Université de Montréal

Étude de l'effet de l'insertion de chaînes latérales sur la conformation et les propriétés spectroscopiques d'oligothiophènes

par

Nicolas Di Césare

Département de chimie

Faculté des arts et des sciences

Thèse présentée à la Faculté des études supérieures

en vue de l'obtention du grade de

philosophiæ Doctor (Ph.D.)

en chimie

Janvier, 1999

Université de Montréal

Faculté des études supérieures

Cette thèse intitulée :

Étude de l'effet de l'insertion de chaînes latérales sur la conformation et les propriétés spectroscopiques d'oligothiophènes

présentée par :

Nicolas Di Césare

a été évaluée par un jury composé des personnes suivantes :

François Brisse :	Président-rapporteur
Gilles Durocher :	Directeur de recherche
Christian Reber :	Membre du jury
Benoît Simard :	Examinateur externe
Claude Carignan :	Représentant du doyen

Thèse acceptée le : 99-04-12

Sommaire

Cette thèse porte sur l'étude de l'effet de substituants sur la conformation et les propriétés optiques d'oligothiophènes (dimères et trimères) dans différents milieux. Dans une première partie, il sera question de l'effet de la nature et de la position de substituants sur la conformation et les paramètres spectroscopiques de dérivés du 2,2'-bithiophène. Les substituants ont été initialement insérés dans le but d'augmenter la solubilité des polythiophènes. Les études physico-chimiques effectuées sur ces polymères substitués ont montré que la substitution n'influençait pas seulement la solubilité du polymère, mais également ses propriétés physiques et chimiques. Afin de bien saisir cet effet de substitution, une étude en profondeur est donc de rigueur.

Dans le premier chapitre, nous verrons cet effet de substitution sur les propriétés optiques (spectres d'absorption et de fluorescence) et sur les rendements quantiques de fluorescence qui nous permettront d'extrapoler les conformations et de décrire les contributions électroniques des substituants qui se reflètent sur les paramètres spectroscopiques. Les résultats montrent que le 2,2'-bithiophène (BT) adopte une conformation non plane et qu'une distribution de conformères est attendue en solution ou en phase gazeuse. L'insertion de substituants alkyls, alkoxys ou alkylthios en position 4 et/ou 4' n'influence aucunement la conformation du BT, ainsi, ces dérivés possèdent relativement les mêmes propriétés optiques que le BT. Par contre, l'insertion de substituants alkyls, alkoxys ou alkylthios en position 3 et/ou 3' influence de façon significative la conformation et, donc, les propriétés optiques en comparaison avec le BT. Ces influences sont également dépendantes de la nature du substituant. Les substituants alkyls et alkylthios induisent une grande torsion entre les cycles thiophènes, en comparaison avec le BT, et ainsi induisent un important déplacement hypsochrome de la première transition singulet-singulet combiné avec

une diminution du coefficient d'absorptivité molaire. Cette torsion est causée par l'encombrement stérique créé par ces groupes. Inversement, les groupes alkoxys induisent une plus grande planéité entre les cycles thiophènes en comparaison avec le BT. Cette augmentation de planéité induit un déplacement bathochrome et une augmentation du coefficient d'absorptivité molaire de la première transition singulet-singulet, toujours en comparaison avec le BT. Les spectres de fluorescence nous montrent, qu'au premier état singulet excité relaxé, tous les dérivés adoptent une conformation quasi plane et cela, indépendamment de la présence de substituants ou non.

Afin d'approfondir l'effet de la nature et de la position des substituants sur la conformation et sur les barrières de rotation et également pour appuyer les résultats expérimentaux, une analyse conformationnelle, utilisant la méthode *ab initio* HF/3-21G*, a été effectuée sur plusieurs dérivés du BT comportant des substituants alkyls (chapitre 2), alkoxys (chapitre 3) et alkylthios (chapitre 4). Les résultats obtenus corroborent les résultats expérimentaux décrits plus haut. De plus, l'obtention des conformations les plus basses en énergie et des barrières de rotation, entre la conformation de plus basse énergie et la conformation plane *anti* (180°), a permis de corréler les effets chromiques (thermochromisme, solvatochromisme ...) observés chez les polythiophènes correspondants avec les possibilités de changements conformationnels obtenus à l'aide des calculs sur les dimères modèles (chapitre 5).

Dans la deuxième et dernière partie, il sera question de l'effet des interactions intermoléculaires sur les propriétés optiques des oligothiophènes. Pour cette partie, le terthiophene (TT) et quelques dérivés du TT seront utilisés. La connaissance de ces interactions est primordiale dans la compréhension de l'origine des effets chromiques chez les polythiophènes puisque ces effets s'observent à l'état solide ou suivant l'agrégation en solution. Dans un premier temps (chapitre 6), nous effectuerons une analyse conformationnelle, utilisant la méthode *ab initio* HF/3-21G*, jointe à une étude spectroscopique en solution afin de déterminer les conformations des dérivés et avoir une connaissance des surfaces d'énergie potentielle de chacun d'eux. Ensuite (chapitre 7), les propriétés optiques obtenues dans différents milieux nous permettront d'identifier l'importance des changements conformationnels et des interactions

électroniques intermoléculaires dans les spectres d'absorption et de fluorescence. Ces effets observés expérimentalement seront corroborés (chapitre 8) avec des résultats théoriques de calculs effectués sur les formes cristallines des dérivés étudiés. Les résultats montrent que les interactions intermoléculaires sont très importantes pour le dérivé non substitué, TT, ce qui résulte en l'apparition d'une scission excitonique importante dans les spectres d'absorption. Par contre, les dérivés substitués ne montrent aucune scission excitonique importante et, dans leur cas, les changements conformationnels sont responsables des changements observés dans les spectres d'absorption.

Table des matières

Liste des tableaux

* La numérotation des tableaux suit les règles suivante : le premier chiffre correspond au chapitre comportant la figure et le deuxième chiffre correspond au numéro original de la figure dans l'article.

Liste des figures

* La numérotation des tableaux suit les rêgles suivante : le premier chiffre correspond au chapitre comportant la figure (0 correspond à l'introduction) et le deuxième chiffre correspond au numéro original de la figure dans l'article.

Liste des abréviations

AM1 : Austin Model 1.

BT : 2,2'-bithiophène.

CI : configuration interactions.

DBO33BT : 3,3'-dibutoxy-2,2'-bithiophène.

DBO44BT : 4,4'-dibutoxy-2,2'-bithiophène.

DBS33BT : 3,3'-dibutylthio-2,2'-bithiophène.

DCABT : 4,4'-didécyl-2,2'-bithiophène-5,5'-dicarbonyl dichlorure.

DD33BT : 3,3'-didécyl-2,2'-bithiophène.

DD44BT : 4,4'-didécyl-2,2'-bithiophène.

DE33BT : 3,3'-diéthyl-2,2'-bithiophène.

DE34BT : 3,4'-diéthyl-2,2'-bithiophène.

DETT : 3',4'-diéthyl-2,2' :5'2''-terthiophène.

DFT : Density Funtional Theory.

DHTT : 3',4'-dihexyl-2,2' :5'2''-terthiophène.

DMO34BT : 3,4'-diméthoxy-2,2'-bithiophène.

DMO44BT : 4,4'-diméthoxy-2,2'-bithiophène.

DMO33BT : 3,3'-diméthoxy-2,2'-bithiophène.

DMODM34BT : 3,4'-diméthoxy-3',4-diméthyl-2,2'-bithiophène.

DMOTT : 3,3''-diméthoxy-2,2' :5',2''-terthiophène.

DMS33BT : 3,3'-diméthylthio-2,2'-bithiophène.

DMS34BT : 3,4'-diméthylthio-2,2'-bithiophène.

DMSDM34BT : 3,4'-diméthylthio-3',4-diméthyl-2,2'-bithiophène.

DMTT : 3,3''-diméthyl-2,2' :5',2''-terthiophène.

MP2 : Moller-Plesset Method 2.

PM3 : Parametric Method 3.

PPV : polyparaphénylènevinylène.

PT : polythiophène.

TT : 2,2':5',2''-terthiophène.

ZINDO/S : Zerner Intermediate Neglect of Differential Overlap for Spectroscopy.

Schémas moléculaires

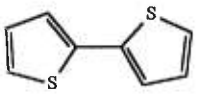

BT

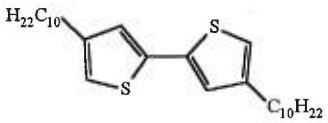

DD44BT

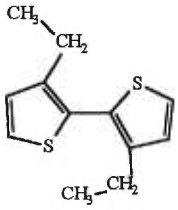

DE33BT

(DD33BT: avec chaînes décyles)

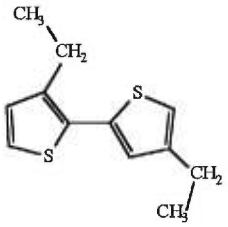

DE34BT

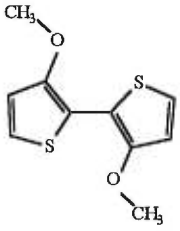

DMO33BT

(DBO33BT: avec chaînes butyles)

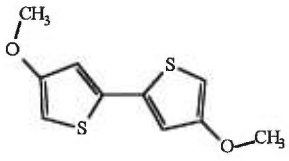

DMO44BT

(DBO44BT: avec chaînes butyles)

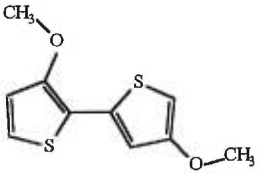

DMO34BT

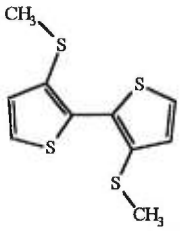

DMS33BT

(DBS33BT: avec chaînes butyles)

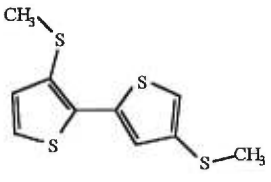

DMS34BT

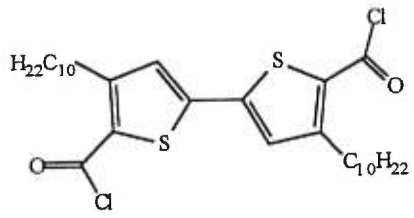

DCABT

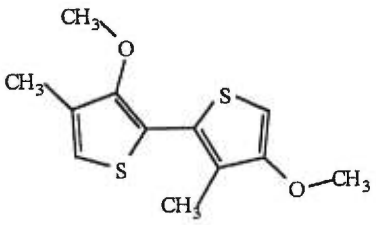

DMODM34BT

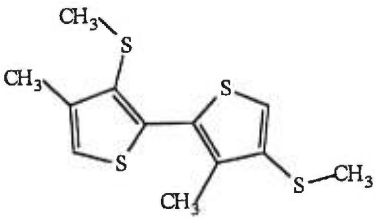

DMSDM34BT

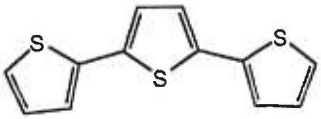

TT

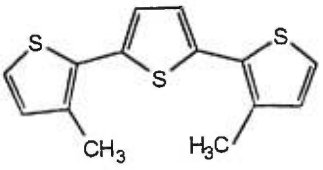

DMTT

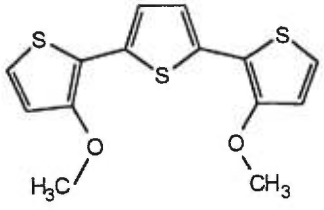

DMOTT

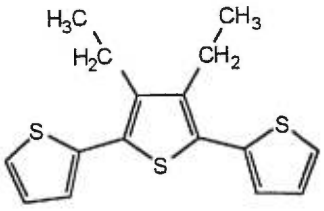

DETT

(DHTT: avec chaînes hexyles)

Remerciements

Je souhaite tout d'abord remercier mon directeur de thèse, le professeur Gilles Durocher du département de chimie de l'Université de Montréal, pour m'avoir accepté dans son groupe de recherche et pour son support tout au long de mes études doctorales. La confiance qu'il m'a témoignée et les discussions générées par ce présent travail ont été, pour moi, très profitables au plan académique et pratique.

Je désire également remercier le professeur Mario Leclerc, également du département de chimie de l'Université de Montréal, qui est à l'origine du projet de recherche sur les oligothiophènes présenté ici. Son expérience et nos discussions sur le sujet ont été grandement appréciées. Je désire également remercier les étudiants de son groupe de recherche (François Raymond, Anne Donat-Bouillud, Claudio Marrano et Ernesto Riviera Garcia) qui ont effectué les synthèses des molécules étudiées.

J'aimerais également remercier le docteur Michel Belletête, agent de recherche au département de chimie de l'Université de Montréal, qui m'a initié aux différentes techniques utilisées dans le cadre de mes travaux de recherche. Je le remercie également pour les discussions partagées et son aide dans la rédaction des différents articles publiés.

En terminant, je remercie le Conseil de Recherche en Sciences Naturelles et en Génie du Canada (CRSNG) pour m'avoir accordé deux bourses d'étude supérieure (ÉS A et ÉS B) qui m'ont permis de réaliser ces travaux à l'abri des soucis financiers. Je remercie également le département de chimie qui m'a accordé des emplois d'auxiliaires à l'enseignement. En terminant, je remercie le CRSNG et le fonds FCAR (Québec) pour leurs subventions à la recherche.

Introduction

L'intérêt des polymères organiques conjugués a montré un essor important depuis les années soixante-dix avec l'étude de la conductivité électrique du poly(acétylène) dopé [1]. Depuis ce temps, plusieurs polymères conjugués (comportant une délocalisation des électrons π tout au long de la chaîne principale) comme le poly(phénylène), le poly(phénylène vinylène), le poly(pyrrole) et le poly(thiophène) (PT) (fig. 1), ont montré des propriétés électriques et électrochimiques intéressantes. De plus, ces polymères composés de cycles aromatiques en conjugaison, ont montré une meilleure stabilité chimique et un meilleur potentiel pour la transformation du matériau brut en un matériau fini et utilisable à l'état neutre ou oxydé, ce qui les avantage sur le poly(acétylène). De ces polymères conjugués, les poly(thiophène)s ont fait montre d'un grand intérêt. Depuis quelques années, plusieurs résumés décrivant les travaux et les résultats obtenus à ce jour sur la synthèse, la structure, l'électrochimie, les propriétés électriques et physico-chimiques ainsi que sur les applications des polythiophènes ont été publiés [2-6].

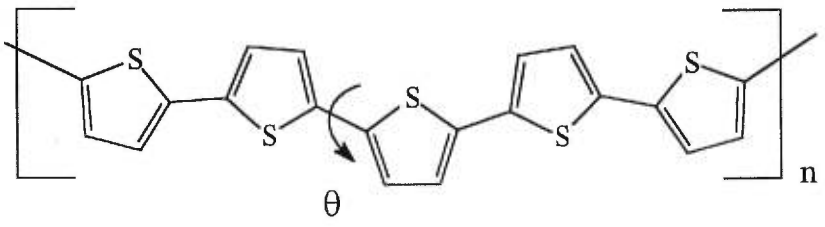

Figure 1: Structure primaire du polythiophène

Le PT non substitué est non soluble dans les solvants organiques communs ce qui rend son utilisation difficile. Pour remédier à ce problème, de nouveaux PTs substitués ont été développés. La grande diversité de substituants possibles a permis

l'essor de nouveaux PTs avec des propriétés électriques, optiques et physico-chimiques différentes. Comme montré sur la figure 1, chaque cycle thiophène du polymère est "libre" (suivant une surface d'énergie potentielle) de rotation. Cette mobilité qui dépendra de la nature et de la position des substituants, confère au PT des relations conformation-propriétés des plus intéressantes. Comme par exemple, les propriétés optiques dépendent directement du degré de conjugaison de la chaîne principale qui diminue avec la torsion entre les cycles thiophènes. Ainsi, pour une conformation plane ($\theta = 0°$ ou $180°$), la délocalisation est maximale comparativement au conformère perpendiculaire ($\theta = 90°$) où la délocalisation est presque nulle entre les cycles thiophènes. Une des propriétés optiques intrigante et intéressante (dont nous allons particulièrement nous intéresser dans ce projet) des PTs substitués est l'effet chromique, c'est-à-dire le changement de couleur (déplacement de la première bande d'absorption) suivant un changement dans les propriétés physiques et/ou chimiques du milieu où se trouve le polymère. Nous pouvons observer cet effet suite à un changement de température (thermochromisme) en solution ou à l'état solide, en présence d'ions (ionochromisme), suite à un changement de pression (piézochromisme) etc. L'observation ou non de ces phénomènes est très dépendante de la nature et de la position des substituants.

Le projet de recherche, dont les résultats sont présentés dans cet ouvrage, a démarré avec l'objectif d'identifier les origines des effets chromiques (ou l'absence de ces effets) observés chez les PTs substitués. Généralement [7-15], les origines des effets chromiques sont discutées en termes de changements conformationnels. Lorsque les chaînes polymériques sont libres les unes par rapport aux autres, les cycles thiophènes de la chaîne principale adoptent une conformation favorable énergétiquement. Cette conformation peut varier grandement dépendamment de la nature et de la position des substituants. Ces formes libres peuvent exister en solution et à l'état solide à haute température. Suivant la diminution de température, en solution et à l'état solide, les chaînes de polymère s'agrègent et s'empilent les unes sur les autres. Cet empilement peut favoriser un changement conformationnel vers des structures plus planes afin d'augmenter l'énergie d'interaction entre les chaînes voisines et ainsi former une structure cristalline plus compacte et plus stable. Ce

changement conformationnel peut se produire si la forme libre est non plane et si la barrière rotationnelle pour la forme plus plane est franchissable. Ainsi les formes libres planes et les formes libres tordues possédant un trop grand encombrement stérique pour former une forme plane ne devraient montrer aucun effet chromique significatif.

Cette interprétation des effets chromiques a été établie en comparant les différents effets chromiques de polythiophènes comportant différents substituants [12-27]. Par contre, les effets des substituants sur les conformations et sur les barrières de rotation étaient alors méconnus et cette interprétation était plutôt spéculative qu'exacte. Une des critiques les plus importantes de cette interprétation est que les interactions intermoléculaires à l'état solide ou suivant l'agrégation des chaînes de polymère en solution ne sont jamais discutées et incluses dans l'interprétation des changements des propriétés optiques de ces matériaux. L'interaction entre deux systèmes conjugués peut conduire à d'importants changements dans les propriétés optiques, comme par exemple la formation d'excitons, et ainsi jouer un rôle clé dans l'interprétation des effets chromiques des polythiophènes.

Pour atteindre l'objectif d'éclaircir l'origine des effets chromiques, nous devions connaître les effets de la position et de la nature des substituants sur les conformations des cycles thiophènes de façon précise. Pour cela, nous avons utilisé plusieurs bithiophènes (BTs) substitués par différents groupes: alkyls, alkoxys et alklylthios. Dans cette étude, l'utilisation d'oligomères est très profitable puisque, chez les polymères, les conformations sont mal définies. De plus, une très grande distribution et une inhomogénéité de conformères sont présentes. De plus, les données expérimentales (bandes d'absorption et de fluorescence) reflètent cette grande dispersion, ce qui rend leur analyse difficile. Également, la nature même du polymère ne permet pas une grande variabilité dans les solvants utilisables. Par ailleurs, la structure des oligomères est beaucoup mieux définie, chaque molécule est identique et les solvants sont beaucoup moins limités. Nous pouvons également noter que l'utilisation des oligothiophènes comme matériaux actifs, en remplacement des polythiophènes, est de plus en plus fréquente [28-34]. Ainsi, l'étude des oligomères

nous informe directement sur les propriétés de ces matériaux. L'utilisation de dimères, pour étudier l'effet de la position et de la nature du substituant, a pour avantage qu'un seul angle dièdre (angle entre les deux cycles thiophènes) est présent; ainsi, tous les paramètres expérimentaux reliés au degré de conjugaison peuvent être directement reliés à la conformation de ces dimères.

Pour déterminer expérimentalement les conformations des différents dérivés étudiés, nous avons recourt à la spectroscopie électronique UV/vis d'absorption et de fluorescence. Comme la conformation des oligothiophènes influence directement le degré de conjugaison présent dans la molécule, l'analyse des bandes d'absorption et de fluorescence présente une méthode physico-chimique des plus appropriée pour cette étude. La spectroscopie d'absorption nous permet d'obtenir de l'information sur la conformation de l'état fondamental (S_0) et la fluorescence, sur celle du premier état excité singulet (S_1) en plus de nous fournir les paramètres photophysiques des dérivés étudiés. La fluorescence ne figure pas dans l'objectif d'étudier les origines des effets chromiques, mais permettra de compléter l'analyse spectroscopique et photophysique de ces molécules. De plus, elle sera utilisée comme moyen de détection pour la caractérisation des agrégats. Les rendements quantiques de fluorescence seront spécialement discutés dû à l'intérêt porté à ces matériaux en électroluminescence. Comme nous allons le voir, les paramètres spectroscopiques nous donnent une idée générale des conformations adoptées par les différents dérivés, mais ne nous permettent pas d'obtenir de façon précise la conformation et surtout ne nous informent pas sur les barrières rotationnelles entre les cycles thiophènes.

Pour compléter l'analyse conformationnelle, nous utiliserons des méthodes de calculs théoriques qui nous donneront une information directe sur les conformations et les barrières de rotation applicables à la phase gazeuse. Il existe principalement trois types de niveau de calculs pour ce genre d'études : les calculs de mécanique moléculaire, semi-empirique et *ab initio*. Comme les calculs de mécanique moléculaire ne considèrent pas la structure électronique des molécules, qui est très importante dans une fine optimisation de structures moléculaires conjuguées comme recherchée ici et dans la recherche de barrières rotationnelles, ce type de calculs s'est montré bien insuffisant pour atteindre nos objectifs. Les calculs semi-empiriques

(AM1 et PM3) sont souvent utilisés chez les oligothiophènes (et autres molécules semblables) afin de déterminer les structures moléculaires, les barrières rotationnelles et les propriétés des différents états électroniques. Ces calculs ont l'avantage d'être très rapides, utilisables pour de gros systèmes et ne nécessitent pas l'utilisation d'ordinateurs puissants. Par contre, certaines approximations sont faites dans la résolution d'intégrales électroniques, ce qui rend souvent ce niveau de calculs insuffisant pour certaines utilisations [35-40]. Dans le premier chapitre de ce travail, nous combinons les résultats expérimentaux de l'analyse conformationnelle sur les dimères avec des calculs semi-empiriques (AM1). Quoique ces calculs montrent des résultats intéressants et concluants pour certains dérivés, spécialement les dérivés alkyls, ils se sont montrés insuffisant pour d'autres, comme les dérivés alkoxys.

Les calculs *ab initio* (HF/3-21G*) utilisés par la suite se sont montrés plus efficaces dans l'obtention des conformations et des barrières rotationnelles de ces molécules (chapitres 2-4). Il existe plusieurs niveaux de calculs *ab initio* (HF, MP2, etc.), la méthode Hartree-Fock (HF) est l'une des méthodes de base qui inclut certaines approximations comme la négligence de la corrélation électronique. Malgré cela, la méthode HF est considérée très bonne pour l'obtention de structures moléculaires pour des molécules organiques simples possédant des atomes légers (H, C, O, S etc.). Cette confiance en la méthode *ab initio* HF se reflète dans le nombre important d'articles où elle est utilisée [41-42]. La taille de nos systèmes ne nous permettait pas l'utilisation de calculs *ab initio* plus évolués parce qu'ils nécessitent un temps de calcul et un espace mémoire trop important. La validation de ces calculs ainsi que la comparaison avec les calculs semi-empiriques seront discutées plus profondément aux chapitres 2-4. Il est à noter que les calculs *ab initio* corroborent très bien les données expérimentales. Au chapitre 5, les résultats des analyses conformationnelles des dimères modèles seront discutés et comparés au thermochromisme observé chez les polymères correspondants. Nous verrons alors que cette analyse conformationnelle appuie l'hypothèse de changements conformationnels comme origine du thermochromisme.

Cette corrélation théorique, quoiqu'intéressante et utile dans la prédiction de futurs polythiophènes thermochromes [25], ne nous informe pas sur les interactions

interchaînes pouvant exister lors de l'agrégation ou à l'état solide. Afin de solutionner ce point, nous nous sommes donnés comme objectif d'étudier le thermochromisme directement chez les oligothiophènes. Ainsi, en travaillant dans différents milieux, nous pourrons identifier la nature des interactions intermoléculaires présentes chez ces molécules et ainsi voir leurs effets sur les propriétés optiques de ces systèmes en comparaison avec les changements conformationnels. Pour atteindre cet objectif, l'utilisation de la spectroscopie UV/vis (absorption et fluorescence) est encore de mise, ainsi que les calculs théoriques, pour la connaissance des conformations et pour la corrélation avec les résultats expérimentaux.

Cette dernière partie couvre les chapitres 6-8. Dû à la nature des différentes expériences réalisées et aux faibles signaux obtenus avec les dimères, l'utilisation d'oligothiophènes plus long s'est avérée plus pertinente pour cette partie. Dans ce travail, nous présenterons les résultats obtenus avec les trimères. Afin d'atteindre les objectifs fixés, le travail est divisé en trois parties distinctes. La première, chapitre 6, comporte l'analyse conformationnelle des dérivés utilisés dans leur forme libre, en solution ou en phase gazeuse. Cette première partie est primordiale puisque tous les changements conformationnels et les effets thermochromes suivant l'agrégation sont discutés en fonction des conformations des molécules libres. Dans la deuxième partie, chapitre 7, les résultats expérimentaux de l'observation des effets chromiques seront présentés et discutés en fonction des changements conformationnels et des interactions intermoléculaires. Comme dernière partie, chapitre 8, des calculs semi-empiriques (ZINDO/S) effectués sur des structures cristallines des dérivés étudiés permettra de construire un modèle théorique en corrélation avec les résultats expérimentaux.

Les articles discutés dans cette thèse ont été choisis en fonction de leur importance par rapport au but de la thèse. Dans le cadre de mes travaux de recherche, d'autres publications en rapport aux oligothiophènes ont été produites. Les résultats de ces articles ont été jugés moins importants en regard des buts fixés dans le présent travail. Je présente donc un bref apperçu et les conclusions importantes de ces articles. Deux de ces d'articles [43,44], présentent les paramètres spectroscopiques et photophysiques d'une série d'oligothiophènes substitués comportant de trois à six

unités thiophènes. Les résultats sont discutés en termes de conformation et d'effet de la longueur de l'oligomère. Ils sont également comparés aux polyesters correspondants. Les résultats montrent que l'insertion de chaînes latérales alkyles induit une plus grande torsion entre les cycles thiophènes et cela peu importe la longueur de l'oligomère. Cette torsion a pour effet de déplacer les bandes d'absorption vers les plus hautes énergies et de diminuer les coefficients d'extinction molaire. Elle conduit également à une diminution des rendements quantiques de fluorescence et des durées de vie de fluorescence. Ces dernières diminutions sont principalement dues à l'augmentation de la constante de désactivation non radiative (k_{nr}). Les résultats ont également montré que les oligomères insérés dans un polyester conservaient les mêmes propriétés optiques que l'oligomère isolé.

Dans un autre article [45], nous présentons l'évolution des paramètres spectroscopiques et photophysiques en solution (pour des molécules isolées) en fonction de la température (25°C à -140°C) pour le TT, le DMOTT, le DMTT et le DHTT. Les résultats montrent que le TT et le DMOTT possèdent des structures très flexibles de sorte qu'une baisse de température est suffisante pour induire un changement conformationnel. Cette flexibilité est due aux très faibles barrières rotationnelles de ces trimères. Les changements conformationnels observés sont expliqués en termes d'augmentation de l'interaction entre molécules de soluté et de solvant lorsque la température est diminuée. Les dérivés DMTT et DHTT possédant des barrières rotationnelles beaucoup plus importantes, ne montrent que très peu de changements dans leurs spectres d'absorption en fonction de la température. Dans tous les cas, les spectres de fluorescence ne montrent aucun déplacement hypsochrome ou bathochrome (seuls des changements d'intensité sont observés) puisqu'il est attendu que pour chaque dérivé, une conformation plane est atteinte au premier état excité singulet relaxé. Quant aux résultats photophysiques, les changements dans les paramètres sont discutés en termes de différence conformationnelle et dans le processus d'intercombinaison qui est le mode majeur de désactivation du premier état singulet excité.

Nous avons également publié [46,47] une étude sur les origines du thermochromisme chez les tétramères. Les tétramères étudiés étaient le

quaterthiophène non substitué, deux tétramères comportant des groupements alkyles (l'un comportant des groupements méthyles et l'autre des groupements décyles) et un dernier comportant des groupements alkoxys. Les résultats du thermochromisme d'un polymère correspondant à un des oligomères ont également été présentés [46]. Les propriétés optiques des oligomères en solution, dans une matrice de substitution et sous forme agrégée sont présentées. Des calculs ZINDO/S sur les structures cristallines sont également rapportés. Les résultats montrent que les effets thermochromes des dérivés substitués avec les groupements alkoxys et décyles sont induits par des changements conformationnels. Par contre, les agrégats du dérivé comportant des groupements méthyles montrent un effet excitonique important, comparable à celui observé chez le quaterthiophène non substitué. Ces résultats sont expliqués en termes d'un arrangement particulier des molécules dans la structure cristalline (ou agrégée). Les oligomères montrant des effets excitoniques importants possèdent tous une structure cristalline ordonnée et compacte favorisant ainsi les interactions intermoléculaires. Les autres dérivés montrent une structure cristalline moins ordonnée et compacte; ainsi, nous observons seulement un effet conformationnel sur les propriétés optiques suite à l'agrégation.

L'ensemble de ce travail nous a permis de faire la lumière sur l'effet de la nature et de la position de la substitution sur les conformations et les propriétés optiques des oligothiophènes substitués. Les résultats montrent que l'insertion de substituants en positions 3 et/ou 3' influence la conformation des oligothiophènes. Comparativement au BT ou au TT qui sont non plans en phase gazeuse ou en solution ($\theta \approx 150°$ entre cycles thiophènes), l'insertion de groupements alkoxys en position 3 et/ou 3' (DMO33BT, DMOTT, etc.) induit une plus grande planéité entre les cycles thiophènes. Inversement, l'insertion de groupements alkyles à ces mêmes positions (DD33BT, DMTT, DHTT, etc.) induit une torsion plus importante entre les cycles thiophènes. Les groupements alkylthios induisent également une plus grande torsion entre les cycles thiophènes, mais de façon moins importante que les groupements alkyls. Cette influence sur les conformations et les différences entre les substituants de nature variée sont dues à un équilibre entre la délocalisation électronique qui favorise une conformation plane et l'encombrement stérique qui favorise une

conformation plus tordue. Les résultats montrent également que l'insertion de groupements en positions 4 et/ou 4' n'influence pas la conformation des oligothiophènes. Ces effets de la substitution sur la conformation influencent directement les propriétés optiques de ces oligothiophènes. Les molécules plus planes, à l'inverse des molécules plus tordues, possèdent des bandes d'absorption déplacées vers les plus basses énergie et possèdent une meilleure structure vibronique. Elles possèdent également des coefficients d'extinction molaire plus élevés. Pour tous les dérivés étudiés, les spectres de fluorescence montrent qu'une conformation plane est fortement favorisée au premier état excité singulet relaxé, et cela indépendamment de la présence ou non de substituants.

Ce travail a également permis de distinguer les changements conformationnels des effets excitoniques résultant des interactions intermoléculaires et ainsi d'identifier les origines du thermochromisme des polythiophènes substitués. Les mesures effectuées sur des trimères dans des matrices de substitution ont permis d'obtenir les propriétés optiques de ces oligothiophènes dans des conformations plus planes que celles adoptées en solution. Pour tous les trimères substitués, ces changements optiques suivant un changement conformationnel sont identiques aux changements optiques suivant l'agrégation. Ces résultats montrent que, suite à l'agrégation, ces molécules adoptent une conformation plus plane et que les changements optiques résultant de ces changements conformationnels sont beaucoup plus importants que les changements optiques pouvant résulter des interactions intermoléculaires. Pour le dérivé non substitué (TT), nous observons l'inverse, c'est-à-dire que les changements optiques résultant des interactions intermoléculaires sont beaucoup plus importants que les changements résultant des changements conformationnels. Cette différence est expliquée en termes de structure micro-cristalline. Les molécules possédant des groupements latéraux forment un agrégat où l'empilement des molécules défavorise les interactions intermoléculaires comparativement à la forme agrégé du TT qui est beaucoup plus compacte.

Chapitre 1

Analyse conformationelle et spectroscopique de dérivés du 2,2'-bithiophène

Dans ce premier chapitre, nous présentons les propriétés optiques (spectres d'absorption et de fluorescence) ainsi que la photophysique des dérivés alkyls et alkoxys du 2,2'-bithiophène. Ces résultats expérimentaux sont discutés en termes de la contribution électronique des substituants sur la première transition singulet-singulet observée et de l'effet des substituants sur la conformation du BT. Les effets de la nature et de la position du substituant sont également discutés. Afin de compléter l'analyse conformationnelle des dérivés étudiés, les surfaces d'énergie potentielle, obtenues avec la méthode semi-empirique AM1 (une brève description des méthodes théoriques utilisée dans le cadre des traveaux présentés est donnée à l'annexe 1), en fonction de l'angle dièdre entre les deux cycles thiophènes (θ), sont également présentées. Les transitions $S_1 \leftarrow S_0$ calculées, en fonction de l'angle dièdre θ, avec la méthode semi-empirique ZINDO/S, sont comparées avec la première transition singulet-singulet observée pour chacun des dérivés. Cette comparaison permet d'extrapoler la conformation de chaque dérivé en solution.

Les résultats obtenus avec cette technique ont montré que la substitution en position 4,4' n'avait aucun effet sur la conformation du BT. Les comparaisons des transitions singulet-singulet calculées et observées montrent, pour chaque dérivé, une conformation à environ 150° similaire à celle du BT. Ces conformations correspondent aux minima des surfaces d'énergie potentielle obtenues avec AM1. De la même manière, le dérivé décyl en position 3,3' montre une conformation au voisinage de 90° similaire au minumum global de la courbe d'énergie potentielle.

Les surfaces d'énergie potentielle ainsi que l'extrapolation de la conformation à l'aide de la première transition singulet-singulet pour les dérivés alkoxys en position 3,3' montrent une conformation à 120°. Une description de la nomenclature utilisée pour identifier les différentes conformations est donnée à l'annexe 2.

Les résultats expérimentaux des dérivés alkoxys ne concordent pas très bien avec l'hypothèse d'une conformation non plane (θ = 120°), du moins, plus tournée que la conformation du BT (où θ = 150°). Les calculs plus évolués qui ont été effectués par la suite, après la sortie de ce premier article, ont montré que les calculs semi-empiriques AM1 se comparaient aux calculs *ab initio* pour le cas des dérivés 4,4' et alkyl en position 3,3' à l'exception des barrières de rotation qui sont sous évaluées par la méthode AM1. Pour ce qui est du cas des alkoxys en position 3,3', les calculs AM1 se sont montrés insuffisants pour l'obtention d'une surface d'énergie potentielle correcte et en accord avec les données expérimentales.

Une analyse conformationnelle plus complète effectuée par différentes méthodes théoriques (semi-empirique et *ab initio*) sera présentée aux chapitres 2-4 pour les dérivés alkyls, alkoxys et alkylthios. Une discussion plus détaillée sur la validité des calculs AM1 *versus ab initio* sera alors présentée. Dans ce premier article, les dérivés thioalkyls sont absents puisqu'ils ne figuraient pas dans le projet initial. Les données expérimentales sont présentées dans le même chapitre que l'analyse conformationnelle détaillée (chapitre 4).

Dans ce chapitre, et dans les suivants, les valeurs rapportées dans les tableaux ne comporte aucune incertitude. Ceci est principalement dû au format des articles où on représente que très rarement les incertitudes sur les mesures spectroscopiques. J'aimerais tout de même spécifier à ce moment, les incertitudes et les précisions considérées sur ces mesures. La première information retenue sur les spectres est la position du maximum. Puisque dans tous les cas nous avons des bandes d'absorption très large et sans résolution vibronique, je considère une incertitude de $\pm$ 1 nm sur la position du maximum de la bande. Ces unités ont ensuite été transformées en cm^{-1}. Ainsi, une incertitude de 100 cm^{-1} peut être calculée. Les mesures des coefficients

d'extinction molaire ont été obtenues avec un graphique de la concentration en fonction de l'absorbance, ainsi par régression linéaire des points expérimentaux, nous obtenons une incertitude de 100 M^{-1} cm^{-1}. Les largeurs de bande ont été mesurées directement sur les spectres, une incertitude de 100 cm^{-1} a été considérée. L'incertitude sur les rendements quantiques de fluorescence est plus difficile à évaluer. Généralement, une incertitude d'environ 10% est considérée pour ces mesures.

1.1 Article 1 : Conformational and spectroscopic analysis of selected 2,2'-bithiophene derivatives

Article publié dans The Journal of Physical Chemistry A, volume 101, numéro 5, pages 776-782 (1997).

Conformational and Spectroscopic Analysis of Selected 2,2'-Bithiophene Derivatives

Nicolas Di Césare, Michel Belletête, François Raymond, Mario Leclerc, and Gilles Durocher

Département de chimie, Université de Montréal
C.P. 6128, Succ. A, Montréal, Québec H3C 3J7, Canada

Abstract

A spectroscopic study has been performed on selected substituted 2,2'-bithiophenes. Absorption and fluorescence spectra of bithiophenes (BT) substituted with alkyl and alkoxy groups in positions 4,4' and 3,3' have been measured in solvents of various polarity and viscosity. AM1 and ZINDO/S semiempirical calculations have also been performed on all molecules in order to evaluate the torsional potential energy surfaces and the singlet-singlet transition energies. They are found by a combined theoretical and experimental technique in which 3,3'-derivatives are more twisted than their 4,4'-analogs in the ground state. After excitation, molecules relax to much more planar S_1 excited states. The sole exceptions are 3,3'-alkoxybithiophene derivatives which seem to remain in the same conformation in their respective relaxed S_1 excited state. For molecules in their T_1 excited states, planar and perpendicular conformations are the most stable. It is also observed that fluorescence quantum yields of all bithiophene derivatives are weak but weaker for 3,3'-substituted compounds. Results are interpreted in terms of a possible substitutional effect on the intersystem crossing process involved in these systems.

1. Introduction

The preparation of soluble conjugated polythiophenes can be done by the incorporation of relatively long and flexible side chains [1]. This approach is based upon a decrease in attractive interchain interactions and the introduction of favorable interactions between the substituents and the solvent. But, the introduction of substituents may have a strong influence on the electronic structure of the resulting material and, consequently, on its optical properties. For instance, some substituted polythiophenes exhibit intriguing thermochromic (in the solid state and in solution) properties [2-5]. These unusual optical effects are believed to be related to a reversible "transition" between a coplanar (highly conjugated) and a nonplanar (less conjugated) conformation of the conjugated main chain [6,7]. Other studies have revealed the strong dependence of the thermochromic properties upon the position and the nature of the substituents [8-10]. Several explanations of the driving force of these optical phenomena have been proposed (crystallization, aggregation, thermally induced steric interactions, etc.), but a detailed description of the structural parameters involved in these optical effects is still lacking.

Knowledge of the structure-property relationships in substituted polythiophenes is still rudimentary [1]. The polymers are complex materials exhibiting a broad and not fully characterized range of conjugation lengths and a distribution of molecular environments and excitonic effects that makes difficult the measurement of vibrationally resolved optical spectra and simple fluorescence decay kinetics. For this reason, we think it is important to focus our attention on the most easily studied oligothiophenes, *i.e.* substituted bithiophenes. A thorough understanding of the optical properties of these molecules upon the nature and the position of the substituents should provide the basis for determining such structural properties as conformation and conjugation length in the more complex polythiophenes.

Recently, gas phase electron diffraction performed at 97-98° C on the unsubstituted bithiophene molecule (BT) has shown the existence of two

conformations, *anti*-like and *syn*-like, with torsional angles of 148° and 36° and conformational weights of 56 and 44%, respectively [11]. These results are in very good agreement with the most recent *ab initio* calculations performed with large basis sets [12-16]. We have recently applied semiempirical quantum-chemical calculation methods (AM1, PM3 and ZINDO/S) to study the ground and excited state conformations of BT as well as other oligothiophenes [17-19]. It was found that the PM3 method does not reproduce accurately the torsional potential of BT. On the contrary, AM1 calculations reproduce minima and maxima at angles similar to those obtained using *ab initio* calculations and in agreement with most stable conformers of BT measured in the vapor phase. The torsional potential curve is flat such that multiple conformations may coexist in the gas phase and in solution. ZINDO/S calculations performed on AM1 optimized conformers predict a fully planar *anti* conformation for BT but give a torsional barrier between thiophene rings close to the experimental values (5 ± 2 kcal mol^{-1}) [20, 21]. Moreover, these calculations suggest that, after excitation, all molecules relax to nearly planar excited singlet electronic states [18, 19]. ZINDO/S also predicts that the most stable conformations of BT in its first excited triplet state are planar ($\phi = 0°$ and 180°), but a local minimum is also predicted for the perpendicular conformation.

The conformation of many alkyl-substituted thiophene oligomers has been studied theoretically [13, 14, 16, 22-24]. Results indicate that 4,4'-dialkylbithiophenes behave similarly to the unsubstituted compound. On the contrary, due to strong repulsive interactions 3,3'-dialkylbithiophenes give conformers with high torsional angles between thiophene rings. These results are conformed with the absorption spectra of these molecules [24].

The fluorescence quantum yield of BT is very small [25, 26]. It has been observed that the intersystem crossing is the major mode of relaxation of the first excited singlet state which is favored by the presence of two heavy atoms [26]. From the first excited triplet state, the system returns to the ground state via intersystem crossing such that no phosphorescence is observed. To our knowledge, the photophysics of substituted bithiophenes is still unknown.

To shed more light on the conformational changes involved in substituted polythiophenes, optical and photophysical properties of bithiophenes having alkyl or alkoxy groups in 3,3' or 4,4' positions have been investigated. 4,4'-Didecyl-2,2'-bithiophene-5,5'-dicarbonyl dichloride (DCABT) has also been investigated. In these simple systems, irregular effects caused by the polymer are eliminated such that absorption and fluorescence bandwidths are smaller and more structured. The study of small oligomers allows also for the use of semiempirical calculations for the interpretation of experimental results. The main objective here in this work is to describe the substituent effect (nature and position) on the molecular conformation and electronic properties of these thiophene dimers. The bithiophenes have been divided in two groups: 4,4'- and 3,3'- substituted molecules. The molecules investigated are shown in Figure 1.

2. Experimental section

2.1. Materials

All solvents were purchased from Aldrich Chemicals (99+%, anhydrous) and used as received. Prior to use, the solvents were checked for spurious emission in the region of interest and found to be satisfactory. 4,4'-Didecyl-2,2'-bithiophene (DD44BT) [27], 4,4'-didecyl-2,2'-bithiophene-5,5'-dicarbonyl Dichloride (DCABT) [28], and 3,3'-didecyl-2,2'-bithiophene (DD33BT) [29] were prepared according to previously published procedures. All alkoxy-substituted bithiophenes were prepared from 3,3'-dibromo-2,2'-bithiophene or 4,4'-dibromo-2,2'-bithiophene following procedures described in a previous publication [30].

2.2. Instrumentation

The absorption spectra were recorded on a Phillips UV/vis spectrometer using 1 cm quartz cells and solute concentrations of (1-3) x 10^{-5} M. The spectra were

then digitized with the use of a GRAPHPAD/IBM-AT system. It has been verified that the Beer-Lambert law is well-respected for these compounds for solute concentrations up to 10^{-4} M. Fluorescence spectra corrected for the emission detection were recorded on a Spex Fluorolog-2 spectrophotometer with a F2T11 special configuration. The excitation and emission band-passes used were 2.6 and 1.9 nm, respectively. Each solution was excited near the absorption wavelength maximum using 1 cm path length quartz cell, and the concentration used for each derivative studied was (0.1-2.0) x 10^{-5} M, giving absorbance of less than 0.1 to avoid any inner-filter effects. For all molecules, a study of the concentration (C) effect has been done on the fluorescence intensities (I_F) and all measurements have been performed in the linear region of the I_F *vs* C curve. Quantum yields of fluorescence were determined at 298 K against DD44BT in chloroform (ϕ_f = 0.017) [28] as a standard. All corrected fluorescence excitation spectra were found to be equivalent to their respective absorption spectra.

2.3. Theoretical methods

Semiempirical calculations were performed using the Hyperchem package, release 4.5, for Windows from Hypercube, Inc on a Pentium computer with an internal memory of 16 Mb. This package has been used to draw the molecules and optimize roughly their geometry using the MM+ force field, which is an extension of MM2 developed by Allinger [31]. A more precise geometry optimization was obtained using the AM1 (Austin Model 1) semiempirical method, including the sulfur atom parameter. AM1 is a modified MNDO method proposed and developed by M.J.S. Dewar and co-workers at the University of Texas at Austin [32-35]. For all derivatives, the dihedral angle (ϕ) between the two thiophene rings was varied in 15° increments from planar cis conformation (ϕ = 0°) to the planar trans conformation (ϕ = 180°). For each increment, ϕ was held fixed while the remainder of the molecule was reoptimized using AM1. We have developed a subroutine to couple CHEMPLUS and EXCEL to make full use of the automatic phipsi routine of

HYPERCHEM after optimization by AM1 at each torsional angle. A root mean square (RMS) gradient in the energy of 0.1 kcal mol^{-1} was use for the optimization criterion.

The electronic transition energies have been calculated within the framework of the semiempirical ZINDO/S method including configuration interaction (CI). ZINDO/S is a modified INDO method parametrized to reproduce UV/visible spectroscopic transitions [36-37]. The electron-repulsion integrals were evaluated using the Mataga-Nishimoto formula. For the singlet-singlet transition, all singly excited configurations involving the five highest occupied and the five lowest unoccupied orbitals (CI = 5/5) were included whereas CI = 3/3 was used for the triplet-triplet energy calculation. The ZINDO/S method also provides the ground state and the first excited triplet energies of the molecule. From these values and the transition energies (singlet-singlet and triplet-triplet), the first excited singlet (S_1) and triplet (T_1) state energies were obtained for each torsional angle. The geometry used for ZINDO/S calculations is that optimized at each torsional angle from the AM1 method.

3. Results and discussion

3.1. Optical Properties

The absorption and fluorescence spectra have been taken in a series of *n*-alkanes (pentane to hexadecane) as well as in perfluorohexane, methanol, hexanol, chloroform, tetrahydrofuran (THF), and acetonitrile. We observed that the absorption and fluorescence maxima of these thiophene derivatives are similar in all solvents. In general, a small red shift (2-3 nm) has been observed in the spectra going from *n*-pentane to *n*-hexadecane. The solvent effects have been previously study on BT [17]. A small red shift is also observed (1-2 nm) in these spectra as the polarity of the solvent increases. Figures 2 and 3 show the absorption and fluorescence spectra of the bithiophenes in *n*-hexane and Table 1 reports the spectral data.

If one compares the three 4,4'-substituted bithiophene derivatives with the unsubstituted molecule (BT: λ_{abs} = 301 nm, λ_f = 360 nm) [24], it is possible to analyze the influence of the nature of the substitution on the first electronic transition assuming that the equilibrium geometry is similar for all the molecules investigated. We will see later that this assumption is reasonable.

It is observed that the addition of decyl chains to the bithiophene chromophore (BT) provokes a red-shift of the absorption and fluorescence bands (see Figure 2 and Table 1). This is surely due to the inductive effect of the decyl chains. These results are in agreement with measurements reported for 4,4'-dioctyl-2,2'-bithiophene [24] and 4,4'-dimethyl-2,2'-bithiophene [38]. The absorption and fluorescence spectra of DD44BT do not show any vibrational fine structure, meaning that this molecule is quite flexible in its ground (S_0) and first relaxed excited singlet states (S_1). However it can be observed that the DD44BT fluorescence band is sharper than its absorption band (see Figure 2 and Table 1), suggesting that the molecule is on average more rigid in the S_1 state. This suggests that the barrier to rotation is higher when the molecule is in its first relaxed singlet excited state. This will be confirmed by ZINDO/S calculations in the next section.

The substitution of BT with methoxy and butoxy groups in the 4,4' positions provokes red shifts in the absorption and fluorescence spectra which are larger than those observed by the incorporation of decyl chains. These results show that, as expected, alkoxy substituents are better electron donor than alkyl groups. Table 1 also shows that the butoxy substituent is a better electron donor group than the methoxy substituent when the molecule is in the ground state whereas this trend is reversed for the molecule in the S_1 relaxed excited state. The Stokes shifts (difference between absorption and fluorescence energy maxima) of DMO44BT and DBO44BT are larger compared to that measured for DD44BT (see Table 1). This indicates that the conformational changes occurring during the relaxation of the Franck-Condon excited state are more important for 4,4'- alkoxy- than for 4,4'-alkylbithiophene derivatives. Like those for DD44BT, absorption and fluorescence bands of alkoxy derivatives are structureless (see Figure 2), showing the mobilility of the thiophene

rings in both S_0 and S_1 states.

The absorption bands of 3,3'-alkoxybithiophene derivatives appear at approximately the same wavelengths as those of 4,4' analogs. This shows that steric effects are not the only factors influencing electronic transition energy values for these systems. The positions of substituents also play a role. Indeed, we have shown by ZINDO/S calculations that alkoxy substituents in the 3-position give $S_1 \leftarrow S_0$ electronic transitions which are red-shifted compared to those observed for 4,4' analogs having the same torsional angles. These calculations together with the absorption spectra suggest that 3,3'-alkoxybithiophenes are more twisted than 4,4'-alkoxy analogs but have similar singlet-singlet transition energies due to better electron donor properties of substituents in 3- and 3'-positions. But, conversely to 4,4'-alkoxy compounds, the absorption spectra of 3,3'-alkoxy bithiophenes are structured. Moreover the bandwidths are smaller by about 1000 cm^{-1} compared to those of 4,4'-alkoxybithiophenes. These results seem to indicate that the 3,3'-alkoxy derivatives are more rigid (higher barrier to rotation) such that the number of conformers available is reduced. This will be confirmed later by semiempirical calculations.

The fluorescence spectrum of DMO33BT is very wide in all of the solvents investigated. Moreover the bandwidths increase with time even if the solutions are kept in the dark. For this reason, it is not possible to assign the fluorescence wavelength at the center of mass of the peak with good accuracy. This behavior is not observed in the DMO33BT absorption spectrum. We believe that this behavior is due to a small degradation of the molecule. The new species is not detected in the absorption spectra but shows a weak luminescence spectrum which overlaps the DMO33BT fluorescence band. The same phenomena are observed for DBO33BT in chloroform, THF and acetonitrile, but, in *n*-alkanes and in *n*-alcohols, the fluorescence bands are much sharper and do not show any changes with time.

It is observed that the fluorescence band of DBO33BT in *n*-hexane is blue shifted by 23 nm compared to DBO44BT, whereas the emission bandwidths of both molecules are similar (see Table 1). Since absorption bands of both molecules appear

at similar wavelengths, these results suggest that the DBO33BT first relaxed excited state is less planar than that of DBO44BT. However, the presence of vibrational structure in the DBO33BT fluorescence spectrum indicates that this molecule remains rigid in the S_1 relaxed excited state. The vibrational Franck-Condon envelope of the absorption and fluorescence spectra is identical, showing that the DBO33BT geometries in S_0 and S_1 are very close.

Figure 3 shows that the first electronic absorption band of DD33BT appears as a shoulder around 35700 cm^{-1} (280 nm). This is an indication that the torsional angle between thiophene rings is very large for this molecule. This will be confirmed below by semiempirical calculations. The absorption spectrum of DD33BT is very similar to that of 3,3'-dioctyl-2,2'-bithiophene reported by Van Hutten *et al.* [24]. However, the first absorption band of the methyl analog derivative is reported at 268 nm [38], which suggests that methyl groups create a slightly larger steric hindrance than longer alkyl chains. The fluorescence band of DD33BT is very weak but appeared at 374 nm, giving a very large Stokes shift of 9000 cm^{-1}. It thus seems that, in the relaxed S_1 excited state, electronic delocalization is favored in such a way that the steric hindrance caused by the alkyl chains is not very effective. Indeed, Table 1 shows that the energetic positions of the fluorescence bands of DD44BT and DD33BT are very close. But one can see that the fluorescence spectrum of DD33BT is wider than that of DD44BT, suggesting that more conformers are present in the S_1 state of DD33BT.

Figure 2 and Table 1 show that the addition of carbonyl chloride groups to the DD44BT molecule to form the DCABT derivative provokes a large red shift of the absorption band (4500 cm^{-1}). This shows that the conjugation length increases by adding two double bonds to the molecular frame. The effect of this process on the geometry of the DCABT molecule will be discussed below. However, the fact that the absorption spectrum is structured seems to indicate that the DCABT molecule is more rigid than DD44BT. Like its absorption spectrum, the fluorescence band of DCABT is red-shifted by a large amount (3000 cm^{-1}) compared to that of DD44BT. This is in agreement with the observation that the DCABT fluorescence band is

structured. Indeed, a better electronic delocalization should reduce the mobility of the thiophene rings. The small value of the Stokes shift observed (see Table 1) strongly suggests that conformational changes occurring upon the relaxation of the S_1 state are less important than those found in other molecules.

In methanol, the DCABT absorption band shows a hypsochromic shift of 1200 cm^{-1} compared to that in *n*-hexane. This blue shift may be interpreted in terms of the formation of hydrogen bonds between the alcohol as proton donor and the carbonyl groups. This should increase the electron acceptor properties of each carbonyl substituent at both ends of the bithiophene, thus reducing the electron density between thiophene rings. The resulting effect would be a more twisted geometry for DCABT in alcohols. A similar blue shift is observed for the fluorescence spectrum of DCABT in methanol, showing that hydrogen bonds are also playing a role in the S_1 relaxed excited state.

Table 2 reports the fluorescence quantum yields (ϕ_F) of the molecules investigated in *n*-hexane, *n*-hexadecane, methanol and *n*-hexanol. Amid the bithiophene derivatives investigated, DCABT possesses the stronger fluorescence (ϕ_F = 0.077), probably due to a better electronic delocalization in the S_1 relaxed excited state. For the other 4,4'-substituted compounds, the fluorescence quantum yields observed are close to the one reported for BT in dichloromethane and in dioxane (0.018) [25, 26]. It thus seems that the alkyl or alkoxy chains at the 4,4'-positions do not affect much the radiative and/or the nonradiative properties of these molecules. Moreover, Table 2 shows that fluorescence quantum yields of these molecules are not much affected by the viscosity of the environment. This suggests that the internal conversion deactivation process is not very important for these derivatives.

For 3,3'-substituted alkoxybithiophenes, Table 2 shows that ϕ_F are about 10 times less than those of the 4,4'-analogs. Conversely to the 4,4'-compounds, 3,3' derivatives show a variation in their fluorescence quantum yields with the viscosity of the environment. It is difficult to believe that this behavior is linked to the internal conversion process since, as observed above, 3,3' derivatives seem more rigid than 4,4'- substituted bithiophenes. Recently, it has been found that the main deactivation

pathway involved in the relaxation of the BT S_1 state is an intersystem crossing process [26]. At present, the substitutional effect on this process is unknown for bithiophene derivatives. We are currently working on this aspect of the problem. However, Rossi *et al.* have reported the triplet quantum yield (ϕ_T) of several 2,2':5',2"-terthiophene derivatives [39]. It was found that the compound having the highest ϕ_T value is the one showing maximum steric effects between thiophene rings. Thus, it is plausible to think that the same behavior can be observed for bithiophene derivatives. The intersystem crossing process involved should be related to the S_1-T_n energy gap of the BT derivatives. We have checked this using ZINDO/S calculations. It was found that the S_1-T_n energy gap decreases as the dihedral angle between thiophene rings increases as observed for the unsubstituted BT molecule [18]. These results will be reported elsewhere. Thus, we think that 3,3'-bithiophene derivatives would have weaker fluorescence quantum yields due to an enhanced intersystem crossing involved in these molecules. The viscosity effects observed on ϕ_F values would be related to an energy barrier involved in the $S_1 \rightarrow T_n$ crossing. For the 4,4'-derivatives, this barrier is probably higher such that the radiationless process is independent of the viscosity of the environment.

3.2. Conformational analysis

3.2.1. AM1 Calculations

A conformational analysis has been carried out on all molecules using the semiempirical AM1 method. For each molecule, a geometry optimization is performed on each value of the dihedral angle between the two rings (ϕ) from the fully planar *syn* ($\phi = 0°$) to the fully planar *anti* ($\phi = 180°$) conformation at each 15° using AM1 calculations. The difference between the total energy of each optimized geometry and the energy of the most stable conformer has been plotted as a function of the dihedral angle in Figure 4A for the 4,4'-substituted bithiophenes and in Figure 4B for the 3,3' analogs. Figure 4A also reports the potential energy surface of the

unsubstituted bithiophene molecule (BT). Recently, we have discussed in detail the AM1 torsional potential of BT [17, 18]. It was found that a qualitative agreement exists between AM1 results and the most recent calculations performed at the *ab initio* level using large basis sets. In particular, the energy minima were reproduced at similar dihedral angles.

Figure 4A shows that 4,4' derivatives have similar potential energy surfaces; *i.e.*, energy minima and maxima appear at similar dihedral angles. The DD44BT potential curve reported here is in good agreement with the AM1 curve obtained for the dioctyl analog [24] and qualitatively similar to that of the 4,4'-methyl derivative as obtained by *ab initio* calculations [14]. The two minima observed are the result of a compromise between steric effects between hydrogen and sulfur atoms, which tend to increase the torsional angle between thiophene rings, and the electronic conjugation along the molecular frame which favors a planar conformation. The fact that the perpendicular and the *cis* conformations have about the same energy shows the strong steric hindrance between sulfur atoms in the *cis* conformation.

The rotational barrier, as calculated by the AM1 method, is about 0.4 kcal mol^{-1} for BT, DD44BT, DMO44BT, and DBO44BT, showing that the equilibrium geometry of these molecules is not much influenced by the substituents in the 4,4' positions. Thus, it was well-justified to interpret changes in the absorption spectra in terms of inductive effects rather than conformational changes. However, the potential energy curves are rather flat, allowing many conformers for these molecules in their ground state. This is in agreement with the relatively large structureless absorption bands observed (see Figure 2). The barrier to rotation of DCABT (0.8 kcal mol^{-1}) is higher than those observed for the other 4,4'-bithiophenes, showing the increase in the π-electron delocalization for this molecule. This should increase the rigidity of this molecule, which is reflected by a sharper absorption band that shows a vibrational progression (see Figure 2).

Figure 4B shows the potential energy curves of 3,3'-substituted bithiophenes. For these molecules, the energy of the planar *cis* conformations ($\phi = 0°$) are very large, showing strong steric interactions between sulfur and alkoxy or alkyl

substituents. Moreover, this energy is much higher for the DD33BT molecule. This indicates that CH_2 groups show much more steric hindrance than oxygen atoms. This is in good agreement with results obtained on poly(3,3'-dialkyl-2,2'-bithiophenes) [29] and poly(3,3'-dialkoxy-2,2'-bithiophenes) [30]. We have observed that the length of the alkyl chains has no effect on the conformational analysis. The AM1 curve of DD33BT is in good agreement with the one reported for the dioctyl analog [24] and with the potential energy curve of the dimethyl analog as obtained by *ab initio* calculations [14]. The planar *trans* conformations (ϕ = 180°) are also destabilized compared to those of the 4,4' analogs. The equilibrium geometry of these molecules is much more twisted (ϕ = 120° for DBO33BT and ϕ = 105° for DMO33BT and DD33BT). The barrier to rotation is higher for the 3,3' derivatives compared to the 4,4' derivatives, which suggests that the molecular frame is more rigid. This is in agreement with the shape of the absorption bands of these systems. Indeed, Table 1 and Figure 3 show that the first absorption bands of DMO33BT and DBO33BT are sharper and more structured compared to the 4,4' analogs. But the vibrational Franck-Condon envelope of the alkoxy compounds shows a (0,0) transition lower in intensity compared to other vibronic transitions, which is a characteristic of nonplanar aromatic skeleton. And since the fluorescence spectrum of DBO33BT is an approximate mirror image of the absorption spectrum, it is suggested that the molecule is also twisted in its first relaxed excited singlet state, as suggested in part 3.1.

3.2.2. ZINDO/S Calculations

For each AM1 optimized geometry, the energies of the ground state (S_0), of the first excited singlet (S_1) and triplet (T_1) states, and of the first electronic transition ($S_1 \leftarrow S_0$) have been calculated using the ZINDO/S semiempirical method. The potential energy surfaces of S_0, S_1 and T_1 of DMO44BT are shown in Figure 5 and are representative of all the molecules investigated. The ground state geometry predicted by ZINDO/S is planar even for the 3,3' derivatives. This clearly indicates

that ZINDO/S underestimates small steric effects and puts more emphasis on the electronic conjugation between thiophene rings. However, the fact that *cis* conformations are destabilized by 1500-5000 cm^{-1} depending on the nature and the position of the substituent compared to *trans* conformations shows that ZINDO/S takes care of important repulsion forces. One can see on Figure 5 that the fully planar *cis* and *trans* conformations are the most stable for the S_1 excited state. It is thus predicted that, after excitation, the molecules should relax to planar S_1 states. This is in agreement with the large Stokes shifts generally found for oligothiophenes (see Table 1) and the observation that fluorescence bands are always sharper than corresponding absorption bands. It has to be pointed out here that just like that for the ground state of the 3,3' derivatives, ZINDO/S failed to predict any distorsion in the S_1 state geometry of the 3,3'-alkoxy derivatives. Figure 5 also shows that the most stable conformations of the T_1 state are planar (ϕ = 0° and 180°). However, contrary to singlet states, potential energy surfaces show local minima when the thiophene rings are in perpendicular arrangement, showing the biradical nature of the first triplet state.

It is well-known that even if ZINDO/S sometimes failed to optimize the ground and excited states geometry perfectly, it is, however, an excellent method to predicting electronic transition energies [17-19, 36, 37]. Then, another way to estimate the ground state geometry of the bithiophenes can be done by correlating the $S_1 \leftarrow S_0$ electronic transition energy (ν) calculated for each AM1 optimized geometry with the first absorption band energy obtained experimentally. Since no vibronic interactions are involved in ZINDO/S calculations, results obtained refer to the 0,0 electronic transition of isolated molecules (vapor phase). The experimental $\nu(0,0)$ of the various molecules have been estimated from the crossing of absorption and fluorescence spectra. To evaluate the $\nu(0,0)$ of the molecules in the vapor phase, the wavenumbers have been plotted as a function of the polarizability function as described elsewhere [17]. The polarizability function is defined by the relation $f(n^2) = 2(n^2-1)/(2n^2+1)$, where n represents the refractive index of the alkane. At n =1, $f(n^2) = 0$ such that the extrapolated curves give the estimated $\nu(0,0)$ values for the

molecules in the gas phase. Figure 6 shows such a plot for the DMO44BT bithiophene derivative. Table 3 reports the best fits between extrapolated and calculated $\nu(0,0)$ values and the corresponding geometry. It is worth noting here that the ZINDO/S method calculates about the same energies for conformations having complementary dihedral angles. Table 3 reports only *trans* conformations. Moreover, ZINDO/S is not parameterized for the chlorine atom such that, in the case of DCABT, Table 3 reports calculations where chlorine atoms are replaced by hydrogen and fluorine atoms. In general, the ground state geometry of these bithiophenes obtained from ZINDO/S are in excellent agreement with those calculated from the AM1 method (see figure 4).

4. Concluding Remarks

This paper shows that electronic spectroscopy coupled with semiempirical calculations can provide valuable information about the conformations adopted by substituted bithiophenes in their ground and excited states. AM1 and ZINDO/S semiempirical calculations coupled with the analysis of absorption spectra predict that 3,3' twisted conformers are more stable when compared to the 4,4' analogs. Fluorescence spectra as well as ZINDO/S calculations suggest that, after excitation, molecules relax to much more planar S_1 excited states. The sole exceptions are 3,3'-alkoxy derivatives which seem to remain in the same conformation in their S_1 relaxed excited states if one correlates the shape of their absorption and fluorescence spectra. ZINDO/S calculations also predict that bithiophene derivatives in their T_1 excited states are characterized by planar as well as perpendicular conformations.

Fluorescence spectra show that 3,3'-alkoxybithiophenes are more rigid than their 4,4' analogs in their relaxed S_1 excited state. However, their fluorescence quantum yields are smaller by 1 order of magnitude compared to those of 4,4'-alkoxy derivatives. We suggest that an enhanced intersystem crossing deactivation process for the 3,3' derivatives might be responsible for this behavior.

Acknowledgment

The authors are grateful to the Natural Sciences and Engineering Research Council of Canada (NSERC) and the Fonds FCAR (Quebec) for their financial support. N.D is grateful to the NSERC for a graduate scholarship. F.R. thanks also NSERC for a B. Sc. scholarship.

References and Notes

[1] Roncali, J. *Chem. Rev.* **1992**, *92*, 711.

[2] Keane, M.P.; Svensson, S.; Naves de Brito, A.; Correia, N.; Lunell, S.; Sjogen, B.; Inganas, O.; Salaneck, R. *J. Chem. Phys.* **1993**, *93*, 6357.

[3] Roux, C.; Leclerc, M. *Macromolecules*, **1992**, 25, 2141.

[4] Robitaille, L.; Leclerc, M. *Macromolecules*, **1994**, *27*, 1847.

[5] Faïd, K.; Fréchette, M.; Ranger, M.; Mazerolle, L.; Lévesque, I.; Leclerc, M. *Chem. Mat.* **1995**, *7*, 1390.

[6] Sandman, D.J. *TRIPS.* **1994**, *2*, 44.

[7] Inganas, O. *TRIPS.* **1994**, *2*, 189.

[8] Roux, C.; Bergeron, J.-Y.; Leclerc, M. *Makromol. Chem.*, **1993**, 194, 869.

[9] Roux, C.; Leclerc, M. *Chem. Mater.* **1994**, *6*, 620.

[10] Roux, C.; Faïd, K.; Leclerc, M. *Polym. News.* **1994**, *19*, 6.

[11] Samdal, S.; Samuelson, E.J.; Volden, H.V. *Synth. Met.* **1993**, *59*, 259.

[12] Quattrocchi, C.; Lazzaroni, R.; Brédas, J.L. *Chem. Phys. Lett.* **1993**, *208*, 120.

[13] Distefano, G.; Dal Colle, M.; Jones, D.; Zambianchi, M.; Favaretto, L.; Modelli, A. *J. Phys. Chem.* **1993**, *97*, 3504.

[14] Hernandez, V.; Navarrete, J.T. *J. Chem. Phys.* **1994**, *101*, 1369.

[15] Orti, E.; Viruela, P.M.; Sanchez-Martin, J.; Tomas, F. *J. Phys. Chem.* **1995**, *99*, 4955.

[16] Alemán, C.; Julia, L. *J. Phys. Chem.* **1996**, *100*, 1524.

[17] Belletête, M.; Leclerc, M.; Durocher, G. *J. Phys. Chem.* **1994**, *98*, 9450.

[18] Belletête, M.; Di Césare, N.; Leclerc, M.; Durocher, G. *Chem. Phys. Lett.* **1996**, *250*, 31.

[19] Belletête, M.; Di Césare, N.; Leclerc, M.; Durocher, G. *J. Mol. Struct. (THEOCHEM)* **1997**, *391*, 85.

[20] Bucci, P.; Longeri, M.; Veracini, C.A.; Lunazzi, L. *J. Am. Chem. Soc.* **1974**, *96*, 1305.

[21] Terbeek, L.C.; Zimmerman, D.S.; Burnell, E.E. *Mol. Phys.* **1991**, *74*, 1027.

[22] Dos Santos, D.A.; Galvão, D.S.; Laks, B.; Dos Santos, M.C. *Chem. Phys. Lett.* **1991**, *184*, 579.

[23] Dos Santos, D.A.; Galvão, D.S.; Laks, B.; Dos Santos, M.C. *Synth. Met.* **1992**, *51*, 203.

[24] Van Hutten, P.F.; Gill, R.E.; Herrema, J.K.; Hadziioannou, G. *J. Phys. Chem.* **1995**, *99*, 3218.

[25] Garcia, P.; Pernaut, J.M.; Hapiot, P.; Wintgens, V.; Valat, P.; Garnier, F.; Delabouglise, D. *J. Phys. Chem.* **1993**, *97*, 513.

[26] Becker, R.S.; Seixas de Melo, J.; Maçanita, A.L.; Elisei, F. *Pure & Appl. Chem.* **1995**, *67*, 9.

[27] Zagorska, M.; Krische, B. *Polymer*, **1990**, *31*, 1379.

[28] Belletête, M.; Mazerolle, L.; Desrosiers, N.; Leclerc, M.; Durocher, G. *Macromolecules*, **1995**, *28*, 8587.

[29] Souto Maior, R.M.; Hinkelmann, K.; Eckert, H.; Wudl, F. *Macromolecules*, **1990**, 23, 1268.

[30] Faïd, K.; Cloutier, R.; Leclerc, M. *Macromolecules*, **1993**, 26, 2501.

[31] Allinger, N.L. *J. Am. Chem. Soc.* **1977**, *99*, 8127.

[32] Dewar, M.J.S.; Zoebisch, E.G.; Healy, E.F.; Stewart, J.J.P. *J. Am. Chem. Soc.* **1985**, *107*, 3902.

[33] Dewar, M.J.S.; Dieter, K. *J. Am. Chem. Soc.* **1986**, *108*, 8075.

[34] Stewart, J.J.P. *J. Comp. Aided Mol. Design*, **1990**, *4*, 1.

[35] Dewar, J.M.S.; Yuan, Y.C. *Inorg. Chem.* **1990**, *29*, 3881.

[36] Ridley, J.; Zerner, M.C. *Theor. Chim. Acta*, **1973**, *32*, 111.

[37] Forber, C.; Zerner, M.C. *J. Am. Chem. Soc.* **1985**, *107*, 5884.

[38] Arbizzani, C.; Barbarella, G.; Bongini, A.; Mastragostino, M.; Zambianchi, M. *Synth. Met.* **1992**, *52*, 329.

[39] Rossi, R.; Ciofalo, M.; Carpita, A.; Ponterini, G. *J. Photochem. Photobiol. A: Chem.* **1993**, *70*, 59.

Table 1

Spectroscopic Parameters of the Bithiophene Derivatives Studied in *n*-Hexane at Room Temperature (298 K)

molecule	λ_A [a] (nm)	ν_A [b] (cm^{-1})	ε ($M^{-1}\,cm^{-1}$)	$Fwhm_A$ [c] (cm^{-1})	λ_F [d] (nm)	ν_F [e] (cm^{-1})	$fwhm_F$ [f] (cm^{-1})	Δ [g] (cm^{-1})
DD44BT	309	32 300	11 000	4700	375	26 700	4000	5500
DMO44BT	316	31 700	10 300	5200	395	25 300	4000	6400
DBO44BT	320	31 300	8 500	5600	393	25 400	4200	5900
DCABT	361	27 700	18 000	5200	422	23 700	3500	4000
DCABT [h]	346	28 900	26 700	4700	413	24 200	3700	4700
DD33BT	280[i]	35 700	4 400	-	374	26 700	5100	9000
DMO33BT	319	31 400	12 900	4300	-	-	-	-
DBO33BT	317	31 500	15 000	4400	370	27 000	4000	4500

[a] Absorption wavelengths taken at the center of mass of the absorption band.

[b] Absorption wavenumbers taken at the center of mass of the absorption band.

[c] Full width at half-maximum (fwhm) of the absorption band.

[d] Fluorescence wavelengths taken at the center of mass of the fluorescence band.

[e] Fluorescence wavenumbers taken at the center of mass of the fluorescence band.

[f] Full width at half-maximum (fwhm) of the fluorescence band.

[g] Stokes shift between absorption (ν_A) and fluorescence (ν_F) bands.

[h] Measure taken in methanol.

[i] Measure evaluated at the shoulder.

Table 2

Fluorescence Quantum Yields (x 10^3) of the Bithiophene Derivatives in *n*-Hexane, *n*-Hexadecane, Methanol and *n*-Hexanol at Room Temperature (298K).

solvent	DD44BT	DMO44BT	DBO44BT	DCABT	DD33BT	DMO33BT	DBO33BT
n-hexane	17	18	22	77	0.77	2.9	3.9
n-hexadecane	19	27	30	73	-	6.2	6.3
methanol	15	27	25	94	0.72	1.8	1.7
n-hexanol	18	27	32	168	1.4	5.7	3.3

Table 3

Dihedral Angle Giving the Best Correlation between $\nu_A(0,0)$ Extrapolated at n=1 and ZINDO/S Calculations (E ($S_1 \leftarrow S_0$)) for Bithiophene Derivatives.

molecule	$\nu_A^{(0,0)}$ (cm^{-1})	$\nu_{S0\rightarrow S1}$ (cm^{-1})	ϕ
DD44BT	30 800	30 400	150
DMO44BT	30 400	30 095	150
DBO44BT	30 000	30 070	150
DCABT	27 800	274 00[a]	135
		276 40[b]	135
DD33BT	35 700[c]	36 400	90
		34 900	105
DMO33BT	31 400[c]	31 300	120
DBO33BT	31 300	31 670	120

[a] Value obtained using an hydrogen atom as a replacement for the chlorine atom.

[b] Value obtained using a fluorine atom as a replacement for the chlorine atom.

[c] Value taken at the maximum of absorption.

Figure 1: Molecular structures of the substituted bithiophenes investigated.

Figure 2: Absorption (—) and fluorescence (---) spectra of 4,4'-substituted molecules in *n*-hexane.

Figure 3: Absorption (—) and fluorescence (---) spectra of 3,3'-substituted molecules in *n*-hexane.

Figure 4: Potential energy curves for the ground state of 4,4'-substituted molecule (A) and of the 3,3'-substituted molecule (B) obtained by the AM1 semiempirical method.

Figure 5: Variation of S_0 (—), S_1 (·····) and T_1 (— — —) state energies of DMO44BT as a function of the dihedral angle between the two thiophene rings.

Figure 6: Plot of the 0,0 absorption wavenumber as a function of the polarizability function $f(n^2)$ of the nonpolar solvents for DMO44BT.

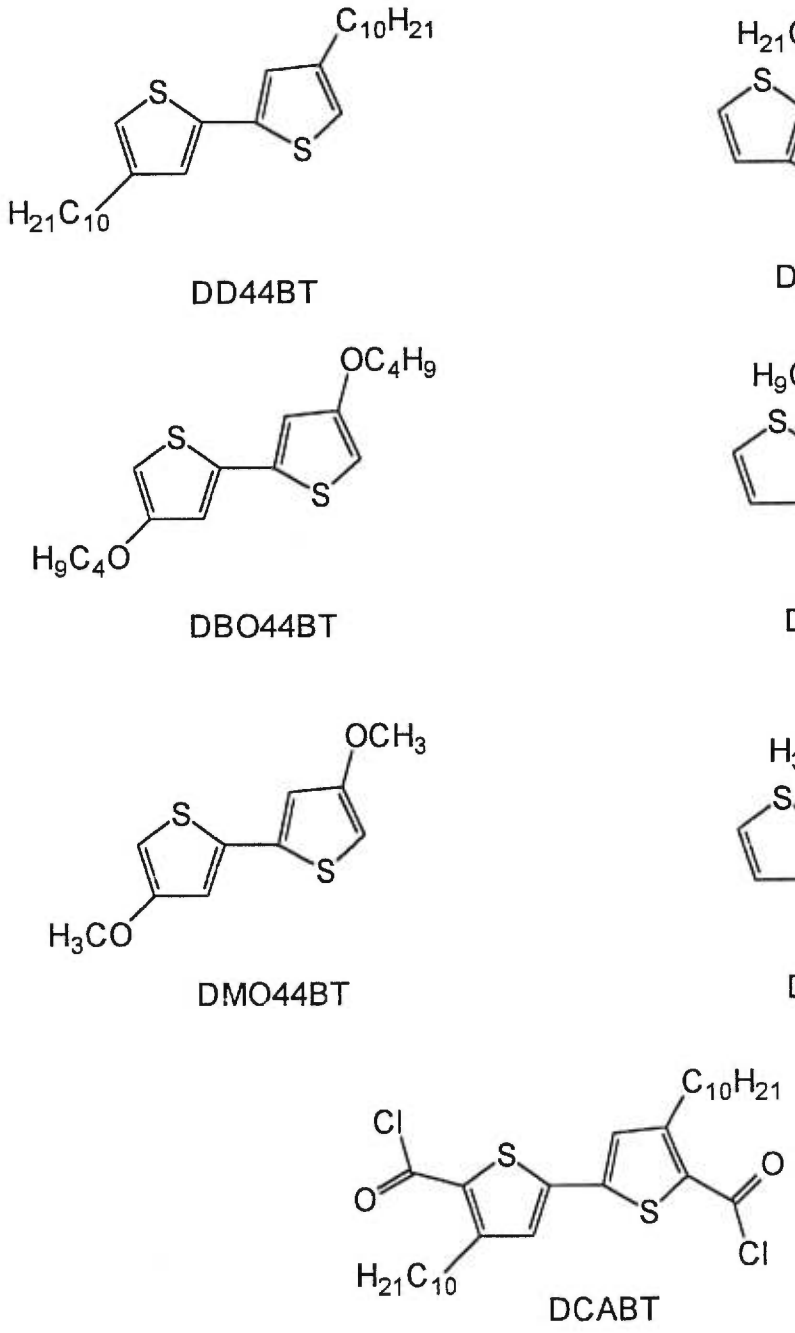

Figure 1: Molecular structures of the substituted bithiophenes investigated.

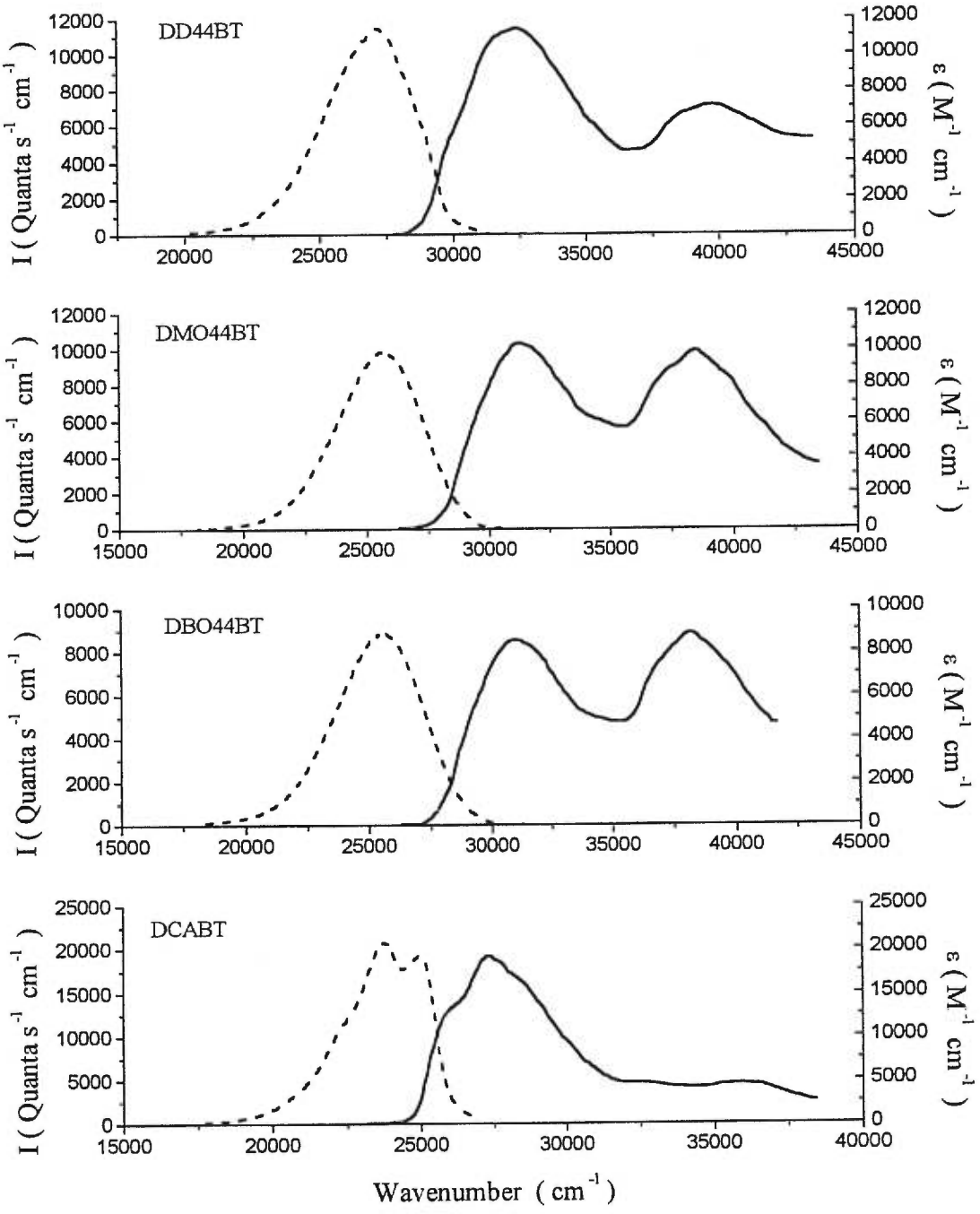

Figure 2: Absorption (—) and fluorescence (---) spectra of 4,4'-substituted molecules in *n*-hexane.

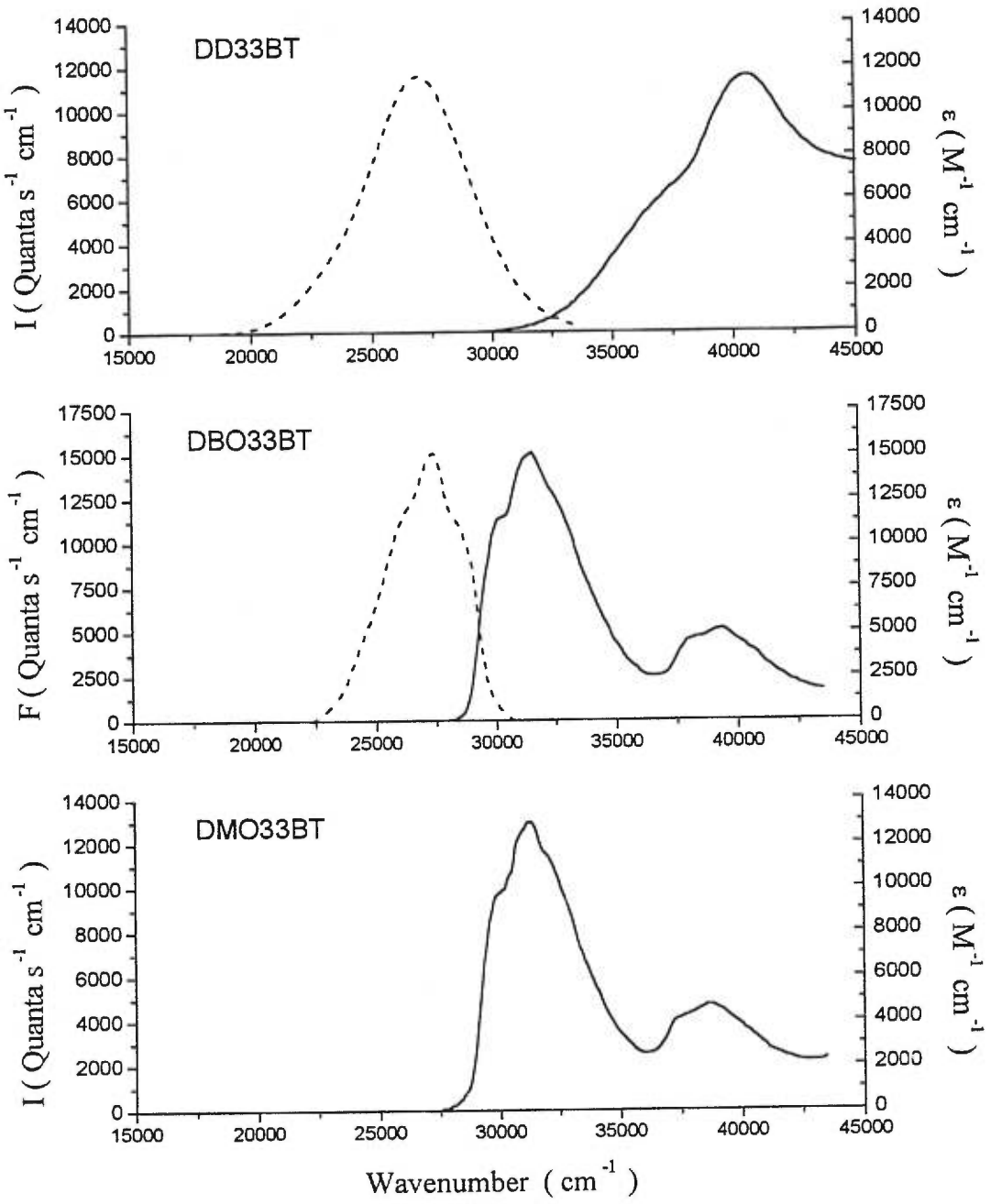

Figure 3: Absorption (—) and fluorescence (---) spectra of 3,3'-substituted molecules in *n*-hexane.

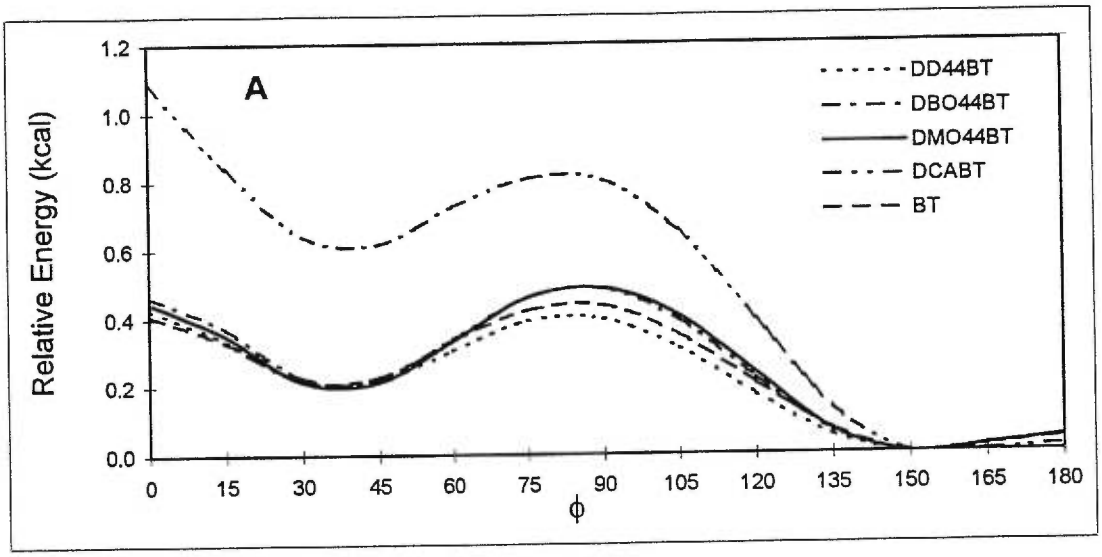

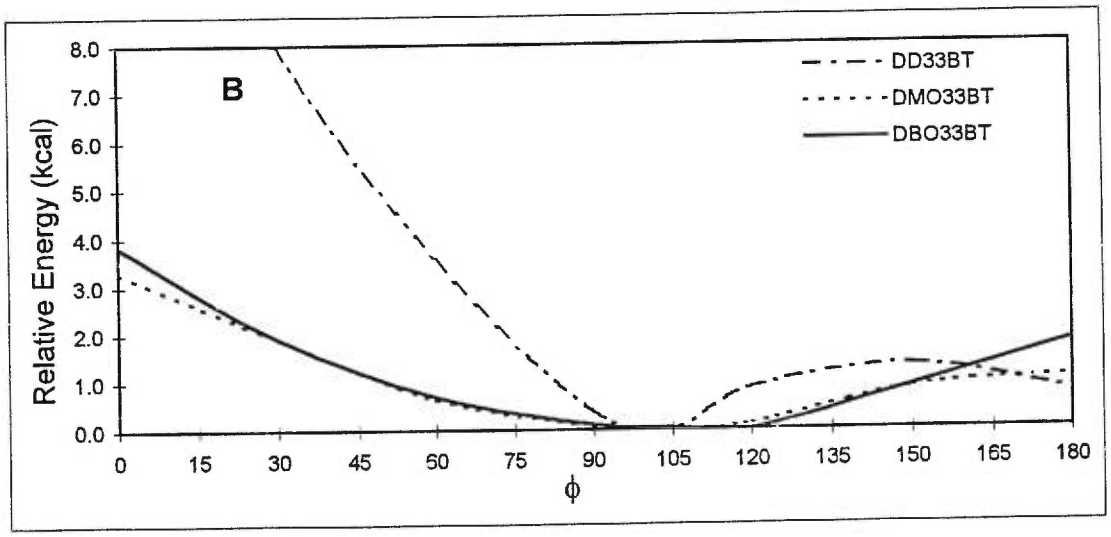

Figure 4: Potential energy curves for the ground state of 4,4'-substituted molecule (A) and of the 3,3'-substituted molecule (B) obtained by the AM1 semiempirical method.

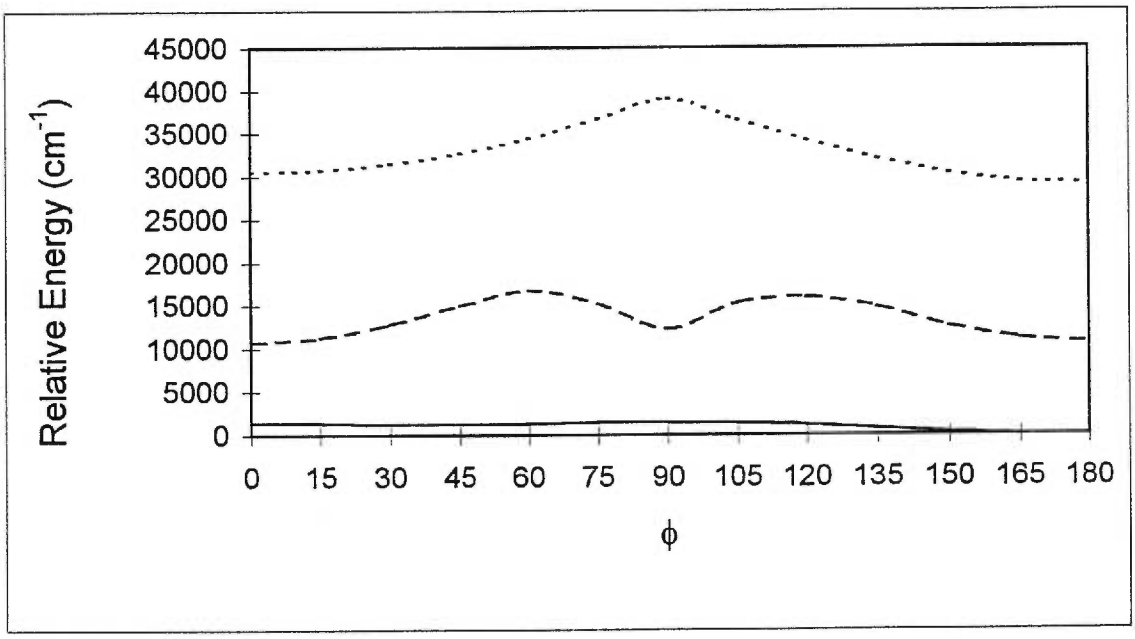

Figure 5: Variation of S_0 (—), S_1 (·····) and T_1 (— — —) state energies of DMO44BT as a function of the dihedral angle between the two thiophene rings.

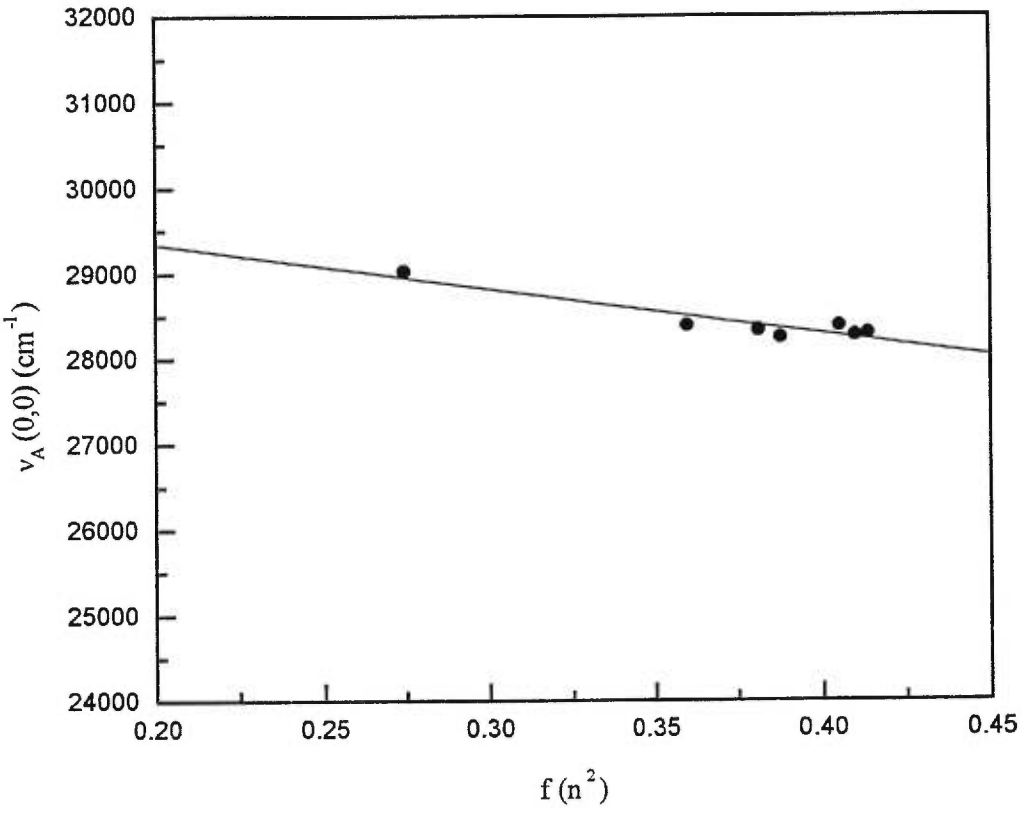

Figure 6: Plot of the 0,0 absorption wavenumber as a function of the polarizability function f(n^2) of the nonpolar solvents for DMO44BT.

Chapitre 2

Étude structurale et conformationelle de dérivés alkyls du 2,2'-bithiophène

Avec ce chapitre commence l'analyse conformationnelle des dimères utilisant les méthodes de calculs théoriques *ab initio* et semi-empiriques. Les trois prochains chapitres porteront sur l'obtention des conformations minimales, des barrières de rotation et des structures géométriques des dérivés alkyls, alkoxys et alkylthios, respectivement.

Dans ce chapitre, nous discuterons de l'importance de l'encombrement stérique créé par les groupes alkyls en position 3,3' et 3',4. Nous verrons que l'insertion de tels groupes induit une torsion importante entre les cycles thiophènes comparativement au BT. Conjointement, les barrières rotationnelles pour les formes planes sont également plus importantes. Ces résultats théoriques sont en accord avec les données expérimentales décrites dans le précédent chapitre. Le dérivé alkyl en position 4,4' n'a pas été considéré dans ce chapitre parce qu'il est bien connu qu'à ces positions les substituants alkyls n'ont aucun effet sur la conformation du dimère comme vu au chapitre 1 et comme nous allons le voir dans le prochain chapitre avec les dérivés alkoxys.

Les résultats des calculs *ab initio* (HF/3-21G*) sont également comparés aux résultats obtenus avec les méthodes semi-empiriques (AM1 et PM3). Nous verrons que, pour ces dérivés alkyls, les calculs semi-empiriques sont satisfaisants pour l'obtention des conformations minimales mais ils sous-estiment les barrières rotationnelles. La validité des calculs semi-empiriques obtenue pour ces dérivés

alkyls est due principalement à la nature même des substituants. La contribution électronique, comparativement à la contribution stérique, est faible dans le cas des substituants alkyls ce qui rend valide l'utilisation des calculs semi-empiriques. Par contre, la faiblesse des barrières de rotation obtenues démontre le peu d'importance qu'accordent les calculs AM1 et PM3 à la délocalisation électronique du dimère considéré.

2.1 Article 2 : A conformational study of ethyl-substituted bithiophenes. Semi-empirical *versus ab initio* methods.

Article publié dans Synthetic Metals, volume 94, pages 291-298 (1998).

A Conformational Study of Ethyl-Substituted Bithiophenes. Semi-Empirical Versus Ab Initio Methods

Nicolas Di Césare [a], Michel Belletête [a], Mario Leclerc [b] and Gilles Durocher [a]

[a] Laboratoire de Photophysique Moléculaire

[b] Laboratoire des Polymères Électroactifs et Photoactifs

Département de Chimie, Université de Montréal

C.P. 6128, Succ. A, Montréal, Québec, H3C 3J7, Canada

Abstract

Semi-empirical (AM1, PM3) and *ab initio* calculations (STO-3G, 3-21G*) are employed to obtain the equilibrium optimized geometries and the torsional potential surfaces of 2,2'-bithiophene as well as its 3,4'- and 3,3'-ethyl-substituted derivatives. For the unsubstituted molecule , *ab initio* calculations have also been performed at the HF/6-31G* level. The geometries were completely optimized along the torsional potential curves to account for the molecular relaxation, yielding a physically meaningful picture of the nonrigid rotation. The results given by each theoretical method are compared and discussed. It is found that ethyl substitution causes rather small changes in the thiophene ring structure. Contrary to these results, ethylation dramatically influences the overall shape of the torsional potentials, leading to a large tilt from planarity. The barrier against planarity is found much higher for the 3,3'-ethyl derivative. It is also observed that the steric hindrance created by ethyl groups is much higher than that induced by methyl substituents.

1. Introduction

Polythiophenes are among the most studied polymeric materials because of their good chemical stability and high electrical conductivity in the oxidized (doped) state [1]. However, characterization and processing of these conjugated polymers have been limited by their inherent insolubility and infusibility. This problem of processability has been solved by the incorporation of relatively long and flexible side chains onto the polymer backbone. The development of these new substituted polythiophenes has led to the discovery of interesting optical phenomena which are not observed in the unsubstituted parent polymers. For instance, intriguing thermochromic properties (both in the solid state and in solution) have been found in several substituted polythiophenes. [2-9]. These observations have been interpreted in terms of a reversible loss of conjugation due to out-of-plane twisting of thiophene rings. It is believed that the torsion energies around thiophene-thiophene bonds are affected by the nature and the position of the lateral groups, since they may lead to both steric hindrance and electronic delocalization. We have recently shown that the occurrence of thermochromism in polythiophenes can be related to the values of the rotational energy barrier of dimer models which are building blocks of the macromolecules [10].

Geometry optimizations have been reported mainly for 2,2'-bithiophene (BT) [11-21] and its methyl-substituted derivatives [22-25]. In this work, the equilibrium conformations and torsional potentials of BT, 3,4'-diethyl-2,2'-bithiophene (DE34BT) and 3,3'-diethyl-2,2'-bithiophene (DE33BT) are investigated theoretically using semi-empirical (AM1, PM3) and *ab initio* (STO-3G, 3-21G*) methods. These molecules should act as better models than methyl-substituted oligomers for poly(alkylthiophene)s. Much emphasis is put on the conformational particularities of each theoretical method used. The molecules investigated are shown in Fig. 1.

2. Methodology

2.1. Semi-empirical calculations

It is well known that the MNDO (modified neglect of differential overlap) semi-empirical method [26,27] is not able to reproduce dihedral angles in conjugated systems. AM1 (Austin model 1) is an improved version of MNDO which has been developed to correct some of its weaknesses [28-31]. PM3 (parametric method 3) is a re-parameterization of AM1 which differs only in the values of the parameters [32]. The parameters for PM3 were derived by comparing a much larger number and wider variety of experimental versus computed molecular properties. Typically, nonbonded interactions are less repulsive in PM3 than in AM1.

AM1 and PM3 calculations including the sulfur atom parameter sets were performed using the HYPERCHEM package, release 4.5 for Windows from Hypercube, Inc., on a Pentium computer with an internal memory of 32 Mbytes. A r.m.s. gradient in the energy of 0.1 kcal mol^{-1} was use for the optimization criterion. The conformational analysis was done by changing the torsional angle θ by 15° steps between $\theta = 0°$ (planar *syn* conformation) and $\theta = 180°$ (planar *anti* conformation). For each conformer, the dihedral angle was held fixed while the remainder of the molecule was optimized (the rigid-rotor approximation was not applied). The energy differences are always relative to the corresponding absolute minimum conformation. Potential energy surfaces have been drawn using a spline fitting.

2.2. *Ab initio* calculations

The *ab initio* calculations were performed on a Silicon Graphics Challenge R4000 work station at the University of Montreal using the Gaussian 90 program [33]. STO-3G and 3-21G* basis sets were used for the calculations. The 6-31G* basis set has also been used for BT. The Berny analytical gradient method was used for the optimizations. For BT, a C_{2h} symmetry restriction was applied for the planar

anti conformation and a C_{2v} symmetry restriction was applied for the planar *syn* conformer. A locally C_2 symmetry restriction between the two rings was applied for nonplanar BT conformers and DE33BT but no constraint was applied to the side groups. For DE34BT, no symmetry restriction was applied. The requested HF convergence on the density matrix was 10^{-8} and the threshold values for the maximum force and the maximum displacement were 0.00045 and 0.0018 a.u., respectively. To obtain the final torsional angles of the most stable conformers, calculations of these geometries were performed without constraint on the dihedral angle. *Ab initio* calculations were done at each 30° due to the longer time of the calculations. The geometries were completely optimized at each value of the dihedral angle *i.e.* the rigid-rotor approximation was not used.

3. Results and Discussion

3.1. Geometry optimizations

The structural parameters of the optimized equilibrium geometries of BT, DE34BT and DE33BT as obtained by the various theoretical methods investigated are compiled in Tables 1-3, respectively. Table 1 also reports bond lengths and bond angles of BT in the vapor phase as obtained by the electron diffraction technique [16]. The atomic numbering is indicated in Fig. 1.

Table 1 shows that the agreement between experimental and theoretical data is good and rather similar for each theoretical method . Indeed the standard deviation varies between 0.018 and 0.025 Å for bond lengths and between 0.7 and 1.3° for bond angles depending on the theoretical method used. Surprisingly the PM3 semi-empirical method gives the best overall agreement with electronic diffraction data. Thus, we can conclude that, except for the dihedral angle (see Section 3.2), semi-empirical calculations are good enough to obtain the accurate structure of BT. The same behavior has been found for methoxy-substituted bithiophenes [34].

One can see from Tables 1-3 that the incorporation of an ethyl group in 3 and/or 3' position(s) induces only small changes in the structural parameters of BT which are consistent for each theoretical method. For example, C2-C2', S1-C2 and C3-C4 bond distances are stretched, whereas the C4-C5 bond length is shortened upon ethylation. Moreover C2'-C2-C3, S1-C2-C3 and C3-C4-C5 bond angles increase, while the C2-C3-C4 bond angle decreases in the presence of ethyl groups. The small geometrical perturbation contributes to relieve some of the steric hindrance created by ethyl groups. It is worth mentioning that all the theoretical methods employed show that, as the torsion between thiophene rings increases, the C2-C2' bond length also increases. This is in agreement with a reduction of the electronic delocalization along the molecular frame for hindered molecules. However, this correlation is much stronger using the *ab initio* methods as shown in Table 1-3.

3.2. Conformational analysis

We illustrate in Fig. 2 the torsion potential surfaces of BT, as calculated with the various theoretical methods. *Ab initio* calculations performed at the HF/6-31G* level show the existence of two-well defined potential wells separated by a relatively small energy barrier (1.69 kcal mol^{-1}). These results suggesting the coexistence of *syn* and *anti* conformers are in good agreement with *ab initio* calculations performed at the same level of theory (or with more sophisticated basis sets) [17,18,21,24] and with the experimental studies on the isolated BT molecules [16,35,36] and in solution [37]. However, according to *ab initio* calculations performed on BT [21] and biisothiathianaphthene [38], the rotational energy barrier calculated at the HF/6-31G* level is overestimated compared to that obtained at the MP2 (Moller Plesset Method) level. The absolute energy minimum corresponds to the *anti* conformation with a dihedral angle θ = 147.3°. This equilibrium geometry arises from a compromise between the electronic conjugation between thiophene rings and steric repulsions occuring between sulfur and hydrogen atoms. But the energy barrier

against planarity is so small (0.37 kcal mol^{-1}) that, in the solid state, packing effects lead to a coplanar conformation (θ = 180°) [39-41]. The *syn*-like conformer is located at 45° and is less stable than the global minimum by 0.68 kcal mol^{-1}. It is interesting to note that the planar *syn*-conformer is more energetic than the perpendicular conformation. Although the planar *syn* conformer possesses high π conjugation, the steric interactions between sulfur atoms are strong enough to destabilize the system by about 1.9 and 1.2 kcal mol^{-1} relative to the optimal *anti* and *syn* conformers, respectively. From Fig. 2, one can see that HF/3-21G* and HF/6-31G* potential energy surfaces are very similar. Indeed the minimum energy twist angles are calculated at identical values and the rotational barriers are close enough. The 3-21G* calculations shown here are in very good agreement with those reported by Hernandez and Lopez Navarrete [19]. Moreover, these authors found that 3-21G* and 6-31G** *ab initio* calculations performed on BT as well as on 3,4'- and 3,3-methyl-substituted bithiophenes are in excellent agreement with each other. On the other hand, the use of the 3-21G basis set gives a rotational energy barrier which is largely overestimated and a gobal minimum for a planar *anti* conformation [24]. It was found that this basis set overestimates the conjugative interactions and to a smaller extent the nonbonded interactions [24]. A similar behavior has been observed from the STO-3G potential energy surface (see Fig. 2). Thus, as expected, *ab initio* calculations performed with the minimal basis set are not able to represent the conformational preferences of BT and overestimate the rotational energy barrier in agreement with STO-3G calculations reported elsewhere [12-14].

Surprisingly, the overall shape of the torsional potential curve obtained from AM1 calculations is much more similar of that obtained with HF/3-21G* than that obtained at the HF/STO-3G level. Indeed, the minima (30, 150°) and maxima (0, 90, 180°) are calculated at similar torsional angles to those obtained from HF/6-31G* or HF/3-21G* *ab initio* methods. But the calculated energies are very underestimated by using AM1 as observed before [20,24,42-44]. For instance, the AM1 barrier to rotation is only 0.44 kcal mol^{-1}. On the other hand, the use of PM3 calculations leads to an erroneous rotational profile. Indeed the PM3 method also gives two minima at

similar angles, but the relative positions are inverted, with the *syn*-like conformation more stable by 0.52 kcal mol^{-1} in agreement with similar calculations reported in the literature [25,44]. Comparison between the different methods leads us to consider the 3-21G* basis set as the minimum level necessary to study the conformational preferences of the substituted bithiophenes investigated in this work and elsewhere [34,45]. Energies and torsional angles of the minima and maxima of BT, DE34BT and DE33BT as obtained by the 3-21G* basis set are compiled in Table 4.

The torsional potential surfaces of DE34BT are displayed in Fig. 3. One can see that 3-21G* calculations predict two minima at twisted angles of 60.0 and 108.1° separated by a very small energy barrier (0.1 kcal mol^{-1}). Thus, the presence of an ethyl group in position 3 creates repulsive steric interactions which twist the molecule. But the energy barrier at $\theta = 180°$ is relatively small (2.2 kcal mol^{-1}) such that planar *anti* conformation is probably allowed in the solid state. In agreement with this assumption, X-ray diffraction measurements have revealed co-planar (or nearly co-planar) structures for poly(3-alkylthiophene)s in the solid state, at room temperature [46-48]. Thus interchain (or intrachain, through chain folding) interactions can be large enough to compensate the energy barrier against planarity for these polymers. Fig. 3 also shows that the fully planar *syn* conformation is more destabilized than the planar *anti* structure, indicating that the combined sulfur-sulfur and ethyl-hydrogen steric effects are more important than the combined ethyl-sulfur and sulfur-hydrogen repulsive interactions. 3-21G* calculations have also been performed for torsional angles ranging from θ =180 to $\theta = 360°$ since a small molecular asymmetry does exist in the molecule. A nearly mirror-image symmetry centered at $\theta = 180°$ is observed (figure not shown). The 3-21G* potential energy surface of DE34BT differs from that of DM34BT calculated at the same level of theory [19]. For DM34BT, only one minimum is observed for the nearly orthogonal conformation ($\theta = 108.6°$) but no energy calculation has been performed at $\theta = 60°$. Moreover the rotational barrier against planarity (*anti*-structure) is smaller for DM34BT (about 0.8 kcal mol^{-1}) than for DE34BT (2.2 kcal mol^{-1}). This strongly suggests that an ethyl group creates more steric hindrance than a methyl substituent.

At the HF/STO-3G level, the most stable conformation is predicted as less twisted (θ = 150°). A local minimum is found at around 50° which is destabilized by 1.15 kcal mol^{-1} compared to the global minimum. Moreover, the planar conformational energies are very underestimated compared to that found at the 3-21G* level. Two minima (θ = 45 and θ = 135°) are also obtained from AM1 calculations with the *syn*-like conformer as the most stable. The energy barrier between these two minima (0.43 kcal mol^{-1}) is higher than that observed from *ab initio* calculations performed at the HF/3-21G* level (0.1 kcal mol^{-1}). The AM1 results reported here are quite different to those reported by dos Santos and Bohland-Filho [44] where the planar *anti* conformer of DE34BT is predicted as the most stable. The reason for this discrepency may be the possible use of the rigid-rotor approximation in their calculations. PM3 calculations also predict a *syn* conformer (θ = 50°) as the most stable but no local minimum is displayed in the *anti* portion of the curve. These results reproduce PM3 calculations reported in [44].

The above theoretical results are in good agreement with the spectroscopic evidence that the first absorption band of 3-octyl-2,2'-bithiophene in *n*-hexane (λ_A = 293 nm) is blue-shifted by 8 nm compared to that of BT (λ_A = 301 nm) [49]. This is caused by a decrease in the electronic conjugation arising from a more tilted angle between thiophene rings. This behavior has been well supplemented using ZINDO/S calculations [20,49,50].

From Fig. 4, one can see that the structure of DE33BT predicted by 3-21G* calculations is very twisted (θ = 101.5°) with a barrier against planarity (at θ = 180°) of 7.6 kcal mol^{-1} compared to 2.2 kcal mol^{-1} found for DE34BT. This clearly shows that the addition of a second ethyl group in the 3' position largely increases the steric hindrance. Along the same line, it is worth noting that, contrary to poly(3-alkyl-thiophene)s, interchain interactions are not sufficient to allow a co-planar conformation for poly(3,3'-dialkyl-2,2'-bithiophene)s [5,51]. The same behavior has been found for 3-21G* [19] an 6-31G* [24] *ab initio* calculations performed on DM33BT. But the rotational barrier at 180° is much lower for DM33BT (4.2 kcal

mol^{-1} at the HF/3-21G* level) than for DE33BT (7.6 kcal mol^{-1}) confirming the assumption mentioned above that an ethyl group induces stronger steric effects than a methyl substituent.

The same profile is observed when STO-3G calculations are performed on DE33BT but the whole curve is less energetic than the 3-21G* energy profile and the dihedral angle of the most stable conformer is shifted to 115°. AM1 calculations predict two minima located at 135° and 60° which are almost isoenergetic (ΔE = 0.029 kcal mol^{-1}) with a small rotational barrier (0.25 kcal mol^{-1}). As in the case of DE34BT, our AM1 calculations do not agree with those published by dos Santos and Bohland-Filho [44] which predict the global minimum at θ = 180°. PM3 and 3-21G* potential energy surfaces are quite similar in the *anti* section of the curves. But the *syn* conformers are less energetic than those calculated using the 3-21G* basis set as observed elsewhere [44].

According to the above results, DE33BT should be very twisted. This assumption agrees well with spectroscopic data showing that the first absorption band of 3,3'-dioctyl-2,2'-bithiophene [49] and 3,3'-didecyl-2,2'-bithiophene [50] in *n*-hexane are blue-shifted by about 20 nm and are much more reduced in intensity compared to that observed for BT. Indeed, as predicted from ZINDO/S calculations [20,49,50], the singlet-singlet electronic energy increases and the oscillator strength decreases as the torsional angle between thiophene rings becomes more tilted. Another spectroscopic evidence in favor of the theoretical results reported above is the fact that the Stokes shift between absorption and fluorescence spectra of DD33BT in solution is very large (about 9000 cm^{-1}) compared to that of the 4,4'-didecyl derivative (about 5500 cm^{-1}) [50]. This indicates that large conformational changes occur during the relaxation of the Franck-Condon excited state. According to semi-empirical [50] and *ab initio* calculations [52] and following spectroscopic data [50], BT derivatives adopt a planar conformation in the first relaxed singlet excited state. Thus, the large Stokes shift observed strongly suggests that DD33BT is twisted in the ground state. Since the length of the alkyl chain should not have

significant effects on this behavior. DE33BT is expected to give the same type of results.

4. Concluding remarks

We have presented semi-empirical and *ab initio* calculations for the investigation of equilibrium structures and torsional potential curves of 2,2'-bithiophene (BT), 3,4'-diethyl-2,2'-bithiophene (DE34BT) and 3,3'-diethyl-2,2'-bithiophene (DE33BT). The overall agreement between theoretical and experimental structural parameters of BT is about the same for each theoretical method investigated. This suggests that semi-empirical methods are sufficiently accurate to provide reliable bond distances and angles of oligothiophenes.

Potential energy surfaces compiled for BT at HF/6-31G* and HF/3-21G* levels are very similar. From these calculations, a nonplanar *anti* conformer is predicted as the more stable but the energy barrier against planarity is rather small (0.39 kcal mol^{-1}). Another local minimum is located at aroud 45° in agreement with experimental data. On the other hand, STO-3G calculations predict the BT molecule as planar with an *anti* configuration. No other local minimum is detected by this method. These results show that a minimal basis set is not large enough to calculate small details in the torsional potential surface of this type of molecule. Surprisingly the AM1 potential energy surface qualitatively agrees with that obtained at the HF/3-21G* level but the energies are largely underestimated. Finally, a *syn*-like conformer is predicted as the minimal energy structure from PM3 calculations.

The incorporation of ethyl groups causes rather small changes in the thiophene ring structure. These small variations in the structural parameters are consistent within each theoretical method investigated. On the other hand, the shape of the torsional potential curves changes dramatically with the presence of ethyl groups. Each theoretical method clearly shows that ethyl-substituted oligomers are very twisted. It is found that the barrier against planarity is much higher for the 3,3'-ethyl-substituted derivative in agreement with the nonplanar conformation of the

parent polymer in the solid state. It is also observed that ethyl groups create more steric hindrance than methyl groups. Thus, the former compounds should be more adequate as models in the conformational analysis of poly(alkylthiophene)s.

Acknowledgments

The authors are grateful to the Natural Sciences and Engineering Research Council of Canada (NSERC) and the "Fonds FCAR" (Québec) for their financial support. N.D.C. is grateful to the NSERC for a graduate scholarship.

References

[1] P. Garcia, J.M. Pernaut, P. Hapiot, V. Wintgens, P. Valat, F. Garnier and D. Delabouglisse, *J. Phys. Chem.*, 97 (1993) 513.

[2] S.D.D.V. Rughooputh, S. Hotta, A.J. Heeger and F. Wudl, *J. Polym. Sci., Polym. Phys. Ed.*, 25 (1987) 1071.

[3] O. Inganas, W.R. Salaneck, J.E.Osterholm and J. Laakso, *Synth. Met.*, 22 (1988) 395.

[4] C. Roux and M. Leclerc, *Macromolecules*, 25 (1992) 2141.

[5] C. Roux, J.-Y. Bergeron and M. Leclerc, *Makromol. Chem.*, 194 (1993) 869.

[6] C. Roux and M. Leclerc, *Chem. Mater.*, 6 (1994) 620.

[7] K. Faïd, M. Fréchette, M. Ranger, L. Mazerolle, I. Lévesque, M. Leclerc, T.-A. Chen and R.D. Rieke, *Chem. Mater.*, 7 (1995) 1390.

[8] R. Hanna and M. Leclerc, *Chem. Mater.*, 8 (1996) 1512.

[9] M. Leclerc, M. Fréchette, J.-Y. Bergeron, M. Ranger, I. Lévesque and K. Faïd, *Macromol. Chem. Phys.*, 197 (1996) 2077.

[10] N. Di Césare, M. Belletête, G. Durocher and M. Leclerc, *Chem. Phys. Lett.*, 275 (1997) 533.

[11] J.L. Brédas, B. Thémans, G. Fripiat, J.M. André and R.R. Chance, *Phys. Rev. B*, 29 (1984) 6761

[12] J.L. Brédas, B. Thémans, J.M. André, A.J. Heeger and F. Wudl, *Synth. Met.*, 11 (1985) 343.

[13] J.L. Brédas, G.B. Street, B. Thémans and J.M. André, *J. Chem. Phys.*, 83 (1985) 1323.

[14] D. Jones, M. Guerra, L. Favoretto, A. Modelli, M. Fabrizio and G. Distefano, *J. Phys. Chem.*, 94 (1990) 5761.

[15] M. Kofranek, T. Kovár, H. Lischka and A. Karpfen, *J. Mol. Struct. (THEOCHEM)*, 259 (1992) 181.

[16] S. Samdal, E.J. Samuelsen and H.V. Volden, *Synth. Met.*, 59 (1993) 259.

[17] C. Quattrocchi, R. Lazzaroni and J.L. Brédas, *Chem. Phys. Lett.*, 208 (1993) 120.

[18] G. Distefano, M. Dal Colle, M. Zambianchi, L. Favaretto and A. Modelli, *J. Phys. Chem.*, 97 (1993) 3504.

[19] V. Hernandez and J.T Lopez Navarrete, *J. Chem. Phys.*, 101 (1994) 1369.

[20] M. Belletête, M. Leclerc and G. Durocher, *J. Phys. Chem.*, 98 (1994) 9450.

[21] E. Orti; P.M. Viruela, J. Sanchez-Marin and F. Tomas, *J. Phys. Chem.*, 99 (1995) 4955.

[22] M. Belletête, N. Di Césare, M. Leclerc and G Durocher, *Chem. Phys. Lett.*, 250 (1996) 31.

[23] V. Hernandez and J.T Lopez Navarrete, *Synth. Met.*, 76 (1996) 221.

[24] C. Alemán and L. Julia, *J. Phys. Chem.*, 100 (1996) 1524.

[25] M. Belletête, N. Di Césare, M. Leclerc and G. Durocher, *J. Mol. Struct. (THEOCHEM)* 391 (1997) 85.

[26] M.J.S. Dewar and M.L. McKee, *J. Am. Chem. Soc.*, 99 (1977) 5231.

[27] L.P. Davis, R.M. Guidry, J.R. Williams, M.J.S. Dewar and H.S. Rzepa, *J. Comp. Chem.*, 2 (1981) 433.

[28] M.J.S. Dewar, E.G. Zoebisch, E.F. Healy and J.J.P Stewart, *J. Am. Chem. Soc.*, 107 (1985) 3902.

[29] M.J.S. Dewar and K. Dieter, *J. Am. Chem. Soc.*, 108 (1986) 8075.

[30] J.J.P. Stewart, *J. Comp. Aided Mol. Design*, 4 (1990) 1.

[31] J.M.S Dewar and Y.C. Yuan, *Inorg. Chem.*, 29 (1990) 3881.

[32] J.J.P. Stewart, *J. Comput. Chem.*, 10 (1989) 209; 10 (1989) 221.

[33] M.J. Frisch, M. Head-Gordon, G.W. Trucks, J.B. Foresman, H.B. Schlegel, K. Raghavachari, M. Robb, J.S. Bimkley, C. Gonzales, D.J. Defrees, D.J. Fox, R.A. Whiteside, R. Seeger, C.F. Melius, J. Baker, R.L. Martin, L.R. Kahn, J.J.P.Stewart, S. Topiol and J.A. Pople, *Gaussian 90, Revision F ; Gaussian : Pittsburgh, PA*, (1990).

[34] N. Di Césare, M. Belletête and G. Durocher; *J.Mol. Struct. (TheoChem)*, in press.

[35] J.E. Chadwick and B.E. Kohler, *J. Photochem.*, 98 (1994) 3631.

[36] M. Takayanagi, T. Gejo and I. Hanazaki, *J. Phys. Chem.*, 98 (1994) 12893.

[37] P. Bucci, M. Longeri, C.A. Veracini, and L. Lunazzi, *J. Am. Chem. Soc.*, 96 (1974) 1305.

[38] P. M. Viruela, R. Viruela, E. Orti and J.-L. Brédas, *J. Am. Chem. Soc.*, 119 (1997) 1360.

[39] G.J. Visser, G.J. Heeris, J. Wolters and A. Vos, *Acta Cryst.B.*, 24 (1968) 467.

[40] P.A. Chaloner, S.R. Gutatunga and P.B. Hitchcock, *Acta Cryst.*, C50 (1994) 1941.

[41] M. Pelletier and F. Brisse, *Acta Cryst.*, C50 (1994) 1942.

[42] D.A. dos Santos, D.S. Galvao, B. Laks and M.C. dos Santos, *Chem. Phys. Lett.*, 51 (1992) 203.

[43] D.A. dos Santos, D.S. Galvao, B. Laks and M.C. dos Santos, *Synth. Met.*, 51 (1992) 203.

[44] M.C. Dos Santos and J Bohland- Filho,. *SPIE*, 2528, (1995) 143.

[45] N. Di Césare, M. Belletête, F. Raymond, M. Leclerc and G. Durocher, *J. Chem. Phys.*, 102 (1998) 2700.

[46] A. Bolognesi, M. Catellani, S. Destri and W. Porzio, *Makromol. Chem., Rapid Commun.*, 12 (1991) 9.

[47] T.J. Prosa, M.J. Winokur, J. Moulton, P. Smith and A.J. Heeger, *Macromolecules*, 25 (1992) 4364.

[48] J. Mardalen, E.J. Samuelsen, O.R. Gautun and P.H. Carlsen, *Synth. Met.*, 48 (1992) 363.

[49] P.F. van Hutten, R.E. Gill, J.K. Herrema, and G. Hadziioannou, *J. Phys. Chem.*, 99 (1995) 3218.

[50] N. Di Césare, M. Belletête, F. Raymond, M. Leclerc and G. Durocher, *J. Phys. Chem.*, 101 (1997) 776.

[51] J. Mardalen, H.J. Fell, E.J. Samuelsen, E. Bakken, P.H.J. Carlsen and M.R. Andersson, *Macromol. Chem. Phys.*, 196 (1995) 553.

[52] Unpublished results.

Table 1

Optimized Geometry of BT

Parameter [a]	HF/6-31G*	HF/3-21G*	HF/STO-3G	AM1	PM3	e. diff. [b]
C2-C2'	1.465	1.458	1.479	1.424	1.440	1.456
S1-C2	1.739	1.735	1.744	1.687	1.746	1.733
C2-C3	1.352	1.353	1.346	1.387	1.376	1.370
C3-C4	1.434	1.434	1.448	1.427	1.432	1.452
C4-C5	1.344	1.347	1.336	1.379	1.366	1.363
C5-S1	1.725	1.721	1.730	1.665	1.721	1.719
C3-H3	1.074	1.069	1.080	1.092	1.091	1.124
C4-H4	1.073	1.069	1.080	1.092	1.090	1.123
C5-H5	1.071	1.067	1.079	1.089	1.089	1.122
C2'-C2-C3	128.3	127.8	127.6	126.7	124.6	126.3
S1-C2-C3	110.8	111.0	111.5	110.7	111.2	111.8
C2-C3-C4	113.2	113.0	112.8	111.8	112.6	111.9
C3-C4-C5	112.6	112.5	112.2	111.6	112.4	112.3
C4-C5-S1	111.8	111.9	112.7	111.9	112.5	112.3
C5-S1-C2	91.6	91.6	90.8	94.0	91.3	91.7
C2-C3-H3	123.3	123.3	124.2	124.9	124.5	123.1
C3-C4-H4	123.6	123.5	123.1	123.1	122.7	123.6
C4-C5-H5	127.9	127.1	126.9	125.3	125.7	127.9
S1-C2-C2'-S1'	147.3	146.3	180.0	150.0	30.0	148.4

[a] Distances (Å), angles and the dihedral angle (°).

[b] Taken from Ref. [16].

Table 2

Optimized Geometry of DE34BT

parameter [a]	HF/3-21G*	HF/STO-3G	AM1	PM3
C2-C2'	1.468	1.486	1.426	1.442
S1-C2	1.735	1.748	1.691	1.748
C2-C3	1.349	1.346	1.384	1.373
C3-C4	1.441	1.458	1.433	1.438
C4-C5	1.348	1.335	1.381	1.369
C5-S1	1.723	1.729	1.666	1.720
C3-H3	1.070	1.079	1.093	1.093
C5-H5	1.068	1.078	1.089	1.090
C4-Ca	1.509	1.526	1.477	1.485
Ca-Cb	1.548	1.548	1.511	1.515
C2'-C2-C3	127.2	128.5	126.8	125.3
S1-C2-C3	111.0	111.7	110.7	111.4
C2-C3-C4	113.6	112.5	112.0	112.5
C3-C4-C5	111.5	112.1	111.3	112.2
C4-C5-S1	112.6	113.0	112.1	112.6
C5-S1-C2	91.4	90.8	93.9	91.3
C2-C3-H3	122.9	124.8	124.8	124.9
C4-C5-H5	126.5	126.5	125.2	125.2
C3-C4-Ca	123.2	122.5	123.2	122.8
C4-Ca-Cb	110.2	110.5	112.1	111.4
C3-C4-Ca-Cb	285.9	287.2	-77.9	-78.5
S1'-C2'	1.737	1.748	1.691	1.749
C2'-C3'	1.353	1.346	1.389	1.377
C3'-C4'	1.441	1.458	1.435	1.440
C4'-C5'	1.346	1.335	1.375	1.364
C5'-S1'	1.717	1.729	1.667	1.721
C4'-H4'	1.070	1.080	1.092	1.091
C5'-H5'	1.068	1.079	1.089	1.089
C3'-Ca'	1.509	1.526	1.477	1.485
Ca'-Cb'	1.548	1.548	1.511	1.515
C2-C2'-C3'	128.1	128.5	127.6	126.6
S1'-C2'-C3'	111.8	111.7	110.9	111.3
C2'-C3'-C4'	111.8	112.5	111.3	112.1
C3'-C4'-C5'	113.1	112.1	112.0	112.6
C4'-C5'-S1'	111.9	113.0	111.8	112.5
C5'-S1'-C2'		90.8	94.0	91.4
C3'-C4'-H4'	122.9	122.8	122.5	122.2
C4'-C5'-H5'	126.9	126.7	125.5	125.6
C2'-C3'-Ca'	125.6	126.6	126.2	126.4
C3'-Ca'-Cb'	110.1	110.6	112.2	111.6
C2'-C3'-Ca'-Cb'	262.5	254.2	-107.7	-108.2
S1-C2-C2'-S1'	108.1	40.4	45.0	50.0

[a] Distances (Å), angles and dihedral angles (°).

Table 3

Optimized Geometry of DE33BT

parameter [a]	HF/3-21G*	HF/STO-3G	AM1	PM3
C2-C2'	1.470	1.491	1.427	1.445
S1-C2	1.739	1.749	1.690	1.749
C2-C3	1.353	1.346	1.388	1.376
C3-C4	1.442	1.458	1.435	1.440
C4-C5	1.345	1.332	1.376	1.363
C5-S1	1.718	1.728	1.666	1.722
C4-H4	1.070	1.080	1.092	1.091
C5-H5	1.068	1.079	1.089	1.089
C3-Ca	1.509	1.526	1.477	1.485
Ca-Cb	1.546	1.546	1.510	1.515
C2'-C2-C3	128.1	128.1	128.3	126.3
S1-C2-C3	111.6	112.0	111.0	111.4
C2-C3-C4	111.9	111.8	111.2	112.1
C3-C4-C5	113.1	112.8	112.0	112.6
C4-C5-S1	111.9	112.7	111.9	112.6
C5-S1-C2	91.4	90.7	93.9	91.3
C3-C4-H4	123.0	122.5	122.7	122.2
C4-C5-H5	126.9	126.8	125.4	125.6
C2-C3-Ca	125.7	126.3	125.6	126.2
C3-Ca-Cb	111.4	112.4	113.0	111.6
C2-C3-Ca-Cb	250.8	252.9	-132.0	-106.6
S1-C2-C2'-S1'	101.5	115.7	60.0	95.0

[a] Distances (Å), angles and dihedral angles (°).

Table 4

Relative energies (kcal mol^{-1}) and torsional angles (θ) of BT, DE34BT and DE33BT obtained by *ab initio* calculations performed at the HF/3-21G* level

Molecule	*syn* (θ = 0°)		θ = 90°		*anti* (θ = 180°)
BT	1.72	0.57	1.49	0.0	0.39
		(44.7°)		(146.3°)	
DE34BT	3.81	0.014	0.1	0.0	2.2
		(60.0°)		(108.1°)	
DE33BT	15.9	-	0.0	-	7.6
			(101.5°)		

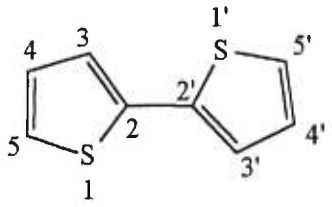

BT

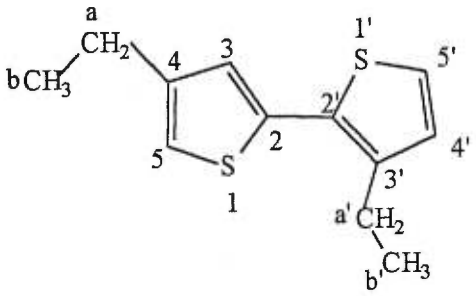

DE34BT

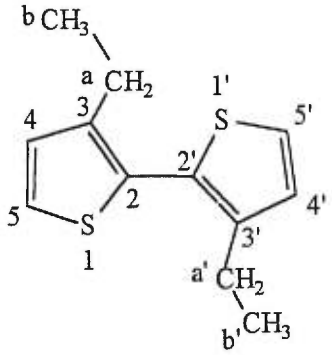

DE33BT

Figure 1. Molecular structures of the bithophenes investigated.

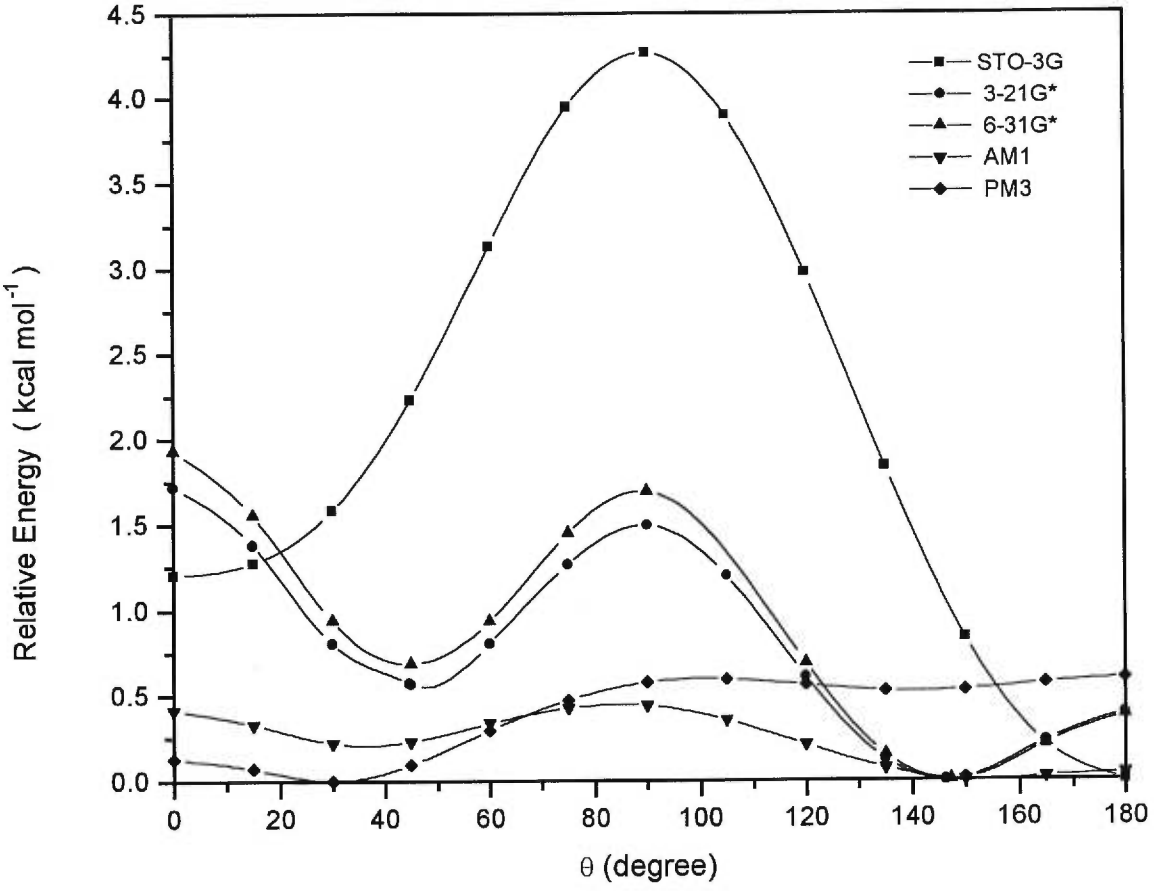

Figure 2. Potential energy curves of BT as obtained from semi-empirical (AM1, PM3) and *ab initio* (STO-3G, 3-21G*, 6-31G*) calculations.

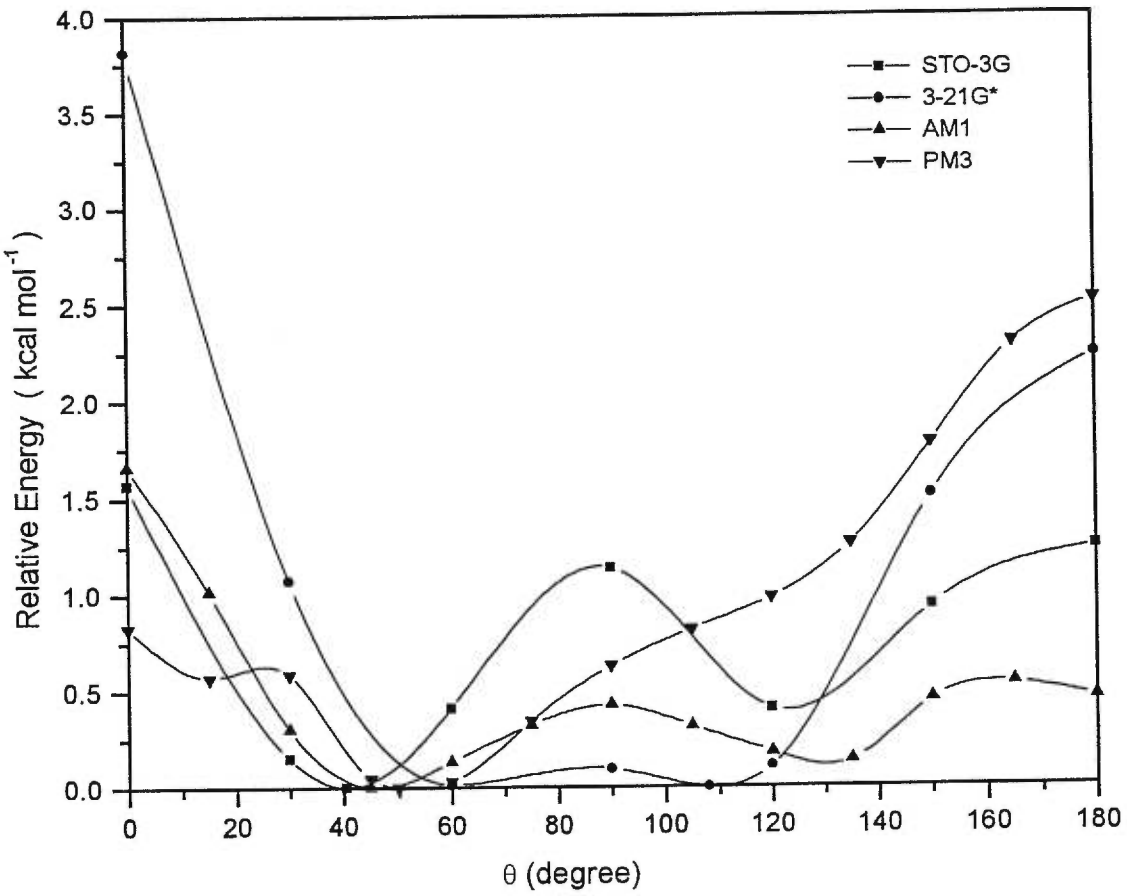

Figure 3. Potential energy curves of DE34BT as obtained from semi-empirical (AM1,PM3) and *ab initio* (STO-3G, 3-21G*) calculations.

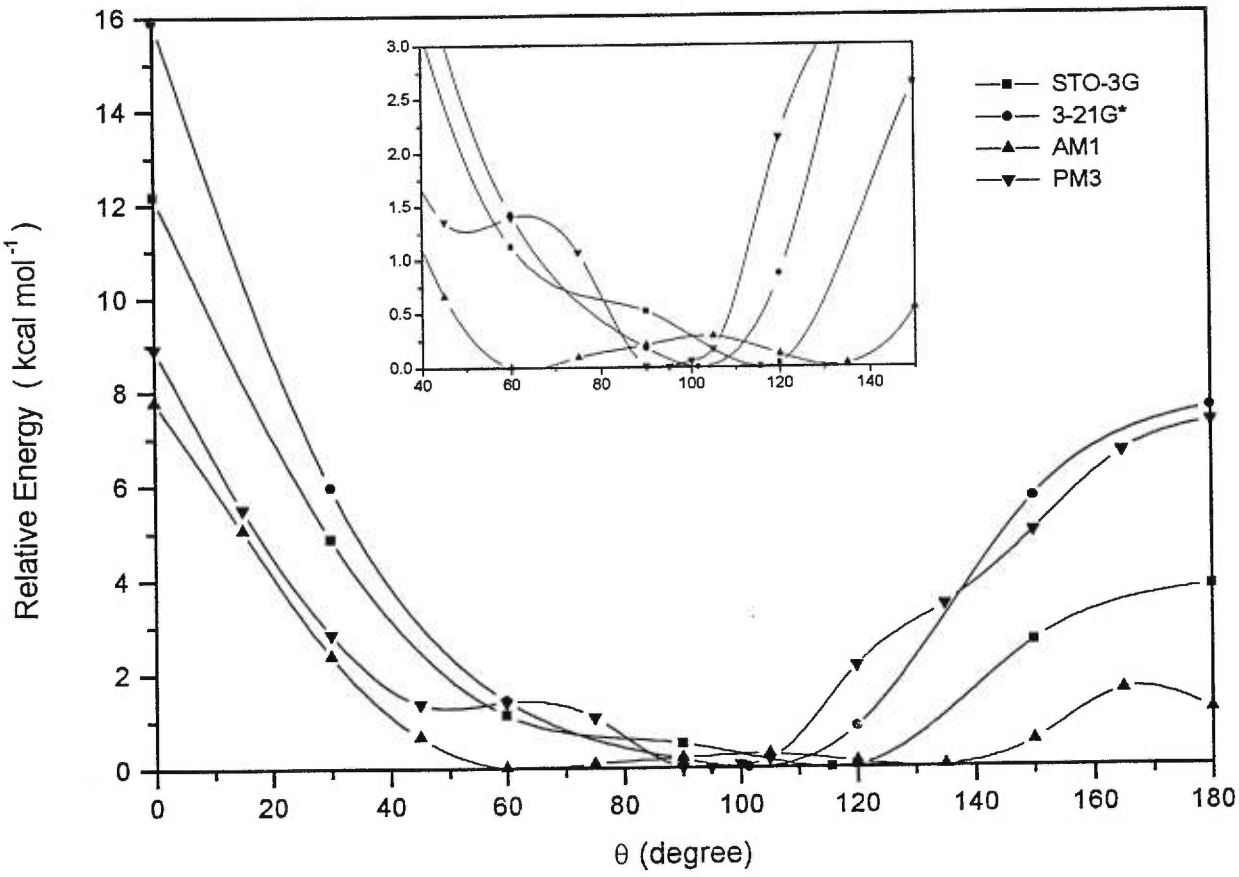

Figure 4. Potential energy curves of DE33BT as obtained from semi-empirical (AM1,PM3) and *ab initio* (STO-3G, 3-21G*) calculations.

Chapitre 3

Étude structurale et conformationnelle de dérivés alkoxys du 2,2'-bithiophène

L'analyse conformationnelle des dimères se poursuit ici avec la présentation des résultats théoriques obtenus sur les dérivés alkoxys. Contrairement aux substituants alkyls, la contribution électronique des substituants alkoxys en position 3 et/ou 3' est plus importante. Ceci se reflète sur les conformations minimales et les barrières rotationnelles de ces substituants. La présence des substituants alkoxys induit une plus grande planéité entre les cycles thiophènes et une barrière rotationnelle à 90° plus importante. Cet effet est expliqué par une combinaison des effets mésomères entre le doublet libre de l'oxygène et les électrons π du système aromatique et la variation des densités de charge créée par l'insertion des groupements alkoxys. L'insertion des groupements alkoxys en position 4,4' n'affecte aucunement la surface d'énergie potentielle du dimère comparativement au BT. Les résultats sur un dimère possédant des groupements alkoxys et alkyls sont également présentés.

Les résultats semi-empiriques présentés dans ce chapitre montrent un désaccord important comparativement aux résultats obtenus avec les calculs *ab initio*. Ce désaccord est principalement dû à la faiblesse des méthodes semi-empiriques utilisées pour obtenir les surfaces d'énergie potentielle des systèmes où les facteurs électroniques sont importants.

3.1 Article 3 : HF/3-21G* *ab initio* calculations on methoxy-substituted bithiophenes

Article accepté dans Journal of Molecular Structures (TheoChem), novembre 1998.

HF/3-21G* *AB INITIO* CALCULATIONS ON METHOXY-SUBSTITUTED BITHIOPHENES

Nicolas DiCésare [a], Michel Belletête [a], Mario Leclerc [b] and Gilles Durocher [a]

[a] Laboratoire de photophysique moléculaire
[b] Laboratoire des polymères électroactifs et photoactifs

Département de Chimie, Université de Montréal
C.P. 6128, Succ. A, Montréal, Québec, H3C 3J7, Canada

Abstract

We report, for the first time, the lowest energy structures as well as a detailed conformational analysis of several bithiophenes substituted with methoxy and methyl groups in various positions. For each molecule, geometrical parameters and potential energy surfaces have been obtained from HF/3-21G* *ab initio* calculations. The effect of the position of substituents on structural parameters and on torsional potentials has been examined. These calculations give results, which are in good agreement with available experimental data. For oligomers having methoxy groups in positions 3,3' and 3,4', planar *anti* conformations are well stabilized with large rotational barriers at 90°. This phenomenon has been interpreted in terms of charge transfer in the thiophene units induced by the methoxy groups in the 3 and/or 3' positions and delocalization throughout the molecular frame. For 4,4'-methoxy-2,2'-bithiophene, the alkoxy groups do not show any influence on the electronic structure of the molecule and do not create steric hindrance such that the most stable conformer is very similar to that of the unsubstituted bithiophene molecule. On the other hand, it is found that the most stable conformer of 3,4'-dimethoxy-4,3'-

dimethyl-2,2'-bithiophene is much twisted due to the presence of the methyl group in the 3'-position. This work also reports on theoretical results performed at lower levels (AM1 and PM3) since these levels of calculation are often the only ones practically available for large substituted oligothiophenes. It is shown that these calculations fail to predict accurate conformations of the molecules studied here mainly due to the methoxy group substituent. A ZINDO/S analysis performed on the geometries obtained by the various theoretical methods employed is also reported. It is observed that, for the same torsional angle, the ZINDO/S method is very sensitive to the starting geometry.

1. Introduction

Some substituted polythiophenes with relatively long and flexible side chains show interesting thermochromic properties, both in solution and in the solid state [1-7]. It has been found that these thermochromic properties are strongly related to the nature and the position of the side chains in the repetitive units of the polymer [8]. The optical properties presented by these macromolecules involve the intramolecular delocalization of the π electrons along the conjugated chain. This delocalization depends on the extent of the overlapping between the p_z orbitals of the carbon atoms in the α,α'-positions which is governed by the internal rotation around the single bonds between adjacent thiophene rings.

Ab initio calculations have been used to obtain the torsional potential of 2,2'-bithiophene (BT) [9-18] as well as of various alkyl-substituted derivatives [19-23]. For BT, the most advanced calculations show the existence of two well-defined potential wells separated by a relatively small barrier suggesting that *syn-gauche* and *anti-gauche* conformers should coexist [17, 18, 22]. The incorporation of alkyl-substituents in 3 and/or 3' positions creates a large steric hindrance, which induces a large torsion of the molecule, giving rise to an increase in the rotational barrier against planarity. It was shown that the occurrence of thermochromism in

polythiophenes could be related to the values of the rotational barrier of dimer models, which are building blocks of the macromolecules [24]. To reduce the time of calculation, semiempirical calculations have also been performed on BT and on substituted bithiophenes [25-31]. It was observed that the potential energy surface of BT calculated by the AM1 method [26, 27] is qualitatively similar to those found out by the most advanced *ab initio* calculations [17, 18, 22]. Even though the energy curve is too flat compared to *ab initio* result, the lowest energy conformations are well reproduced. The AM1 method also detects steric effects caused by alkyl substituents giving rise to much twisted conformations for alkyl-substituted bithiophenes. Alkoxy-substituted derivatives are also predicted to be much twisted from these semiempirical calculations [30, 31]. However, these calculations seem to neglect the electronic properties of the alkoxy substituents, which should favor a better planarity of the molecule.

To the best of our knowledge, *ab initio* calculations have never been performed on alkoxy-substituted bithiophenes. In order to obtain more reliable information about the conformation of this type of molecules, we will report on a conformational analysis of 4,4'-dimethoxy-2,2'-bithiophene (DMO44BT), 3,3'-dimethoxy-2,2'-bithiophene (DMO33BT) and 3',4-dimethoxy-2,2'-bithiophene (DMO34BT) using HF/3-21G* *ab initio* calculations. The HF/3-21G* method has been selected because of the relatively large size of our systems. The results obtained with this *ab initio* method can be successfully compared with more elaborate *ab initio* calculation as HF/6-31G*, MP2/6-31G* and DFT calculations for BT [17,18,32] and substituted bithiophenes [20,22,33]. Moreover, preliminary results have shown that HF/3-21G* and HF/6-31G** performed on 2-methoxy thiophene show very similar torsional potentials. The theoretical results obtained show that the incorporation of methoxy substituents in 3 and/or 3' positions greatly improves the molecular planarity in agreement with experimental data reported in the literature. This paper also reports HF/3-21G* calculations performed on 3,4'-dimethoxy-4,3'-dimethyl-2,2'-bithiophene (DMODM34BT) which is the dimer model for the

corresponding thermochromic polythiophene [24]. It is shown that the presence of a methyl group in the 3'-position induces a twisting in the molecule. Semiempirical (AM1, PM3) calculations are also reported. It is observed that these calculations fail to give reliable results for the geometry of the molecules studied involving methoxy groups. Finally a ZINDO/S analysis have been performed on the molecular geometries optimized by the various theoretical methods used. It is shown that, for the same twisting angle, the ZINDO/S method is very sensitive to the starting geometry. The molecules investigated are shown in Figure 1.

2. Theoretical Methods

Ab initio calculations were performed on a Silicon Graphics Challenge R4000 workstation at the University of Montreal using the Gaussian 90 program [34]. The HF/3-21G* basis set was used for the calculations. The Berny analytical gradient method was used for the optimizations. For the 3,3'- and 4,4'-methoxy bithiophenes, a locally C_2 symmetry restriction was applied between the two rings but no constraint was applied to the side groups. For the other molecules, no symmetry restriction was applied. The requested HF convergence on the density matrix was 10^{-8} and the threshold values for the maximum force and the maximum displacement were 0.00045 and 0.0018 a.u. (atomic unit), respectively. To obtain the final torsion angles of the most stable conformers, calculations of these geometries were performed without constraint on the dihedral angle. Potential energy surfaces have been drawn using a simple analytical form (1) least-squares-fitted which has been used by most workers in the field [18, 32]:

$$V(\theta) = \sum_{n=1}^{m} 1/2\ V_n(1-\cos(n\theta)) \qquad (1)$$

with m varying from 4 to 6. For the complete potential energy surface of DMODM34BT (Fig. 5), the fitting has been done separately for 0 to 180° and for 180 to 360° due to the asymmetry of the potential energy surface.

AM1 (Austin model 1) [35-38] and PM3 (Parametric Method 3) [39] semiempirical methods including the sulfur atom parameter sets were performed using the HYPERCHEM package, release 4.5 for Windows from Hypercube, Inc. PM3 is a reparametrization of AM1, which is based on the neglect of diatomic overlap (NDDO) approximation. Typically, nonbonded interactions are less repulsive in PM3 than in AM1. A RMS gradient in the energy of 0.1 kcal mol^{-1} was used for the optimization criterion.

The semiempirical conformational analysis was done by changing the torsional angle θ by 15° steps between θ = 0° (*syn* conformation) and θ = 180° (*anti* conformation). *Ab initio* calculations were compiled at each 30° due to the longer time of the calculations. For each conformer, the dihedral angle was held fixed while the remainder of the molecule was optimized (the rigid rotor approximation was not applied).

The ZINDO/S method including configuration interaction (CI) as employed in the HYPERCHEM package has been used to calculate the singlet-singlet electronic transition energies of the optimized conformers. ZINDO/S is a modified INDO method parameterized to reproduce UV/Visible spectroscopic transitions [40,41]. The electron-repulsion integrals were evaluated using the Mataga-Nishimoto formula. All singly excited configurations involving the five highest occupied and the five lowest unoccupied orbitals (CI = 5/5) were included in the energy calculation.

3. Results and Discussion

3.1. Equilibrium structures

Fully optimized geometric structures of the lowest energy conformer of each bithiophene derivative as obtained by the HF/3-21G* method are compiled in Tables 1 to 4. The atomic numbering is indicated in Figure 1. For the sake of comparison, X-Ray measurements of DMO44BT [42] and DMO33BT [43] are included in Tables 1 and 3, respectively. It is observed that X-Ray structures of both molecules are well reproduced by *ab initio* calculations performed at the HF/3-21G* level.

Insertion of methoxy groups in 4,4'-positions does not significantly change the geometrical parameters of BT (see Table 1 and ref. [20]). The sole exception is the C2-C3 bond length, which is shorter for DMO44BT than BT. This can be explained by the electron-donor properties and/or an inductive effect of the methoxy groups which can produce a resonance structure and/or a charge transfer involving C4, C5 and S1 atoms (or C4'-C5'-S1' in the other thiophene ring). This resonance structure should not increase the electronic delocalization between the two heterocycles. Indeed, this behavior has no effect on the value of the C2-C2' bond length but favors a slightly better planarity for DMO44BT (S1-C2-C2'-S1' dihedral angle = 148.4°) compared to BT (S1-C2-C2'-S1' dihedral angle = 146.3°) as well as a slightly higher rotational barrier between thiophene rings for the former molecule (see next section).

Tables 1 and 2 show that the C2-C2' bond length of DMO34BT is shorter than that of DMO44BT. This shows the importance of the methoxy group in the 3' position in the electronic structure of the dimer. The consequence of this behavior is the increase of the molecular planarity (S1-C2-C2'-S1' torsion angle = 170.9°) which causes a reduction of the inter-ring bond length (see next section). The incorporation of a second methoxy group in the 3 position (DMO33BT) further decreases the C2-C2' bond length due to the increase of the planarity of the molecule

(S1-C2-C2'-S1' torsion angle = 180°) compared to DMO34BT. This shows the additive effect of the two methoxy groups in the 3,3' positions. On the other hand, the presence of a methyl group in the 3'-position of DMODM34BT induces a large twisting between thiophene rings, which contributes to increase the C2-C2' bond distance. The same behavior has been observed for alkyl-substituted bithiophenes [20, 23]. From Table 4, one can also observe that C3-C4 (or C3'-C4') bond lengths are longer showing the repulsion between methyl and methoxy groups. It is worth mentioning that all molecules show a stretching of the C2-C2' bond length as the torsion between thiophene rings increase.

It is interesting to note that the orientation of the methoxy groups relative to the molecular frame depends upon the position of this substituent on the molecule. Indeed methoxy substituents in 3 and/or 3'-positions adopt a twisted conformation (C2-C3-Oa-Cb) while these groups in 4 and/or 4'-positions are planar (C3-C4-Oa-Cb) with neighboring thiophene rings. This difference will be discussed later in the text with the presentation of the potential energy profiles. It will be shown below that the orientation of the methoxy groups does not significantly affect potential energy surfaces but can influence singlet-singlet electronic transitions as calculated by the ZINDO/S semiempirical method.

Finally, we have observed that all the theoretical methods investigated are in good agreement with each other as far as the geometrical parameters are concerned. The sole exceptions are the orientation of methoxy groups in 3 and/or 3'-positions, which are predicted as nearly planar for all the molecules by the semiempirical methods and the inter-ring torsion as discussed below.

3.2. Conformational analysis

Torsional potentials of the various dimers as obtained by *ab initio* HF/3-21G* as well as semiempirical (AM1 and PM3) calculations are represented in Figures 2 to 5. The energies and torsional angles of the minima and maxima of each molecule as

obtained by the HF/3-21G* method are compiled in Table 5. Recently, we have shown that torsional potential energy surfaces of BT obtained from *ab initio* calculations using HF/3-21G* and HF/6-31G* basis sets are very close [23]. This, and a comparison with the literature results on *ab initio* calculations (HF with large basis sets, MP2 (Moller-Plesset Method) and DFT (Density Functional Theory) on BT [17,18,22,32] and on alkyl-substituted bithiophenes [20-22,33], strongly suggest that the HF/3-21G* basis set is sufficiently accurate for a conformational analysis on substituted bithiophenes.

The complete conformational analysis of the molecules investigated here should involve the dihedral angle between thiophene rings as well as the orientation of the methoxy groups relative to the molecular plane. In a first step, a conformational analysis of the methoxy group in the 4 (or 4') position (for DMO44BT) has been obtained keeping the inter-ring torsion angle fixed. The results show that the methoxy substituents adopt an *anti* conformation (C3-C4-Oa-Cb dihedral angle = 180°) in agreement with X-Ray data [42]. It was observed that the perpendicular and *syn* conformations of the methoxy groups are more energetic regardless of the value of the inter-ring torsional angle. In a second step, the inter-ring torsional potential has been obtained for two sets of methoxy groups orientations, *syn* and *anti*. It was found that the relative potential energy surface is not significantly influenced by the above orientations of the methoxy groups. This indicates that the relative torsion potential involving the two thiophene rings is mostly independent of the conformation adopted by the methoxy groups. On the other hand, calculations performed on DMO33BT shows that methoxy groups in 3,3'-positions are much twisted relative to the molecular plane for any value of the inter-ring dihedral angle. At this position, the methoxy group can not adopt a planar *syn* conformation (C2-C3-Oa-Cb = 0°) due to a large steric hindrance existing between the methyl group (Cb) and the neighboring thiophene ring. The perpendicular and the *anti* conformations are suspected to be less energetic. The

effect of this torsion on the electronic contribution of the methoxy groups to the conformation of DMO33BT will be discussed later in the text.

For the asymmetrical DMO34BT molecule, energy calculations have been done for many sets of torsional angles of the methoxy groups. The results confirm the data reported above that, in the 4 (or 4') position, the methoxy group is coplanar (*anti*) with the molecular frame for any dihedral angle between thiophene rings. In the 3 (or 3') position, this substituent adopts a minimum energy twisted conformation for any conformation of the molecular frame but the inter-ring torsional potential shows a little dependence with the conformation adopted by the methoxy groups. Since the twisted conformation of the methoxy group is always the minimum conformation, we present only the potential energy surface for this methoxy conformation. The effect of the conformation of the methoxy groups in 3 (or 3') position will be discussed with the presentation of the respective potential energy surface. It is important to mention that, for all the calculations presented here, the substituents have always been free to relax.

4,4'-dimethoxy-2,2'-bithiophene (DMO44BT)

Ab initio calculations performed at the HF/3-21G* level show that the most stable conformation of DMO44BT corresponds to an *anti-gauche* structure with a torsional angle $\theta = 148.4°$ (see Figure 2 and Table 5). This twisted conformer is found to be more stable than the *anti* structure ($\theta = 180°$) by 0.34 kcal mol^{-1}. Two main factors are involved in the description of the molecular structure of BT derivatives: the steric hindrance between thiophene rings, which favors twisted conformations and the π-electron conjugation along the molecular frame, which favors the planarity of the molecule. The actual equilibrium geometry of the molecule can be considered as a compromise between these two factors. However the energy difference between the *anti-gauche* conformer and the *anti*-conformer is so small that, at room temperature, DMO44BT could adopt any in-between

conformations as suggested by the absorption spectrum of this compound in solution at room temperature [30]. Thus it is easy to understand that, in the solid state, packing effects are strong enough to overcome this small energy barrier such that DMO44BT is reported to be planar [42]. A stable *syn-gauche* conformer is also calculated at a torsional angle $\theta = 41.1°$ which is more energetic than the *anti-gauche* conformer by 0.54 kcal mol^{-1}. The maximum in the HF/3-21G* energy surface corresponds to the conformation where the thiophene rings are in a perpendicular arrangement ($\theta = 90°$). It is interesting to note that the *syn*-conformer ($\theta = 0°$) is almost as energetic as the perpendicular conformer showing the strong steric hindrance between sulfur atoms.

The HF/3-21G* potential energy surface of DMO44BT is very close to that of BT performed at the same level of theory [17, 20] and at higher levels [17,18,32]. Particularly the torsional angles of the lowest energy conformers are calculated at similar angles than those predicted for BT ($\theta = 44.3°$and $\theta = 146.3°$) [20]. Moreover, the rotational barrier between *anti-gauche* and perpendicular conformations (1.84 kcal mol^{-1}) is relative close to that found for BT (1.49 kcal mol^{-1}). These results show that the presence of methoxy groups at 4,4'-positions does not seem to have significant effect on the conformation of the molecule. The same behavior has been observed for 4,4'-dimethyl-2,2'-bithiophene [20, 22]. Moreover, it was found that the absorption spectra of BT and DMO44BT in solution are quite similar [30]. Indeed the first absorption band of each molecule has about the same width ($\cong$ 5200 cm^{-1}) and is structureless showing the mobility of the thiophene rings (small energy difference between the *anti-gauche* structure and the *anti* conformation). However, the first absorption band of DMO44BT in *n*-hexane is red-shifted by 1600 cm^{-1} compared to that of BT. This is probably due to the electron-donating properties of the methoxy groups.

Figure 2 shows that the results provided by the AM1 semiempirical method are in qualitative agreement with HF/3-21G* data. Indeed the minima (45°, 150°) and maxima (0°, 90°, 180°) are calculated at similar torsion angles. However the

calculated energies are largely underestimated by AM1. For instance, the barrier to rotation between *anti-gauche* and perpendicular conformers is only 0.44 kcal mol^{-1}. On the other hand, the PM3 semiempirical method predicted a *syn-gauche* conformation (θ = 30°) as the most stable geometry but the barrier to rotation (0.57 kcal mol^{-1}) is close to that obtained by AM1. The same behavior has been reported for AM1 and PM3 semiempirical calculations performed on BT [26-29].

3',4-dimethoxy-2,2'-bithiophene (DMO34BT)

Figure 3 shows that the HF/3-21G* potential energy surface of DMO34BT predicts the molecule as nearly planar (θ = 170.6°). Indeed this conformation is found to be more stable than the *anti* conformation by only 0.13 kcal mol^{-1}. It would be surprising that the presence of a methoxy group in 3'-position causes weaker repulsive steric interactions than those induced by an hydrogen atom in the unsubstituted molecule. We believe that the increase of planarity is due to an important electronic contribution of the methoxy group in 3'-position, which favors electronic delocalizations between thiophene rings that can overcome the steric hindrance between sulfur and oxygen atoms. This contribution might involve the electron donor properties of the methoxy groups, an inductive effect due to the electron attractive properties of the methoxy groups and a charge transfer involving the sulfur atoms. A detailed discussion of these contributions will be presented later on after the presentation of the potential energy surface of DMO33BT. It is found that the *syn* conformation of DMO34BT is destabilized by 1.19 kcal mol^{-1} compared to the lowest energy conformer indicating that steric effects between sulfur atoms are still important. The barrier of rotation between *anti-gauche* and perpendicular conformations is 3.88 kcal mol^{-1} compared to 1.84 kcal mol^{-1} found for DMO44BT. Calculations have also been performed on DMO34BT for torsional angles ranging from θ =180° to θ = 360° since a small asymmetry in the molecule does exist. It is observed that this energy profile is very similar to the 0 - 180° one.

AM1 and PM3 semiempirical methods predict the DMO34BT molecule as twisted with a *syn-gauche* arrangement. Moreover both methods indicate that the *anti* conformation is strongly destabilized compared to the *syn* conformation. Thus, for these semiempirical methods, the main geometric factor seems to be the repulsive interactions between oxygen and sulfur atoms, which are stronger than those between sulfur atoms. The electronic contribution of the methoxy groups seems to be completely neglected by this type of calculations. This behavior is important since the only conformational analyses of methoxy substituted bithiophenes reported in the literature are obtained with molecular mechanic and semiempirical calculations [30,31], where twisted ($\theta = 120°$ [30] et $\theta = 135°$ [31]) molecular conformations are found.

3,3'-dimethoxy-2,2'-bithiophene (DMO33BT)

The conformation of DMO33BT predicted by HF/3-21G* calculations is *anti* (see Figure 4). The rotational energy barrier between *anti* and the perpendicular conformer (6.69 kcal mol^{-1}) is much higher than that found for DMO34BT (3.88 kcal mol^{-1}). A second local minimum, *syn-gauche*, is also calculated at $\theta = 55.2°$ but this conformation is less stable by 3.34 kcal mol^{-1} compared to the *anti* conformation. The *syn* conformer is almost as unstable as the perpendicular conformer showing strong steric repulsive interactions in this structure.

This decrease of twisting and the important increase of the rotational barrier at 90° compared to BT [23] (or DMO44BT) show the important contribution of the methoxy groups in the 3 and/or 3' positions. The electron donor properties of the methoxy groups may be involved. But since the charge density (Mulliken population), as calculated from HF/3-21G*, on the oxygen atom does not significantly change with the value of the dihedral angle between the thiophene rings and since the methoxy groups are nearly perpendicular to the plane of the thiophene rings, this contribution is small and might not influence the molecular conformation

and the rotational barrier. In contrast, important changes in the charge density (Mulliken population) of the S1 and C3 atoms are observed as the torsional angle is varied. Indeed, the charge density on S1 is 0.455 for the perpendicular conformation and is more positive as the molecule becomes planar (0.505 for the *anti* conformation). For the C3 atom, the charge density is 0.415 and 0.360 for the perpendicular and *anti* conformations, respectively. This indicates that an important charge transfer occurs between S1 and C3 atoms when the molecule becomes planar. On the other hand, the charge density on the sulfur atom of BT does not significantly change with the rotation of the thiophene rings. However we can observe a small change in the charge density of the C3 atom (-0.205 and -0.240 for the perpendicular and the *anti* conformations, respectively). The important charge transfer observed in DMO33BT is thus induced by the presence of the methoxy groups linked to the C3 and C3' atoms. This effect is greater when the molecule is planar showing that the delocalization over the molecular frame contributes to this phenomenon. It is worth noting that the decrease of twisting could also be due to attractive interaction forces taking place between the oxygen atom (negatively charged) and the sulfur atom in the opposite thiophene ring (positively charged) as suggested previously by Meille *et al* [44]. Both mechanisms, the intramolecular charge transfer interaction and the Coulombic interaction between non-bonded sulfur and oxygen atoms, are likely to play a role in explaining the planarity of these molecules.

From AM1 calculations, the molecular structure of DMO33BT is predicted to be much twisted (θ = 105°). But to the contrary of AM1 calculations performed on DMO34BT, the minimum conformation is *anti*-gauche. Moreover, *anti*-like conformers are much lower in energy than *syn*-like conformers. This indicates that the combined sulfur-sulfur and oxygen-oxygen steric interactions are more important than repulsive steric effects between oxygen and sulfur atoms in this type of calculations. The reverse situation is true for PM3 calculations where *anti*-like conformations are very unstable. The lowest energy conformer predicted by this method appears for a *syn-gauche* conformation (θ = 75°). Like in the case of

DMO34BT, both methods seem to minimize the electronic contribution of the methoxy groups on the conformation of the molecule.

According to the above *ab initio* theoretical results, the DMO33BT molecule should be planar and rigid compared to DMO44BT and BT. This assumption is in good agreement with the experimental evidence that, to the contrary of DMO44BT and BT, the absorption spectrum of DMO33BT is structured [30]. This is a spectroscopic behavior of planar rigid systems. Moreover, the bandwidth of the first absorption band of DMO33BT (4300 cm^{-1}) is much smaller than that of DMO44BT (5200 cm^{-1}) suggesting that a lower amount of conformers are present in the case of DMO33BT. Another spectroscopic evidence in favor of an average planarity of this 3,3'-alkoxy derivative is the fact that the absorption and fluorescence spectra of 3,3'-butoxy-2,2'-bithiophene (DBO33BT) form very good mirror images [30]. Since BT derivatives are expected to be almost planar in the first relaxed singlet excited state [28-30], the good mirror-image relationship strongly suggests that DBO33BT is nearly planar in the ground state. The length of the alkoxy chain should not have any significant effects on this behavior. Thus DMO33BT is expected to give the same behavior. Recently, the structure of DMO33BT has been predicted as twisted from AM1 [30] and MM2 [31] conformational analyses. Using AM1 as a geometry optimizer, the ZINDO/S semiempirical method has also predicted DMO33BT as twisted [30]. But we have clearly shown above that semiempirical theoretical results totally disagree with *ab initio* calculations. It will be shown below that the calculations of electronic transition energies of alkoxy bithiophene derivatives are very sensitive upon the starting geometry obtained from the various optimization methods employed.

3,4'-dimethoxy-4,3'-dimethyl-2,2'-bithiophene (DMODM34BT)

Since DMODM34BT is an asymmetrical molecule, HF/3-21G* calculations have been performed for torsional angles between $\theta = 0°$ and $\theta = 360°$. The potential

energy surface obtained is not symmetrical (see Figure 5). The orientation of the methoxy group in the 3 position is responsible for this behavior. Indeed, this substituent is twisted relative to the thiophene ring attached to it such that, at θ = 210° and θ = 240°, the methoxy substituent and the adjacent thiophene ring are pointing in the same direction creating large steric interactions between the methyl group (C_b) of the methoxy substituent and S1'. On the other hand, for conformers having torsion angles of 150° and 120°, respectively, the methoxy group and the neighboring thiophene ring are pointing in opposite directions resulting in lower steric effects, which explains the smaller energy that is found for these conformers. Similarly, the non-coplanarity of the methoxy group is responsible for the energetic differences found between corresponding *syn*-gauche conformers (30° and 60° *vs* 330° and 300°). In the latter case, steric interactions involved the methyl group of the methoxy substituent in the 3 position and the methyl group of the adjacent thiophene ring located in the 3'-position.

Figure 5 shows that the lowest energy conformer is located at θ = 305.9° with high barriers against planarity (*syn*, 8.00 kcal mol^{-1}; *anti*, 4.18 kcal mol^{-1}). However, a local minimum is also found at θ = 123.4°, which is relatively close in energy to the *anti* conformer (0.81 kcal mol^{-1}) but a high barrier to rotation at θ = 0° (6.63 kcal mol^{-1}). The higher rotational barriers against planarity obtained for this molecule relative to those of the other methoxy-substituted bithiophenes investigated are explained by the presence of the methyl group in the 3'-position, which creates large steric effects. A similar behavior has been observed for alkyl-substituted bithiophenes [20, 22, 23]. Moreover, starting from the local minimum, the energy to reach θ = 180° is very similar to that obtained for 3,4'-dimethyl-2,2'-bithiophene [20]. This indicates that the electronic contribution (charge transfer) induced by the methoxy group in the 3 position partly compensates for the combined steric effects induced from methoxy and methyl groups in 3 and 3'-positions, respectively. On the other hand, *syn*-like conformers are much destabilized emphasizing the strong steric

interactions between methoxy and methyl groups on one side of the molecule and between sulfur atoms on the other molecular side.

Recently, we have reported the potential energy surface of DMODM34BT for conformers having dihedral angles between 0° to 180° with the lowest energy conformer located at 88° [24]. However, the latter conformer was obtained starting from a planar conformation of the methoxy group in the 3-position (Cb-Oa-C3-C2 ≈ 0°). For this molecular arrangement, thiophene rings are not free to rotate (relax) because the methyl of the methoxy group (in the 3 position) is very close to the thiophene ring. Thus the corresponding potential energy surface has not been calculated. On the other hand, the potential energy surfaces have been obtained with the other possible planar conformation of the methoxy group (Cb-Oa-C3-C2 ≈ 180°) as illustrated on Figure 1. The torsion potential obtained (figure not shown) shows important differences compared to that obtained with a perpendicular conformation of the methoxy group. For instance, the lowest energy conformer is located at θ = 180° whereas lower rotational barriers are obtained for *syn-gauche* conformers. But all conformers optimized with the latter conformation of the methoxy group are much more energetic than those obtained with a perpendicular conformation of the methoxy group. Thus, Figure 5 features the most stabilized conformers of DMODM34BT in the gas phase, except for the conformer having a dihedral angle of 88° as discussed above. The latter conformer represents a local minimum in another part of the three dimensional torsion potential. To conclude this conformational analysis, one can see that it is rather difficult to have a complete view of the potential energy surface of DMODM34BT. Indeed this kind of molecule has a high degree of freedom leading to a wide distribution of possible conformers. However, we think that the potential energy surface illustrated in Figure 5 gives a good idea of the minimum conformation and the rotational barriers involved in this substituted bithiophene.

3.3. ZINDO/S Analysis

The first electronic transition energies have been calculated from the ZINDO/S semiempirical method using the optimized geometry obtained at each theoretical level. Table 6 reports the transition wavelengths obtained for DMO33BT. The same trend has been obtained for the other bithiophene derivatives studied here such that the same conclusions could be applied.

For each theoretical method used to obtain optimized geometries, the wavelength of the electronic transition decreases as the molecule becomes more twisted. This behavior is well known and is due to the decrease in the overlapping between p_z orbitals of the inter-ring carbon atoms as the torsional angle increases. This induces a reduction in the electronic conjugation and hence an increase in the transition energy (decrease of the wavelength). However, ZINDO/S data are very sensitive to the starting geometry used in the calculations for the same torsional angle. Indeed, transition energies are lowered when ZINDO/S is performed from semiempirical AM1 and PM3 geometries compared with geometries optimized at *ab initio* level. Each geometrical parameter may influence ZINDO/S data, particularly the dihedral angle formed between methoxy groups and the bithiophene moiety. It has been mentioned in the previous section that the structure of DMO33BT as calculated from the HF/3-21G* method gives the methoxy groups as twisted relative to the molecular frame whereas semiempirical methods place methoxy groups as planar with the rest of the molecule. To investigate further the effect of the orientation of methoxy groups on the transition energy, we have done a HF/3-21G* geometry optimization keeping methoxy groups of DMO33BT planar. For the *anti* conformation, the transition wavelength obtained was 335.2 nm. The same trend was observed for other torsional angles. Thus, the fact that HF/3-21G* calculations give the lowest energy conformer of DMO33BT with tilted methoxy groups is partly

responsible for the high energies found compared to those obtained from semiempirical calculations where the optimized structures show the methoxy groups as planar. ZINDO/S calculations performed on the AM1 and PM3 equilibrum structured (θ = 150°) of BT give transition wavelengths of 325.4 nm and 317.3 nm respectively. These wavelengths obtained with the semiempirical structures are also red shifted compared to that obtained with the HF/3-21G* structure (301.3 nm). Since no methoxy groups are present in the BT molecule, this behavior should involve small variations in the C-C and C-S bond lengths for both BT and DMO33BT.

ZINDO/S calculations performed at the HF/3-21G* equilibrium structures (θ = 150°) for bithiophene (BT) and DMO44BT give transition wavelengths of 301.3 nm [23] and 310.8 nm, respectively. The red-shift observed (1000 cm^{-1}) for DMO44BT shows the electron-donor properties of the methoxy groups. The same behavior has been found experimentally [30]. Moreover, it was found that DMO33BT absorption wavelengths are higher than those calculated for DMO44BT for the same dihedral angle. This indicates that methoxy groups located in the 3,3'-positions induce a higher electron delocalization throughout the entire molecule.

From ZINDO/S transition energy calculations on AM1 optimized geometries and the position of the 0,0 absorption wavenumber extrapolated at n =1, we have reported that DMO33BT is twisted with θ = 120° [30]. Recently, the same geometry has been reported for this molecule using transition energy calculations on geometries optimized from molecular mechanics (MM2) [31]. These results are not in agreement with *ab initio* calculations reported above. But we have seen that the starting geometry is critical in ZINDO/S calculations. The wavenumber [ν_A (0, 0)] extrapolated at n = 1 for DMO33BT gives a value of 31400 cm^{-1} (318 nm) [30]. According to Table 6, this corresponds to a torsion angle θ = 150° from HF/3-21G*/ZINDO/S calculations. This is in a better agreement with the conformational analysis performed at *ab initio* levels. Moreover, a value of 30900 cm^{-1} (324 nm) is obtained for the DMO33BT's *anti* conformer. The difference (500 cm^{-1}) is inside the

1000 cm^{-1} bracket generally accepted for this kind of calculations. To conclude this part, we believe that ZINDO/S calculations are too sensitive to starting geometries, when one compares the variation of the transition energy with the torsion angle, to be used in the determination of precise conformations for this type of molecules in solution. It has to be mentioned though, that in all ZINDO/S calculations discussed here, the σ and π scaling parameters have been kept fixed at 1.267 and 0.585, respectively. Better correlations between ZINDO/S and experiments might be obtained for a particular geometry optimizer by changing the scaling parameters.

4. Concluding remarks

Ab initio calculations performed at the HF/3-21G* level give torsional potentials which correlate well with available absorption data. It is found that the potential energy surface of DMO44BT is very similar to that of BT showing the small effect of methoxy substituents in 4,4'-positions. On the other hand, DMO34BT and DMO33BT are predicted as planar with an *anti* conformation. This behavior is interpreted mainly by the charge transfer occurring between the sulfur atom and the carbon C3, which is induced by the presence of the methoxy group on the same carbon atom. This charge transfer has a direct influence on the resonance between the thiophene rings. Finally, the DMODM34BT molecule is reported to be much twisted due to the presence of the methyl group in position 3, which creates steric hindrance. On the other hand, semiempirical calculations are not precise enough to obtain accurate rotational energy profiles for alkoxy-substituted bithiophenes. It is also shown that the ZINDO/S semiempirical method is very sensitive to the starting geometry used in the calculations.

Acknowledgment

The authors are grateful to the Natural Sciences and Engineering Research Council of Canada (NSERC) and the "Fonds FCAR" (Québec) for their financial support. N.D. is grateful to the NSERC for a graduate scholarship.

References

[1] S.D.D.V. Rughooputh, S. Hotta, A.J. Heeger and F. Wudl, J. Polym. Sci., Polym. Phys. Ed., 25 (1987), 1071.

[2] O. Inganas, W.R. Salaneck, J.E. Osterholm and J. Laakso, Synth. Met., 22 (1988), 395.

[3] C. Roux and M. Leclerc, Macromolecules, 25 (1992), 2141.

[4] C. Roux, J-Y. Bergeron and M. Leclerc, Makromol. Chem., 194 (1993), 869.

[5] C. Roux and M. Leclerc, Chem. Mater., 6 (1994), 620.

[6] K. Faïd, M. Fréchette, M. Ranger, L. Mazerolle, I. Lévesque, M. Leclerc, T-A. Chen and R.D. Rieke, Chem. Mater., 7 (1995), 1390.

[7] I. Lévesque and M. Leclerc, Chem. Mater., 8 (1996), 2843.

[8] M. Leclerc, M. Fréchette, J-Y. Bergeron, M. Ranger, I. Lévesque and K. Faïd, Macromol. Chem. Phys., 197 (1996), 2077.

[9] J-L. Brédas, B. Thémans, G. Fripiat, J-M. André and R.R. Chance, Phys. Rev. B., 29 (1984), 6761.

[10] J-L. Brédas, G.B. Street, B. Thémans and J.M. André, J. Chem. Phys., 83 (1985), 1323.

[11] V. Barone, F. Lelj, N. Russo and M. Toscano, J. Chem. Soc., Perkin Trans 2 (1986), 907.

[12] G. Jones, M. Guerra, L. Favoretto, A. Modelli, M. Fabrizio and G. Distefano, J. Phys. Chem., 94 (1990), 5761.

[13] C.X. Cui, M. Kertesz and H. Eckhart, Synth. Met., 41 (1991), 3491.

[14] M. Kofranek, T. Kovár, H. Lischka and A. Karpfen, J. Mol. Struct. (THEOCHEM), 259 (1992), 181.

[15] S. Samdal, E.J. Samuelsen and H.V. Volden, Synth. Met., 59 (1993), 259.

[16] C. Quattrocchi, R. Lazzaroni and J-L. Brédas, Chem. Phys. Lett., 208 (1993), 120.

[17] E. Orti, P.M. Viruela, J. Sanchez-Marin and F. Tomas, J. Phys. Chem., 99 (1995), 4955.

[18] A. Karpfen, C.H. Choi and M. Kertesz, J. Phys. Chem., 101 (1997), 7426.

[19] G. Distefano, M. Dal Colle, M. Zambianchi, L. Favaretto and A. Modelli, J. Phys. Chem., 97 (1993), 3504.

[20] V. Hernandez and J.T. Lopez Navarrete, J. Chem. Phys., 101 (1994), 1369.

[21] V. Hernandez and J.T. Lopez, Navarrete, Synth. Met., 76 (1996), 221.

[22] C. Alemán and L. Julia, J. Phys. Chem., 100 (1996), 1524.

[23] N. Di Césare, M. Belletête, M. Leclerc and G. Durocher, Synth. Met., 94 (1998), 291.

[24] N. Di Césare, M. Belletête, G. Durocher and M. Leclerc, Chem. Phys. Lett., 275 (1997), 533.

[25] D.A. dos Santos, D.S. Galvao, B. Laks and M.C. dos Santos, Synth. Met., 51 (1992), 203.

[26] M. Belletête, M. Leclerc and G. Durocher, J. Phys. Chem., 98 (1994), 9450.

[27] M.C. Dos Santos and J. Bohland- Filho, SPIE, 2528 (1995), 143.

[28] P.F. van Hutten, R.E. Gill, J.K. Herrema and G. Hadziioannou, J. Phys. Chem., 99 (1995), 3218.

[29] M. Belletête, N. Di Césare, M. Leclerc and G. Durocher, J. Mol. Struct. (THEOCHEM), 391 (1997), 85.

[30] N. Di Césare, M. Belletête, F. Raymond, M. Leclerc and G. Durocher, J. Phys. Chem. A, 101 (1997), 776.

[31] A. Bongini, F. Brioni M. Panunzio, J. Chem. Soc., Perkin Trans.2 (1997), 927.

[32] C. Aleman, V.M. Domingo, L. Fajari, L. Julia and A. Karpfen, J. Org. Chem., 63 (1998), 1041.

[33] P.M. Viruela, R. Viruela, E. Orti, E and J-L. Brédas, J. Am. Chem. Soc., 119 (1997), 1360.

[34] M.J. Frisch, M. Head-Gordon, G.W. Trucks, J.B. Foresman, H.B. Schlegel, K. Raghavachari, M. Robb, J.S. Bimkley, C. Gonzales, D.J. Defrees, D.J. Fox, R.A.

Whiteside, R. Seeger, C.F. Melius, J. Baker, R.L. Martin, R.L. Kahn, J.J.P. Stewart, S. Topiol and J.A. Pople, Gaussian 90, Revision F ; Gaussian :Pittsburgh, PA, 1990.

[35] M.J.S. Dewar, E.G. Zoebisch, E.F. Healy and J.J.P. Stewart, J. Am. Chem. Soc., 101 (1985), 3902.

[36] M.J.S. Dewar and K. Dieter, J. Am. Chem. Soc., 108 (1986), 8075.

[37] J.J.P. Stewart, J. Comp. Aided Mol. Design, 4 (1990), 1.

[38] J.M.S. Dewar and Y.C. Yuan, Inorg. Chem., 29 (1990), 3881.

[39] J.J.P. Stewart, J. Comput. Chem., 10 (1989), 209; 10 (1989), 221.

[40] J. Ridley and M.C. Zerner, Theor. Chim. Acta, 32 (1973), 111.

[41] C. Forber and M.C. Zerner, J. Am. Chem. Soc., 107 (1985), 5884.

[42] E.F. Paulus, K. Siam, K. Wolinski and L. Schäfer, J. Mol. Struct., 196 (1989), 171.

[43] E.F. Paulus, R. Dammel, G. Kämpf and P. Wegener, Acta Cryst., B44 (1988), 509.

[44] S.V. Meille, A. Farina, F. Bezziccheri and M.C. Gallazzi, Adv. Mater., 6 (1994), 848.

Table 1

Optimized Geometry for the lowest energy structure of DMO44BT

bond length	HF/3-21G* (Å)	X-RAY [a] (Å)	angle	HF/3-21G* (degree)	X-RAY [a] (degree)
C2-C2'	1.457	1.462 (4)	C2'-C2-C3	127.4	128.4 (3)
S1-C2	1.735	1.723 (2)	S1-C2-C3	111.4	111.4 (1)
C2-C3	1.348	1.356 (3)	C2-C3-C4	112.7	112.3 (2)
C3-C4	1.436	1.427 (3)	C3-C4-C5	112.9	113.2 (2)
C4-C5	1.348	1.355 (4)	C4-C5-S1	111.5	111.1 (2)
C5-S1	1.727	1.716 (2)	C5-S1-C2	91.5	92.1 (1)
C3-H3	1.068	0.906 (24)	C2-C3-H3	125.1	127.8 (13)
C5-H5	1.065	1.018 (22)	C4-C5-H5	128.0	128.3 (15)
C4-Oa	1.360	1.357 (3)	C3-C4-Oa	118.4	118.9 (2)
Oa-Cb	1.439	1.426 (3)	C4-Oa-Cb	118.7	114.8 (2)
			C3-C4-Oa-Cb	180.6	178.1 (2)
			S1-C2-C2'-S1'	148.4	180.0 (2)

[a] Taken from ref. [42].

Table 2

Optimized Geometry for the lowest energy structure of DMO34BT

bond length	HF/3-21G* (Å)	angle	HF/3-21G* (degree)
C2-C2'	1.451	C2'-C2-C3	126.7
S1-C2	1.741	S1-C2-C3	111.1
C2-C3	1.351	C2-C3-C4	113.0
C3-C4	1.433	C3-C4-C5	112.7
C4-C5	1.348	C4-C5-S1	111.9
C5-S1	1.726	C5-S1-C2	91.3
C3-H3	1.068	C2-C3-H3	125.2
C5-H5	1.066	C4-C5-H5	127.8
C4-Oa	1.362	C3-C4-Oa	118.4
Oa-Cb	1.439	C4-Oa-Cb	118.5
S1'-C2'	1.736	C3-C4-Oa-Cb	179.9
C2'-C3'	1.352		
C3'-C4'	1.434	C2-C2'-C3'	127.2
C4'-C5'	1.344	S1'-C2'-C3'	110.5
C5'-S1'	1.722	C2'-C3'-C4'	113.6
C4'-H4'	1.068	C3'-C4'-C5'	112.0
C5'-H5'	1.067	C4'-C5'-S1'	112.2
C3'-Oa'	1.375	C5'-S1'-C2'	91.6
Oa'-Cb'	1.457	C3'-C4'-H4'	123.3
		C4'-C5'-H5'	127.0
		C2'-C3'-Oa'	122.4
		C3'-Oa'-Cb'	116.5
		C2'-C3'-Ob'-Cb'	251.3
		S1-C2-C2'-S1'	170.9

Table 3

Optimized Geometry for the lowest energy structure of DMO33BT

bond length	HF/3-21G* (Å)	X-RAY [a] (Å)	angle	HF/3-21G* (degree)	X-RAY [a] (degree)
C2-C2'	1.448	1.425 (7)	C2'-C2-C3	126.3	128.9 (4)
S1-C2	1.740	1.733 (3)	S1-C2-C3	110.4	108.9 (3)
C2-C3	1.354	1.373 (5)	C2-C3-C4	113.8	114.0 (4)
C3-C4	1.432	1.401 (7)	C3-C4-C5	111.7	112.2 (4)
C4-C5	1.345	1.327 (7)	C4-C5-S1	112.7	113.2 (5)
C5-S1	1.720	1.693 (5)	C5-S1-C2	91.4	91.8 (2)
C4-H4	1.068	0.83 (4)	C3-C4-H4	123.5	116.0 (3)
C5-H5	1.067	0.72 (4)	C4-C5-H5	126.6	131.0 (3)
C3-Oa	1.378	1.371 (5)	C2-C3-Oa	121.9	118.6 (4)
Oa-Cb	1.457	1.414 (5)	C3-Oa-Cb	116.5	116.5 (3)
			C2-C3-Oa-Cb	246.2	-178.6 (3)
			S1-C2-C2'-S1'	180.0	180.0

[a] Taken from ref. [43].

Table 4

Optimized Geometry for the lowest energy structure of DMODM34BT

bond length	HF/3-21G* (Å)	angle	HF/3-21G* (degree)
C2-C2'	1.460	C2'-C2-C3	127.6
S1-C2	1.736	S1-C2-C3	110.6
C2-C3	1.350	C2-C3-C4	113.9
C3-C4	1.440	C3-C4-C5	111.4
C4-C5	1.345	C4-C5-S1	112.6
C5-S1	1.723	C5-S1-C2	91.5
C5-H5	1.068	C4-C5-H5	126.6
C3-Oa	1.377	C3-C4-Cc	121.7
Oa-Cb	1.459	C2-C3-Oa	125.7
C4-Cc	1.503	C3-Oa-Cb	116.6
S1'-C2'	1.741	C2-C3-Oa-Cb	286.1
C2'-C3'	1.350		
C3'-C4'	1.445	C2-C2'-C3'	127.2
C4'-C5'	1.347	S1'-C2'-C3'	112.1
C5'-S1'	1.724	C2'-C3'-C4'	111.4
C5'-H5'	1.065	C3'-C4'-C5'	113.7
C3'-Cc'	1.506	C4'-C5'-S1'	111.5
C4'-Oa'	1.363	C5'-S1'-C2'	91.3
Oa'-Cb'	1.440	C4'-C5'-H5'	127.8
		C2'-C3'-Cc'	126.4
		C3'-C4'-Oa'	118.1
		C4'-Oa'-Cb'	118.8
		C3'-C4'-OA'-Cb'	181.3
		S1-C2-C2'-S1'	305.9

Table 5

Relative energies (in kcal mol^{-1}) and torsional angles (θ) of DMO44BT, DMO34BT, DMO33BT and DMODM34BT obtained by *ab initio* calculations performed at the HF/3-21G* level

Molecule	*syn*[a]	*syn-gauche*	perpendicular[a]	*anti-gauche*	*anti*[a]
DMO44BT	1.55	0.54 (41.1°)	1.84	0.0 (148.4°)	0.34
DMO34BT	1.19		3.88	0.0 (170.6°)	0.13
DMO33BT	6.26	3.34 (55.2°)	6.69		0.0
DMODM34BT	8.00	0.0 (305.9°)	-	1.37 (123.4°) 4.18 (210.0°)	2.18

[a] *Syn*, θ = 0° ; *anti*, θ = 180° ; perpendicular, θ = 90°.

Table 6

First Singlet-Singlet Electronic Transition Wavelength (nm) of DMO33BT as Obtained by ZINDO/S from Starting Geometries Optimized at Various Theoretical Levels and for Various Dihedral Angles θ.

θ (degree)	HF/3-21G*	AM1	PM3
0	321.5	358.1	357.1
30	311.2	345.7	338.7
60	293.5	318.8	313.6
90	255.6	280.4	270.7
120	291.7	319.7	310.3
150	318.2	348.8	338.1
180	324.2	358.5	349.2

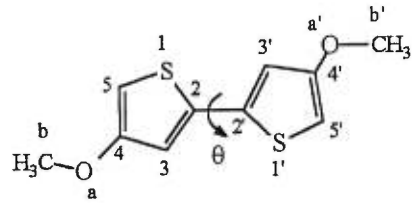

DMO44BT

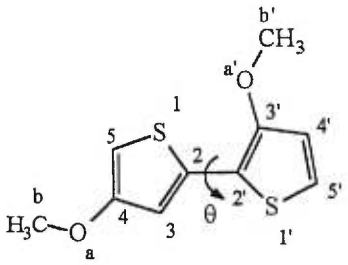

DMO34BT

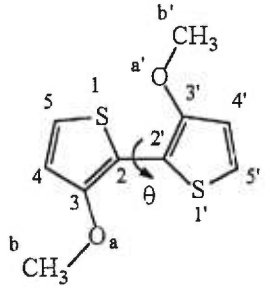

DMO33BT

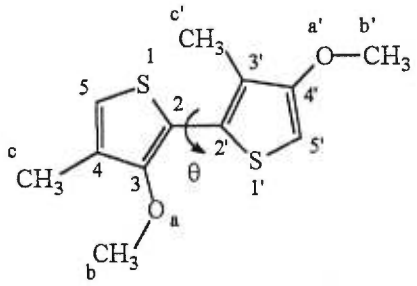

DMODM34BT

Figure 1. Molecular structures of the bithiophenes investigated.

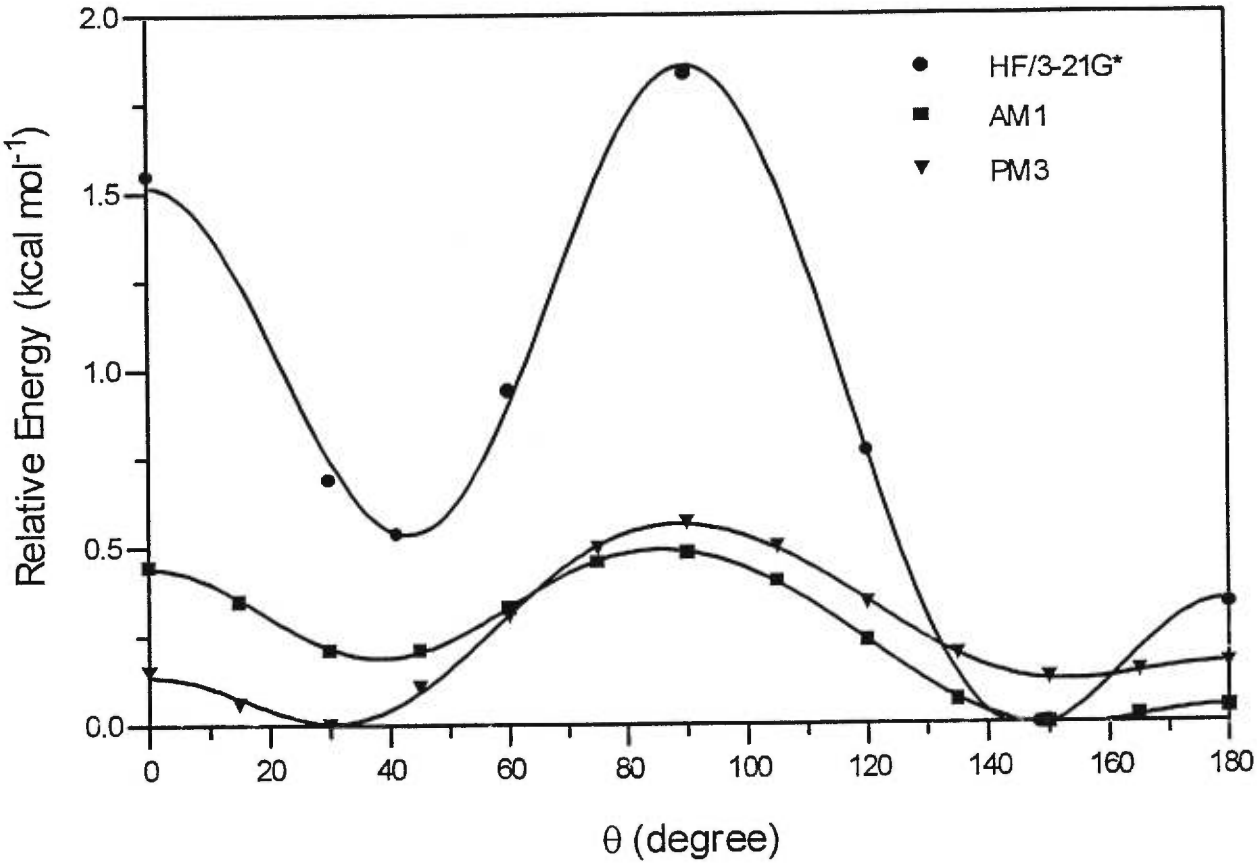

Figure 2. Potential energy curve of DMO44BT as obtained from semiempirical (AM1, PM3) and *ab initio* (HF/3-21G*) calculations.

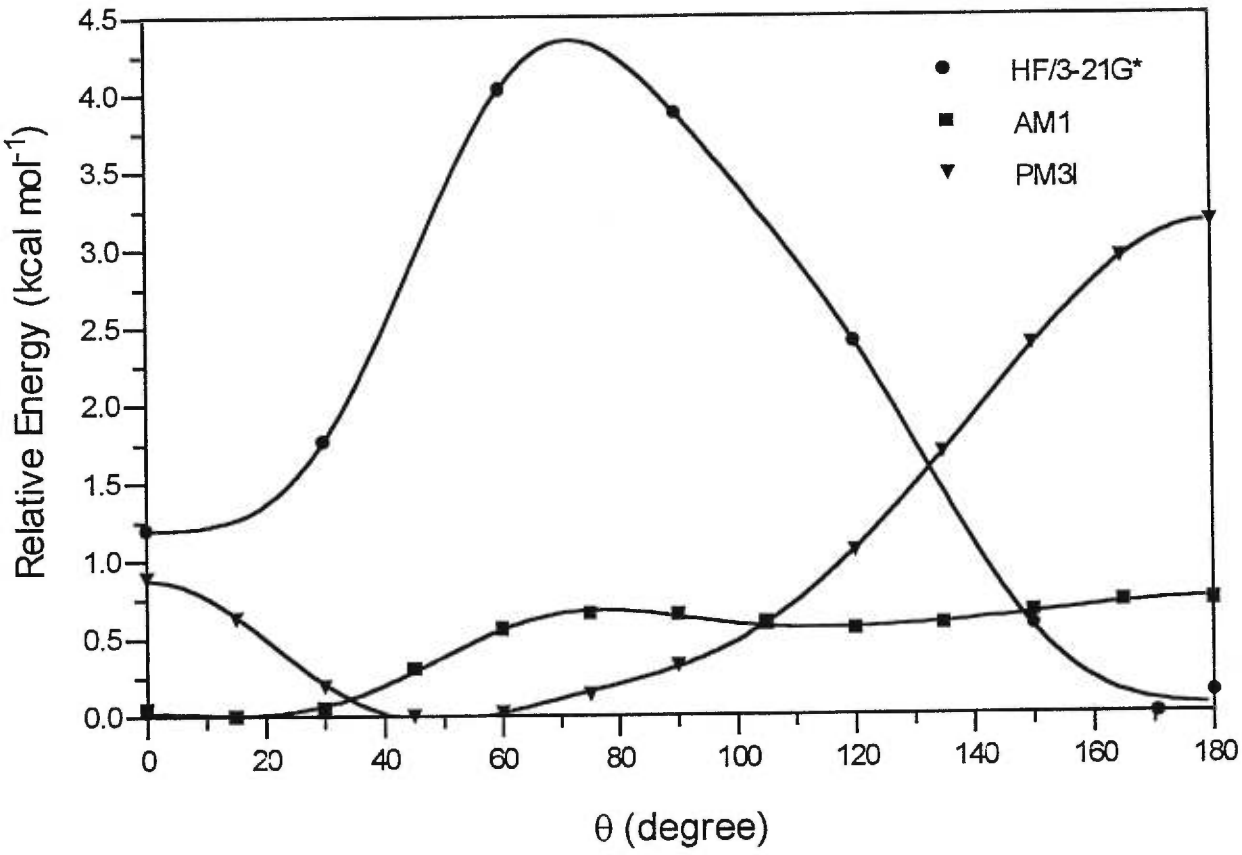

Figure 3. Potential energy curve of DMO34BT as obtained from semiempirical (AM1, PM3) and *ab initio* (HF/3-21G*) calculations.

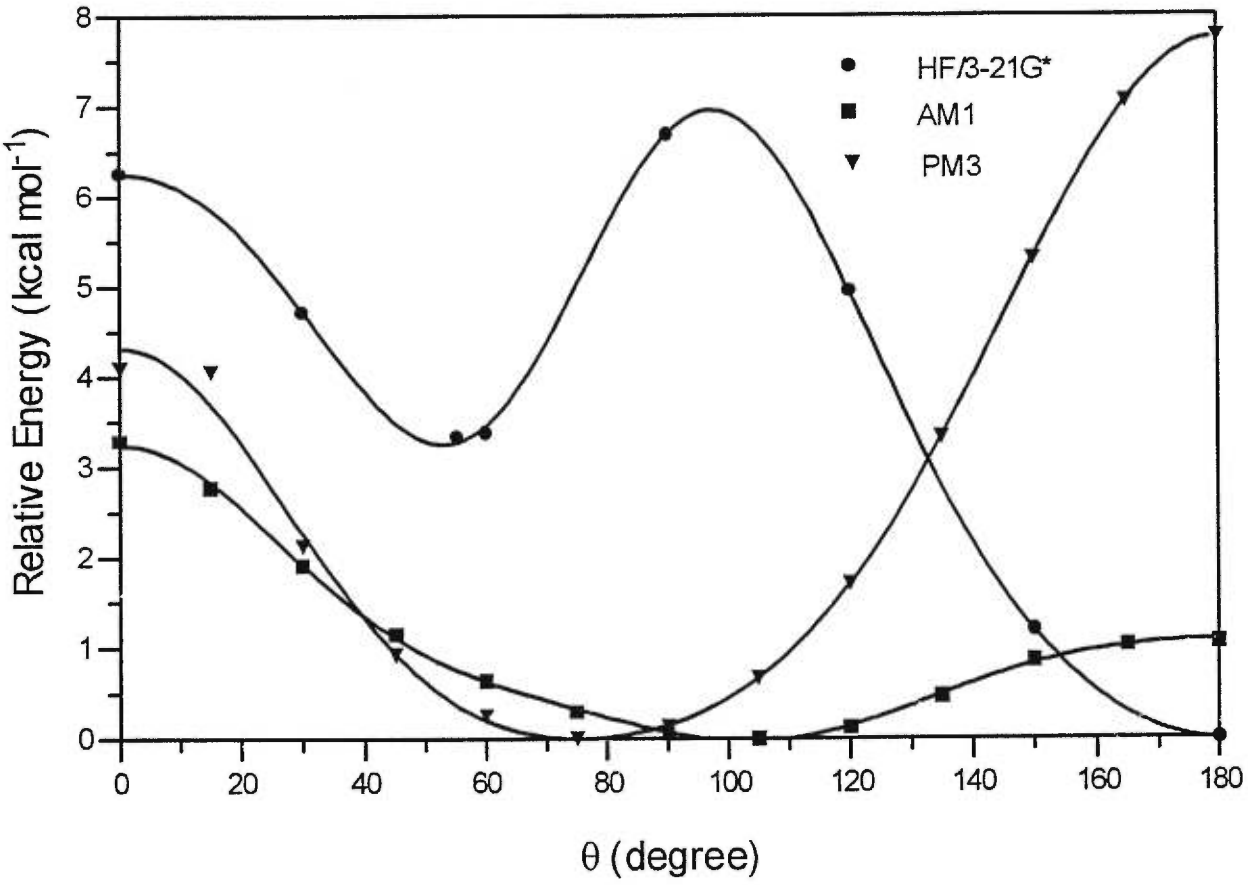

Figure 4. Potential energy curve of DMO33BT as obtained from semiempirical (AM1, PM3) and *ab initio* (HF/3-21G*) calculations.

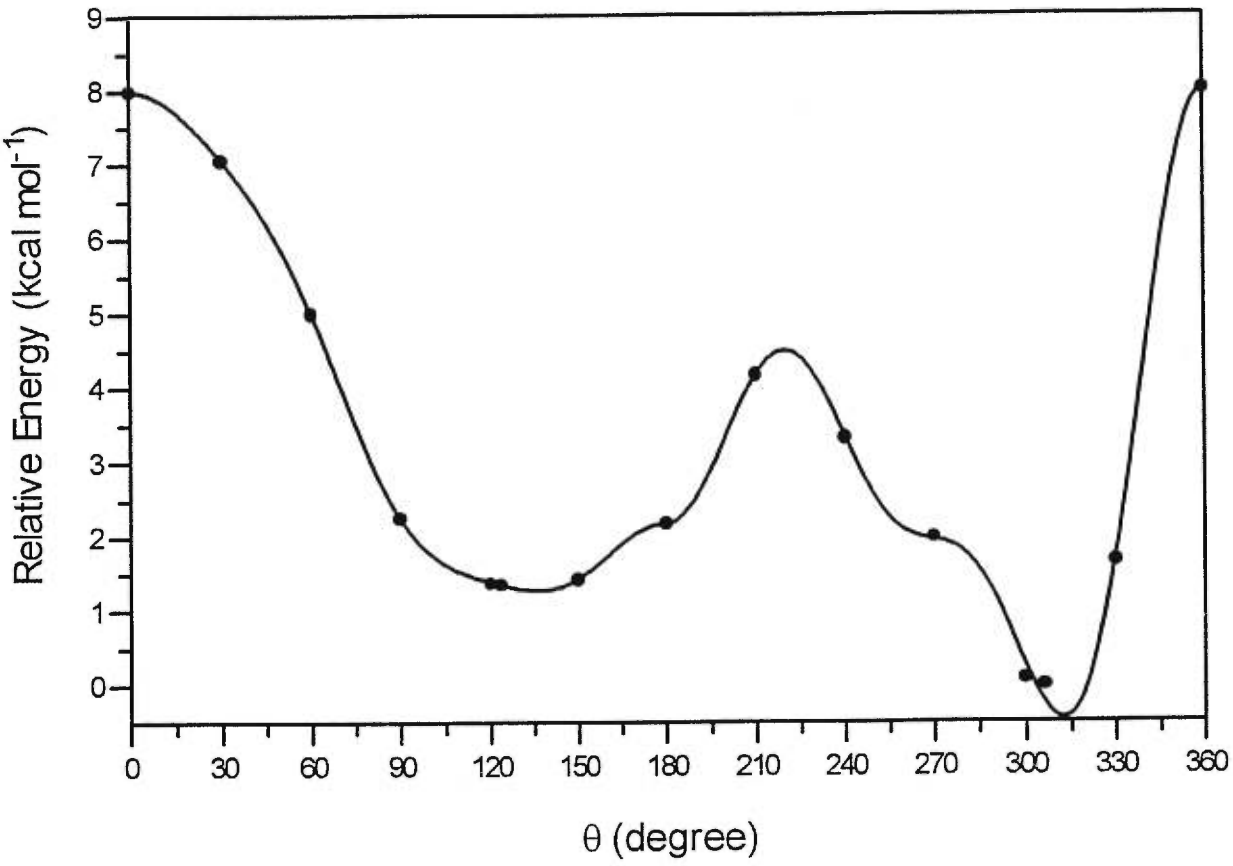

Figure 5. Potential energy curve of DMODM34BT as obtained from the HF/3-21G* *ab initio* calculation.

Chapitre 4

Étude structurale et conformationnelle de dérivés alkylthios du 2,2'-bithiophène

Ce chapitre présente la dernière partie des analyses conformationnelles sur les dimères substitués. Dans ce chapitre, il sera question des substituants alkylthio, plus précisément de groupes méthylthio substitués en position 3 (et/ou 3') et 4 (et/ou 4'). Il sera aussi question d'une molécule combinant des groupes méthylthios et méthyles.

Comme discuté dans les deux chapitres précédents, les surfaces d'énergie potentielle sont présentées et discutées en termes d'encombrement stérique et d'effet électronique (tel que discuté avec les substituants méthoxys). Les résultats montrent que l'insertion de deux groupes méthylthios en position 3,3' crée une importante torsion entre les cycles thiophènes. Cet effet est dû à la grosseur des groupes méthylthios (spécialement celle du soufre) qui crée un encombrement stérique important. Cet encombrement stérique est tout de même moins important comparativement aux substituants éthyles (chapitre 2). Comme le soufre fait partie de la même famille que l'oxygène, on pourrait s'attendre à observer un effet électronique similaire à celui observé avec les substituants méthoxys (chapitre 3). Ceci n'est pas le cas à cause de la moins grande électronégativité du soufre. L'encombrement stérique compense cet effet électronique et cause l'importante torsion calculée. Par contre, pour le bithiophène substitué en position 3,4' par des méthylthios, l'encombrement stérique créé par un substituant méthylthio est moins important et l'effet électronique est moins négligeable. La surface d'énergie

potentielle de cette molécule est similaire à celle obtenue pour le BT montrant que l'effet électronique et l'encombrement stérique se compensent mutuellement. Naturellement, lorsque l'on combine un méthylthio en position 3 et un méthyle en position 3', l'encombrement stérique est tel que l'on obtient une molécule très tordue.

Dans la dernière partie de cet article, les résultats spectroscopiques du 3,3'-dibutylthio-2,2'-bithiophène (DBS33BT) seront présentés. Ces résultats complètent les résultats expérimentaux présentés au chapitre 1. Ces résultats sont présentés dans ce chapitre puisque la molécule n'était pas disponible lors de la publication de l'article présenté au chapitre 1. Les données spectroscopiques du DBS33BT sont également comparées à celles du BT, du DE33BT et du DBO33BT. Les résultats montrent l'importante torsion entre les cycles thiophènes du DBS33BT en accord avec les calculs théoriques présentés.

4.1 Article 4 : Molecular structure and conformational analysis of some alkylthio-substituted bithiophenes. Theoretical and experimental investigation

Article publié dans The Journal of Physical Chemistry A, volume 102, numéro 16, pages 2700-2707 (1998).

Molecular Structure and Conformational Analysis of Some Alkylthio-Substituted Bithiophenes. Theoretical and Experimental Investigation

Nicolas DiCésare [a], Michel Belletête [a], Francois Raymond [b], Mario Leclerc [b] and Gilles Durocher [a]

[a] Laboratoire de photophysique moléculaire
[b] Laboratoire des polymères électroactifs et photoactifs

Département de Chimie, Université de Montréal,
C.P. 6128, Succ. A, Montréal, Québec, H3C 3J7, Canada

Abstract

The conformational analysis and molecular structure of 3,3'-dimethylthio-2,2'-bithiophene (DMS33BT), 3,4'-dimethylthio-2,2'-bithiophene (DMS34BT) and 3,4'-dimethylthio-3,4'-dimethyl-2,2'-bithiophene (DMSDM34BT) were investigated by *ab initio* calculations at the Hartree-Fock level (HF/STO-3G and HF/3-21G*) as well as by semiempirical calculations [Austin Model 1 (AM1) and Parametric Method 3 (PM3)]. *Ab initio* calculations (HF/3-21G*) indicated that the insertion of two alkylthio chains in the 3,3' positions creates a sufficiently high steric hindrance to twist the molecule to a minimum conformation at 71.0° (and a second minimum at 120°), with an energy barrier of 2.3 kcal mol^{-1} compared with the coplanar *trans* (180°) conformation. For this molecule (DMS33BT), one can see an absorption band characteristic of a twisted molecule with a large range of conformations. The fluorescence spectrum demonstrates that the molecule adopts, in the first singlet excited state, a less twisted conformation. The presence of only one alkylthio substituent in the 3-position (DMS34BT) decreases the steric hindrance such that a

less twisted conformation (141.5°, (HF/3-21G*)) is obtained, with a lower energy barrier of 0.5 kcal mol^{-1}. The insertion of an alkylthio and a methyl group in the 3,3' positions (DMSDM34BT) creates the maximum steric hindrance and the more twisted molecule (102.2°), with the higher energy barrier compared with the planar conformation (5 kcal mol^{-1}). It is concluded from these results that the steric hindrance created by an alkylthio group is less than that of a methyl or an ethyl group in the same positions. It is also shown that the *ab initio* HF/STO-3G and the semiemperical AM1 and PM3 calculations are not sophisticated enough to predict good energy minimum conformers and potential energy surfaces for these kinds of molecules.

1. Introduction

Polythiophenes are frequently studied because of their high conductivity [1] in the doped state and also because of their interesting optical properties [1,2]. These properties make polythiophene a good candidate for electronic and optoelectronic composites [3,4]. To improve the solubility of polythiophene, new substituted polythiophenes with different lateral chains have been synthesized [5-10]. These substituted polythiophenes show new interesting optical properties, such as thermochromism and solvatochromism [8-11]. Variation in the optical properties of the different substituted polymers are related to the change of conformation of the backbone caused by the lateral chain. To have a good description of the conformation and of the effects of the position and nature of the substitution on the optical properties of polythiophene, theoretical and experimental studies of well-defined substituted oligothiophene models have been very useful. Recently, the conformations and spectroscopic properties of bithiophene (BT) and of some alkyl- and alkoxy- substituted bithiophenes have been studied [12-16]. Also, the potential energy surfaces of a series of substituted BTs have been used to obtain a theoretical understanding of the thermochromism observed in the parent polymers [17]. These

results have successfully correlated the potential energy surface of the dimer with the thermochromism of many polymers and have allowed to successful predictions of the 3,3'-dimethylthio-2,2'-bithiophene (DMS33BT) polymeric system [18].

To date, the conformational analysis of BT [19,20] and some alkyl derivatives [21,22] have been well studied by *ab initio* calculations as well as by semiempirical calculations [12,13,23]. The potential energy surface of bithiophene is well defined by using *ab initio* HF/3-21G* and more elaborated basis sets. On the other hand, using the *ab initio* HF/STO-3G basis set and semiempirical calculations [Austin Model 1 (AM1) and Parametric Method 3 (PM3)], the potential energy surface is not defined with sufficient accuracy [12,13]. It is interesting to note that the semiempirical method AM1 predicts similar conformers than those obtained with more elaborated methods but with smaller rotational energy barriers. From the most elaborate methods, two minima are obtained, one at 30° and the global minimum at 150°. Three maxima are found: one at 0°, a second at 90°, and one at 180°. The rotational energy barrier between 0° and 30° is ~1.3 kcal mol^{-1}, the rotational barrier at 90° is ~1.5 kcal mol^{-1}, and a low rotational barrier, 0.5 kcal mol^{-1}, is obtained between 150° and 180°. For BT and substituted BTs, two important forces determine the conformation and the rotational barrier of the molecule. One force is the electron delocalization throughout the molecule, which favors a planar conformation, and the second force is the steric hindrance between the sulfur atom and the group of atoms in the 3-position, a hydrogen atom in the case of BT, which is responsible for the twisting of the molecule.

For the first time, we propose in this paper a theoretical analysis of alkylthio substituents on BT. The effects of the nature and of the position of the substituent are discussed together with the potential energy surfaces and the geometry. It is shown that the insertion of two alkylthio lateral chains in the 3,3'-positions creates sufficiently high steric hindrance to induce a large twisting of the molecule. The presence of only one alkylthio lateral chain in the 3-position creates less steric hindrance and gives rise to a molecular structure much less twisted, near the

conformation of BT. The presence of an alkylthio and a methyl group in the 3,3'-positions, on the other hand, create the most important steric hindrance, with a concomitant high rotational energy barrier compared with the planar *trans* conformation. It is also shown that the basis set HF/STO-3G from *ab initio* calculations and the semiempirical AM1 and PM3 methods are not sophisticated enough in comparison with the *ab initio* HF/3-21G* basis set to make good predictions on the minimum energy conformers and on the potential energy surfaces. The molecular structures investigated are shown in Figure 1.

2. Methodology

2.1. *Ab initio* calculations

The *ab initio* calculations were performed on a Silicon Graphics Challenge R4000 work station at the University of Montreal using the Gaussian 90 program [24]. The conformational analysis was done by changing the torsional angle θ by 30° steps. The geometries were optimized at the Hartree-Fock (HF) level with the STO-3G and 3-21G* basis sets. The Berny analytical gradient method was used for the optimizations. In the geometry optimization of the DMS33BT, a locally C_2 symmetry restriction was applied between the two rings to reduce the calculation time, but no constraint was applied to the side groups. No constraint was applied on the other molecules. The requested HF convergence on the density matrix was 10^{-8}, and the threshold values for the maximum force and the maximum displacement were 0.00045 and 0.0018 a.u. (atomic unit), respectively. To obtain the final torsional angles of the most stable conformers, calculations of these geometries were performed without constraint on the dihedral angle.

2.2. Semiemperical calculations

Semiempirical calculations were performed using the HYPERCHEM package, release 4.5, for Windows from Hypercube, Inc., on a Pentium personal computer. This package has been used to draw the molecules and roughly optimize their geometry using the MM+ force field, which is an extension of MM2 developed by Allinger [25]. A more precise geometry optimization was obtained using the AM1 or PM3 semiempirical methods, including the sulfur atom parameter. AM1 is a modified MNDO method proposed and developed by M.J.S. Dewar and co-workers at the University of Texas at Austin [26-29]. For all derivatives, the dihedral angle (θ) between the two thiophene rings was varied in 15° increments from planar *trans* conformation ($\theta = 180°$) to the planar *cis* conformation ($\theta = 0°$). For each increment, θ was held fixed while the remainder of the molecule was optimized using AM1. A root-mean-square (rms) gradient in the energy of 0.1 kcal mol^{-1} was use for the optimization criterion.

2.3. Materials

Hexane was purchased from Aldrich Chemicals (99+%, anhydrous) and used as received. Prior to use, the solvent was checked for spurious emissions in the region of interest and found to be satisfactory. The synthesis of 3,3'-dibutylthio-2,2'-bithiophene (DBS33BT) will be described in a forthcoming publication [18]. All NMR and elemental analysis data were consistent with the expected structure.

2.4. Instrumentation

Absorption spectra were recorded on a Varian spectrometer model Cary 1 Bio using 1-cm path length quartz cells and a solute concentration of 2.18×10^{-5} M. It

has been shown that the Beer-Lambert law applies for the concentration used. Fluorescence spectra corrected for the emission detection were recorded on a Spex Fluorolog-2 spectrophotometer with a F2T11 special configuration. The excitation and emission band-passes used were 2.6 and 1.9 nm, respectively. Each solution was excited near the absorption wavelength maximum using a 1-cm path length quartz cell, and the concentration used was 2.18×10^{-5} M, giving an absorbance near 0.1 to avoid any inner filter effects. A study was made of the effect of concentration (C) on the fluorescence intensity (I_F), and all measurements were made in the linear region of the I_F versus C curve.

3. Results and Discussion

We have used the HF/3-21G* method as the more elaborated calculation in this paper to have reasonable calculation times and because this basis set gives similar results in comparison with more elaborated basis sets. We used the results obtained with this basis set for comparison with the other methods. For BT, it was shown that a basis set without polarization functions is not good enough to predict good potential energy surfaces [19,22]. Methods and basis sets HF/3-21G* [20,21], HF/6-31G* [20,22], HF/6-31G** [21], HF/6-311G** [22], and MP2/6-31G* [20] give very similar potential energy surfaces with the same minima and similar potential energy barriers. For the alkyl-substituted bithiophenes in the 3,3'-positions [21], it is also clear that the HF/3-21G* and the HF/6-31G** basis sets give identical potential energy surfaces with similar energy barriers and minima. From these results, the use of polarization functions seems essentials and the HF/3-21G* is the minimal basis set acceptable for the determination of potential energy surfaces. Moreover, results obtained with the basis set HF/3-21G* have been recently shown to give a very good correlation between the calculated conformation and the rotational energy barrier of substituted BTs and the experimental optical properties of the parent polymer [17].

If one compares the structural parameters of BT with the basis set HF/3-21G* [21], HF/6-31G* [20], HF/6-31G** [21], and MP2/6-31G* [20], very similar values are obtained. Indeed, we have compared the optimized geometries obtained from HF/3-21G*, HF/6-31G*, and MP2/6-31G* with experimental results from electron-diffraction [30]. Standard deviations (SDs) on the bond lengths (including carbon-hydrogen bond lengths) of 0.024 Å for HF/3-21G*, 0.024 Å for HF/6-31G*, and 0.022 Å for MP2/6-31G* are obtained. For the angles, SDs of 0.81° for HF/3-21G*, 1.04° for HF/6-31G*, and 1.10° for MP2/6-31G* are obtained. Now, if we compare the calculated planar *trans* conformations with the crystallographic results [31], which show BT as planar, we obtain for bond lengths (excluding carbon-hydrogen bond lengths) SDs of 0.035 Å for HF/3-21G*, 0.037 Å for HF/6-31G* and 0.027 Å for MP2/6-31G*. For the angles, we obtain SDs of 6.4° for HF/3-21G*, 6.5° for HF/6-31G*, and 6.5° for MP2/6-31G*. From these data, one can see that the MP2/6-31G* method seems to give better results on bond lengths but not necessarily on bond angles. The results obtained using the two other Hartree-Fock methods on bond lengths are very close to those obtained from MP2/6-31G*.

We have also confirmed that even the semiempirical methods (AM1 and PM3) give good structural parameters on BT such that any differences observed in the potential energy surfaces based on the dihedral angle from one calculation to the other cannot be ascribed or correlated to any structural parameter defects. In the following, the molecular structures as obtained from HF/3-21G* will be described and a comparison of the energy surfaces, based on the dihedral angle, calculated from various methods will be discussed.

3.1. 3,3'-Dimethylthio-2,2'-bithiophene (DMS33BT)

The potential energy surfaces of DMS33BT calculated from various methods are represented in Figure 2. The rotational barrier and the minimum conformations calculated from HF/3-21G* are shown in table 1. Very shallow minima are obtained

at 71.0° and at 120°. The geometry at 120° was optimized without constraint on the dihedral angle and we obtained a relaxed conformation at 73.8°, which is very close to the 71.0° angle previously obtained. For this reason we can confirm that the minimum obtained at 71.0° in Figure 2 is the global minimum. The energy barrier between these two minima is very low, 0.11 kcal mol^{-1}. In comparison with kT at room temperature (298 K), 0.59 kcal mol^{-1}, one can expect that many conformers will coexist at room temperature in solution or in the gas phase. At 180°, we obtain a rotational barrier of 2.3 kcal mol^{-1}. This barrier corresponds to the steric hindrance existing between the methylthio side group and the sulfur atom of the thiophene ring. This rotational barrier is very similar to that obtained with one ethyl side group in the 3-position [32], but is higher than the one obtained with one methyl group in the 3-position [21,22]. From these results, one can see that the presence of two methylthio groups creates the same steric hindrance as one ethyl side group. In other words, the steric hindrance of one methylthio group is less than that of one ethyl side group as will be shown later for 3,4'-dimethylthio-2,2'-bithiophene (DMS34BT). For the co-planar *syn* conformation ($\theta = 0°$), one obtains a high rotational barrier of 13.6 kcal mol^{-1} because of the steric hindrance caused by the presence of two lateral chains very close each other. This rotational barrier is smaller than that found for the 3,3'-diethyl derivative [32], showing that two methylthio groups on the same side of the molecule create less steric hindrance than two ethyl groups at the same positions.

Using the basis set HF/STO-3G, one obtains a potential energy surface very similar to that calculated from HF/3-21G*. This basis set predicts two minima, at 61.1° and 124.8°. The barrier at 90° is higher but the rotational barrier at 0° is lower. The barrier at 180° is also similar with that calculated from HF/3-21G*. For this molecule, one can see that HF/STO-3G is quite good though it cannot reproduce the fine details of the more elaborate basis set and it gives always a higher rotational barrier at 90° and a lower barrier for the *syn* conformation. The same behaviour has been found for BT [33,34] and alkyl derivatives [32]. As for the semiempirical AM1 calculations, the potential energy surface obtained is not at all realistic. The

minimum obtained is for the coplanar *syn* conformation where there is the larger steric hindrance. For PM3, the surface looks better. We obtain the global minimum at 90° but the energy falls off for the planar conformations, *syn* and *anti*, which is not realistic either. It is surprising that the results obtained by these two semiempirical methods are so different because they were much more similar when applied to BT. These results were rather similar to the *ab initio* results [23,35], except that the rotational barriers were largely underestimated compared with that obtained at the *ab initio* level.

The molecular structure parameters of the lowest energy conformer of DMS33BT using the four theoretical methods already described are listed in Table 2. A restricted C_2 symmetry between the two thiophene rings has been applied such that only parameters of one thiophene ring and one side group is shown. From the results in Table 2 we can see that few parameters are quite different from one method to another. The bond length between the two thiophene rings, C2-C2', is much higher for *ab initio* methods than for semiempirical methods. The double bonds in the thiophene ring, C2-C3 and C4-C5, are predicted to be smaller by the *ab initio* calculations in comparison with the semiemperical methods. This result shows the difference in the electronic distribution is taken care of by the *ab initio* and semiemperical methods. The bond lengths between the sulfur atom and carbons in the ring, S1-C2 and C5-S1, are much smaller for the AM1 method compared with other methods which is the reason the potential energy barrier calculated by *ab initio* methods are higher than those obtained by semiempirical methods for the planar conformation (180°). These small bond lengths explain the favored planar conformation calculated by AM1 because of the more compact ring giving rise to less steric hindrance between the sulfur atom and the group in the adjacent thiophene ring. Another difference is the bond length of the carbon and the sulfur of the side group, C3-Sa, which is larger for the *ab initio* methods compared with semiemperical methods. It is also noteworthy that the side group is perpendicular to the thiophene ring (C2-C3-Sa-Cb ~94°) for HF/3-21G*, which decreases the

resonance of the nonbonding electron lone-pair on the sulfur atom with the aromatic ring.

The absorption and fluorescence spectra of BT, DBS33BT, and decyl- and butoxy- substituted bithiophenes in the 3,3'-positions are shown in Figure 3 and the spectroscopic parameters for these molecules are reproduced in Table 3. The absorption spectrum of BT has already been discussed [13]. The first absorption band is well explained by using a twisted angle of 150° with a certain distribution of conformers. The absorption spectrum of 3,3'-dibutoxy-2,2'-bithiophene (DBO33BT) is characteristic of a planar conformation [36]. On the other hand, the absorption spectrum of 3,3'-didecyl-2,2'-bithiophene (DD33BT) is characteristic of a twisted conformation of ~100°, as shown recently [12]. Figure 3A shows that the absorption band maximum of DBS33BT is not far from that of DD33BT, and in both cases the absorbtivity coefficient is less than that of BT and DBO33BT. This result clearly shows that DBS33BT is on the average much more twisted than BT or DBO33BT but probably a little less than DD33BT. Indeed, the minimum obtained by HF/3-21G*, 120° (or 71.0°), is between the minima of BT (150°) [20] and DE33BT (101.5°) [32], which shows the good evaluation of the minimum energy conformer by using the HF/3-21G* basis set.

We can see that the absorption band of DBS33BT is spread over a large wavelength region. The part of the band in the region of lower energy shows the presence of more planar conformers. The absorption band of DBS33BT extends to the red of that of DBO33BT in the region of 27 500 cm^{-1}, this suggesting that the methylthio group has better electron donor properties compared with the butoxy group. This result is in agreement with the spectral data observed on substituted thiophenes. Indeed the maximum of the absorption band of thiophene is at 231 nm [37], that of 3-methoxythiophene is at 255 nm [37], and that of the 3-methylthiothiophene is at 270 nm [38]. The same behavior has been observed on the 4,4'-substituted-2,2'-bithiophenes [12,39,40]. It is worth mentioning that ZINDO/S calculations performed on HF/3-21G*-optimized geometries of DMO33BT and

DMS33BT do not predict the methythio substituent as a better electron donor group. Indeed the calculated energies of the first electronic transition of each compound are very similar.

DBS33BT possesses a very particular absorption spectrum that allows for many possible conformers at room temperature because the rotational energy barrier is quite low (see Figure 2 and Table 1). We have already mentioned that the minima of the potential energy surfaces of DMS33BT and of the ethyl substituents in the 3,4'-positions are in the same position and that the surfaces between 90° and 180° are very similar. In agreement with these results, it is observed that the absorption spectra of DBS33BT and 3-octyl-2,2'-bithiophene (O3BT) [14] (parameters are reported in Table 3) are much blue-shifted in comparison with the BT absorption spectrum. These spectra are also very wide, which is a characteristic of twisted molecules with a large distribution of conformers. However, it is worth pointing out that the first absorption band of DBS33BT shows a larger blue-shift, is less intense and is spread over a larger region compared with that of O3BT.

The fluorescence spectrum of DBS33BT shows a large red-shift in comparison with the absorption band (the Stokes shift is 11300 cm^{-1}) and a decrease of the bandwidth. For the BT derivatives, it is well-known that, in the first excited singlet state, the planar conformation is favored [12]. The spectral data reported here lead us to the same conclusion for this molecule. However, the fluorescence band of DBS33BT is much red-shifted in comparison with that of alkyl- and alkoxy-substituted BTs (see Table 3). This result is in agreement with the assumption already mentioned that the methylthio substituent is a better electron donor group than alkyl and alkoxy substitutents. But another contribution to the red shift observed may also involve conformational changes of the methylthio group in the excited state. Indeed in the ground state, *ab initio* calculations performed at the HF/3-21G* level predict that this side group is perpendicular to the molecular frame (see Table 2). Thus, it is quite possible that in the first relaxed singlet excited state, the

methylthio group reaches a less twisted conformation, which should induce a better electronic delocalization along the molecular frame.

3.2. 3,4'-Dimethylthio-2,2'-bithiophene (DMS34BT)

The potential energy surface of DMS34BT is presented in Figure 4. From the basis set HF/3-21G*, two minima are obtained: one minimum at θ = 50° and the global minimum at 141.5°. Three maxima are also obtained, at θ = 0°, 90°, and 180°. The rotational barrier for these maxima are listed in Table 1. For this molecule, the steric hindrance created by only one alkylthio group is smaller and one obtains a less twisted conformation in comparison with the 3,3'-substituted compound. If one compares the potential energy surfaces of DMS34BT and BT [19,20], it is seen that these two surfaces are quite similar. The minimum energy conformations of each molecule are close; for BT there are two minima, one at 44.7° and the global minimum at 146.3°. The energy barriers are also very similar, for BT, the barrier at 180° is 0.39 kcal mol^{-1} in comparison with 0.31 kcal mol^{-1} for DMS34BT: at 90°, the barrier for BT is 1.49 kcal mol^{-1} compared with 0.86 kcal mol^{-1} for DMS34BT; and at 0°, the barrier for BT is 1.72 kcal mol^{-1} in comparison with 2.1 kcal mol^{-1} for DMS34BT. These similarities do not mean that the steric hindrance caused by an alkylthio group is similar to that of a hydrogen atom in the unsubstituted BT. It is more plausible that the more planar conformation obtained for DMS34BT is due to the donor effect of the alkylthio group that improves the delocalization over the molecular frame, which favors the planar conformation. The delocalization effect of a donor group in position 3 has also been clearly demonstrated with the results on the alkoxy substituted BTs [36]. The maximum of the absorption band of DMS34BT is at 331 nm [39,40], wich is at the same position as the 4,4'-methylthio-2,2'-bithiophene (327 nm) [39,40]. The absorption spectra of these two compounds are very similar [38], except for the second transition, at 265 nm, where the intensity in comparison with the intensity of the first transition is higher for the 4,4'-substituted

derivative. As already mentioned, the substitution in the 4,4'-positions does not influence the conformation [12] and a minimum conformation at 150° is expected for the 4,4'-derivative with a similar potential energy surface as that of BT. The fact that the 3,4'-derivative possesses a similar spectrum suggests that the conformation and the distribution of conformers in solution are rather identical to those of the 4,4'-substituted derivative and also nearly identical as those of BT.

The *ab initio* HF/STO-3G basis set gives a similar potential energy surface but the two minima are moved in the direction of the more planar conformations. This shift of the minima is also observed in the case of BT where the two minima are at 180° and 0°. We have observed that the HF/STO-3G basis set favored the planar conformations for many molecules [32,36], except for the molecules with very high steric hindrance. This shows the inability of this basis set to calculate the fine details in the conformational analysis of the thiophene oligomers. The rotational barrier at $\theta = 90°$ is also often larger than the energy barrier obtained by HF/3-21G*. It seems that the HF/STO-3G basis set put to much emphasis on the delocalization rather than on the nonbonded interactions, in other words, HF/STO-3G underestimates the steric hindrance and/or overestimates the electronic delocalization. Finally, for this molecule, AM1 calculations failed again. The minimum obtained, $\theta = 175°$, is close to one of the minima obtained by the *ab initio* methods but the other part of the curve makes no sense. The potential energy surface obtained by PM3 calculations gives a preference for the *syn* conformer. We obtained the global minimum at 30° and a local minimum at 180°. This preference of the *syn* conformation for PM3 calculations has also been found for BT [23,34] and the reasons were then discussed [35].

The optimized geometries of the lowest energy conformers for each theoretical method are presented in Table 4. The geometric parameters of DMS34BT and of DMS33BT, for the HF/3-21G* basis set, are very similar without any important difference except for the angles between the two cycles, C2'-C2-C3 and C2-C2'-C3', which are larger for the latter compound. For the asymmetric

DMS34BT, some structural parameters of each thiophene ring differ. The bond length C2-C3 is smaller than the bond length C2'-C3' and the bond C4-C5 is larger than the bond C4'-C5'. The angles C2'-C2-C3 and C2-C2'-C3' are also different. These differences show clearly the effect of the steric hindrance caused by the alkylthio group in position 3 and the possibility of the asymmetric molecule to adopt a conformation that will favor a less twisted conformation with a lower rotational barrier. Again for this molecule, the position of the two alkylthio groups is perpendicular to the plane of the thiophene ring. As for the difference between the methods, again, the bond length between the two cycles, C2-C2', is smaller for the semiemperical methods. As for the other geometric parameters, the same effects observed for the DMS33BT can also be observed here.

3.3. 3',4-Dimethyl-3,4'-dimethylthio-2,2'-bithiophene (DMSDM34BT)

The potential energy surface of DMSDM34BT is shown in Figure 5, which shows one minimum at 102.3°, a rotational barrier of 4.5 kcal mol^{-1} at $\theta = 180°$, and a barrier of 15.0 kcal mol^{-1} at $\theta = 0°$. The minimum obtained for this molecule is approximately at the same position as that observed for the 3,4'-dimethyl-2,2'-bithiophene [21] and the 3,4'-diethyl-2,2'-bithiophene [32]. But, the rotational barriers for both planar conformations are higher for the DMSDM34BT than for the diethyl substituents in the 3,4-positions. From these results, it is clear that the methyl group in the 3-position in DMSDM34BT creates a more important steric hindrance and is responsible for the twisted conformation. The presence of the alkylthio group in the 3-position does not play an important role in the determination of the conformation of the molecule, as seen for DMS34BT, which presents a similar potential energy surface as BT but plays a more important role in the rotational barrier as indicated by the comparison of the potential energy surface of DMSDM34BT and DM34BT [21]. At $\theta = 0°$, the presence of the two substituents face to face creates the maximum steric hindrance and is responsible of the high

rotational barrier. This rotational barrier is grossly identical to that observed for the 3,3'-dimethyl and 3,3'-diethyl-2,2'-bithiophene [21,32]. The rotational barrier at 180° is higher for DMSDM34BT because there are two substituents in the 3-position such that the molecule cannot relax like the asymmetric one (DMS34BT). Rather, this barrier at 180° for DMSDM34BT is of the same order as those of the methyl and ethyl substituents in the 3,3'-positions.

The potential energy surface for the *ab initio* HF/STO-3G basis set is relatively similar to that obtained by HF/3-21G*. The important difference is that HF/STO-3G gives a less twisted conformation, at 120°, but the rotational barriers at 180° are predicted to be very similar by both methods. For this molecule, AM1 failed to predict the minimum conformation and the potential energy surface. Calculations on BT [13,23] and on alkyl-substituted BT [12,23] by AM1 were good enough to predict the minimum conformations and for the determination of rotational barriers but not for this molecule containing these kinds of lateral chains. PM3 can reproduce quite well the potential energy surface except for the planar *trans* conformation, where one observes a shallow minimum.

The structural parameters for the lowest energy conformation are listed in Table 5. The angle C2'-C2-C3 is greater for DMSDM34BT than for DMS33BT. This difference can be correlated with the higher steric hindrance caused by the presence of the methyl group in the 3-position, which forces the two rings to adopt this conformation to reduce the steric hindrance. When we compare the structural parameters of DMSDM34BT with those of DMS34BT, we can see that the structural parameters of the two rings for the former are very similar, which is in contrast with the asymmetric DMS34BT. As observed in the other molecules, the bond length C2-C2' obtained by HF/STO-3G is the largest and it is the smallest from AM1. All the methods give a twisted conformation (C2-C3-Sa-Cb) for the alkylthio group in the 3-position, but HF/STO-3G and the semiempirical methods suggest a planar conformation for the alkylthio group in the 4'-position.

4. Concluding Remarks

The results reported here show that insertion of two alkylthio substituents in positions 3,3' creates a sufficiently important steric hindrance to twist the molecule. The potential energy surface of this molecule is very similar to those obtained for the 3,4'-dimethyl- and 3,4'-diethyl-2,2'-BTs. The low rotational energy barrier allows for the presence of many conformations, which is responsible for the wide, diffuse and unstructured absorption spectrum observed. The electron donor property of the alkylthio group is important, so the fluorescence is red-shifted in comparison with that of the alkyl- and alkoxy-substituted BTs. The blue-shift of the absorption band caused by the twisted conformations and the red-shift of the fluorescence band caused by the electron donor properties of a more planar conformer are responsible for the very large Stokes shift observed that characterizes the spectral properties of this 3,3`-substituted derivative. The presence of only one alkylthio lateral chain does not create such a large steric hindrance and gives rise to a potential energy surface that is very similar to that of BT. The presence of the methyl group in the DMSDM34BT is responsible for the twisted conformation obtained for this molecule, but the presence of the alkylthio group in the 3-position creates a sufficiently high steric hindrance to give a high rotational barrier for the planar *trans* conformation. The semiemperical AM1 method fails in the determination of the minimum energy conformer and potential surfaces of these kinds of substituted molecules. On the other hand, HF/STO-3G and the semiemperical PM3 method give better results. Amongst the theoretical methods investigated in this paper, however, the *ab initio* HF/3-21G* method is the only one capable to explaining the fine details of the energy surfaces necessary to make good correlations with experiments.

Acknowledgement.

The authors are grateful to the Natural Sciences and Engineering Research Council of Canada (NSERC) and the fonds FCAR (Quebec) for their financial support. N.D.C. and F.R. are grateful to the NSERC for a graduate scholarship.

References and Notes

[1] Schopf, G.; Kossmehl, G. *Adv. Polym. Sci.* **1997**, *127*, 1.

[2] Busisio, R.; Botta, C.; Colombo, A.; Destri, S.; Porzio, W.; Grilli, E.; Tubino, R.; Bongiovanni, G.; Mura, A.; Di Silvestro, G. *Synth. Met.* **1997**, *87*, 23.

[3] Kunugi, Y.; Miller, L.L.; Maki, T.; Canavesi, A. *Chem. Mater.* **1997**, *9*(5), 1061.

[4] Katz, H.E. *J. Mater. Chem.* **1997**, *7*(3), 369.

[5] Zotti, G.; Salmaso, R.; Gallazzi, M.C.; Marin, R.A. *Chem. Mater.* **1997**, *9*, 791.

[6] Goldoni, F.; Iarossi, D.; Mucci, A.; Schenetti, L.; Zambianchi, A. *J. Mater. Chem.* **1997**, *7*(4), 593.

[7] Buvat, P.; Hourquebie, P. *Macromolecules* **1997**, *30*, 2685.

[8] Leclerc, M.; Fréchette, M.; Bergeron, J-Y.; Ranger, M.; Lévesque, I.; Faïd, K. *Macromol. Chem. Phys.* **1996**, *197*, 2077.

[9] Roux, C.; Bergeron, J-Y.; Leclerc, M. *Makromol. Chem.* **1993**, *194*, 869.

[10] Ingagnas, O. *Trends Polym. Sci.* **1994**, *2*, 189.

[11] Langeveld-Voss, B.M.W.; Peeters, E.; Janssen, R.A.J.; Meijer, E.W. *Synth. Met.* **1997**, *84*, 611.

[12] DiCésare, N.; Belletête, M.; Raymond, F.; Leclerc, M.; Durocher, G. *J. Phys. Chem. A* **1997**, *101*(5), 776.

[13] Belletête, M.; Leclerc, M.; Durocher, G. *J. Phys. Chem.* **1994**, *98*(38), 9450.

[14] Van Hutten, P.F.; Gill, R.E.; Herrema, J.K.; Hadziioannou, G. *J. Phys. Chem.* **1995**, *99*, 3218.

[15] Bongini, A.; Brioni, F.; Panunzio, M. *J. Chem. Soc. Perkin Trans. 2* **1997**, 927.

[16] Becker, R.S.; de Melo, J.S.; Maçanita, A.L.; Elisei, F. *J. Phys. Chem.* **1996**, *100*, 18683.

[17] DiCésare, N.; Belletête, M.; Leclerc, M.; Durocher, G. *Chem. Phys. Lett.* **1997**, *275*, 533.

[18] Raymond, F.; DiCésare, N.; Belletête, M.; Durocher, G.; Leclerc, M. *Adv. Mater.* **1998**, *10*, 599

[19] Quattrocchi, C.; Lazzaroni, R.; Brédas, J.L. *Chem. Phys. Lett.* **1993**, *208*, 120.

[20] Orti, E.; Viruela, P.M.; Sanchez-Marin, J.; Tomas, F. *J. Phys. Chem.* **1995**, *99*, 4955.

[21] Hernandez, V.; Lopez-Navarrete, J.T. *J. Chem. Phys.* **1994**, *101*(2), 1369.

[22] Aleman, C.; Julia, L. *J. Phys. Chem.* 1996, *100*, 1524.

[23] dos Santos, M.C.; Bohland-Filho, J. *Proc. SPIE* **1994**, *2528*, 143.

[24] Frisch, M.J.; Head-Gordon, M.; Trucks, G.W.; Foresman, J.B.; Schlegel, H.B.; Raghavachari, K.; Robb, M.; Bimkley, J.S.; Gonzales, C.; Defrees, D.J.; Fox, D.J.; Whiteside, R.A.; Seeger, R.; Melius, C.F.; Baker, J.; Martin, R.L.; Kahn, L.R.; Stewart, J.J.P.; Topiol, S.; Pople, J.A. *Gaussian 90*, Revision F, Gaussian : Pittsburgh, P.A. 1990.

[25] Allinger, N.L. *J. Am. Chem. Soc.* **1977**, *99*, 8127.

[26] Dewar, M.J.S.; Zoebisch, E.G.; Healy, E.F.; Stewart, J.J.P. *J. Am. Chem. Soc.* **1985**, *107*, 3902.

[27] Dewar, M.J.S.; Dieter, K. *J. Am. Chem. Soc.* **1986**, *108*, 8075.

[28] Stewart, J.J.P. *J. Comput. Aided Mol. Des.* **1990**, *4*, 1.

[29] Dewar, J.M.S.; Yuan, Y.C. *Inorg. Chem.* **1990**, *29*, 3881.

[30] Samdal, S.; Samuelson, E.J.; Volden, H.V. *Synth. Met.* **1993**, *59*, 259.

[31] Pelletier, M.; Brisse, F. *Acta Cryst.* **1994**, *C50*, 1942.

[32] DiCésare, N.; Belletête, M.; Leclerc, M.; Durocher, G. *Synth. Met.* **1998**, *94*, 291.

[33] Baron, V.; Lelj, F.; Russo, N.; Toscano, M. *J. Chem. Soc. Perkin Trans 2* **1986**, 907.

[34] Brédas, J.L.; Street, G.B.; Thémans, B.; André, J.M. *J. Chem. Phys.* **1985**, *83*, 1323.

[35] Belletête, M.; DiCésare, N.; Leclerc, M.; Durocher, G. *J. Mol. Struct. (TheoChem)* **1997**, *391*, 85.

[36] DiCésare, N.; Belletête, M.; Leclerc, M.; Durocher, G. *J. Mol. Struct. (TheoChem)*, in press.

[37] Unpublished results.

[38] Barbarella, G. private communication.

[39] Folli, U.; Iarossi, D.; Montorsi, M.; Mucci, A.; Schenetti, L. *J. Chem. Soc. Perkin Trans. 1* **1995**, 537.

[40] Barbarella, G.; Zambianchi, M.; Antolini, L.; Folli, U.; Goldoni, F.; Iarossi, D.; Schenetti, L.; Bongini, A. *J. Chem. Soc. Perkin Trans. 2* **1995**, 1869.

[41] Frost, D.C.; Herring, F.G.; Katrib, A.; McDowell, C.A.; McLean, R.A.N. *J. Phys. Chem.* **1972**, *76*, 1030.

Table 1

Relative Energy (in kcal mol^{-1}) and Torsional Angle (θ) Obtained by the 3-21G* Basis Set

molecule	*syn* [a]	*syn*-gauche	perpendicular	*anti*-gauche	*anti* [a]
DMS33BT	13.6	0.0	0.11	0.031	2.3
		(71.0°)		(120°)	
DMS34BT	2.1	0.049	0.86	0.0	0.31
		(50.0°)		(141.5°)	
DMSDM34BT	15.0	-	0.0	-	4.5
			(102.3°)		

[a] *Syn*, θ = 0° ; *anti*, θ = 180°.

Table 2

Optimized Geometry for the Lowest Energy Conformer of DMS33BT

parameter [a]	HF/3-21G*	HF/STO-3G	AM1	PM3
C2-C2'	1.4651	1.4901	1.4191	1.4456
S1-C2	1.7321	1.7477	1.6971	1.7464
C2-C3	1.3546	1.3493	1.3945	1.3803
C3-C4	1.4399	1.4603	1.4375	1.4415
C4-C5	1.3450	1.3325	1.3716	1.3628
C5-S1	1.7195	1.7276	1.6671	1.7173
C4-H4	1.0683	1.0802	1.0931	1.0964
C5-H5	1.0673	1.0793	1.0892	1.0893
C3-Sa	1.7661	1.7733	1.6730	1.7462
Sa-Cb	1.8232	1.8028	1.7519	1.8062
C2'-C2-C3	120.6	128.1	129.0	126.7
S1-C2-C3	111.4	112.1	110.5	111.6
C2-C3-C4	112.3	111.6	111.1	111.5
C3-C4-C5	112.8	112.8	112.4	113.0
C4-C5-S1	111.9	112.8	111.7	1112.5
C5-S1-C2	91.6	90.7	94.2	91.4
C3-C4-H4	122.6	122.9	122.4	121.7
C4-C5-H5	127.1	126.7	125.6	125.3
C2-C3-Sa	124.9	124.7	124.7	124.5
C3-Sa-Cb	98.9	99.0	106.4	103.6
C2-C3-Sa-Cb	94.2	126.2	153.2	164.9
S1-C2-C2'-S1'	71.0	124.8	0.0	90.0

[a] Distance in angstroms, angle and dihedral angle in degrees.

Table 3

Spectroscopic Parameters of Bithiophene and Bithiophene Derivatives in *n*-Hexane at Room Temperature (298K)

Molecule	λ_{Abs} [a] (nm)	ν_{Abs} [a] (cm^{-1})	ε (M^{-1} cm^{-1})	$FWHM_{Abs}$ [b] (cm^{-1})	λ_F [a] (nm)	ν_F [a] (cm^{-1})	$FWHM_F$ [b] (cm^{-1})	Δ [c] (cm^{-1})
BT	300	33300	12490	5560	355	28100	4310	5200
DBS33BT	280	35700	7530	-	410	24400	4470	11300
O3BT[d]	293	34100	-	5870	366	27300	4550	6800
DBO33BT[e]	317	31500	15000	4440	370	27000	4000	4500
DD33BT[f]	280	35700	4380	-	374	26700	5050	9000

[a] taken at the maximum of the band.

[b] Full-width at half-maximum.

[c] Stokes shift between absorption (ν_A) and fluorescence (ν_F) bands.

[d] 3-Octyl-2,2'-Bithiophene, ref [14].

[e] 3,3'-Dibutoxy-2,2'-Bithiophene, ref [12].

[f] 3,3'-Didecyl-2,2'-Bithiophene, ref [12].

Table 4

Optimized Geometry for the Lowest Energy Conformer of DMS34BT.

parameter [a]	HF/3-21G*	HF/STO-3G	AM1	PM3
C2-C2'	1.4625	1.4842	1.4232	1.4407
S1-C2	1.7380	1.7459	1.6947	1.7472
C2-C3	1.3545	1.3465	1.3840	1.3739
C3-C4	1.4343	1.4554	1.4304	1.4374
C4-C5	1.3510	1.3391	1.3872	1.3728
C5-S1	1.7129	1.7295	1.6562	1.7166
C3-H3	1.0691	1.0797	1.0923	1.0977
C5-H5	1.0675	1.0793	1.0904	1.0910
C4-Sa	1.7652	1.7732	1.6797	1.7429
Sa-Cb	1.8232	1.8027	1.7491	1.8029
C2'-C2-C3	125.7	125.5	129.5	125.5
S1-C2-C3	110.7	111.1	111.1	111.1
C2-C3-C4	113.4	113.7	111.7	112.9
C3-C4-C5	111.8	110.9	111.1	111.7
C4-C5-S1	112.6	113.6	112.6	112.8
C5-S1-C2	91.5	90.8	93.5	91.4
C2-C3-H3	123.8	123.7	125.0	123.9
C4-C5-H5	126.1	126.5	123.9	125.4
C3-C4-Sa	124.0	124.7	127.4	126.5
C4-Sa-Cb	99.6	99.0	105.0	104.7
C3-C4-Sa-Cb	277.6	58.2	-6.9	-1.7
S1'-C2'	1.7342	1.7494	1.6692	1.7485
C2'-C3'	1.3600	1.3536	1.4007	1.3846
C3'-C4'	1.4388	1.4599	1.4258	1.4409
C4'-C5'	1.3446	1.3319	1.3778	1.3631
C5'-S1'	1.7182	1.7266	1.6688	1.7142
C4'-H4'	1.0682	1.0804	1.0924	1.0923
C5'-H5'	1.0672	1.0791	1.0889	1.0896
C3'-Sa'	1.7675	1.7734	1.6857	1.7470
Sa'-Cb'	1.8221	1.8031	1.7567	1.8030
C2-C2'-C3'	130.4	130.6	121.4	127.6
S1'-C2'-C3'	110.9	111.8	110.9	111.3
C2'-C3'-C4'	112.5	111.6	111.5	111.5
C3'-C4'-C5'	113.0	113.1	111.4	113.0
C4'-C5'-S1'	111.7	112.5	112.0	112.5
C5'-S1'-C2'	92.0	91.0	94.1	91.6
C3'-C4'-H4'	122.4	122.6	123.2	122.8
C4'-C5'-H5'	127.18	126.6	125.4	125.3
C2'-C3'-Sa'	126.1	126.6	118.3	124.4
C3'-Sa'-Cb'	99.8	98.7	104.5	105.1
C2'-C3'-Sa'-Cb'	281.7	239.6	131.9	174.2
S1-C2-C2'-S1'	141.5	180.0	165.0	30.0

[a] Distances in angstroms, angle and dihedral angle in degrees.

Table 5

Optimized Geometry for the Lowest Energy Conformer of DMSDM34BT

parameter [a]	HF/3-21G*	HF/STO-3G	AM1	PM3
C2-C2'	1.4690	1.4916	1.4228	1.4471
S1-C2	1.7282	1.7455	1.6687	1.7422
C2-C3	1.3560	1.3481	1.4014	1.3800
C3-C4	1.4491	1.4685	1.4317	1.4486
C4-C5	1.3465	1.3350	1.3821	1.3685
C5-S1	1.7199	1.7294	1.6644	1.7148
C5-H5	1.0679	1.0787	1.0889	1.0901
C3-Sa	1.7677	1.7764	1.6866	1.7567
Sa-Cb	1.8220	1.8039	1.7579	1.8063
C4-Cc	1.5066	1.5212	1.4702	1.4776
C2'-C2-C3	128.3	127.9	121.9	126.9
S1-C2-C3	111.3	112.1	111.0	112.0
C2-C3-C4	112.8	112.0	111.5	111.4
C3-C4-C5	111.6	111.8	111.0	112.3
C4-C5-S1	112.7	113.4	112.3	112.8
C5-S1-C2	91.5	90.6	94.1	91.4
C4-C5-H5	126.3	126.4	124.9	125.0
C3-C4-Cc	123.6	123.0	124.1	124.1
C2-C3-Sa	124.0	125.5	118.4	124.2
C3-Sa-Cb	99.6	98.4	105.1	102.6
C2-C3-Sa-Cb	271.1	280.4	122.3	-119.6
S1'-C2'	1.7352	1.7446	1.6940	1.7423
C2'-C3'	1.3525	1.3456	1.3884	1.3770
C3'-C4'	1.4485	1.4692	1.4391	1.4490
C4'-C5'	1.3499	1.3363	1.3833	1.3715
C5'-S1'	1.7095	1.7315	1.6568	1.7132
C5'-H5'	1.0675	1.0767	1.0900	1.0912
C3'-Cc'	1.5068	1.5216	1.4693	1.4775
C4'-Sa'	1.7661	1.7678	1.6808	1.7450
Sa'-Cb'	1.8233	1.7976	1.7496	1.8026
C2-C2'-C3'	127.7	127.9	129.7	125.5
S1'-C2'-C3'	112.0	112.2	111.3	112.0
C2'-C3'-C4'	111.7	112.2	111.1	111.9
C3'-C4'-C5'	112.5	111.7	111.4	111.7
C4'-C5'-S1'	112.5	113.3	112.6	113.3
C5'-S1'-C2'	91.3	90.6	93.6	91.2
C4'-C5'-H5'	125.9	127.4	124.2	125.4
C2'-C3'-Cc'	125.4	126.1	126.0	124.9
C3'-C4'-Sa'	124.4	119.1	119.7	120.8
C4'-Sa'-Cb'	99.9	100.6	104.3	104.2
C3'-C4'-Sa'-Cb'	273.2	180.5	-176.3	176.4
S1-C2-C2'-S1'	102.3	120.9	180.0	80.0

[a] Distances in angstroms, angle and dihedral angle in degrees.

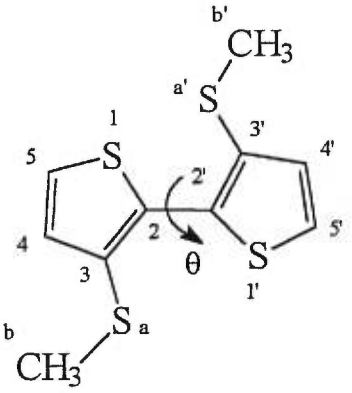

DMS33BT

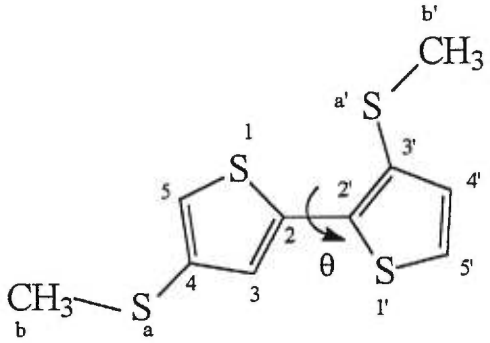

DMS34BT

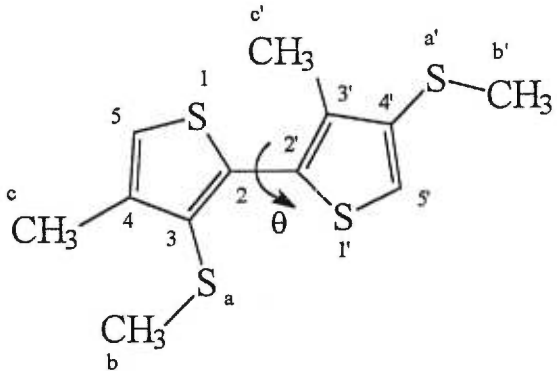

DMSDM34BT

figure 1 : Molecular structures of the substituted bithiophenes investigated.

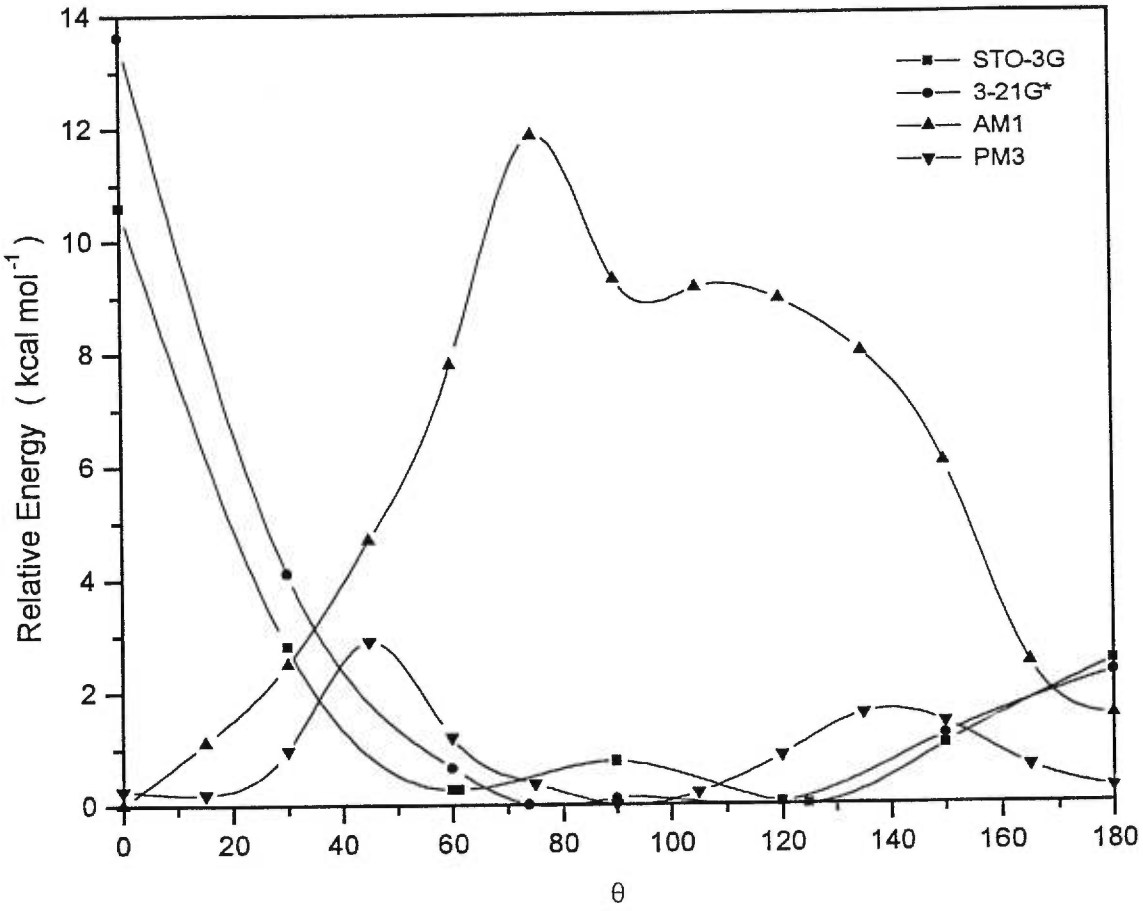

Figure 2 : Potential energy curves for the ground state of DMS33BT.

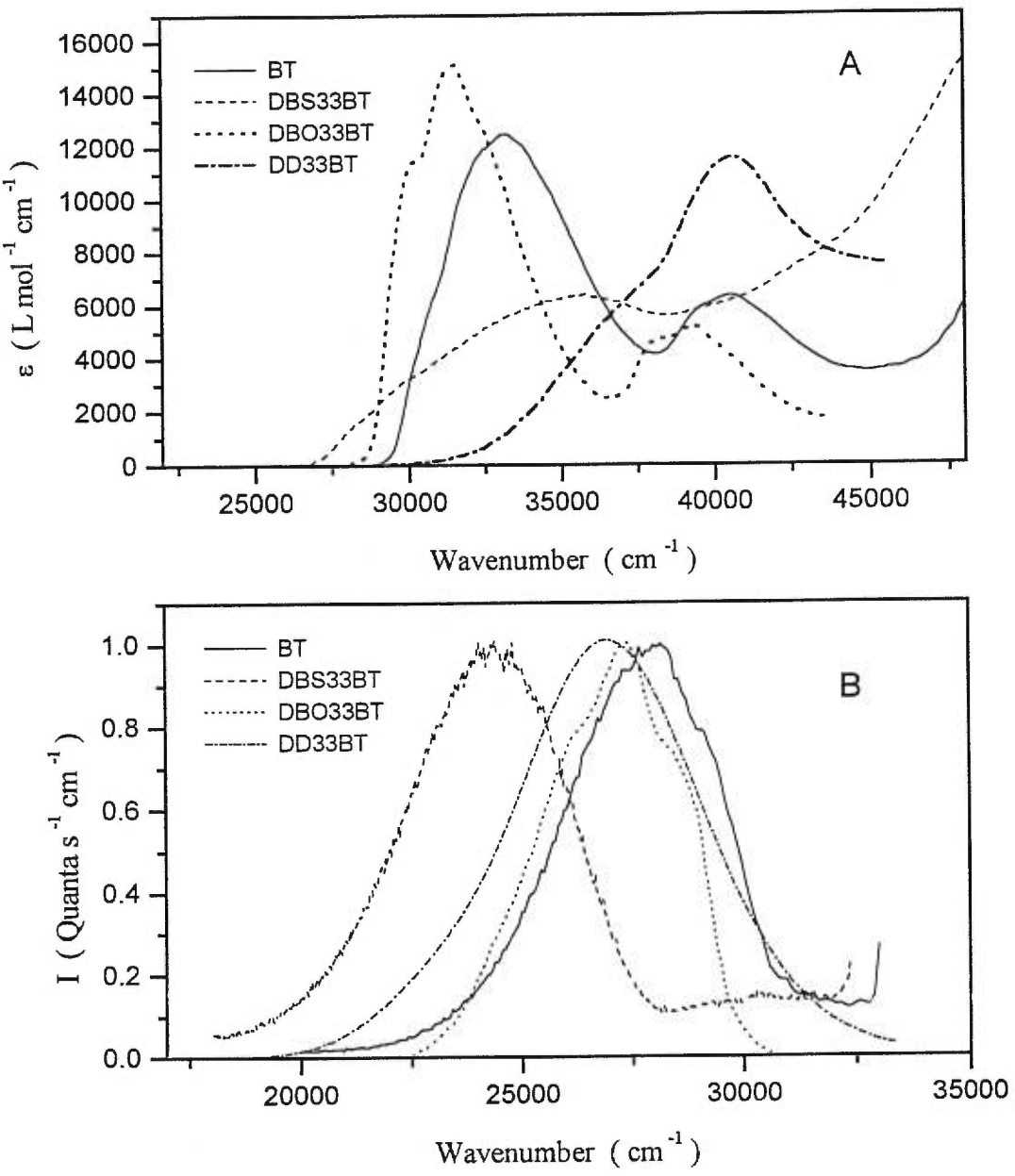

Figure 3 : (**A**) Absorption and (**B**) normalized fluorescence spectra of BT (2,2' bithiophene), DBS33BT (3,3'-dibutylthio-2,2'-bithiophene), DBO33BT (3,3'-dibutoxy-2,2'-bithiophene) and DD33BT (3,3'-didecyl-2,2'-bithiophene) all taken from ref [12]. All spectra were measured in *n*-hexane at room temperature.

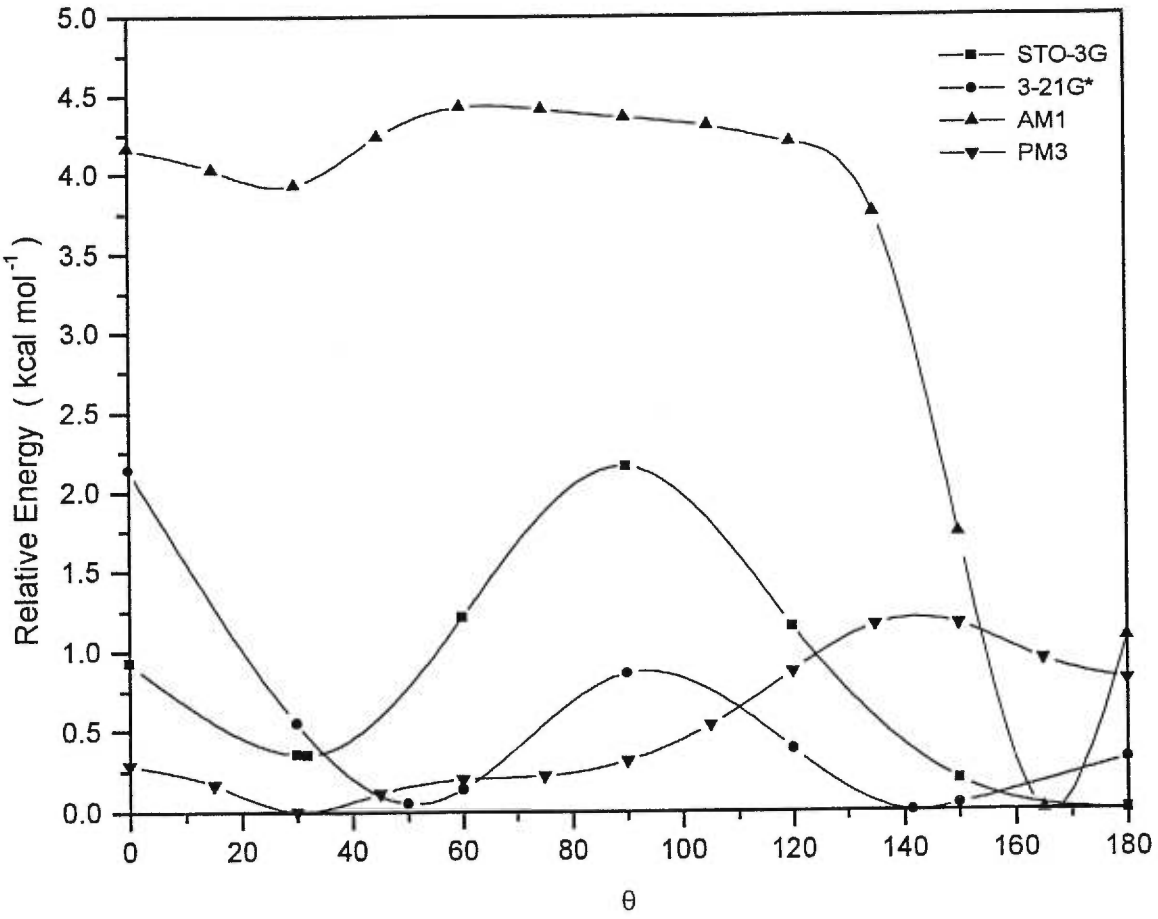

Figure 4 : Potential energy curves for the ground state of DMS34BT.

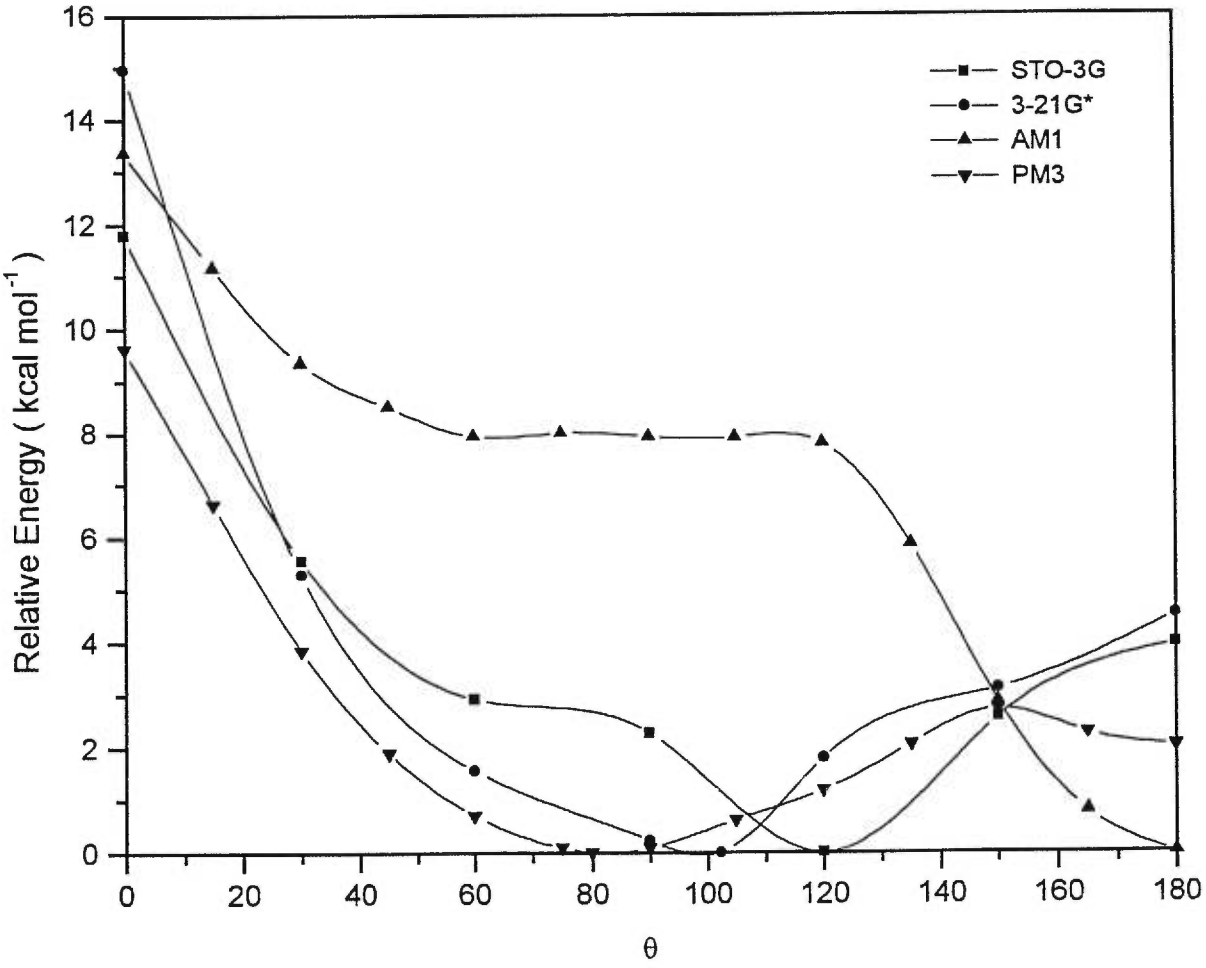

Figure 5 : Potential energy curves for the ground state of DMSDM34BT.

Chapitre 5

Étude de l'origine du thermochromisme observé chez les polythiophènes par détermination des surfaces d'énergie potentielle des dimères modèles

Dans ce chapitre, les surfaces d'énergie potentielle des dimères, présentées dans les trois chapitres précédents, sont analysées et comparées en fonction de l'observation ou non d'effets chromiques chez les polythiophènes substitués correspondants. Comme les changements conformationnels sont une origine possible de ces effets chromiques, les surfaces d'énergie potentielle des unités répétitives devraient montrer une corrélation entre les conformations et les barrières rotationnelles des unités répétitives et les effets chromiques des polymères correspondants.

Les résultats montrent effectivement une corrélation entre les surfaces d'énergie potentielle des dimères et les effets chromiques des polythiophènes correspondants. Les polymères possédant une unité répétitive ayant une conformation plane (barrière nulle ou très faible), tel DMO33BT et DMO34BT, ne montrent aucun effet chromique puisque l'interaction inter-chaîne dans le polymère favorise une conformation plane identique à celle de la forme libre (calculée). À l'inverse, les polymères possédant des unités répétitives très tordues et possédant une barrière rotationnelle pour la forme plane très élevée, tel DE33BT, ne montrent également aucun effet chromique. Ceci est dû au fait que l'interaction inter-chaîne n'est pas assez forte pour surpasser la barrière rotationnelle et favoriser une

conformation plane. Quant aux autres dimères modèles, DE34BT, DMS34BT et DMODM34BT, ils montrent tous une conformation non plane avec une barrière rotationnelle pour les formes planes relativement faible. Tous les polymères correspondants montrent un effet chromique.

Dans cet article, nous faisions également deux prédictions avec les dimères modèles DMS33BT et DMSDM34BT. La surface d'énergie potentielle du DMS33BT montre une conformation tordue avec une barrière rotationnelle relativement faible. Selon les résultats obtenus précédemment, le polymère correspondant devrait être thermochrome. Suite à ces résultats, le poly(3,3'-dibutylthio-2,2'-bithiophène) a été synthétisé et ses effets chromiques ont été démontrés dans un autre article [25]. Le polymère correspondant au DMSDM34BT n'a toujours pas été synthétisé à ce jour.

La corrélation entre les possibilités de changements conformationnels et les effets chromiques des polythiophènes appuie la thèse des changements conformationnels pour expliquer l'origine de ces phénomènes. Par contre, cette étude ne tient compte, en aucun moment, des effets des interactions interchaînes sur les propriétés électroniques de ces systèmes. Les trois prochains chapitres, après celui-ci, traiteront de ces interactions intermoléculaires chez les trimères. Les effets des interactions interchaînes sur les propriétés spectroscopiques seront alors comparés aux effets des changements conformationnels sur les mêmes propriétés spectroscopiques.

4.1 Article 5 : Towards a theoretical design of thermochromic polythiophenes

Article publié dans Chemical Physics Letters, volume 275, pages 533-539 (1997).

Towards a Theoretical Design of Thermochromic Polythiophenes

Nicolas Di Césare [a], Michel Belletête [a], Gilles Durocher [a] and Mario Leclerc [b]

[a] Laboratoire de photophysique moléculaire
[b] Laboratoire des polymères électroactifs et photoactifs

Département de chimie, Université de Montréal
C.P. 6128, Succ. A, Montréal, Québec, H3C 3J7, Canada

Abstract

Ab initio calculations have been performed on several bithiophene derivatives which are the building blocks of substituted polythiophenes in order to correlate their torsional potential energy curves with the thermochromic properties of the parent polymers. It is found that the occurrence of thermochromism in polythiophenes can be related to the values of the energy barrier calculated for the dimer models. Moreover, trends in the thermally induced blue-shift observed with some polythiophene derivatives can be related to the difference in the torsional angles between a co-planar conformation and the more stable conformation of the corresponding bithiophene moieties.

1. Introduction

Some substituted polythiophenes with relatively long and flexible side chains show intriguing thermochromic phenomena, both in solution and in the solid state [1-7]. These optical effects are believed to be related to a planar-to-nonplanar conformational transition of the conjugated backbone [8]. Indeed, any twisting in the polymeric chain should lead to a decrease in the effective conjugation length which produces a blue-shift of the absorption spectrum. It has been found that these thermochromic properties are strongly related to the nature and the position of the side chains in the repetitive units of the polymers [8]. More precisely, it has been suggested that these optical effects are driven by a delicate balance between repulsive intrachain steric interactions and attractive interchain interactions [4, 7, 8]. For instance, at low temperatures, poly(3-alkoxy-4-methylthiophene)s, poly(3-alkylthiophene)s, and poly(3-(alkylthio)thiophene)s can form co-planar (highly conjugated) assemblies which are disrupted upon heating due to a disordering of the side chains; a twisting of the main chain (a less conjugated form) being assumed with this diassembly. On the other hand, as observed with poly(3,3'-dialkyl-2,2'-bithiophene)s, when the steric interactions are too large, no co-planar conformation is accessible whereas, in the absence of significant steric interactions, the conjugated polymer (e.g. poly(3-alkoxythiophene)s and poly(3,3`- dialkoxy-2,2`-bithiophene)s) can maintain nearly co-planar conformations even at high temperatures. However, despite all these interesting results, a clear description of the driving force and of the structural requirements related to these optical phenomena is still lacking. For this purpose, we would like to report a conformational study using *ab initio* theoretical results of several substituted bithiophenes which are building blocks of polythiophene derivatives. We have recently investigated the spectroscopy, photophysics and conformational analysis using semi-empirical methods on bithiophene [9-11], terthiophene [10, 11] alkyl-substituted terthiophene [11], a series of substituted thiophene oligomers [12] and on various 3,3' and 4,4'-substituted

bithiophene derivatives [13]. It is shown here that these calculations can be highly useful to understand and predict the thermochromic behavior of some polythiophene derivatives. The molecules investigated are shown in Fig. 1.

2. Theoretical method

The *ab initio* calculations were performed on a Silicon Graphics Challenge R4000 work station at the University of Montreal using the Gaussian 90 program [14]. The conformational analysis was done by changing the torsional angle θ by 30° steps between θ = 0° (planar *syn* conformation) and θ = 180° (planar *anti* conformation). The geometries were optimized at the HF level with the 3-21G* basis set. The Berny analytical gradient method was used for the optimizations. In the geometry optimization of the unsubstituted bithiophene , C_{2v}, C_2 and C_{2h} symmetry restrictions were imposed for planar *syn*, twisted and planar *anti* conformations respectively. For the 3,3'-substituted bithiophenes, a local C_2 symmetry restriction was applied between the two rings but no constraint was applied to the side groups. For all other molecules, no symmetry restriction was applied. The requested HF convergence on the density matrix was 10^{-8} and the threshold values for the maximum force and the maximum displacement were 0.00045 and 0.0018 a.u. (atomic unit), respectively. To obtain the final torsional angles of the most stable conformers, calculations of these geometries were performed without constraints. The potential energy curves have been drawn using a spline fitting.

3. Results and discussion

3.1. Conformational analysis

The potential energy curves of the bithiophene derivatives investigated are shown in Fig. 2A, B, Fig. 3A and B. Table 1 reports the torsional angles of the most

stable conformer of each dimer as well as the energetic differences between the energy of these conformers and that of a co-planar *anti* conformation. It is shown that the most stable conformation of 2,2'-bithiophene (BT) corresponds to a torsion angle $\theta = 146°$, the *syn* and perpendicular conformations being the most unstable (Fig. 2A). For the *syn* conformation, a local minimum is also found at around $\theta = 45°$. These results are in good agreement with the most recent *ab initio* calculations performed with 3-21G* and larger basis sets [15-17]. The energetic difference between the most stable conformation and the perpendicular structure is calculated to be 1.5 kcal mol^{-1} . A similar value was also obtained with larger basis sets like 6-31G* and MP2/6-31G* [15] showing that energy barriers are rather insensitive to the details of the basis set as far as it is large enough [18, 19]. In the gas phase, electron diffraction performed at 97-98°C on BT has shown the existence of two conformations, *anti*-like and *syn*-like, with torsional angles of 148° and 36° and conformational weights of 56% and 44%, respectively [20]. Two species were indeed identified and assigned to cis and trans conformers in a seeded free-jet expansion. The energy difference between these conformers was given to be 1.16 kcal mol^{-1} with the trans conformer being the most stable [21]. Two species were also identified in a hole-burning supersonic jet experiment. The authors have found, by simulating the progressions in the fluorescence excitation spectra, a double-minimum torsional potential, whose equilibrium structures are twisted by about 21° from the trans-planar structure. The height of the barrier between the minima is estimated to be about 0.1 kcal mol^{-1} [22]. The last three experiments can be largely interpreted by the 3-21G* calculations (see Fig. 2A). But due to packing effects (interchain interactions), BT was reported to be planar with an *anti* conformation ($\theta = 180°$) in the solid state [23, 24].

Fig. 2B shows that the planar conformations (*syn* and *anti*) of 3,3'-diethyl-2,2'-bithiophene (DE33BT) are destabilized compared to that of BT. This is due to strong steric interactions between sulfur atoms and ethyl groups. These results are in reasonable agreement with the most recent *ab initio* calculations performed on 3,3'-

dimethyl-2,2'-bithiophene [16, 19] as well as semi-empirical calculations (AM1) performed on 3,3'-didecyl-2,2'-bithiophene (DD33BT) [13]. The torsional angle for the equilibrium geometry of DE33BT is located around 90° and the energetic difference between this conformer and the planar *anti* structure is 7.6 kcal mol^{-1}. This is in agreement with the experimental evidence that the first absorption band of DD33BT is highly forbidden [13]. Indeed, the electronic delocalization throughout the two thiophene rings should be reduced when they are in a near orthogonal arrangement.

As shown in Fig. 2B, *ab initio* calculations predict that the most stable conformer of 3,3'-dimethoxy-2,2'-bithiophene (DMO33BT) is planar with an *anti* conformation. Surprisingly the presence of methoxy groups in positions 3,3' seems to provide weaker repulsive steric interactions than those found in the unsubstituted molecule (BT). This is probably due to mesomeric effects induced by this substituent which favor the electronic delocalisation between thiophene rings and then overcome the steric hindrance between sulfur and oxygen atoms. This geometry is different than the one predicted by AM1 semiempirical calculations (θ = 105°) [13]. AM1 calculations probably neglect the mesomeric effects of methoxy groups. Moreover this semi-empirical method is well known to put emphasis on repulsions between nonbonded atoms [25] which might explain why it failed for some 3,3'-substituted bithiophenes. The effect of methoxy groups on bithiophene derivatives will be discussed in more detail in a forthcoming publication [26]. The absorption spectrum of DMO33BT is well explained by a planar conformation of the molecule [13]. Indeed the first absorption band is quite intense, compared to that of DD33BT indicating a much better electronic conjugation between thiophene rings. Moreover, both bands of the DMO33BT absorption spectrum show vibrational structures which is a characteristic of highly conjugated (planar) systems. On the other hand, *ab initio* calculations suggest that the most stable conformer of 3,3'-dimethylthio-2,2'-bithiophene (DMS33BT) is twisted (Fig. 2B).This is probably due to the size of the sulphur atoms of the thiomethyl group which should produce stronger steric

interactions than that of a methoxy substituent. Moreover, it has been predicted by ZINDO/S calculations that a thiomethyl group is less of an electron donor than a methoxy substituent [26].

The potential energy curves of 3,4'-diethyl-2,2'-bithiophene (DE34BT) and 3,4'-dimethylthio-2,2'-bithiophene (DMS34BT) (Fig. 3A) suggest that these molecules are twisted but the planar conformations are less destabilized than those of the respective 3,3'-disubtituted derivatives as observed for 3,4'-dimethyl-2,2'-bithiophene [16,19]. These results can be explained in terms of the steric hindrance which should be smaller for 3,4'-disubstituted compounds than for 3,3'-disubstituted derivatives. Fig. 3A shows that the most stable conformation of 3,4'-dimethoxy-2,2'-bithiophene (DMO34BT) is nearly planar but that the barrier to rotation is reduced compared to that of DMO33BT. This is understandable because a methoxy group in position 4 cannot take part in the resonance structure involving the two thiophene rings. This explanation is in agreement with ZINDO/S calculations performed on methoxy derivatives showing that a methoxy group in position 4 is less electron donor than one in position 3 [13]. Fig. 3B shows that the most stable conformation of 3,4'-dimethoxy-4,3'-dimethyl-2,2'-bithiophene (DMODM34BT) is twisted compared to that of DMO34BT due to large steric effects created by the methyl group. Finally, for 3,4'-dimethylthio-4,3'-dimethyl-2,2'-bithiophene (DMSDM34BT), the steric hindrance created by the sulphur atom combined with the weaker electron-donor properties of the thiomethyl substituent are probably responsable for the significantly higher energy barrier calculated for DMSDM34BT compared to that of DMODM34BT.

3.2. Thermochromism

It is interesting to note that all these calculations on bithiophenes can be useful in understanding the thermochromic properties of the corresponding polythiophenes. Indeed, one can see from Table 1 that, with the notable exception of

alkoxy-substituted bithiophenes, all dimers should show a twisted conformation in the gas phase but with a relatively low energy barrier from a co-planar conformation. However, X-ray diffraction measurements have revealed co-planar (or nearly co-planar) structures for poly(3-alkoxy-4-methylthiophene)s [6, 27], poly(3-alkylthiophene)s [28-30], poly(3-(alkylthio)thiophene)s [31] and polythiophene [32] in the solid state, at room temperature. In other words, interchain (or intrachain, through chain folding) interactions can be large enough to compensate the energy barrier against planarity for these polymers. It is worth noting that interchain interactions are not sufficient to allow a co-planar conformation with poly(3,3'-dialkyl-2,2'-bithiophene)s [4,33].

Therefore, assuming that calculations on bithiophenes can reflect the trends observed in the polymers, it seems that when the energy barrier between a co-planar conformation and the more stable torsional angle is equal or less than 2.2 kcal mol^{-1} for a bithiophene unit, a co-planar conformation is then accessible in the solid state for the corresponding polymer, at low temperatures. With an energy barrier of 2.3 kcal mol^{-1} for DMS33BT, a co-planar conformation should be possible for the corresponding poly(3,3'-di(thioalkyl)-2,2'-bithiophene)s (to be synthesized) whereas with an energy barrier of 4.5 kcal mol^{-1} for DMSDM34BT, it is not clear whether the related poly(3-(thioalkyl)-4-methylthiophene)s could be planar in the solid state. Although perfectly head-to-tail poly(3-(alkylthio)-4-methylthiophene)s have not yet been reported, 75% head-to-tail poly(3-(thiobutyl)-4-methylthiophene) shows a maximum of absorption at 364 nm in the solid state at room temperature [34] which seems to preclude any co-planar conformation of the backbone. Finally, the 7.6 kcal mol^{-1} energy barrier calculated for DE33BT seems sufficient to inhibit, as reported above, a co-planar conformation for the parent polymer whereas, not surprisingly, a highly conjugated co-planar conformation has been reported for poly(3,3'-dialkoxy-2,2'-bithiophene)s [7] and non-regioregular poly(3-alkoxythiophene)s [4].

These calculations on bithiophenes can not only indicate if some polythiophenes can adopt a co-planar conformation in the solid state (or aggregated

state) but could also give some information about the extent of the blue-shift observed in the optical spectra when these co-planar assemblies are broken (through side-chain disordering). Indeed, it is believed that the blue-shift observed in the polymers upon heating can be correlated to the difference in the torsional angles between a co-planar conformation (made possible due to interchain interactions) and the calculated conformation for an *isolated* (in absence of strong interchain interactions) molecule. For instance, a blue-shift of 0.34 eV (from 568 to 492 nm) has been observed with poly(3-(alkylthio)thiophene)s [8]. From calculations on the model dimer, the preferred conformation of an *isolated* molecule would involve a torsion angle of about 142°. With poly(3-alkylthiophene)s [8], a 0.47 eV (from 520 to 440 nm) blue-shift has been observed while a torsional angle of 108° has been calculated for the corresponding model compound in the gas phase. A much larger blue-shift of 0.85 eV (from 548 to 398 nm) has been found with poly(3-alkoxy-4-methylthiophene)s [8] which is in agreement with the large twisting angle (88°) calculated for the corresponding dimer. On the other hand, poly(3,3'-dialkyl-2,2'-bithiophene)s do not show any significant change of their absorption maximum upon heating, since these polymers can only exhibit some small thermally induced modifications of their twisted conformation. Conversely, because both aggregated and *isolated* forms can adopt nearly co-planar conformations, poly(3-alkoxythiophene)s and poly(3,3'-dialkoxy-2,2'-bithiophene)s show essentially no thermochromic effect. Moreover, on the basis of our calculations on 2,2'-bithiophene, polythiophene should show some thermochromic effect, but since the stacked structure of this unsubstituted polymer is very stable, degradation of the polymer is observed before any disordering and since this polymer is also insoluble, no thermochromic study is possible in solution. Finally, since both DMS33BT and DE34BT model compounds show similar features, it could be predicted that poly(3,3'-di(alkylthio)-2,2'-bithiophene)s should exhibit thermochromic features similar to those found with regioregular poly(3-alkylthiophene)s whereas assuming that a co-planar struture can be accessible for regioregular poly(3-(alkylthio)-4-

methylthiophene)s (see above), a larger blue-shift of the maximum of absorption could be observed upon heating. The synthesis and characterization of these new polymers is now in progress and should give a good evaluation of our theoretical model.

3.3. Concluding remarks

This study shows that the thermochromism observed on several substituted polythiophenes can be rationalized using *ab initio* calculations performed on dimers which are the repetitive units of the polymers. It is suggested that the extent of the blue-shift observed at high temperatures in some polythiophenes can be related to the difference in the torsional angles between a co-planar conformation (made possible through interchain interactions) and the twisted structure adopted by the polymers when such assemblies are disrupted. Amid the systems examined here, only twisted dimers having an energy barrier $\leq$ 2.2 kcal mol^{-1} against planarity show interesting thermochromic properties in the parent polymers. A delicate balance between the conformer geometries and the energy barrier crossing between them seems to be at the origin of the thermochromic phenomenon in these polymers. For instance, it is shown that poly(3,3'-dialkoxy-2,2'-bithiophene)s and poly(3-alkoxythiophene)s do not show any significant thermochromic effects because their structure is almost co-planar in both aggregated and *isolated* forms. On the other hand, the fact that non-thermochromic poly(3,3'-dialkyl-2,2'-bithiophene)s cannot reach a co-planar conformation in the solid state can be explained by a large energy barrier. Finally, it is believed that these theoretical calculations can not only be useful for the rational design of new thermochromic polythiophene derivatives but also for the development of novel classes of chromic polymeric materials.

Acknowledgment

The authors are grateful to the Natural Sciences and Engineering Research Council of Canada (NSERC) and the "Fonds FCAR" (Québec) for their financial support. ND is grateful to the NSERC for a graduate scholarship. The authors would like also to acknowledge Dr. K. Faïd for the analysis of the thermochromic properties of polythiophene.

References

[1] S.D.D.V. Rughooputh, S. Hotta, A.J. Heeger and F. Wudl, J. Polym. Sci., Polym. Phys. Ed., 25 (1987) 1071.

[2] O. Inganas, W.R. Salaneck, J.E. Osterholm and J. Laakso, Synth. Met. 22 (1988) 395.

[3] C. Roux and M. Leclerc, Macromolecules 25 (1992) 2141.

[4] C. Roux, J.-Y. Bergeron and M. Leclerc, Makromol. Chem. 194 (1993) 869.

[5] C. Roux and M. Leclerc, Chem. Mater. 6 (1994) 620.

[6] K. Faïd, M. Fréchette, M. Ranger, L. Mazerolle, I. Lévesque, M. Leclerc, T.-A. Chen and R.D. Rieke, Chem. Mater. 7 (1995) 1390.

[7] R. Hanna and M. Leclerc, Chem. Mater. 8 (1996) 1512.

[8] M. Leclerc, M. Fréchette, J.-Y. Bergeron, M. Ranger, I. Lévesque and K. Faïd, Macromol. Chem. Phys. 197 (1996) 2077.

[9] M. Belletête, M. Leclerc and G. Durocher, J. Phys. Chem. 98 (1994) 9450.

[10] M. Belletête, N. Di Césare, M. Leclerc and G. Durocher, Chem. Phys. Lett. 250 (1996) 31.

[11] M. Belletête, N. Di Césare, M. Leclerc and G. Durocher, Theochem. 391 (1997) 85.

[12] M. Belletête, L. Mazerolle, N. Desrosiers, M. Leclerc and G. Durocher, Macromolecules, 28 (1995) 8587.

[13] N. Di Césare, M. Belletête, F. Raymond, M. Leclerc and G. Durocher, J. Phys. Chem. A, 101 (1997) 776.

[14] M.J. Frisch, M. Head-Gordon, G.W. Trucks, J.B. Foresman, H.B. Schlegel, K. Raghavachari, M. Robb, J.S. Bimkley, C. Gonzales, D.J. Defrees, D.J. Fox, R.A. Whiteside, R. Seeger, C.F. Melius, J. Baker, R.L. Martin, L.R. Kahn, J.J.P. Stewart, S. Topiol and J.A. Pople, Gaussian 90, Revision F ; Gaussian :Pittsburgh, PA, 1990.

[15] E. Orti, P.M. Viruela, J. Sanchez-Marin and F. Tomas, J. Phys. Chem. 99 (1995) 4955.

[16] V. Hernandez and J.T. Lopez Navarrete, J. Chem. Phys. 101 (1994) 1369.

[17] G. Distefano, M. Dal Colle, D. Jones, M. Zambianchi, A. Favaretto and A. Modelli, J. Phys. Chem. 97 (1993) 3504.

[18] C. Quattrocchi, R. Lazzaroni and J.L. Brédas, Chem. Phys. Lett. 208 (1993) 120.

[19] C. Aleman and L. Julia, J. Phys. Chem. 100 (1996) 1524.

[20] S. Samdal, E.J. Samuelsen and H.V. Volden, Synth. Met. 59 (1993) 259.

[21] J.E. Chadwick and B.E. Kohler, J. Photochem., 98 (1994) 3631.

[22] M. Takayanagi, T. Gejo and I. Hanazaki, J. Phys. Chem., 98 (1994) 12893.

[23] G.J. Visser, G.J. Heeres, J. Wolters and A. Vos, Acta Crystallogr. B24 (1968) 467.

[24] M. Pelletier and F. Brisse, Acta Crystallogr. C50 (1994) 1942.

[25] M.J.S. Dewar and W. Thiel, J. Am. Chem. Soc. 99 (1977) 4899; 99 (1977) 4907.

[26] N. Di Césare, M. Belletête, M. Leclerc and G. Durocher, J. Phys. Chem. A, in preparation.

[27] I. Lévesque and M. Leclerc, Chem. Mater. 8 (1996) 2843.

[28] A. Bolognesi, M. Catellani, S. Destri and W. Porzio, Makromol. Chem., Rapid Commun. 12 (1991) 9.

[29] T.J. Prosa, M.J. Winokur, J. Moulton, P. Smith and A.J. Heeger, Macromolecules 25 (1992) 4364.

[30] J. Mardalen, E.J. Samuelsen, O.R. Gautun and P.H. Carlsen, Synth. Met. 48 (1992) 363.

[31] X. Wu, T.A. Chen and R.D. Rieke, Macromolecules 29 (1996) 7671

[32] Z. Mo, K.-B. Lee, Y.B. Moon, M. Kobayashi, A,J. Heeger and F. Wudl, Macromolecules 18 (1985) 1972.

[33] J. Mardalen, H.J. Fell, E.J. Samuelsen, E. Bakken, P.H.J. Carlsen and M.R. Andersson, Macromol. Chem. Phys. 196 (1995) 553.

[34] M. Fréchette, M. Belletête, J.-Y. Bergeron, G. Durocher and M. Leclerc, Macromol. Chem. Phys. 198 (1997) 1709.

Table 1

Torsional Angle of the Most Stable Conformer of Bithiophene Derivatives, Energy Difference between the Most Stable Conformer and the Co-planar Conformation and Optical Properties of the Parent Polythiophenes.

MOLECULE	θ (°)	ΔE (kcal mol^{-1})	λ_{max} [a] (nm)	λ_{max} [b] (nm)	Δ [g] (eV)
DE33BT	102	7.6	396[c]	384[c]	0.10
DMSDM34BT	102	4.5	-	-	-
DMS33BT	74	2.3	-	-	-
DE34BT	108	2.2	520[d]	440[d]	0.43
DMODM34BT	88	0.9	548[d]	398[d]	0.85
BT	146	0.4	454[e]	450[e]	0.024
DMS34BT	142	0.3	568[d]	492[d]	0.34
DMO34BT	171	0.1	570[c]	538[c]	0.13
DMO33BT	180	0	580[f]	580[f]	0

[a] Maximum of absorption in the UV-visible range of the parent polymer in the solid state at room temperature.

[b] Maximum of absorption in the UV-visible range of the parent polymer in the solid state at 150 - 200 °C.

[c] Taken from Ref. [4].

[d] Taken from Ref. [8].

[e] This work.

[f] Taken from Ref. [7].

[g] Energy difference between the maxima of absorption of the parent polymer in the solid state at room temperature and at 150 - 200°C.

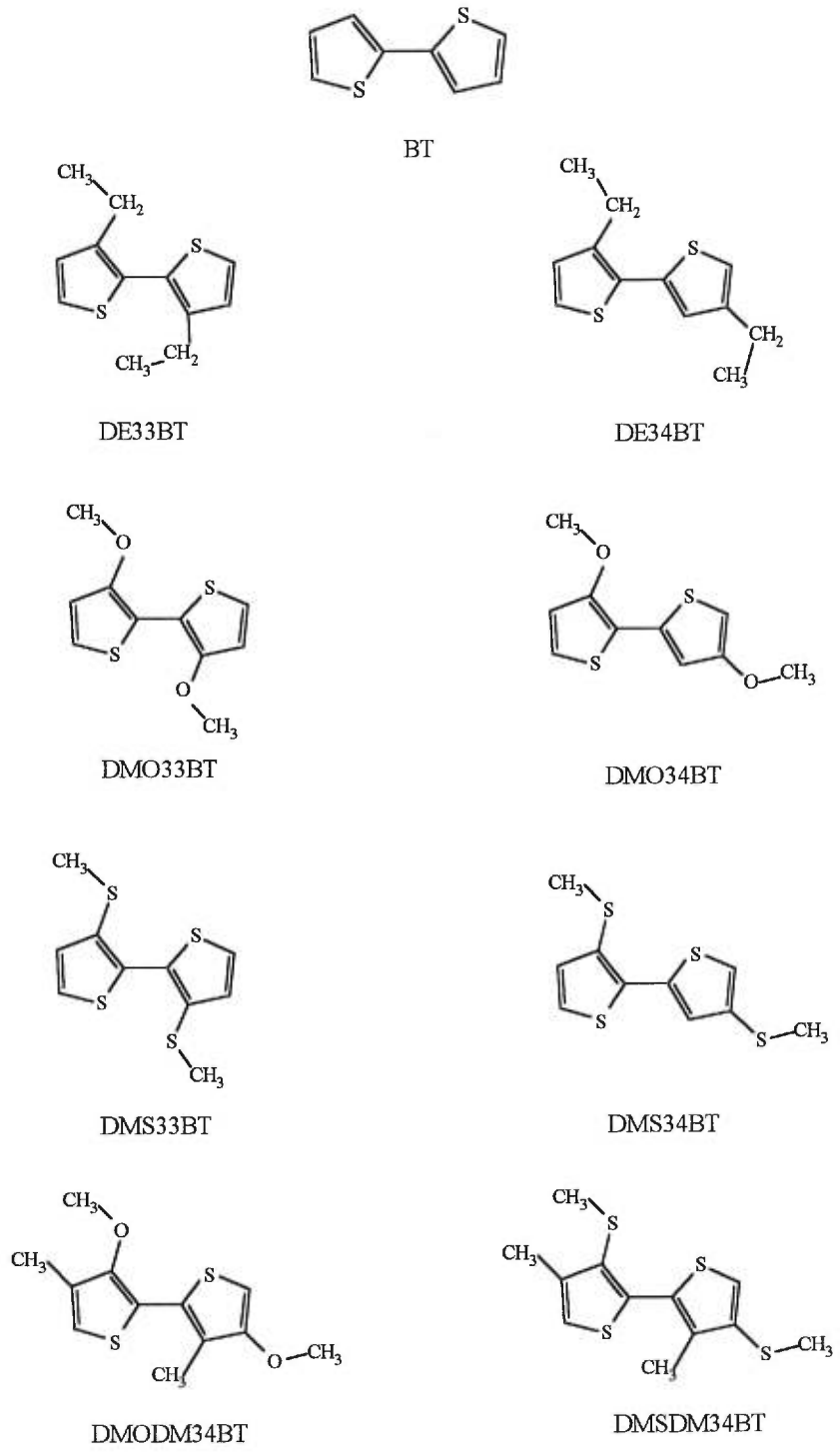

Figure 1: Molecular structure of the substituted bithiophenes investigated

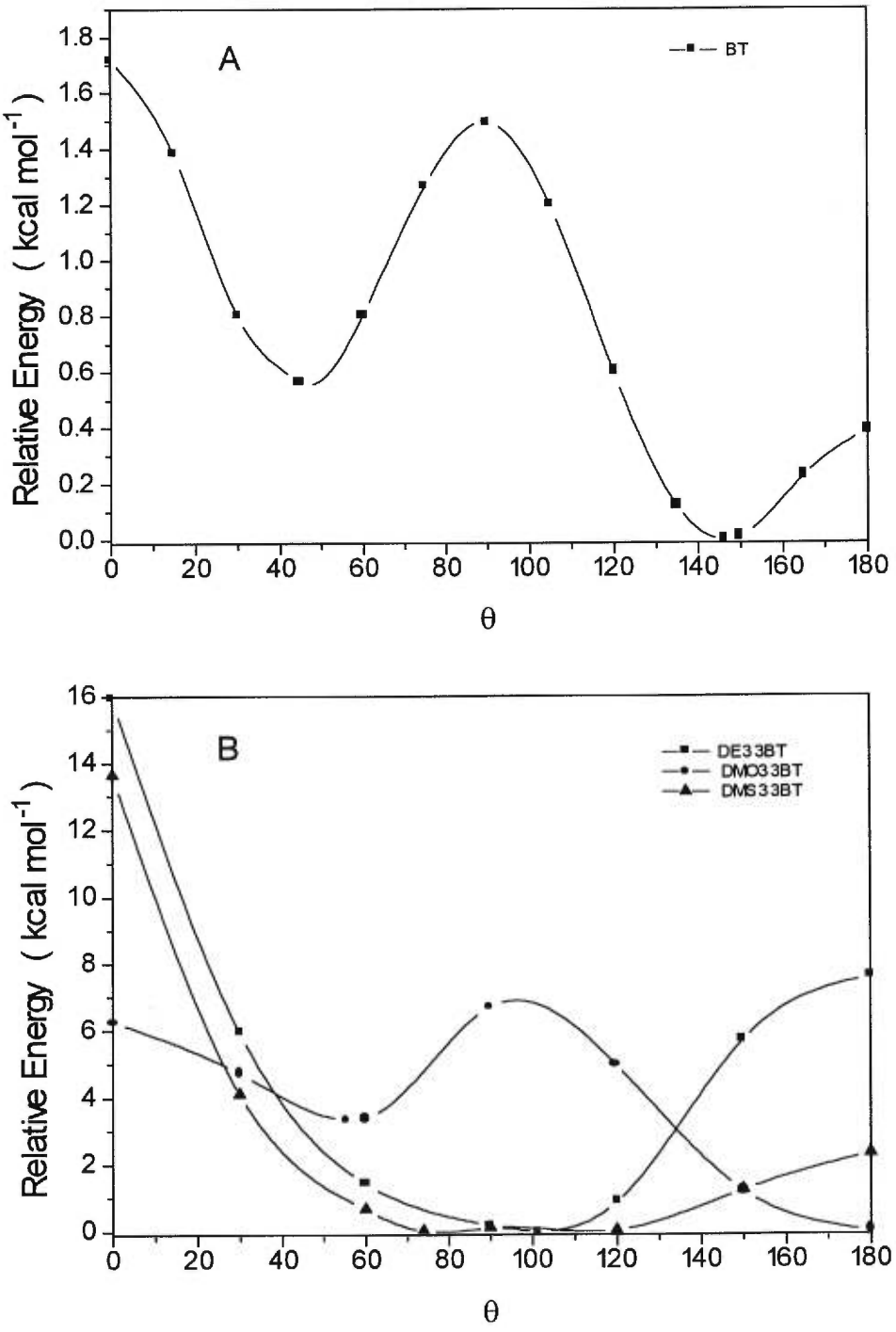

Figure 2: Potential energy curves of bithiophene (A) and 3,3'-substituted bithiophenes (B) as obtained by *ab initio* calculations (3-21 G*).

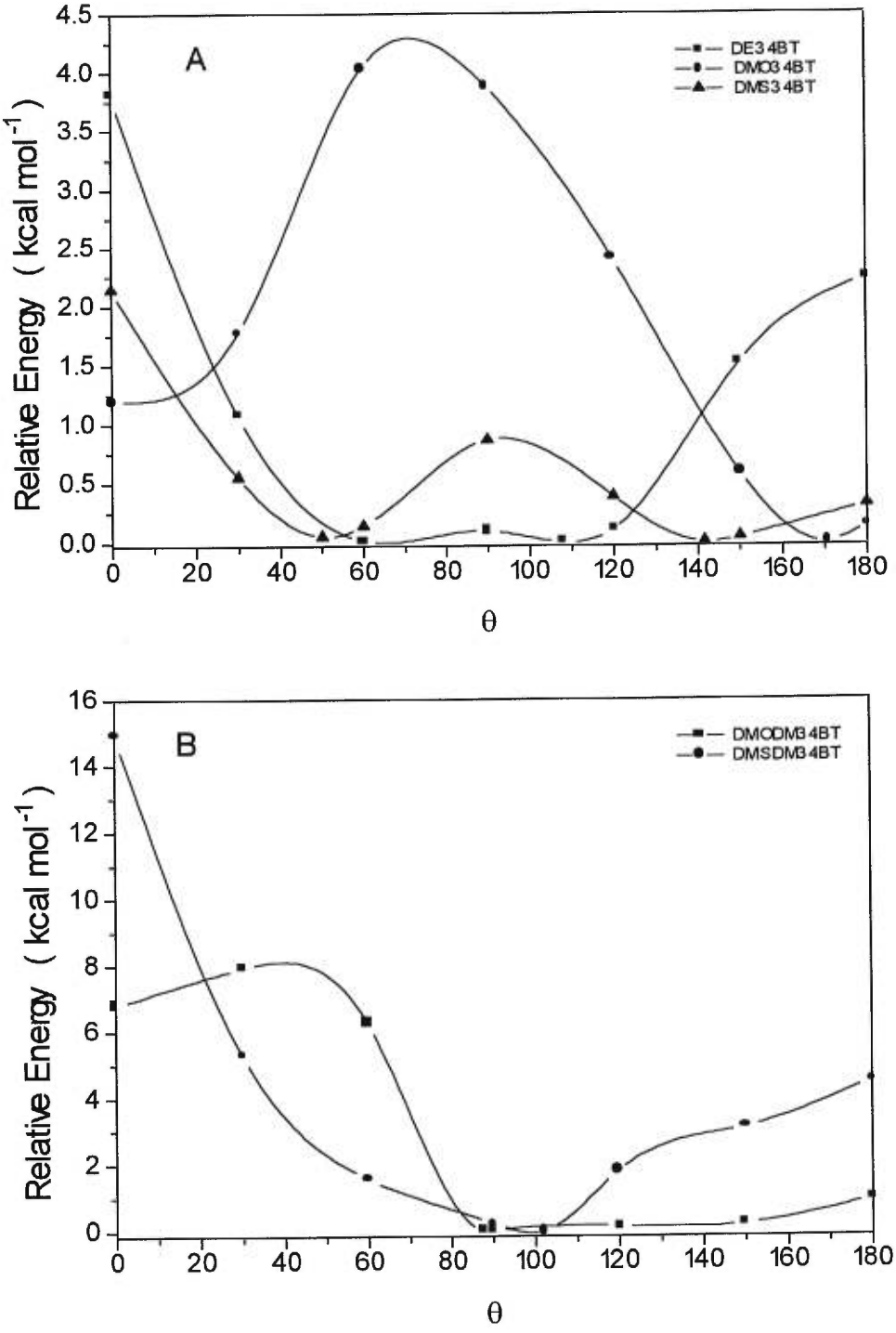

Figure 3: Potential energy curves of 3,4'-substituted bithiophenes (A) and 3,3',4,4' substituted bithiophenes as obtained by *ab initio* calculations (3-21 G*).

Chapitre 6

Étude structurale et conformationnelle de dérivés du 2,2':5',2''-terthiophène

Avec ce chapitre, débute l'étude des trimères. Les trois prochains chapitres auront comme but principal d'observer des effets chromiques chez des oligothiophènes et de déterminer les origines de ces phénomènes. Pour ce faire, il faut dans une première partie, ce présent chapitre, déterminer les conformations et les barrières rotationnelles des trimères étudiés dans leur état libre (solution ou phase gazeuse). Pour ce faire, nous avons utilisé les calculs théoriques *ab initio* (HF/3-21G*) pour l'obtention des surfaces d'énergie potentielle et les données spectroscopiques afin de corréler les résultats théoriques et expérimentaux.

Dans cette étude, nous avons utilisé quatre trimères, soit le terthiophène non substitué (TT) qui est notre molécule de référence, un dérivé possédant des substituants alkoxys et deux dérivés possédant des groupements alkyls. Selon nos attentes et les résultats obtenus avec les dimères, le dérivé alkoxy devrait posséder une conformation quasi plane, le TT est bien connu et possède une conformation non plane (~150° entre les cycles thiophènes) avec une barrière très faible pour la forme plane. Les deux dérivés alkyls, DMTT et DHTT, devraient posséder des conformations plus tordues avec des barrières rotationnelles plus élevées. Nous verrons dans ce chapitre que nos attentes et prédictions des conformations des trimères étaient bonnes.

Ces molécules forment un ensemble complet, c'est-à-dire nous avons une molécule relativement rigide plane (DMOTT), une molécule un peu tordue avec une

barrière rotationnelle faible (TT) et deux molécules tordues avec des barrières rotationnelles plus élevées (DMTT et DHTT). De cet ensemble, il ne manquerait qu'un trimère possédant encore plus de substituants alkyls que le DMTT et le DHTT (qui n'en possèdent que deux) afin d'avoir une molécule très tordue avec une barrière rotationnelle très importante et quasi infranchissable (du type de DE33BT). Malheureusement, aucune molécule de ce genre n'était disponible. Cependant, il est important de mentionner que ce genre de molécule donne des signaux très faibles en absorption et en emission dû à l'important bris de délocalisation chez ces molécules de sorte que des résultats significatifs avec ces molécules sont plus difficiles à obtenir.

6.1 Article 6 : Conformational analysis (*ab initio* HF/3-21G*) and optical properties of symmetrically disubstituted terthiophenes

Article publié dans The Journal of Physical Chemistry A, volume 102, numéro 26, pages 5142-5149 (1998).

Conformational Analysis (*ab initio* HF/3-21G*) and Optical Properties of Symmetrically Disubstituted Terthiophenes

Nicolas DiCésare [a], Michel Belletête [a], Claudio Marrano [b], Mario Leclerc [b] and Gilles Durocher [a]

[a] Laboratoire de photophysique moléculaire
[b] Laboratoire des polymères électroactifs et photoactifs

Département de Chimie, Université de Montréal,
C.P. 6128, Succ. A, Montréal, Québec, H3C 3J7, Canada

Abstract

We report a conformational analysis of several substituted terthiophenes using *ab initio* calculations performed at the HF/3-21G* level. Geometries of terthiophenes having methoxy substituents in 3,3'' positions (DMOTT), methyl groups in the same positions (DMTT), and ethyl substituents in 3',4' positions (DETT) are compared with that of the unsubstituted molecule (TT). For all these symmetrical molecules, it is observed that the two dihedral angles are independent of each other. The most stable conformation of TT is found for dihedral angles $\theta = \phi =$ 147.2°, whereas three maxima are located at 0°, 90° and 180°. The insertion of methoxy groups in 3,3'' positions favors a more planar conformation with a higher rotational barrier at 90°. This behavior is explained by the electron donor properties of the methoxy groups. By contrast, the addition of two methyl groups at the same positions induces a twisting in the molecule which is caused by the steric hindrance between the methyl substituents and the sulfur atom. The presence of two ethyl groups in 3',4' positions creates an even stronger steric effect, giving rise to a more twisted conformation for DETT compared to that of DMTT. Absorption and fluorescence spectra of each terthiophene derivative are also reported and are

correlated with their respective potential energy surfaces. The more planar molecule (DMOTT) shows a red shifted absorption band with a higher vibrational resolution and a smaller bandwidth. For more twisted molecules, the blue shift and the bandwidth of the absorption bands increase with twisting while the absorption coefficient decreases. The fluorescence bands, in all molecules, show a better vibrational resolution with a smaller bandwidth compared to their absorption counterparts, while their maximum wavelengths are practically the same, showing that in the first excited singlet state, all molecules relax to a more planar conformation.

1. Introduction

Polythiophenes and oligothiophenes show very interesting conductive and optical properties [1]. Since these properties strongly depend on the degree of electronic delocalization present in these materials, the length of the oligomer and the insertion of side chains at specific positions are two parameters that can be used to control the final output. Recently, the effect of the molecular length on spectroscopic and photophysical properties of unsubstituted oligothiophenes has been reported by Becker et al [2]. However the combined effects of the presence of side chains and of the oligomer length on the latter properties have been scarcely investigated. Recently we have studied the effect of the nature and position of alkyl and alkoxy substituents on the optical properties of bithiophene (BT) [3]. From these results, it was shown that the presence of substituents in 4,4' positions does not significantly change the molecular conformation, whereas insertion of groups in 3,3' positions greatly affects the geometry of the molecules. More recently, we have completed an analysis of the spectroscopic and photophysical properties of alkyl-substituted oligothiophenes, from trimer to hexamer, combined with semiempirical calculations of their respective potential energy surfaces [4]. It is clearly shown that

the alkyl groups influence the conformation of the oligomers but the geometric changes are mostly independent of the length of the oligomers.

To better understand the substitutional effect on oligothiophene molecular conformations and consequently on their physical properties, theoretical calculations have been of prime importance. *Ab initio* calculations performed at the HF/3-21G* level on many substituted bithiophenes have allowed one to obtain potential energy surfaces that are in good agreement with their spectral data [5-7]. Moreover, these theoretical results have provided rotational barriers [8] that have been correlated with the thermochromism observed on the parent polymers [9-11]. It was shown in these papers [5-7] that the 3-21G* basis set is the minimum *ab initio* level of calculations that gives results in close agreement with those obtained from more elaborate basis sets and methods including MP2 [12-15]. It was also shown that semiempirical AM1 and PM3 methods failed in the prediction of the minimum conformation and rotational barrier for alkoxy- and alkylthio- substituted bithiophenes but give more acceptable results for alkyl-substituted bithiophenes as well as for the unsubstituted molecule.

To the best of our knowledge, the analysis of the substitutional effect using *ab initio* calculations on longer oligothiophenes is still missing in the literature. On the other hand, the conformation of the unsubstituted terthiophene molecule (TT) using HF/6-21G* calculations has been reported recently [16]. It was shown that the two dihedral angles are independent of each other and are very close to that obtained for BT. We report in this paper the potential energy surfaces of TT and three symmetrical disubstituted terthiophene derivatives (shown in Figure 1) as obtained by HF/3-21G* calculations. Results show that, for each molecule, the two dihedral angles are independent of each other. The alkoxy substituents favor a higher planarity of the molecule, while alkyl substituents created steric hindrance and favor more twisted conformations. Absorption and fluorescence spectra of each molecule are also reported and are in good agreement with the molecular torsional potentials. For more planar molecules, the absorption spectrum shows a red shift, a better

vibronic resolution, and a smaller bandwidth. Twisted molecules show absorption spectra blue shifted with a lowering in the absorption coefficient and an increase of the bandwidth. Fluorescence spectra show that all molecules relax to a more planar conformation in their first singlet excited state.

2. Methodology

2.1. *Ab initio* calculations

Ab initio calculations were performed on a Silicon Graphics Challenge R4000 workstation at the University of Montreal using the Gaussian 90 program [17]. The conformational analysis was done by changing the torsional angle θ (and/or ϕ) by 30° steps. The geometries were optimized at the HF level with the 3-21G* basis set. The Berny analytical gradient method was used for the optimizations. In the geometry optimization of TT, DMOTT and DMTT, a locally C_2 symmetry restriction was applied between the thiophene rings for $\theta = \phi$ to reduce the calculation time, but no symmetric constraint was applied to the side groups. No symmetric constraint was applied on DETT and for all molecules where $\theta \neq \phi$. The requested HF convergence on the density matrix was 10^{-8}, and the threshold values for the maximum force and the maximum displacement were 0.00045 and 0.0018 a.u. (atomic unit) respectively. To obtain the final torsional angles of the conformers in each minima, calculations of these geometries were performed without constraint on the dihedral angle.

2.2. Materials

Terthiophene (TT) and *n*-hexane were purchased from Aldrich Chemicals (99% for TT and 99+%, anhydrous for *n*-hexane) and used as received. Prior to use, the compounds were checked for spurious emissions in the region of interest and found to be satisfactory. 3',4'-Dihexyl-2,2':5',2''-terthiophene (DHTT) and 3',3''-

dimethyl-2,2':5',2''-terthiophene (DMTT) were prepared according to previously published procedures [18,19]. 3',3''-Dimethoxy-2,2':5',2''-terthiophene (DMOTT) was prepared following procedures similar to those previously reported in the literature [20].

2.3. Instrumentation

Absorption spectra were recorded on a Varian spectrometer model Cary 1 Bio using 1 cm quartz cells and solute concentrations of (5-8) x 10^{-6} M. It has been shown that the Beer-Lambert law applies for the concentrations used. Fluorescence spectra corrected for the emission detection were recorded on a Spex Fluorolog-2 spectrophotometer with a F2T11 special configuration. The excitation and emission band-passes used were 2.6 and 1.9 nm, respectively. Each solution was excited near the absorption wavelength maximum using a 1 cm path length quartz cell, and the concentrations used were (5-8) x 10^{-6} M, giving absorbances near 0.1 to avoid any inner-filter effects. A study of the concentration (C) effect has been done on the fluorescence intensity (I_F), and all measurements have been performed in the linear region of the I_F *vs* C curve.

3. Results and Discussion

3.1. Structural and Conformational Analysis

The use of the 3-21G* basis set in the *ab initio* calculations has been justified in previous papers [5,7]. Indeed this level of calculations gives similar potential energy surfaces as those obtained from more elaborate basis sets and methods (including MP2) for 2,2'-bithiophene [12,14] and substituted bithiophenes [12,13,15]. Due to the size of the molecules investigated in this paper, we have limited our calculations at this level.

3.1.1. Terthiophene (TT)

Since a C_2 symmetry was used in the geometry optimization, the two thiophene rings at each molecular end are identical, whereas the central ring is symmetric. The structural parameters of TT are listed in Table 1. All geometric parameters are close to those found from X-ray data [21]. In the crystal, TT adopts a nearly planar conformation, about 5-10° from planarity. Moreover two different conformations are obtained; the majority of the molecules are in an *anti-anti* conformation (97%), but some *anti-syn* conformers are present (3%). Table 1 shows that the parameters of each thiophene ring are very close to each other. Only the C3'-C4' bond length and C2'-C3'-C4' and C5'-S1'-C2' bond angles differ significantly from equivalent parameters found in the first thiophene ring. The decrease of the C3'-C4' bond length suggests that the π charge density is higher in the central thiophene ring, resulting in the higher values of the angles mentioned above. As the molecular twisting varies, two parameters, namely, C2-C2' and C3'-C4' bond lengths, are mainly affected. The C2-C2' bond length variation as a function of θ (= ϕ) is illustrated in Figure 2. It is shown that the C2-C2' bond length increases from 1.4545 Å for the *anti-anti* planar conformation to reach its maximum value at 1.4692 Å for the perpendicular conformer and decreases as the *syn-syn* planar geometry is reached (1.4574 Å). A similar effect, but to a lesser extent, is also found for the C3'-C4' bond length (figure not shown). These structural changes are caused by a reduction of the electronic delocalization as the twisting between adjacent thiophene rings increases. It is worth noting that C2-C2' and C3'-C4' bond lengths are shorter for the planar *anti-anti* conformer compared to the respective values in the planar *syn-syn* conformer. This shows the importance of nonbonded interactions (steric hindrance) in the latter conformation causing an increase in the bond length. A similar behavior has been observed in bithiophene [7,12]. Table 1 also shows that all bond lengths and angles for the most stable conformation of TT are very similar to those obtained for BT [7,12,13,14] (a difference smaller than 0.001 Å has been found

for bond lengths). Moreover each molecule has about the same dihedral angle between thiophene rings, namely 147.2° for TT and 147.7° for BT [7]. These results clearly indicate that the thiophene rings at the ends of the molecule are mostly independent of the length of the oligomer. On the other hand, as mentioned above, the central thiophene ring shows small differences.

Potential energy surfaces for $\theta = \phi$ are displayed in Figure 3. Energies and relaxed optimized geometries for minima and maxima are listed in Table 2. As mentioned above, potential energy surfaces involving one dihedral angle (θ or ϕ) are independent of the value of the other dihedral angle. Thus we present only the results of the diagonal energy matrix (θ by ϕ) to illustrate torsional potentials in two dimensions and because it represents the most probable conformations, the global minimum conformation being located on the diagonal. Figure 3A shows that the potential energy surface of TT is very similar to that obtained for BT [7,12-14]. Indeed two minima, a local minimum at 42.8° and the global minimum at 147.2°, are obtained compared to the respective minima of BT located at 44.7° and 146.3° [7]. However the minima obtained for TT are slightly shifted toward more planar conformations. This behavior may be due to the increase in the electronic delocalization going from the dimer to the trimer, but the changes are too small to have any significant importance on the geometry. Three maxima are also observed on the potential energy surface, two for the planar conformations and one for the perpendicular one. The barriers of rotation displayed in Table 2 involve the torsion of the two thiophene rings. However, if we compare the potential energy surface for one dihedral angle, the second remaining fixed at any value (the two dihedral angles are independent of each other), with that obtained for BT [7], we can observe a decrease in the energy barrier for the planar conformations of TT. Indeed $\Delta E = 0.31$ and 1.64 kcal mol^{-1} for planar *anti* and *syn* conformations, respectively, whereas the respective energy barrier values of BT are 0.39 and 1.72 kcal mol^{-1} . These small differences are probably due to the increase in the electronic delocalization found in TT which favors more planar conformations. This effect can also explain the small

increase in the rotational barrier at 90° observed for TT (1.53 and 1.49 kcal mol^{-1} for TT and BT, respectively).

3.1.2. 3,3''-Dimethoxy-2,2':5',2''-terthiophene (DMOTT)

Structural parameters of DMOTT are displayed in Table 3. One can see that bond lengths of end thiophene rings are close to those found for TT. However, small structural changes are oberved between these two molecules. For instance, S1-C2 and C5-S1 bond lengths slightly increase whereas the C4-C5 bond length decreases for DMOTT. However, Table 3 shows that changes are more important for C2-C2' and C3'-C4' bond lengths, which are shorter than those obtained for TT. It is worth mentioning here that this behavior is also observed for TT and DMOTT having identical torsional angles between adjacent thiophene rings, as illustrated in Figure 2. As mentioned above, C2-C2' and C3'-C4' bond lengths are largely dependent on the electronic delocalization along the long molecular axis. The electron-donor properties of the methoxy groups in 3,3'' positions increase the electronic conjugation, favoring a more planar conformation, which reduces the C2-C2' and C3'-C4' bond lengths. A similar behavior has been observed for methoxy-substituted bithiophenes [5]. Figure 2 also shows that the variation of the C2-C2' bond length with the torsion is less for DMOTT than for TT. Indeed, for DMOTT, the difference of the C2-C2' bond length between planar *anti* and perpendicular conformations is 0.0139 Å, whereas a value of 0.0147 Å is observed for TT. Finally, one can see that methoxy groups are nearly perpendicular (angle of 254°, see Table 3) to the molecular plane (see Figure 4), as observed for 3,4'-dimethoxy-2,2'-bithiophene (DMO34BT) [5].

The potential energy surface of DMOTT shows two minima, one at 22.9° and the global minimum located at 171.3° (see Figure 3A). As discussed above, the increase of the molecular planarity following insertion of methoxy groups is due to the increase of the electronic delocalization along the molecular frame caused by the

electron donor properties of these substituents. According to the *ab initio* calculations, this effect is stronger than the steric hindrance created by the methoxy groups which should favor twisted conformations. However, steric effects induced by methoxy groups are reflected in the values of the rotational barriers at the planar *syn* and *anti* conformations. Indeed, the fact that rotational barriers for these two conformations are similar to the respective values obtained for TT (see Figure 3) can be explained in terms of two opposing forces, *i.e.* higher steric effects and a higher electronic delocalization which act in opposite directions with about the same magnitude. For the perpendicular conformation, the rotational barrier of DMOTT is higher than that obtained for TT because the electronic delocalization is no longer playing any role at all. The potential energy surface involving the rotation of only one thiophene ring (the other remaining constant at his minimum conformation) shows a global minimum slightly more planar (171.3°) than that obtained for DMO34BT (170.6°) [5]. This shift toward planarity is very small as observed going from BT to TT. However the rotational barriers seem a little more affected by the length of the molecule. Indeed, the barrier to rotation of one thiophene ring of DMOTT at the perpendicular conformation (4.08 kcal mol^{-1}) is higher than that observed for DMO34BT (3.88 kcal mol^{-1}) [5]. Thus, as observed for TT, the increase in the molecular length seems to provoke a small increase of the rotational barrier at 90°. It is interesting to note that the rotational barrier for the planar *anti* conformation is slightly higher for DMOTT (0.16 kcal mol^{-1}) than for DMO34BT (0.13 kcal mol^{-1}) whereas the reverse is true for rotational barriers for planar *syn* conformations (DMOTT 1.79 kcal mol^{-1}, DMO34BT 1.19 kcal mol^{-1}). This seems to indicate that the location of the sulfur atom and the methoxy substituent on the same side of the molecule creates a stronger steric hindrance for a longer oligothiophene chain.

3.1.3. 3',3''-Dimethyl-2,2':5',2''-terthiophene (DMTT)

Structural parameters of DMTT are displayed in Table 4. All parameters are comparable with the crystallographic data [22]. In the crystalline phase, DMTT adopts a twisted conformation of about 30° from planarity with a proportion of 85% in the *anti-syn* conformation and 15% in the *anti-anti* conformation. The fact that DMTT adopts a less twisted conformation in the crystalline phase compared to that found for the optimized geometry at the *ab initio* level is attributed to packing forces which favor more planar conformations as observed for TT. All geometrical changes induced by the methyl groups are attributed to the change of conformation going from TT to DMTT except for S1-C2, C3-C4 and C2-C2' bond lengths, which are longer compared to that found for TT having the same conformation as DMTT (120°). As mentioned above for TT, S1-C2 and C3-C4 are nearly independent of the twisting of thiophene rings such that the increase in these bond lengths is due to the insertion of methyl groups themselves without involving any significant changes in the torsional angle. The higher value of C2-C2' observed in the case of DMTT can be attributed to the steric hindrance caused by the methyl groups. This steric hindrance causes a smaller variation of the C2-C2' bond length as the molecule becomes more twisted (see Figure 2). As a result, one can see in Figure 2 that the steric hindrance caused by the methyl groups is high enough in the planar *syn* conformation such that the C2-C2' bond length is longer than that calculated for the 30° conformation.

The DMTT potential energy surface shows two minima located at 57.9° and 118.2° which are very close in energy (see Figure 3B). The equivalence of these two minima are reflected in the crystallographic data of this compound, where a majority of *syn-anti* conformations is observed [22]. Twisted conformations predicted by *ab initio* calculations are surely due to the steric hindrance induced by the methyl groups. Moreover, the minima obtained are very close to those found for 3,4'-dimethyl-2,2'-bithiophene (DM34BT) [7]. A very low rotational energy barrier at 90° is observed, which allows a wide range of conformations for this molecule. The rotational energy barriers against planarity are much higher than those observed for

TT or DMOTT. The barrier for the rotation of only one thiophene ring (the other remaining fixed at this minimum conformation) at the planar *anti* conformation (1.43 kcal mol^{-1}) is smaller than that found for DM34BT (2.29 kcal mol^{-1}), showing that the increase of the molecular length stabilizes the *anti* planar conformation. The rotational barriers at 90° (0.18 kcal mol^{-1} for DMTT and 0.16 kcal mol^{-1} for DM34BT) and for the *syn* planar conformation (2.84 kcal mol^{-1} for DMTT and 2.89 kcal mol^{-1} for DM34BT) are much less affected by the number of thiophene rings involved.

3.1.4. 3',4'-Diethyl-2,2':5',2''-terthiophene (DETT)

Structural parameters of DETT are listed in Table 5. All parameters are in good agreement with the crystallographic data of 3',4'-dibutyl-2,2':5',2''-terthiophene (DBTT) [23]. In the crystalline phase, DBTT adopts a conformation of about 30° from planarity with a majority of *anti-anti* conformers. Even though the geometry optimization was done without any symmetry restriction, a symmetrical molecule is obtained both in thiophene rings and ethyl lateral chain parameters. This confirms the molecular symmetry of this molecule and justifies the C_2 local symmetry used for the other molecules when $\theta = \phi$. Most of the structural parameters are similar to those obtained for DMTT except for C3-C4, C3'-C4', and S1'-C2' bond lengths. The increase in the C3'-C4' bond length observed for DETT is caused by the steric effects of the two ethyl chains on the same thiophene ring. Ethyl groups are perpendicular to the plane of the central thiophene ring and point in opposite directions (see Figure 4 and Table 5). It has been calculated that the conformation having ethyl groups pointing in the same direction is less stable by about 1 kcal mol^{-1} compared to that having ethyl groups pointing in opposite directions. By contrast, DBTT in the solid phase shows that the two butyl chains are pointing in the same direction. The reason for this behavior might involve packing forces which should be stronger for the latter conformation because molecules are allowed to approach

closer to each other. It is also possible that the minimum energy conformation calculated in the gas phase has no crystalline form (the compound having hexyl chains on the central thiophene ring (DHTT) is liquid at room temperature). The variation of the C2-C2' bond length with the twisting is much smaller than that observed for other molecules (see Figure 2). This bond length is much longer for the planar *syn* conformation than for the 30° conformation compared to that of DMTT and is still relatively long for the planar *anti* conformation. This clearly indicates the high steric hindrance created by the two ethyl chains in the 3',4' positions. The steric effect in all of these substituted terthiophene derivatives is emphasized by the fact that the increase in the C2-C2' bond length vary as the twisting proceeds and is directly proportional to the reciprocal of the energy barrier against planarity (see Figures 2 and 3).

As one can see in Figure 3B, the insertion of two ethyl groups on the same thiophene ring induces a more important twisting between the rings compared to that found for DMTT. This demonstrates the increase in the steric hindrance of the ethyl groups in these positions where the presence of a second ethyl chain prevents the first ethyl chain from adopting an energy-favored conformation. However, it is worth mentioning here that ethyl groups create stronger steric effects than methyl substituents [7]. This behavior may be partly responsible for the more twisted conformation found in DETT. By contrast with DMTT, we observed that only one minimum at 104.7° is observed for DETT. This is in agreement with crystallographic data showing mainly the presence of *anti* conformers. Both rotational barriers against planarity (*syn* and *anti*) are larger than that obtained for DMTT, reflecting the larger steric hindrance created by the ethyl groups in the 3',4' positions. An experimental determination of the rotational barrier of DBTT has been reported by DeWitt *et al.* [23]. From NMR measurements, they have obtained a value of 8 kcal mol^{-1} for the ground state rotational barrier, which is larger than that calculated for the *anti* conformation (5.1 kcal mol^{-1}) but similar to that predicted for the *syn* conformation (8.4 kcal mol^{-1}). Recently, we have reported a conformational analysis of DHTT

using AM1 and PM3 semiempirical methods [4, 24]. Two minima located at 60° and 120° have been obtained, but the rotational barriers are smaller than those obtained at the *ab initio* level. Smaller rotational barriers obtained with the semiemperical AM1 method have also been observed for unsubstituted oligothiophenes [25,26] as well as for alkyl-substituted bithiophenes [7,26]. The presence of two minima in the DHTT potential energy surface suggests that AM1 underestimates the steric hindrance of the two alkyl chains, giving steric effects similar to those created by the insertion of methyl substituents in positions 3 and 3'' as in DMTT (see Figure 3B).

3.2. Optical properties

The normalized absorption and fluorescence spectra of the molecules investigated are shown in Figure 5. All spectroscopic parameters are listed in Table 6. It is important to note that experimental measurements have been done for DHTT and not for DETT because DETT was not available. However, it is well-known that the length of the side chains does not practically influence the potential energy surface such that similar *ab initio* torsional potentials are expected for DHTT and DETT [3,4]. All spectral measurements have been done in many solvents without showing any important changes in spectroscopic parameters. Figure 5A shows that the absorption spectrum of TT is broad and does not show any resolvable vibrational structures that are characteristics of a nonrigid system giving rise to a wide range of conformations. This result is in agreement with the TT potential energy surface, where the global minimum corresponds to a twisted *anti* conformation having a low rotational barrier. The absorption spectrum of DMOTT is red shifted, shows vibrational structures, and is sharper than that of TT. The bathochromic shift observed is attributed both to the electron donor properties of the methoxy groups and to an increase in the molecular planarity. ZINDO/S calculations [3,24] performed on the optimized geometry obtained from the *ab initio* HF/3-21G* show that the former is responsible for about half of the red shift observed. The presence

of vibrational structures is a characteristic of more planar rigid systems, whereas sharper bands indicate a narrower distribution of conformers. This agrees quite well with theoretical results predicting a more planar conformation for DMOTT. Moreover the rotational barrier at 90° is higher than that found for TT, which should favor a smaller number of conformers for DMOTT. Compared to TT, the absorption spectrum of DMTT is blue shifted, its absorption coefficient is much reduced, ands its bandwidth is larger (see Table 6). This is experimental evidence that DMTT molecules are very twisted. Indeed a larger twisting between adjacent thiophene rings induces a reduction in the electronic delocalization, causing an increase in the transition energy as well as a decrease in the oscillator strength (which is proportional to the absorption coefficient). ZINDO/S shows that this blue shift is even counterbalanced by a 10 nm red shift caused by the methyl groups in the 3,3'' positions. This emphazises the importance of the steric effect between the methyl group and the sulfur atoms in this molecule. On the other hand, the broad and unstructured band indicates the presence of a wider distribution of conformations. All these results are corroborated by the potential energy surface of DMTT. Finally the absorption spectrum of DHTT is slightly blue shifted and its absorption coefficient is reduced compared to that of DMTT. This behavior indicates the presence of higher twisting between thiophene rings in DHTT, as suggested by the comparison of the potential energy surfaces of DMTT and DETT in Figure 3B. It is worth noting that again here for the same dihedral angle in TT and DETT, ZINDO/S shows a bathochromic shift of about 7 nm in the latter compound. Thus, blue shifts observed in the absorption spectra of DMTT and DHTT caused by the twisting of thiophene rings are always counterbalanced by the donor properties of the alkyl chains and would be even larger without the inductive effect of these substituents.

Figure 5B shows that the fluorescence maxima of all the molecules are closer to each other compared to their respective absorption spectra. Moreover, all fluorescence bands have the same vibrational structure and have similar bandwidths. This strongly suggests that all molecules adopt about the same conformation in the

first relaxed singlet excited state. More structured and sharper fluorescence bands compared to their respective absorption bands also suggest that the molecules adopt more planar conformations in their first relaxed singlet excited states with higher barrrier to rotation.

The red shift of the DMOTT fluorescence band compared with that of TT is attributed to the electron donor properties of the methoxy groups. However this spectral shift is much smaller than that found in the absorption spectra. Since an increase of the donor properties of the methoxy groups is expected in the excited state, the reduction in the red shift is explained by a larger conformational changes of TT compared to DMOTT between the ground and first relaxed singlet excited states, as shown from Figure 3A, comparing both minima to 180°. It is also worth noting that a change of the conformation of methoxy groups in the first singlet excited state would also contribute to the red shift observed for the fluorescence band of DMOTT.

Table 6 shows that the fluorescence band maximum of DMTT is very close to that observed for TT. Since a red shift of the DMTT fluorescence band should be observed for a conformation similar to that of TT, we believe that DMTT in the first relaxed singlet excited state is more twisted than TT. The steric hindrance induced by the methyl groups is probably too large for the molecules to reach totally planar conformations, as observed in the crystallographic data [22] for the ground electronic state. Along the same line, we do not believe that the excited-state conformation of DHTT is more planar than that of DMTT, as suggested by their respective fluorescence maxima. The red shift observed for the DHTT fluorescence band relative to that of TT is probably due to the donor properties of the hexyl chains.

Conformational changes between the ground state and first relaxed singlet excited state are well illustrated by the Stokes shifts. Indeed one can see in Table 6 that, as the ground-state conformation of terthiophenes becomes more twisted, the Stokes shift increases indicating an important conformational change between these two states.

4. Concluding Remarks

Ab initio calculations at the HF/3-21G* level performed on terthiophene derivatives have shown that the structural parameters of thiophene rings are little affected by the length of the molecule and the presence and/or the nature of substituent. On the other hand, the inter-ring bonds (C2-C2') and bond angles are the most affected because they depend directly on the electronic delocalization which is strongly related to the molecular conformation. Indeed, the C2-C2' bond length is shorter for the planar *anti-anti* conformers and increases as the twisting proceeds between 180° and 90°. This increase has shown to vary from molecule to molecule and depends linearly on the reciprocal of the potential energy barrier against planarity, which is obviously related to the minimum energy dihedral angle of each thiophene oligomer.

It has been shown that the insertion of methoxy groups in the 3,3'' positions of terthiophene (DMOTT) improves the molecular planarity and rigidity due to the electron donor properties of the methoxy substituents. On the other hand, the steric hindrance caused by the insertion of methyl groups in the same positions (DMTT) induces a large twisting between thiophene rings and produces a more flexible molecule. For these molecules, potential energy surfaces are very close to that of the respective 3,4'-substituted bithiophenes, showing the local effect of the substitution. The presence of two ethyl chains on the central thiophene ring (DETT) seems to produce an even larger steric hindrance, giving rise to a more twisted conformation. Indeed, the rotational barrier against planarity is much higher for DETT compared to those for DMTT, DMOTT, and TT.

Absorption measurements are in good agreement with theoretical results. Indeed the almost planar conformation of DMOTT predicted by *ab initio* calculations is reflected in its absorption band, which is red shifted, more structured,

and sharper than that of the unsubstituted molecule. On the other hand, twisted molecules (DMTT and DHTT) show absorption bands that are blue shifted, unstructured, and broad. Moreover absorption coefficients are smaller for twisted molecules.

After excitation, all terthiophenes become more planar, following the relaxation of the first excited singlet state. This is reflected by sharper fluorescence bands showing resolvable fine structures. We suggest that the relaxed conformation of DMTT and DHTT in the S_1 excited state are less planar than that of TT and DMOTT.

Acknowledgement

The authors are grateful to the Natural Sciences and Engineering Research Council of Canada (NSERC) and the Fonds FCAR (Quebec) for their financial support. N.D.C. is grateful to the NSERC for a graduate scholarship.

References and Notes

[1] Schopf, G.; Kossmehl, G. *Adv. Polym. Sci.* **1997**, *127*, 1.

[2] (a)Becker, R.S.; de Melo, J.S.; Maçanita, A.L.; Elisei, F. *J. Phys. Chem.* **1996**, *100*, 18683. (b) Becker, R.S.; de Melo, J.S.; Maçanita, A.L.; Elisei, F. *Pure & Appl. Chem.* **1995**, *67*, 9.

[3] DiCésare, N.; Belletête, M.; Raymond, F.; Leclerc, M.; Durocher, D. *J. Phys. Chem. A* **1997**, *101*, 776.

[4] (a) DiCésare, N.; Belletête, M.; Donat-Bouillud, A.; Leclerc, M.; Durocher, G. *J. Luminescence*, sent for publication. (b) DiCésare, N.; Belletête, M.; Donat-Bouillud, A.; Leclerc, M.; Durocher, G. *macromolecules*, sent for publication.

[5] DiCésare, N.; Belletête, M.; Raymond, F.; Leclerc, M.; Durocher, G. *J. Phys. Chem. A*, **1998**, *102*, 2700.

[6] DiCésare, N.; Belletête, M.; Leclerc, M.; Durocher, G. *J. Phys. Chem.*, sent for publication.

[7] DiCésare, N.; Belletête, M.; Leclerc, M.; Durocher, G. *Synth. Met*, in press.

[8] DiCésare, N.; Belletête, M. ; Durocher, G. ; Leclerc, M. *Chem. Phys. Lett*, **1997**, *275*, 533.

[9] Leclerc, M.; Fréchette, M.; Bergeron, J-Y.; Ranger, M.; Lévesque, I.; Faïd, K. *Macromol. Chem. Phys.* **1996**, *197*, 2077.

[10] Roux, C.; Bergeron, J-Y.; Leclerc, M. *Makromol. Chem.* **1993**, *194*, 869.

[11] Raymond, F. ; DiCésare, N. ; Belletête, M. ; Durocher, G. ; Leclerc, M. *Adv. Mater.*, in press.

[12] Hernandez, V.; Lopez-Navarrete, J.T. *J. Chem. Phys.* **1994**, *101*, 1369.

[13] Aleman, C.; Julia, L. *J. Phys. Chem.* **1996**, *100*, 1524.

[14] Orti, E.; Viruela, P.M.; Sanchez-Marin, J.; Tomas, F. *J. Phys. Chem.* **1995**, *99*, 4955.

[15] Viruela, P.M.; Viruela, R.; Orti, E.; Brédas, J.L. *J. Am. Chem. Soc.* **1997**, *119*, 1360.

[16] Ciofalo, M.; La Manna, G. *Chem. Phys. Lett.* **1996**, *263*, 73.

[17] Frisch, M.J.; Head-Gordon, M.; Trucks, G.W.; Foresman, J.B.; Schlegel, H.B.; Raghavachari, K.; Robb, M.; Bimkley, J.S.; Gonzales, C.; Defrees, D.J.; Fox, D.J.; Whiteside, R.A.; Seeger, R.; Melius, C.F.; Baker, J.; Martin, R.L.; Kahn, L.R.; Stewart, J.J.P.; Topiol, S.; Pople, J.A. Gaussian 90, Revision F, Gaussian : Pittsburgh, P.A. 1990.

[18] Faïd, K,; Leclerc, M. *J. Chem. Soc., Chem. Commun.* **1993**, *11*, 962.

[19] Georges, G. Ph.D. Thesis, Université de Montréal, 1997.

[20] Zotti, G. ; Gallazi, M.C. ; Zerbi, G. ; Meilla, S.V. *Synth. Met.* **1995**, *73*, 217.

[21] Van Bolhuis, F.; Wynberg, H.; Havinga, E.E.; Meijer, E.W.; Staring, G.J. *Synth. Met.* **1989**, *30*, 381.

[22] Chaloner, P.A.; Gunatunga, S.R.; Hitchcock, P.B. *J. Chem. Soc., Perkin Trans. 2* **1997**, 1596.

[23] (a) DeWitt, L.; Blanchard, G.J.; LeGoff, E.; Benz, M.E.; Liao, J.H.; Kanatzidis, M.G. *J. Am. Chem. Soc.* **1993**, *115*, 12158. (b) Horne, J.C.; Blanchard, G.J.; LeGoff, E. *J. Am. Chem. Soc.* **1995**, *117*, 9551.

[24] Belletête, M.; DiCésare, N.; Leclerc, M.; Durocher, G. *J. Mol. Struct. (TheoChem)* **1997**, *391*, 85.

[25] Belletête, M.; DiCésare, N.; Leclerc, M.; Durocher, G. *Chem. Phys. Lett.* **1996**, *250*, 31.

[26] dos Santos, M.C.; Bohland-Filho, J. *SPIE* **1995**, *2528*, 143.

Table 1

Optimized Structural Parameters of TT

parameter	bond length (Å)	parameter	angle and dihedral angle
S_1-C_2	1.7351	S_1-C_2-C_3	111.0
C_2-C_3	1.3538	C_2-C_3-C_4	112.9
C_3-C_4	1.4335	C_3-C_4-C_5	112.5
C_4-C_5	1.3475	C_4-C_5-S_1	112.0
C_5-S_1	1.7206	C_5-S_1-C_2	91.6
C_3-H_3	1.0694	C_2-C_3-H_3	123.4
C_4-H_4	1.0687	C_3-C_4-H_4	123.5
C_5-H_5	1.0672	C_4-C_5-H_5	127.1
C_2-C_2'	1.4570	S_1-C_2-C_2'	121.2
S_1'-C_2'	1.7342	S_1'-C_2'-C_3'	110.9
C_2'-C_3'	1.3534	C_2'-C_3'-C_4'	113.1
C_3'-C_4'	1.4292	C_5'-S_1'-C_2'	91.9
C_3'-H_3'	1.0692	S_1'-C_2'-C_2	121.2
		C_2'-C_3'-H_3'	123.4
		S_1-C_2-C_2'-S_1'	147.6

Table 2

Relative Energy (in kcal mol^{-1}) and Torsional Angle ($\theta = \phi$) Obtained From *ab initio* Calculations (HF/3-21G*) for the Molecules Investigated.

molecule	*syn* [a]		perpendicular		*anti* [a]
DMOTT	3.5	1.8	7.7	0.0	0.32
		(22.9°)		(171.3°)	
TT	3.4	1.2	3.2	0.0	0.67
		(42.8°)		(147.2°)	
DMTT	5.6	0.047	0.37	0.0	3.0
		(57.9°)		(118.2°)	
DETT	8.4	-	0.23	0.0	5.1
				(104.7°)	

[a] *Syn*, $\theta = \phi = 0°$; *anti*, $\theta = \phi = 180°$.

Table 3

Optimized Structural Parameters of DMOTT

parameter	bond length (Å)	parameter	angle and dihedral angle
S_1-C_2	1.7372	S_1-C_2-C_3	110.4
C_2-C_3	1.3530	C_2-C_3-C_4	113.7
C_3-C_4	1.4339	C_3-C_4-C_5	112.1
C_4-C_5	1.3441	C_4-C_5-S_1	112.1
C_5-S_1	1.7231	C_5-S_1-C_2	91.7
C_4-H_4	1.0680	C_3-C_4-H_4	123.2
C_5-H_5	1.0669	C_4-C_5-H_5	127.1
C_3-O_a	1.3757	C_2-C_3-O_a	122.6
O_a-C_b	1.4592	C_3-O_a-C_b	116.3
C_2-C_2'	1.4511	S_1-C_2-C_2'	122.2
S_1'-C_2'	1.7380	S_1'-C_2'-C_3'	111.2
C_2'-C_3'	1.3559	C_2'-C_3'-C_4'	113.1
C_3'-C_4'	1.4232	C_5'-S_1'-C_2'	91.4
C_3'-H_3'	1.0697	C_2'-C_3'-H_3'	123.8
		S_1'-C_2'-C_2	122.1
		C_2-C_3-O_a-C_b	254.4
		S_1-C_2-C_2'-S_1'	171.3

Table 4

Optimized Structural Parameters of DMTT

parameters	bond length (Å)	parameters	angle and dihedral angle
S_1-C_2	1.7380	S_1-C_2-C_3	111.7
C_2-C_3	1.3538	C_2-C_3-C_4	111.8
C_3-C_4	1.4414	C_3-C_4-C_5	113.2
C_4-C_5	1.3455	C_4-C_5-S_1	111.9
C_5-S_1	1.7177	C_5-S_1-C_2	91.4
C_4-H_4	1.0698	C_3-C_4-H_4	122.8
C_5-H_5	1.0675	C_4-C_5-H_5	126.9
C_3-C_a	1.5087	C_2-C_3-C_a	126.0
C_2-C_2'	1.4665	S_1-C_2-C_2'	119.6
S_1'-C_2'	1.7326	S_1'-C_2'-C_3'	111.0
C_2'-C_3'	1.3521	C_2'-C_3'-C_4'	113.1
C_3'-C_4'	1.4312	C_5'-S_1'-C_2'	91.9
C_3'-H_3'	1.0691	C_2'-C_3'-H_3'	123.1
		S_1'-C_2'-C_2	121.9
		S_1-C_2-C_2'-S_1'	118.2

Table 5

Optimized Structural Parameters of DETT

parameter	bond length (Å)	parameter	angle and dihedral angle
S1-C2	1.7352	S1-C2-C3	111.0
C2-C3	1.3506	C2-C3-C4	113.0
C3-C4	1.4356	C3-C4-C5	112.4
C4-C5	1.3477	C4-C5-S1	112.0
C5-S1	1.7199	C5-S1-C2	91.6
C3-H3	1.0691	C2-C3-H3	123.0
C4-H4	1.0688	C3-C4-H4	123.6
C5-H5	1.0675	C4-C5-H5	127.0
C2-C2'	1.4695	S1-C2-C2'	121.7
S1'-C2'	1.7290	S1'-C2'-C2	120.2
C2'-C3'	1.3528	S1'-C2'-C3'	112.0
C3'-C4'	1.4491	C2'-C3'-C4'	112.3
C4'-C5'	1.3528	C3'-C4'-C5'	112.3
C5'-S1'	1.7290	C4'-C5'-S1'	112.0
C5'-C2''	1.4694	C5'-S1'-C2'	91.4
S1''-C2''	1.7352	S1'-C5'-C2''	120.1
C2''-C3''	1.3508	S1''-C2''-C5'	121.7
C3''-C4''	1.4355	S1''-C2''-C3''	111.0
C4''-C5''	1.3477	C2''-C3''-C4''	113.0
C5''-S1''	1.7199	C3''-C4''-C5''	112.4
C3''-H3''	1.0691	C4''-C5''-S1''	112.0
C4''-H4''	1.0688	C5''-S1''-C2''	91.6
C5''-H5''	1.0675	C2'-C3'-Ca	124.0
C3'-Ca	1.5117	C3'-Ca-Cb	111.0
Ca-Cb	1.5471	C3'-C4-Ca'	123.6
C4'-Ca'	1.5118	C4'-Ca'-Cb'	111.0
Ca'-Cb'	1.5471	C2''-C3''-H3''	123.0
		C3''-C4''-H4''	123.6
		C4''-C5''-H5''	127.0
		C2'-C3'-Ca-Cb	91.2
		C3'-C4'-Ca'-Cb'	274.6
		S1-C2-C2'-S1'	255.7
		S1'-C5'-C2''-S1''	254.4

Table 6

Spectroscopic Parameters of Terthiophene Derivatives in *n*-hexane at Room Temperature

Molecule	λ_A[a] (nm)	ν_A[a] (cm^{-1})	ε[b] (M^{-1} cm^{-1})	$fwhm_A$[c] (cm^{-1})	λ_F[a] (nm)	ν_F[a] (cm^{-1})	$fwhm_F$[c] (cm^{-1})	Δ[d] (cm^{-1})	$\theta = \phi$[e] (deg)
DMOTT	372	26900	-	4600	431	23200	3600	3700	171.3
TT	349	28700	28700	5200	422	23700	3400	5000	147.2
DMTT	335	29900	16100	6100	419	23900	3600	6000	118.2
DHTT[f]	331	30200	13400	6700	426	23500	3500	6700	104.7

[a] Taken at the band maxima.

[b] Molar absorption coefficient at the band maxima.

[c] Full width at half maximum.

[d] Stokes shift between maxima of absorption and fluorescence bands.

[e] Dihedral angle of the minimum energy conformer obtained from the HF/3-21G* basis set.

Figure 1 : Molecular structures of the substituted terthiophenes investigated.

Figure 2: Variation of the C2-C2' bond length with the dihedral angles θ and ϕ.

Figure 3 : Ground-state potential energy curves for dihedral angles $\theta = \phi$.

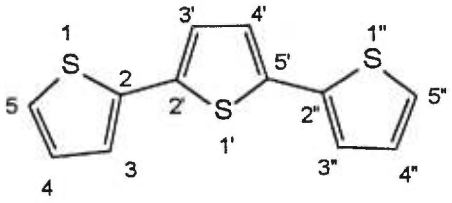

TT

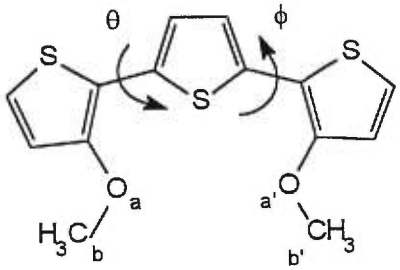

DMOTT

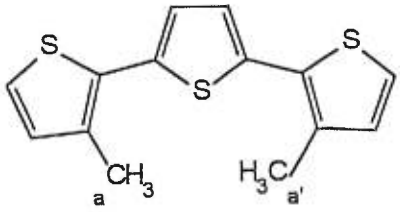

DMTT

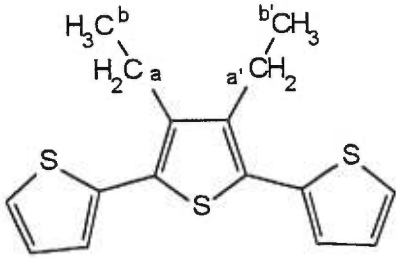

DETT

Figure 1 : Molecular structures of the substituted terthiophenes investigated.

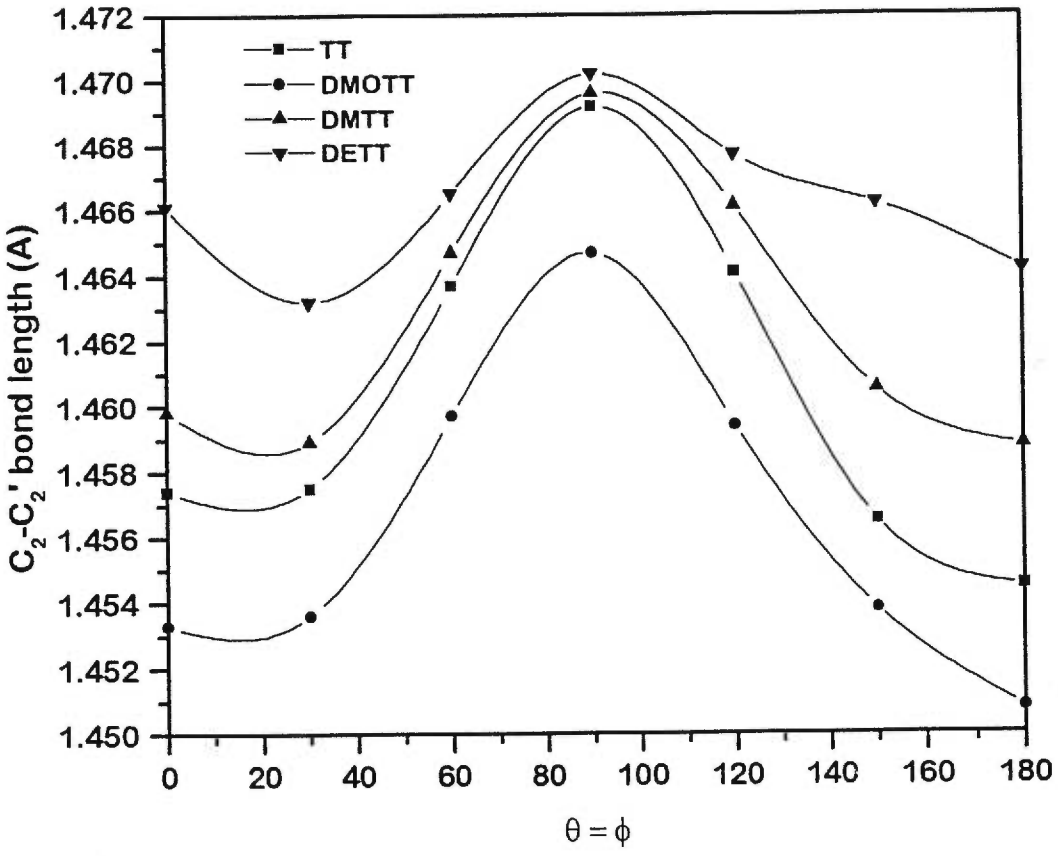

Figure 2: Variation of the C2-C2' bond length with the dihedral angles θ and ϕ.

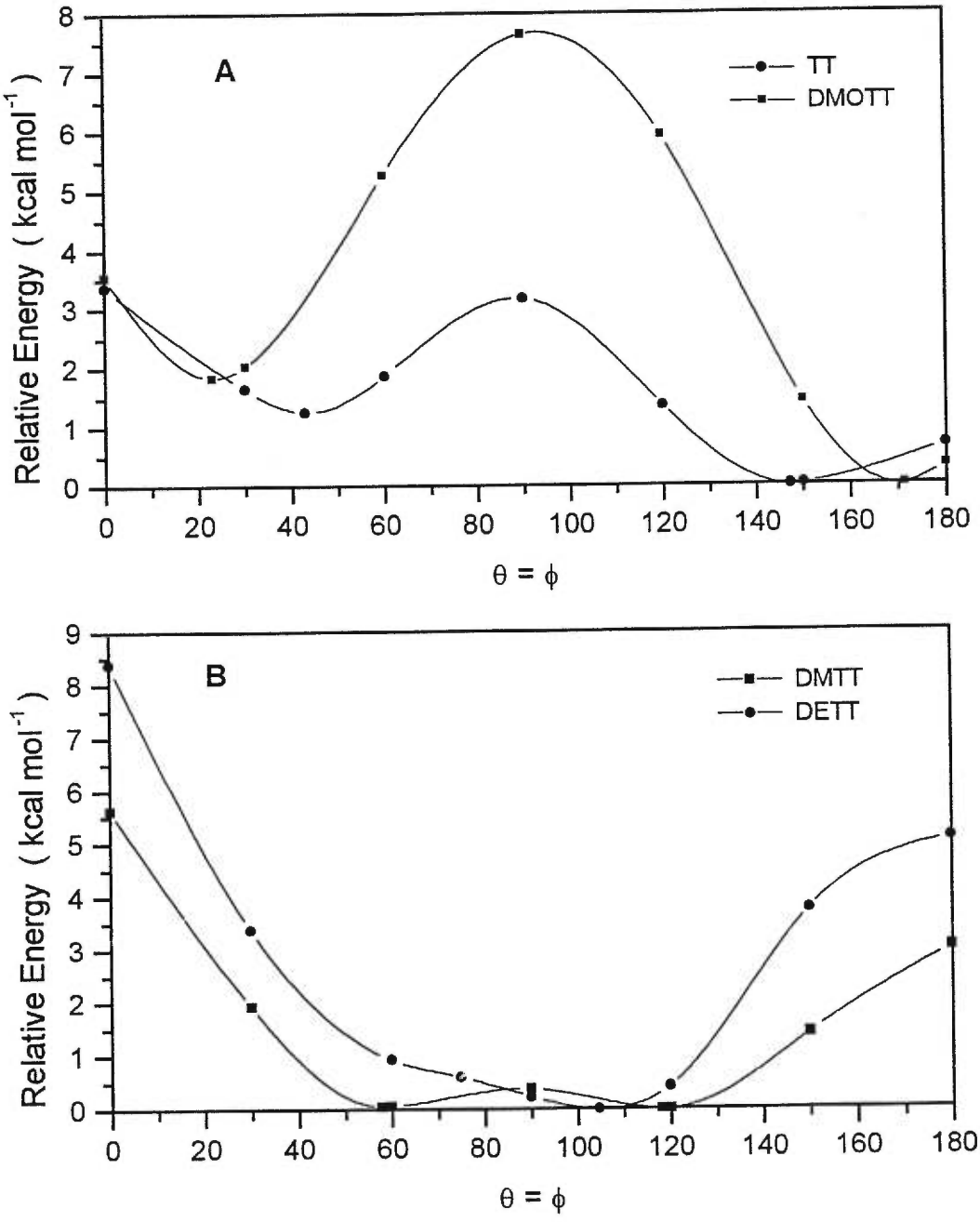

Figure 3 : Ground-state potential energy curves for dihedral angles $\theta = \phi$.

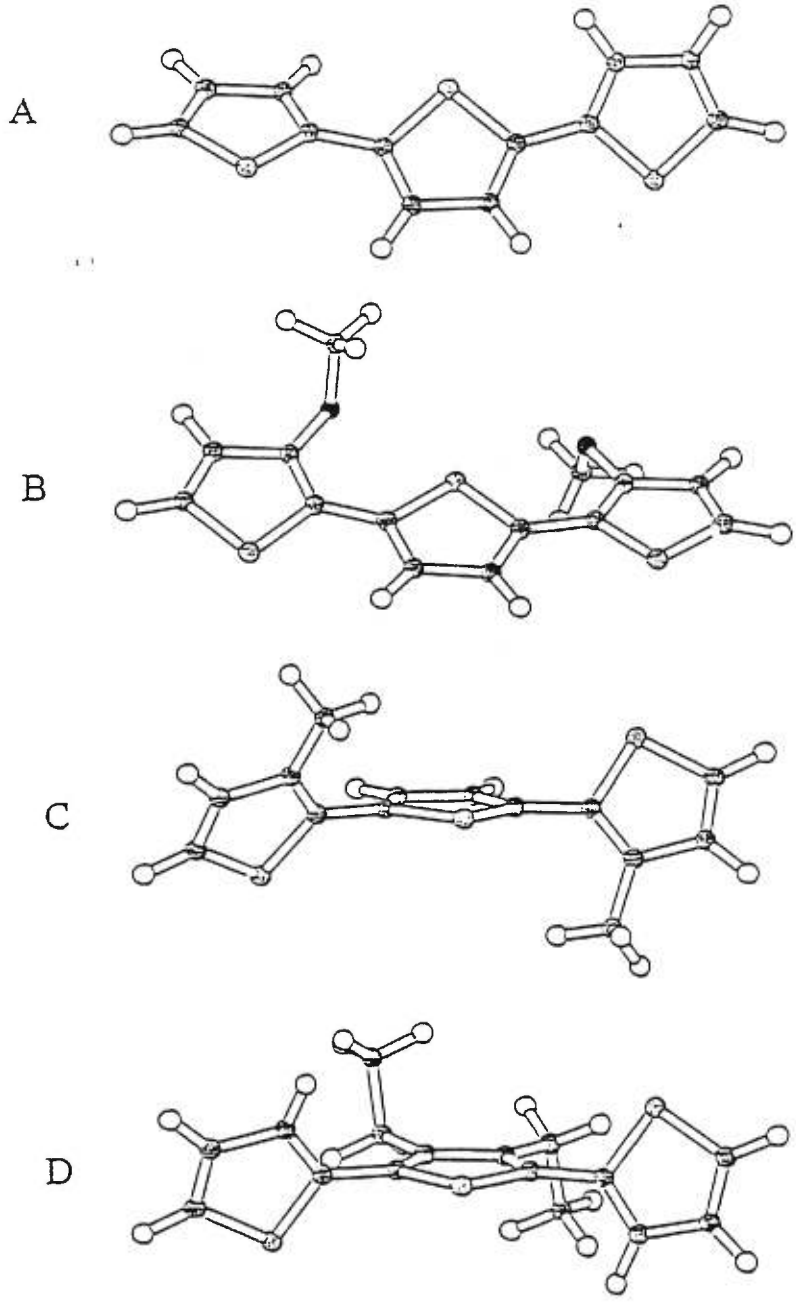

Figure 4 : Optimized molecular structures of the molecules investigated : (A) TT, (B) DMOTT, (C) DMTT, and (D) DETT.

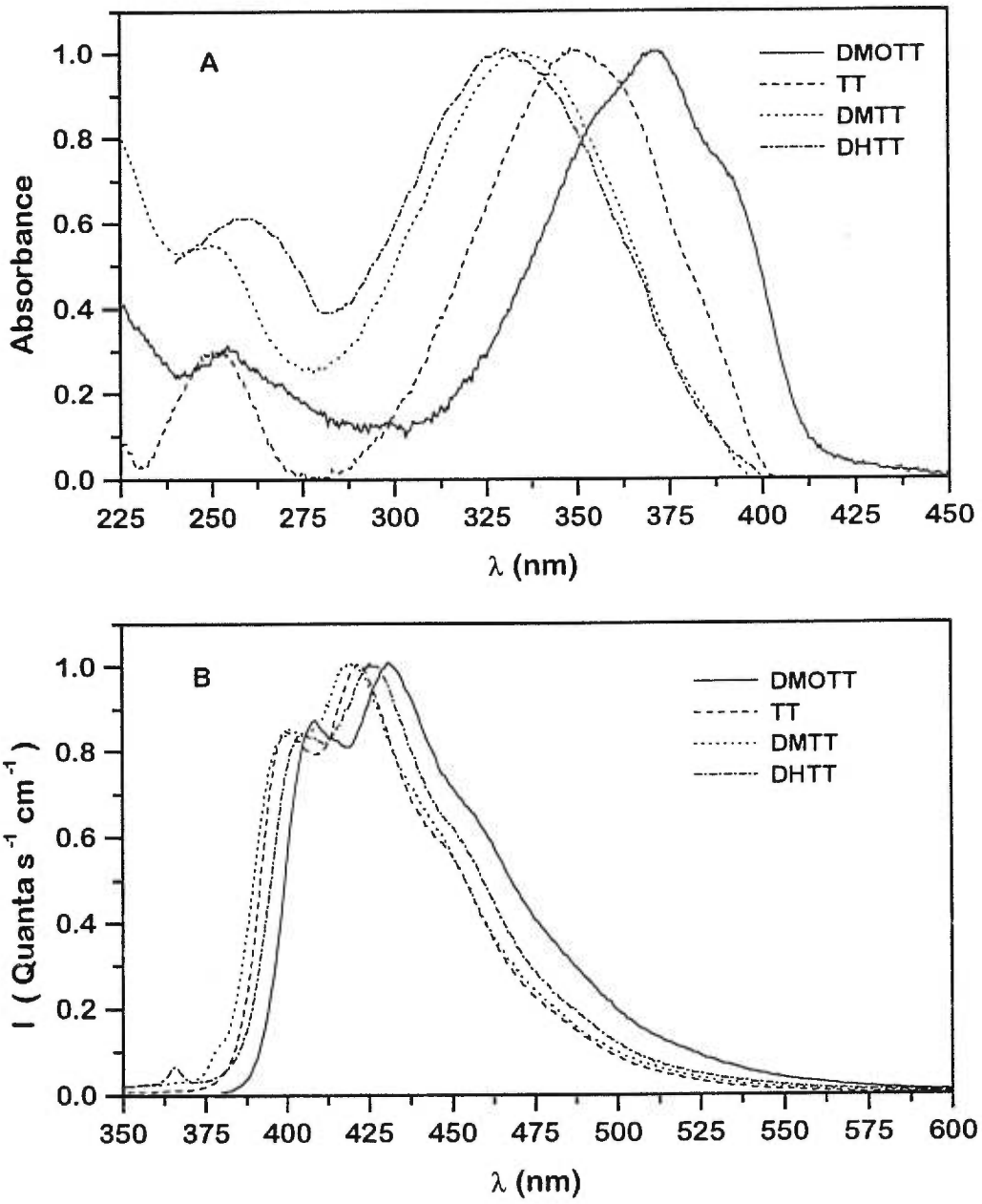

Figure 5 : Absorption (**A**) and fluorescence (**B**) spectra of TT, DMTT, DMOTT, and DHTT. All spectra have been measured in *n*-hexane at room temperature.

Chapitre 7

Étude expérimentale des effets chromiques de dérivés du 2,2':5',2''-terthiophène

L'observation et la description du thermochromisme chez les oligothiophènes sont présentées dans ce chapitre. Le TT ainsi que les mêmes dérivés du TT décrits dans le chapitre précédent, ont été utilisés. Les trimères ont été utilisés dans cette étude des effets chromiques des oligothiophènes contrairement aux dimères pour deux raisons principales. Premièrement, la fluorescence des dimères est très faible (le rendement quantique de fluorescence (ϕ_F) des dimères est voisin de 0.01). Comme la fluorescence est la méthode privilégiée dans cette étude dû aux environnements particuliers, qui ne favorisent pas la détection d'un signal net, l'utilisation d'oligothiophènes avec des ϕ_F plus élevés est préférable. Deuxièmement, comme l'agrégation est utilisée dans cette partie, il nous faut utiliser des oligothiophènes qui s'associent facilement. Comme la solubilité des oligothiophènes diminue avec la longueur de ceux-ci, l'agrégation est plus facile à obtenir pour des oligomères plus longs. Les dimères ont une bonne solubilité dans les solvants organiques communs de sorte que l'agrégation est difficile à obtenir. De plus, la synthèse des trimères permet une plus grande diversité de molécules. Ainsi, les trimères étaient les plus petits oligothiophènes permettant d'atteindre nos objectifs. La longueur des oligomères utilisés est non négligeable dans l'atteinte de nos objectifs. Les oligomères courts permettent un grand choix d'environnements de travail dû à leur bonne solubilité et le nombre restreint de degrés de liberté (spécialement de torsion) simplifie beaucoup l'interprétation des résultats spectroscopiques.

Notre but principal dans ce chapitre est d'observer le thermochromisme chez les trimères et de voir si les changements dans les propriétés optiques ont pour origine un changement conformationnel de l'oligomère ou une interaction électronique (de type excitonique) entre molécules semblables. Naturellement, ces deux effets ne s'excluent pas mutuellement et peuvent être tous les deux à l'origine des changements optiques observés. Afin d'identifier l'effet conformationnel seul, nous avons étudié les changements dans les propriétés optiques suite à un changement conformationnel pour des molécules isolées, c'est-à-dire piégées dans une matrice substitutionnelle (matrice de *n*-décane) à 77K. Comme les molécules sont isolées, aucune interaction intermoléculaire ne peut exister. Les changements des propriétés optiques résultant des changements conformationnels sont alors comparés à ceux observés suite à l'agrégation de sorte que l'on puisse identifier l'importance de ces derniers dans les effets chromiques des trimères. Les changements des propriétés optiques ne correspondant pas aux changements conformationnels sont alors identifiés comme résultants d'effets excitoniques. Il est à noter que, comme chez les polythiophènes, les effets chromiques des trimères s'observent aussi bien en solution qu'à l'état solide. Comme les mesures en solution permettent une plus grande liberté expérimentale, nous ne présenterons pas les mesures à l'état solide.

Les résultats montrent que les effets chromiques du TT sont parfaitement expliqués par une scission de nature excitonique. Par contre, tous les trimères substitués donnent des effets chromiques fort différents de ceux du TT. Ces effets chromiques sont très similaires à ceux induits par les changements conformationnels observés chez les molécules isolées et sont interprétés en termes de changements conformationnels. Cette différence entre le TT et les trimères substitués est expliquée en termes de désordre dans la structure agrégée induit par la présence des substituants qui défavorisent un bon empilement et une interaction électronique forte entre molécules voisines, comme observée pour le TT. Cette dernière hypothèse sera d'ailleurs discutée plus en détails dans le prochain chapitre (chapitre 8) où les

structures cristallines et les calculs semi-empiriques ZINDO/S permettant de calculer les effets des interactions intermoléculaires sur les diverses transitions singulet et triplet seront présentées.

7.1 Article 7 : Intermolecular interactions in conjugated oligomers: I – Optical spectra of terthiophene and substituted terthiophenes recorded in various environments.

Article publié dans The Journal of Physical Chemistry A, volume 103, numéro 7, pages 795-802 (1999).

Intermolecular Interactions in Conjugated Oligothiophenes: I – Optical Spectra of Terthiophene and Substituted Terthiophenes Recorded in Various Environments

Nicolas DiCésare [a], Michel Belletête [a], Claudio Marrano [b], Mario Leclerc [b] and Gilles Durocher [a]

[a] Laboratoire de photophysique moléculaire

[b] Laboratoire des polymères électroactifs et photoactifs

Département de Chimie, Université de Montréal, C.P. 6128, Succ. A, Montréal, Québec, H3C 3J7, Canada

Abstract

The absorption and fluorescence spectra of terthiophene (TT) as well as three substituted terthiophene derivatives, namely 3,3''-dimethoxy-2,2':5',2''-terthiophene (DMOTT), 3,3''-dimethyl-2,2':5',2''-terthiophene (DMTT) and 3',4'-dihexyl-2,2':5',2''-terthiophene (DHTT) isolated in an alkane matrix and in their aggregated forms are reported. The thermochromic properties of substituted oligothiophenes are reported for the first time. The optical changes observed for the isolated molecules in the alkane matrix are interpreted in terms of conformational changes caused by the packing effect. After aggregation, TT exhibits a splitting in the excitation spectrum, which is provoked by an excitonic effect. On the other hand, it is observed that the changes in the optical properties of substituted terthiophenes

are close to those found in the alkane matrix. This strongly suggests that the aggregation process does not produce any significant optical change, other than those provoked by conformational changes, in the excitation spectra of these molecules. It is suggested that the presence of the side chains weaken the intermolecular interactions, which are responsible for the excitonic effect. Finally, the fluorescence spectra of all the molecules investigated show a new red shifted band, when aggregated. The new emission cannot be explained by conformational changes and has its origin in the aggregation process itself.

1. Introduction

Our knowledge on the electronic and optical properties of organic conjugated polymers has evolved over the past two decades, providing the chemical and physical community with viable tools for probing polymer structures on a molecular scale. By investigating optical phenomena of organic conjugated polymer systems, one can develop an accurate picture of intermolecular interactions taking place in solution and in solid phases. This is indeed in the field of interest of many parts of modern chemistry as organic, bio and solid state chemistry.

Polythiophene is an interesting example of a conjugated polymer because of its high electrical conductivity in its oxidized (doped) state [1]. The high conductivity is ascribed to the movement of delocalized charges and associated structural deformations along and between polymer chains [2]. However, this conducting polymer with a highly conjugated π-system is insoluble and infusible. Although the delocalized electronic structure of polythiophene tends to yield relatively stiff chains with little flexibility, solubility has been achieved by the incorporation of relatively long and flexible side chains [3-5]. Introducing an *n*-alkyl group with a minimum of four carbon atoms at the 3-position of the thiophene ring allows the polymer to be soluble in common organic solvents, fusible, and melt processible, yet retaining a rather high conductivity of about 30 -100 S/cm [6]. The

physical and chemical properties of poly(3-alkylthiophene)s have been applied in a number of applications such as batteries, light-emitting devices, photo-pattern recordings, and photo catalysts [7-9].

Due to the incorporation of side chains to the backbone, some polythiophene derivatives exhibit interesting reversible thermochromic [10-14], solvatochromic [6], and piezochromic [15] properties. These optical phenomena are not unique to polythiophenes and have also been reported for some polysilanes [16] and polydiacetylenes [17]. In most cases, these dramatic color transitions have been associated with conformational changes since, in π-conjugated polymers, there is a strong coupling between the electronic structures and the backbone conformation [10-14, 18]. The thermochromism and solvatochromism were considered at a molecular level as a result of the interruption of the conjugation caused by a generation of twists along the main chain. The increased thermal motion of the side chains is believed to be intimately involved in the thermochromic effect by influencing the planarity of the polymer backbone and therefore the electronic structure. For instance, poly(3-alkylthiophene)s are red in the solid state at room temperature and this material becomes yellow at higher temperatures [14]. Crystallographic data of this material show a lamellar structure with a high degree of planarity of the backbone at room temperature [19-21]. As the temperature is increased, the thermal agitation of the lateral chains would induce a larger repulsion between the chains creating a high deviation from planarity in the main chain. It is important to mention here that X-Ray data provide information over the crystalline region while the UV-visible absorption spectra are sensitive to electronically conjugated local chain segments and also to the interchain interactions [21].

Our goal is to better understand how intermolecular interactions affect the optical properties with respect to those observed in isolated molecules and hence to understand the role played by intermolecular interactions in the phenomenon of thermochromism observed in some substituted polythiophenes. However, the polymers are exhibiting a broad and not fully characterized range of conjugation

lengths that make difficult the measurement of vibrationally resolved optical spectra. For this reason, we have focused our attention on oligothiophenes for which optical properties are better characterized. Indeed, the optical properties of many unsubstituted [22, 23] and substituted [24-29] oligothiophene derivatives, in solution at room temperature, are well known. Despite the fact that the synthesis of many substituted oligothiophenes is reported in the literature, the thermochromic properties of these compounds in solution are still lacking. The only chromic effects reported in the literature deal with unsubstituted oligothiophene derivatives in various environments, such as in thin films [30-34], inclusion complexes [34-37] and in aggregated forms [32, 38]. In thin films or in aggregated forms, the optical properties have been explained using an excitonic model [39].

We have recently reported and described the HF/3-21G* potential energy surfaces of many substituted bithiophenes [40-42]. The unsubstituted bithiophene shows a twisted conformation with a minimum at θ =150° (dihedral angle between thiophene rings) [40]. The insertion of methoxy groups in 3 and/or 3' positions favors planar conformations due to the electron donor properties of these substituents [42]. On the other hand, the incorporation of alkyl groups on the same positions induces a greater torsion between thiophene rings with higher rotational energy barriers against planarity [40]. Finally bithiophenes having thioalkyl groups as well as mixed substituents exhibit a good number of various conformers [41,42]. From these theoretical results, it has been possible to correlate the rotational barriers between the lowest energy conformation and the co-planar conformation of the substituted bithiophenes with the thermochromic properties observed (or not) in the parent polymers [43]. Moreover a new thermochromic polythiophene has been predicted using this correlation [44]. These theoretical results strongly suggest that conformational changes are playing an important role in the thermochromism observed in polymers. In contrast, some authors have recently explained optical changes observed in the absorption spectra of poly(3-alkylthiophene)s on the sole basis of interchain interactions (π-stacking effect) and by neglecting possible

conformational changes along the main chain [45]. It will be shown in this paper that this is certainly in disagreement with the origin of the chromic effect observed in substituted oligothiophenes.

In this work, to obtain spectral evidences about the origin of the thermochromic effect, the absorption and fluorescence spectra of four terthiophene derivatives isolated in an *n*-alkyl matrix at 77K and in aggregated forms (in a glassy medium or in methanol/water mixtures) are reported. Both the packing and the excitonic effects on the optical spectra are analysed. Results show that the optical changes found for the isolated molecules in a 77K matrix are associated to conformational changes (packing effect). Conformational changes are also responsible for the main part of the optical changes found in the absorption spectra of the substituted terthiophenes in their aggregated forms. However the formation of parallel H-type excitons may also play a role in these spectra. On the other hand, the fluorescence spectra of the terthiophene derivatives in their aggregated forms cannot be explained by conformational changes and have their origin in the excitonic effect. This study deals with conformational property relationships and π-stacking of conjugated organic oligomers. These are key properties to control in the developpement of new organic conducting polymers. The molecular structures of the oligothiophenes investigated are displayed in Figure 1.

2. Methodology

2.1. Materials

Terthiophene (TT, 99%), *n*-decane (99+%), isopentane (99.5+%, HPLC grade) and methanol (99.9 %, spectrophotometric grade) were purchased from Aldrich Chemicals and used as received. Distilled water was used in the methanol/water mixtures. Prior to use, all the solvents were checked for spurious emissions in the region of interest and found to be satisfactory. 3',4'-dihexyl-

2,2':5',2''-terthiophene (DHTT) [24] and 3,3''-dimethyl-2,2':5',2''-terthiophene (DMTT) [46] were prepared according to previously published procedures. 3,3''-dimethoxy-2,2':5',2''-terthiophene (DMOTT) was prepared following similar procedures to those previously reported in the literature [47].

2.2. Instrumentation

Room temperature absorption spectra were recorded on a Varian spectrometer, model Cary 1 Bio and temperature-dependent absorption spectra were recorded on a Varian spectrometer, model 5E using 1 cm quartz rectangular cells. Fluorescence spectra corrected for the emission detection were recorded on a Spex Fluorolog-2 spectrophotometer with a F2T11 special configuration (1 cm rectangular quartz cells). The excitation and emission band-passes used were 2.6 and 1.9 nm respectively. The fluorescence and excitation spectra were found independent of the excitation and emission wavelength respectively and the excitation spectra were identical to their respective absorption spectra.

In rigid media at 77 K (*n*-decane matrix, isopentane glass and methanol/water mixtures), excitation and fluorescence spectra were recorded using the front face arrangement of the instrument to avoid any reabsorption or inner filter effects. Measurements were taken in a quartz cylinder tube of 0.4 mm (ID) immersed in a Dewar filled with liquid nitrogen. Excitation and emission band-passes of 0.34 and 3.8 nm, respectively were used for the recording of the excitation spectra while the fluorescence spectra were recorded using excitation and emision band-passes of 1.10 and 0.75 nm, respectively. Temperature-dependent measurements (in fluid media) were done using 1 cm quartz cells and with excitation and emission band-passes similar to those employed for the room temperature measurements. Temperatures were varied using a Cryo Industries cryostat, model RC 152, using liquid nitrogen for the cooling gas and monitoring with a thermocouple immersed in the sample solutions.

3. Results and Discussion

3.1 Conformational Analysis

In a recent paper [48], we have reported and described the *ab initio* HF/3-21G* potential energy surfaces of all terthiophenes investigated here (see figure 1) as well as their respective absorption and fluorescence spectra recorded at room temperature. The potential energy surface of TT has shown that the most stable conformation is *anti*-gauche, about 30° off planarity. Moreover, the rotational barrier against planarity is relatively small (0.67 kcal mol^{-1}) allowing for the presence of many conformers at room temperature. The methoxy substituents in the DMOTT compound induces a more planar conformation compared to that of TT. On the other hand, the presence of alkyl substituents (DMTT and 3',4'-diethyl-2,2':5',2''-terthiophene (DETT)) induces a strong twisting between adjacent thiophene rings and a high rotational energy barrier against planarity. Rotational energy barriers and torsional angles of the lowest energy conformers of each derivative are listed in reference [48].

Absorption spectra, recorded in *n*-decane at room temperature (figures 2 and 3), are in good agreement with theoretical results. Indeed, the large and non-structured absorption band of TT suggests that this molecule is not planar and is flexible in agreement with its potential energy surface. On the other hand, the red shifted and more structured absorption band of DMOTT compared to that of TT shows that the molecule is more planar as predicted by the *ab initio* calculations. However, a part of the red shift is also induced by the electron donor properties of the methoxy groups. Finally, compared to the absorption band of TT, the absorption bands of DMTT and DHTT are blue shifted, their absorption coefficients are smaller [48] and their bandwidths are larger [48]. These optical properties strongly suggest that DMTT and DHTT are much twisted in their ground state as predicted by their respective potential energy surfaces.

Fluorescence spectra of each molecule, recorded in *n*-decane at room temperature (figures 2 and 3), are more structured and narrower than their respective absorption spectra and rather similar. Moreover, the relatively large Stoke shifts and the poor adherence to the mirror image relationship between absorption and fluorescence spectra indicate a non-negligeable conformational change between these two states. This lead to the conclusion that all molecules adopt a more planar conformation in the first relaxed excited singlet state. The red shift observed for the fluorescence band of DMOTT compared to that of TT is very small and is attributed to the electron donor effect of the methoxy groups. The fluorescence bands of DMTT and DHTT are located at about the same energy as the emission band of TT showing that, after relaxation in their excited state, these three molecules adopt similar conformations. A more detailed analysis of the spectroscopic parameters of all these molecules has been done before [48].

3.2 Matrix Isolation of the Terthiophene Derivatives

The optimum conditions for the appearance of the quasi-linear spectra (Shpolskii effect) of linear aromatic molecules is obtained when the length of the long axes of the *n*-alkane solvent and the aromatic molecule are matched [49]. For this reason, *n*-decane has been chosen to form a substitutional matrix, which should totally isolate the trimers even at concentrations where aggregates are observed in other solvents.

Figure 2A shows the absorption (or excitation at 77K) and fluorescence spectra of TT in *n*-decane at room temperature (fluid solution) and isolated in the solvent matrix at 77K. One can see that, in a *n*-decane matrix at 77K, the excitation spectrum of TT is red shifted and more structured compared to its absorption spectrum measured at room temperature. By contrast, the fluorescence spectrum of TT recorded at 77 K does not show any significant shift. However, an increase in the vibronic resolution is observed in the *n*-decane matrix. It is also observed that the

mirror image relationship is well respected at 77 K so that the Stokes shift is small between the excitation and fluorescence spectra. These observations strongly suggest that, at 77 K, the TT conformations in the ground and in the excited state are very close. Since a nearly planar conformation is expected for TT in its first singlet excited state, in solution at room temperature [48], and since, at 77 K, the fluorescence band is not shifted, it can be concluded that TT also adopts a planar ground state conformation in the *n*-decane matrix. The change of conformation in the ground state between room temperature solution and 77 K *n*-decane matrix probably occurs due to a better cohesion energy existing between planar molecules and the matrix (packing effect). This is in agreement with X-ray data showing that bithiophene [50, 51] and terthiophene [52] are planar in the solid state. The change of conformation adopted by TT is responsible for the red shift observed in the excitation spectrum, relatively to the room temperature one, recorded in the *n*-decane matrix. Birnbaum and Kohler reached the same conclusion from the full vibrational analysis of the excitation and fluorescence spectra of TT in *n*-decane at 4K [53]. It is important to mention here that this ground state conformational change between room temperature and 77 K can also be achieved in glassy media (isopentane and *n*-butanol) (figures not shown). These results are also in total agreement with the excitation and fluorescence spectra of unsubstituted oligothiophenes reported by Becker *et al.* in an ethanol glass at 77K [23].The second absorption band, near 40000 cm^{-1} is not affected by the conformational change since this electronic transition is localized on one thiophene ring.

A red shift of the DMOTT absorption spectrum is also observed in the *n*-decane matrix with a much improved vibronic resolution (see Figure 2B). The low temperature fluorescence spectrum also shows a better vibronic resolution but, in contrast with TT, a small but detectable red shift of the band is also observed compared to the room temperature spectrum. The mirror image relationship is relatively good at 77 K and the Stokes shift is small showing that DMOTT adopts rather similar conformations in the ground and first singlet excited states. Since

DMOTT is expected to be almost planar (9° off planarity) in fluid solution [48], it is a good assumption to consider that DMOTT is nearly planar in the *n*-decane matrix. Thus, one would expect a smaller difference between room and low-temperature absorption spectra. The red shift of the excitation spectrum recorded at 77K, though smaller than that observed for TT, might involve both a small conformational change of the backbone combined with a conformational change of the methoxy groups. The latter would also explain the red shift of the fluorescence band recorded in the matrix, which cannot be accounted for by a conformational change of the backbone. The last statement can be correlated with the geometry of alkoxy-substituted oligothiophenes calculated (gas phase) and obtained from crystallographic data (solid state). Indeed HF/3-21G* *ab initio* calculations performed on DMOTT [48], and on 3,3'-dimethoxy-2,2'-bithiophene (DMO33BT) [42] predict that the methoxy groups are perpendicularly oriented relatively to the plane of the molecule. On the other hand, in the solid state, X-Ray data shows that the alkoxy groups of DMO33BT, and other alkoxy-substituted bithiophene derivatives are coplanar with the thiophene rings [54, 55]. It is expected that, in the solid state, the coplanar arrangement of the alkoxy groups maximizes the packing energy.

One can see in Figure 3A that the excitation spectrum of DMTT isolated in the matrix shows a large red shift and an increase of the vibrational structure compared to that measured at room temperature. On the other hand, the fluorescence band recorded at 77 K does not show any significant shift but a better vibronic resolution is observed. According to the above discussion, it can be also concluded that DMTT is more planar in the *n*-decane matrix. However, the excitation band of DMTT in the matrix is slightly blue shifted compared to the excitation band of TT in the same environment (see table 1). But, for the same twisting angles between thiophene rings, a red shift of the absorption band should be observed for DMTT compared to TT due to the electron- donating properties of the methyl groups [56]. Moreover, this terthiophene derivative is twisted (about 30° from planarity) in the solid state [51]. According to these observations, it can be concluded that the

conformation of DMTT is not as planar as that of TT in rigid matrices, which explains the blue shifts observed in the excitation and fluorescence spectra of DMTT at 77 K compared to those of TT.

Figure 3B shows that similar optical changes exist between room and low temperature spectra of DHTT indicating that for this molecule, a more planar conformation is also adopted in the *n*-decane matrix at 77 K. As DHTT and DMTT show very similar shifts following the formation of the *n*-decane matrix, it is expected that both molecules adopt very similar conformations in their ground state. However, the vibronic resolution of the 77 K excitation spectrum of DHTT is less pronounced than that found for DMTT. This is probably caused by the presence of the hexyl chains, which preclude the formation of a perfect substitutional matrix and thus allow for a wider distribution of conformers. One can also see that the fluorescence band of DHTT in the matrix is slightly blue shifted compared to that at room temperature. This can also be attributed to the non-uniformity of the matrix, which may trap more twisted conformers.

The spectral properties of the terthiophene derivatives are listed in Table 1. One can see that the shifts between the maxima of the room temperature absorption spectrum and the low temperature excitation spectrum of these molecules are larger for those molecules which are more twisted in the ground state as suggested theoretically [48]. For the fluorescence bands, the shifts are much less pronounced except for DMOTT where a conformational change of the methoxy groups is expected as discussed above. In conclusion, in a *n*-decane matrix at 77 K, the molecules are well isolated and they adopt conformations similar to those found in the solid state. Thus, by comparing absorption and fluorescence spectra of the terthiophene derivatives in fluid solution with those obtained in the rigid matrix, it has been possible to observe the optical changes induced by the packing effect (giving a conformational change) on isolated molecules. Now, let us see how these optical changes can be compared with those observed for the aggregated forms of these trimers.

3.3 Intermolecular Interactions After Aggregation

To investigate the aggregation phenomenon, high concentrations of the molecules in isopentane or in methanol/water mixtures at 77K were used. Isopentane instead of *n*-decane is employed because, at 77 K, this solvent forms a glass avoiding the possibility to trap molecules in interstitial and/or substitutional lattices. Moreover, the spectral resolution of DMOTT aggregates is improved in isopentane compared to the methanol/water mixtures at 77K. Unfortunately, it was observed that the other terthiophenes investigated do not form significant amount of aggregates in isopentane. For this reason, since terthiophene derivatives are not soluble in water, methanol/water mixtures have been used for the other compounds. It is important to mention here that, for DMOTT, similar optical changes have been measured in isopentane and in methanol/water mixtures at 77K.

Figure 4 shows the excitation (A) and fluorescence spectra (B) of TT in a methanol/water mixture (25:75) at 77K. The respective spectra of TT in *n*-decane at room temperature (298 K) and at 77 K (rigid matrix) are also reported in Figure 4. As discussed in the previous section, the red shift observed for the excitation spectrum of TT isolated in the *n*-decane matrix compared to the room temperature absorption spectrum in the same solvent is caused by conformational changes favoring the planarity of the molecule. On the other hand, the excitation spectra of TT in aggregated forms (methanol/water mixture) show two components, one intense band located at 31700 cm^{-1} which is blue shifted compared to that recorded at room temperature in *n*-decane and a weak peak near 25000 cm^{-1} which is red shifted. One can note that the red shifted part of the excitation spectrum is more red shifted than that of the excitation spectrum of the planar conformation of the isolated molecule in the *n*-decane matrix at 77K. These spectral properties have been observed for several unsubstituted thiophene derivatives [30-34, 38] and have been interpreted on the basis of a parallel excitonic type model [39]. The splitting (Davydov splitting) of the absorption band is induced by the two orientations of the molecular transition dipole

moment in the H-aggregated forms. Indeed, the weak red shifted low-energy band (L) is dipole-forbidden while the intense blue shifted high-energy band (H) is dipole-allowed. This is a consequence of the formation of a local C_{2h} symmetry (parallel type) Frenkel exciton, which is later delocalized throughout the microaggregates.

The fluorescence spectra of TT in the methanol/water mixture recorded at 77 K show some peaks centered at 21500 cm^{-1}. The peaks located at 25000 and 23500 cm^{-1} are very close in energy to those observed in *n*-decane and should correspond to the emission of some free molecules. Indeed, the excitation spectrum monitored at 23500 cm^{-1} (figure not shown) in the methanol/water mixtures shows a red-shifted band, which is similar to the one observed for the isolated molecules in the *n*-decane matrix. The new red shifted fluorescence band observed here and for other unsubstituted oligothiophenes has been assigned to the emission from the L energy level of the aggregate [30-34, 38].

Figure 5 shows the temperature-dependent absorption (A) and fluorescence (B) spectra of DMOTT in isopentane. One can see that both absorption and fluorescence spectra exhibit the presence of a new red shifted band which shows, through the appearence of the isosbestic point, that an equilibrium does exist between two species. In the fluorescence spectra, the formation of the new red shifted band is a spectral evidence that DMOTT can form aggregates in this range of temperature. Indeed, as shown above, the conformational change in the ground state does not induce any significant change in the fluorescence spectrum since the emission always arises from nearly planar conformations at all temperatures. Moreover it will be shown below that the new fluorescence band also appears in the isopentane glass at 77 K with vibrational fine structure ruling out the excimer model since no molecular diffusion should occur in this rigid medium and no vibrational structure is expected in an emission spectrum that involves a ground state with a dissociative energy potential surface. Thus the new emission is attributed to a certain type of aggregation. The appearance of a new band to the red of the high temperature

absorption spectrum might also be a consequence of the aggregation process. But, as discussed above, conformational changes may also induce similar optical changes.

To shed more light on the nature of the process involved, the excitation and fluorescence spectra of DMOTT in isopentane at room temperature and in the glassy medium at 77 K have been recorded and are illustrated in Figure 6A. In the isopentane glass, the excitation spectrum of DMOTT (the second vibrational peak) is slightly red shifted compared to the maximum of the room temperature spectrum. This spectral shift is similar to that observed for the isolated molecules in the *n*-decane matrix and to the red shift observed in low temperature fluid solutions in isopentane (see Figure 6B). Moreover, the vibrational fine structure of the spectra in the *n*-decane matrix and in the isopentane glass are identical. Thus, according to the above discussion, small conformational changes involving the dihedral angles between thiophene rings and/or the orientation of the methoxy groups should be mainly responsible for the optical changes observed in the excitation spectrum of DMOTT in the glassy medium.

One can see that the aggregation process induces quite different optical changes in the excitation spectra of TT and DMOTT. Indeed an H-type excitonic effect is responsible for the spectral properties of TT whereas conformational changes might explain the optical changes found in DMOTT (as well as alkyl-substituted terthiophenes, see below). We believe that this difference may involve the intermolecular distance and orientation in the aggregates. Indeed the presence of side chains should increase intermolecular distances and disorder in substituted terthiophenes, which should weaken the ground state electronic interactions between molecules, interactions that are mainly responsible for the H-type excitonic effect. On the other hand, the good packing of TT molecules should allow for a better intermolecular electronic interaction giving rise to the important splitting of the absorption band. It will be shown in the second part of this series of paper that ZINDO/S calculations performed on the crystalline structures are in good agreement with this statement.

One can see in Figure 6A that the fluorescence spectrum of DMOTT in the isopentane glass shows the appearance of a new band, which presents a large red shift, is structured and is independent of the excitation wavelength used as reported for the temperature-dependent fluorescence spectra (see Figure 5B). Moreover, the relative ratio between the two fluorescence bands is independent of the excitation energy showing that only one absorbing species is responsible for the two emissions. As discussed above, conformational changes cannot explain such a large red shift observed for the new emission. The electronic interactions involved in the aggregation process should be responsible for the new emission observed.

Similar results are obtained for the other two substituted terthiophenes. The excitation spectra of the isolated molecules of DMTT (*n*-decane matrix at 77 K) and of the aggregated forms (methanol/water (25:75) at 77 K) as well as the absorption spectrum at room temperature in *n*-decane are reported in Figure 7A. The respective fluorescence spectra are given in Figure 7B. These results, and the fact that the aggregation process does not induce any optical changes other than conformational changes for DMOTT, strongly suggest that a change in the DMTT conformation might also be responsible for the optical changes found in the aggregated forms. Similar results have also been observed on diluted polymer solutions [13,14,57,58]. Moreover, we also know that going from substituted bithiophenes to substituted sexithiophene does not affect much the conformation of these oligomers [24-27]. All these results are in contradiction with the assumption that no conformational change could explained the optical changes observed in the absorption spectra of some poly(3-alkylthiophene)s in solution [45].

The same methodology, but in a methanol/water (1:10) mixture to promote the aggregation phenomenon, has been applied for DHTT. Results are displayed in figure 8. As discussed above for DMTT and DMOTT, the observed red shift is attributed to a conformational change towards planarity. Figure 8B shows that the fluorescence spectrum of DHTT in the methanol/water mixture at 77 K is red shifted compared to that found at room temperature in *n*-decane. However this shift is

smaller than that observed for DMTT in the same environment. This may be due to the presence of the hexyl chains, which could increase the intermolecular distance and thus could reduce intermolecular electronic interactions in the excited state.

4 Concluding Remarks

This work has shown that well-defined substituted oligomers can be used to study conformation/optical property relationships more efficiently than by using only unsubstituted oligothiophenes. The variety of substituted oligomers having different conformations and potential energy curves allowed us to improve significantly our basic knowledge on these systems by using coupled experimental and theoretical methods. For the first time, the thermochromic properties of substituted oligothiophenes are reported.

It has been observed, in this work, that terthiophene derivatives isolated in an alkane matrix become less twisted in their ground electronic states due to the packing effect as was observed in the pure solid state. Moreover, the resulting red shifts in the excitation spectra are larger for oligothiophenes which are more twisted in solutions. On the other hand, the fluorescence spectra of the isolated molecules in the rigid matrix are not significantly shifted indicating that these molecules in fluid solutions are nearly planar in their S_1 relaxed excited states.

Following aggregation, the band in the excitation spectrum of TT is splitted in two components. This phenomenon has been observed for several unsubstituted oligothiophenes and has been interpreted in terms of a parallel H-type excitonic model. On the other hand, the excitation spectra of the substituted terthiophenes in their aggregated forms are close to those observed for the isolated molecules in an alkane matrix. This indicates that the intermolecular interactions induced by the aggregation process provoke conformational changes, which are similar to those induced by the packing effect in the alkane matrix. We believe that, for the substituted oligothiophenes, the presence of the side chains weakens the

intermolecular interactions, which are responsible for the H-type excitonic effect observed in TT. This assumption will tested in part 2 of this series of studies.

Acknowledgment

The authors are grateful to the Natural Sciences and Engineering Research Council of Canada (NSERC) and the fonds FCAR (Quebec) for their financial support. N.D.C. is grateful to the NSERC for a graduate scholarship.

References and Notes

[1] Schopf, G.; Kossmehl, G. *Adv. Polym. Sci.* **1997**, *127*, 1.

[2] Chance, R.R., Boudreux, D.S. ; Brédas, J.L. ;Silbey, R., in *Handbook of Conducting Polymers,* T.A. Skothein, Ed., Marcel Dekker, New York, 1986.

[3] Roncali, J. *Chem. Rev.* **1992**, *92*, 711.

[4] Chen, S.A. ; Ni, J.M. *Macromolecules* **1992** *25*, 6081.

[5] Hsu, W.P. ; Levon, K. ; Ho, K.S. ; Myerson, A.S. ; Kwei, T.K. *Macromolecules* **1993**, *26*, 1318.

[6] Rughooputh, S.D.D.V. ; Hotta, S. ; Heeger, A.J. ; Wudl, F.J. *J. Polym. Sci., Polym. Phys. Ed.* **1987**, *25*, 1071.

[7] Kawai, T. ; Kuwabara, T. ; Wang, S. ; Yoshino, K. *J. Electrochem. Soc.* **1990**, *137*, 3793.

[8] Ohmori, Y. ; Uchida, M. ; Muro, K. ; Yoshino, K. *Jpn. J. Appl. Phys.* **1991**, *30*, L1938.

[9] Morita, S. ; Kawai, T. ; Yoshino, K. *J. Appl. Phys.* **1991**, *69*, 4445.

[10] Inganäs, O.; Salaneck, W.R.; Österholm, J.E.; Laakso, J. *Synth. Met.* **1988**, *22*, 395.

[11] Roux, C.; Leclerc, M. *Macromolecules* **1992**, *25*, 2141.

[12] Roux, C.; Bergeron, J-Y.; Leclerc, M. *Makromol. Chem.* **1993**, *194*, 869.

[13] Faïd, K.; Fréchette, M.; Ranger, M.; Mazerolle, L.; Lévesque, I.; Leclerc, M.; Chen, T.; Rieke, R.D. *Chem. Mater.* **1995**, *7*, 1390.

[14] Leclerc, M.; Fréchette, M.; Bergeron, J.-Y.; Ranger, M.; Lévesque, I.; Faïd, K. *Macromol. Chem. Phys.* **1996**, *197*, 2077.

[15] Yoshino, K.; Nakajima, S.; Onada, M.; Sugimoto, R. *Synth. Met.* **1989**, *28*, C349.

[16] Schilling, F.C.; Bovey, F.A.; Lovinger, A.J.; Ziegler, J.M. *Adv. Chem.* **1990**, *224*, 341.

[17] Variano, B.F.; Sandroff, C.J. Baker, G.L. ; *Macromolecules* **1991**, *24*, 4376.

[18] Thémans, B.; Salaneck, W.R.; Brédas, J. *Synth. Met.* **1989**, *28*, C359.

[19] Winokur, M.J.; Spiegel, D.; Kim, Y.; Hotta, S.; Heeger, A.J. *Synth. Met.* **1989**, *28*, C419.

[20] Tashiro, K.; Ono, K.; Minagawa, Y.; Kobuyashi, M.; Kawai, I.; Yoshino, K. *J. Polym. Sci., Polym. Ed.* **1991**, *29*, 1223.

[21] Mardalen, J.; Samuelson, E.J.; Gautun, O.R.; Carlsen, P.H. *Synth. Met.* **1992**, *48*, 363.

[22] Chosrovian, H.; Rentsch, S.; Grebner, D.; Dahm, D.U.; Birckner, E.; Naarmann, H. *Synth. Met.* **1993**, *60*, 23.

[23] Becker, R.S.; de Melo, J.S.; Maçanita, A.L.; Elisei, F. *J. Phys. Chem.* **1996**, *100*, 18683.

[24] Belletête, M.; Mazerolle, L.; Desrosiers, N.; Leclerc, M.; Durocher, G. *Macromolecules* **1995**, *28*, 8587.

[25] DiCésare, N.; Belletête, M.; Raymond, F.; Leclerc, M.; Durocher, D. *J. Phys. Chem. A* **1997**, *101*, 776.

[26] DiCésare, N.; Belletête, M.; Donat-Bouillud, A.; Leclerc, M.; Durocher, G. *J. Luminescence* **1999**, *81*, 111.

[27] DiCésare, N.; Belletête, M.; Donat-Bouillud, A.; Leclerc, M.; Durocher, G. *Macromolecules.***1998**, *31*, 6289.

[28] Van Hutten, P.F.; Gill, R.E.; Herrena, J.K.; Hadziioannou, G. *J. Phys. Chem.* **1995**, *99*, 3218.

[29] Rossi, R.; Ciofalo, M.; Carpita, A.; Ponterini, G. *J. Photochem. Photobiol. A* **1993**, *70*, 59.

[30] Fichou, D.; Horowitz, B.; Yu, B. Garnier, F. *Synth. Met.* **1992**, *48*, 167.

[31] Oelkrug, D.; Egelhaaf, H.-J.; Worrall, D.R.; Wilkinson, F. *J. Fluorescence* **1995**, *5*, 165.

[32] Oelkrug, D.; Egelhaaf, H.-J.; Giersehner, J.; Tompert, A. *Synth. Met.* **1996**, *76*, 249.

[33] Kanemitsu, Y.; Shimisu, N. *Phys. Rev. B* **1996**, *54*, 2198.

[34] Bosisio, R.; Botta, C.; Colombo, A.; Destri, S.; Porzio, W.; Grilli, E.; Tubino, R.; Bongiovanni, G.; Mura, A.; DiSilvestro, G. *Synth. Met.* **1997**, *87*, 23.

[35] Bongiovanni, G.; Botta, C.; Brédas, J.L.; Cornil, J.; Ferro, D.R.; Mura, A.; Pioggi, A.; Tubino, R. *Chem. Phys. Lett.* **1997**, *278*, 146.

[36] Botta, C.; Bosisio, R.; Bongiovanni, G.; Mura, A.; Tubino, R. *Synth. Met.* **1997**, *84*, 535.

[37] De Feyter, S.; van Stam, J.; Imans, F.; Viaene, L.; De Schryver, F.C.; Evans, C.H. *Chem. Phys. Lett.* **1997**, *277*, 44.

[38] Gierschner, J.; Egelhaaf, H.-J.; Oelkrug, D. *Synth. Met.* **1997**, *84*, 529.

[39] Kasha, M. *Radiation Res.* **1963**, *20*, 55.

[40] DiCésare, N.; Belletête, M.; Leclerc, M.; Durocher, G. *Synth. Met* **1998**, *94*, 291.

[41] DiCésare, N.; Belletête, M.; Raymond, F.; Leclerc, M.; Durocher, G. *J. Phys. Chem. A* **1998**, *102*, 2700.

[42] DiCésare, N.; Belletête, M.; Leclerc, M.; Durocher, G. *J. Mol. Struct. (TheoChem)*, in press.

[43] DiCésare, N.; Belletête, M.; Leclerc, M.; Durocher, G. *Chem. Phys. Lett.* **1997**, *275*, 533.

[44] Raymond, F.; DiCésare, N.; Belletête, M.; Durocher, G.; Leclerc, M., *Adv. Mater.* **1998**, *10*, 599.

[45] Yamamoto, T.; Komarudin, D.; Arai, M.; Lee, B.L.; Saganuma, H.; Asakawa, N.; Inoue, Y.; Kubota, K.; Sasaki, S.; Fukuda, T.; Matsuad, H. *J. Am. Chem. Soc.* **1998**, *120*, 2047.

[46] Georges, G., Ph.D. thesis, Université de Montréal (1997).

[47] Zotti, G.; Gallazi, M.C.; Zerbi, G.; Meilla, S.V. *Synth. Met.* **1995**, *73*, 217.

[48] DiCésare, N.; Belletête, M.; Marrano, C.; Leclerc, M.; Durocher, G. *J. Phys. Chem. A* **1998**, *102*, 5142.

[49] Birks, J.B. "Photophysics of Aromatic Molecules", Wiley-Interscience, 1970, p. 118.

[50] Pelletier, M. ; Brisse, F. *Acta. Cryst.* **1994**, *C50*, 1942.

[51] Chaloner, P.A. ; Gunatunga, S.R. ; Hitchcock, P.B. *Acta. Cryst.* **1994**, *C50*, 1941.

[52] Van Bolhuis, F. ; Wynberg, H. *Synth. Met.* **1989**, *30*, 381.

[53] Birnbaum, D.; Kohler, B.E. *J. Chem. Phys.* **1989**, *90*, 3506.

[54] Paulus, E.F. ; Dammel, R. ; Kampf, G. ; Wegener, P. *Acta. Cryst.* **1988**, *B44*, 509.

[55] Pelletier, M. ; Brisse, F. ; Cloutier, R. ; Leclerc, M. *Acta. Cryst.* **1995**, *C51*, 1394.

[56] ZINDO/S calculations, unpublished results.

[57] Roux, C.; Leclerc, M. *Chem. Mater.* **1994**, *6*, 620.

[58] Lévesque, I.; Leclerc, M. *Chem. Mater.* 1996, *8*, 2843.

Table 1

Comparison of the absorption (or excitation) and fluorescence maxima between room temperature and 77K in *n*-decane.

	ν_E [a] (cm^{-1})		ν_A [b] (cm^{-1})		ν_F [c] (cm^{-1})	
TRIMERS	77K	298K	77K	298K	77K	298K
TT	26 800	28 350	23 500	23 600		
DMOTT	25 900	26 800	22 750	23 100		
DMTT	27 050	29 300	23 550	23 700		
DHTT	27 250	29 900	23 500	23 300		

[a] Maxima of the excitation spectra.

[b] Maxima of the absorption spectra.

[c] Maxima of the fluorescence spectra.

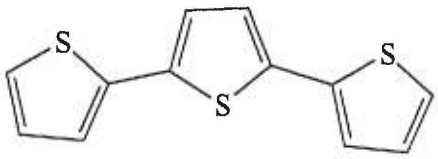

TT

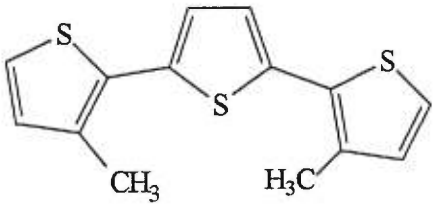

DMTT

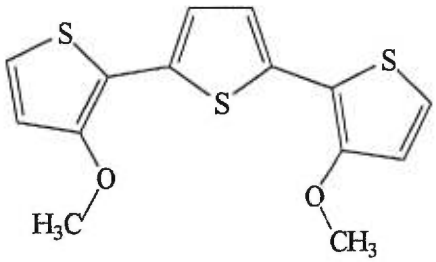

DMOTT

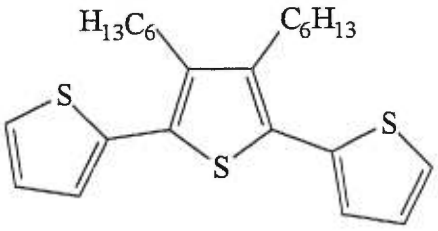

DHTT

Figure 1 : Molecular structures of the substituted terthiophenes investigated.

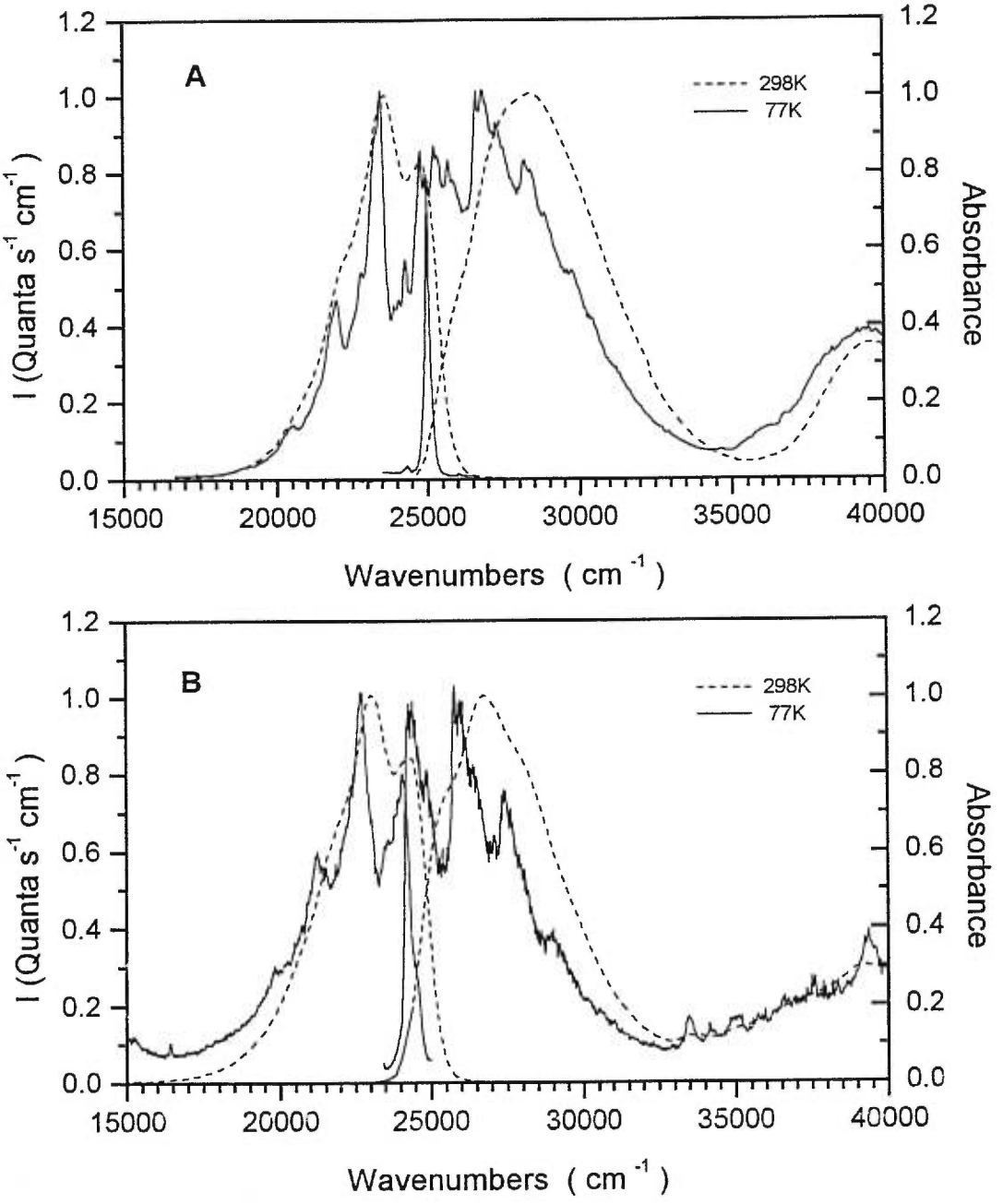

Figure 2 : Absorption (298K), excitation (77K) and fluorescence spectra of TT (**A**) and DMOTT (**B**) in *n*-decane. The excitation and emission wavenumbers were near the maximum of the absorption (or excitation) and emission spectra respectively. The molar concentration were 2.5 $x10^{-5}$ mol dm^{-3} for TT and DMOTT at room temperature.

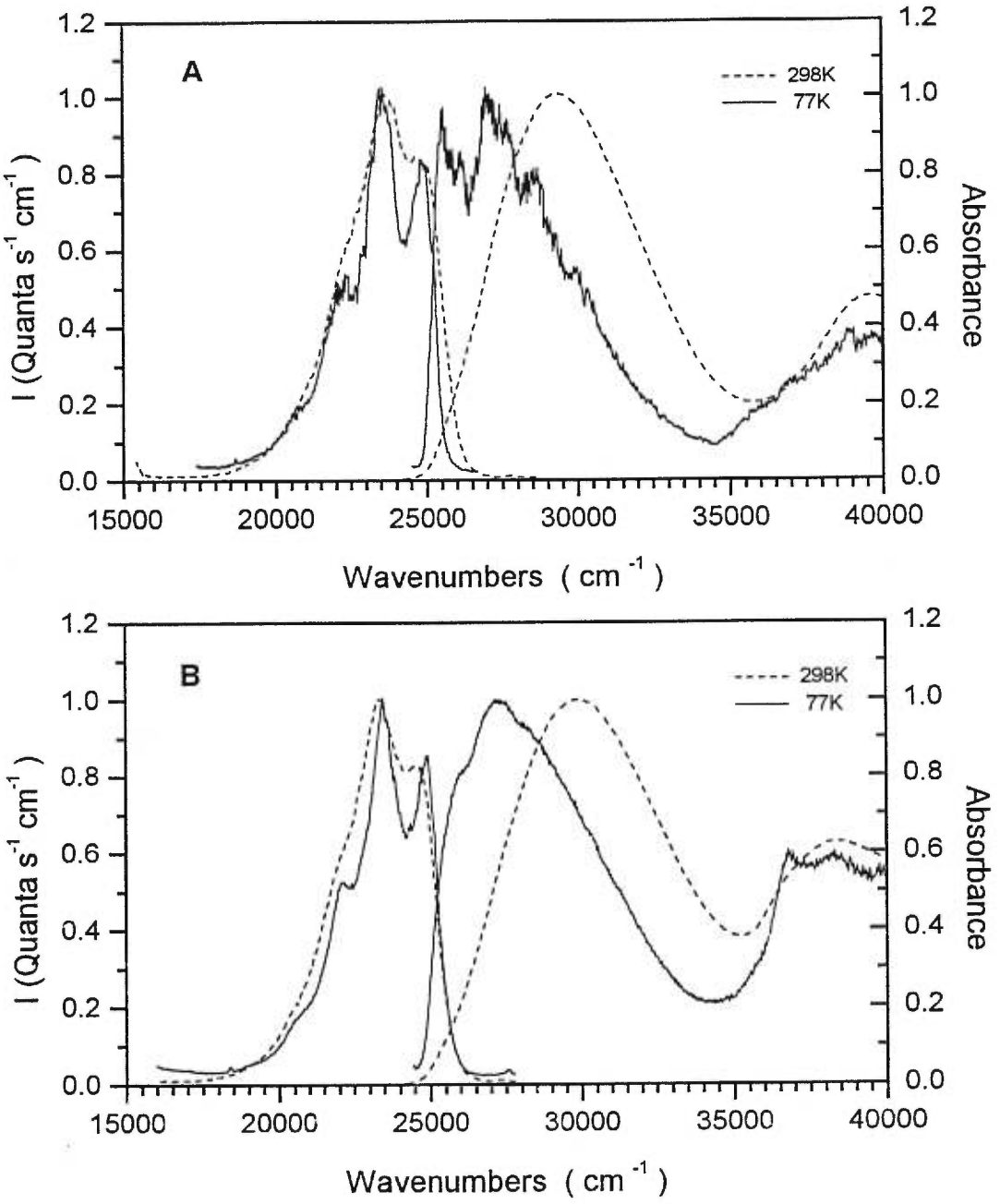

Figure 3 : Absorption (298K), excitation (77K) and fluorescence spectra of DMTT (**A**) and DHTT (**B**) in *n*-decane. The excitation and emission wavenumbers were near the maximum of the absorption (or excitation) and emission spectra respectively. The molar concentration were 5.6 $x10^{-5}$ (DMTT) and 5.2 $x10^{-5}$ (DHTT) mol dm^{-3} at room temperature.

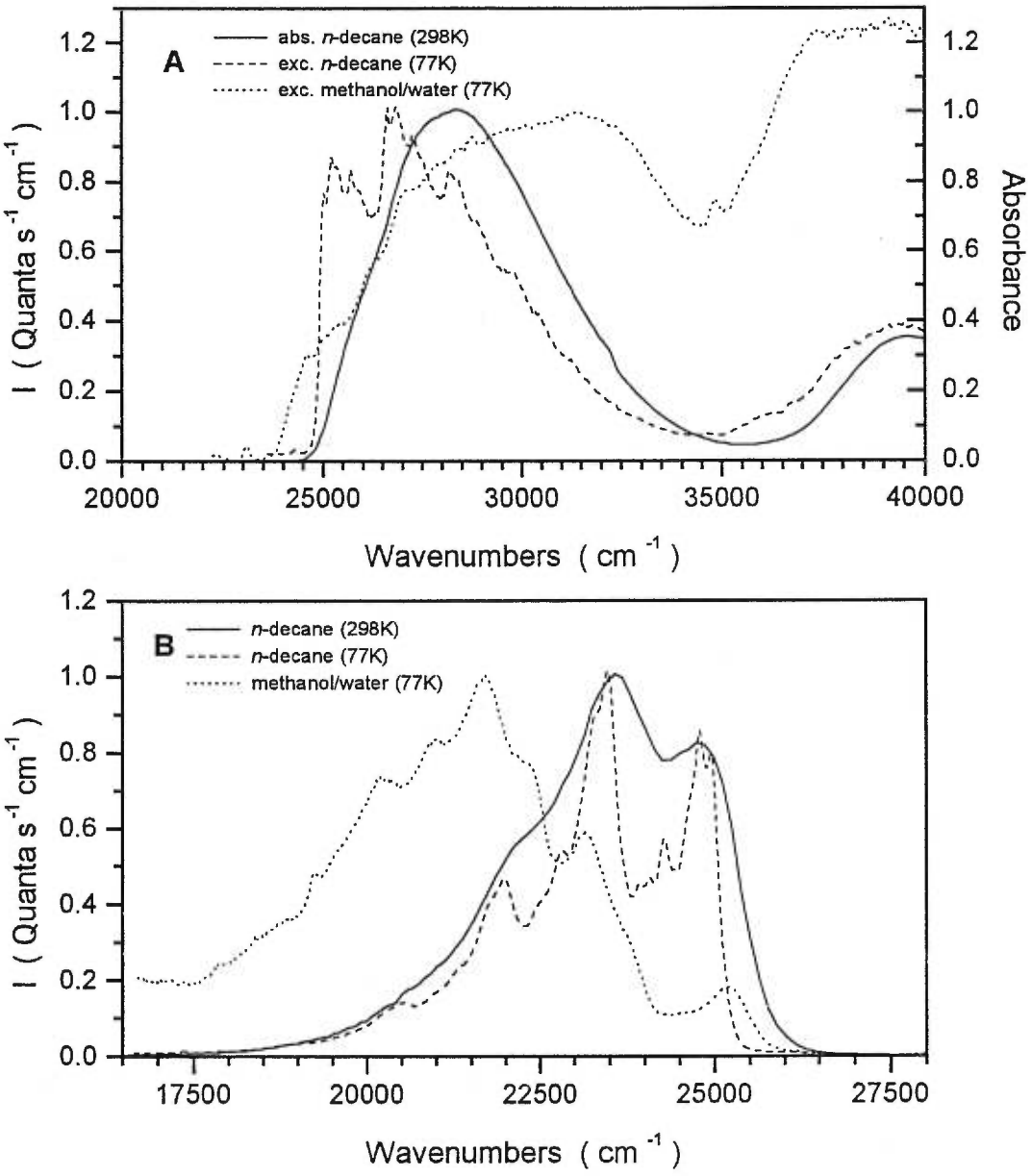

Figure 4 : Absorption **(A)**, excitation **(A)** and fluorescence **(B)** spectra of TT in various environments. The excitation and emission wavenumbers were near the maximum of the absorption (or excitation) and emission spectra respectively. The molar concentration was 4.9 $x10^{-5}$ mol dm^{-3} at room temperature in the methanol/water mixture.

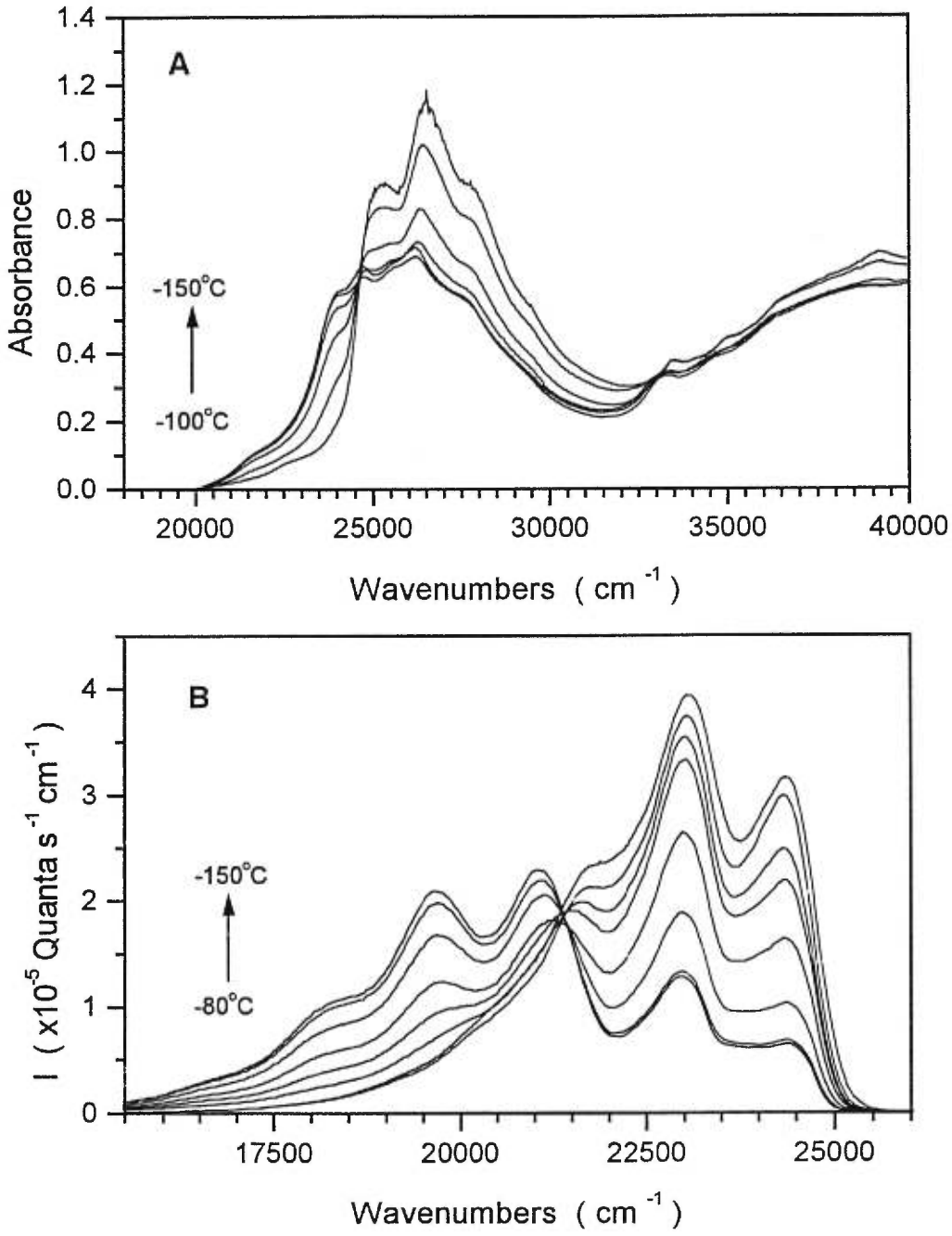

Figure 5 : Temperature dependent absorption (**A**) and fluorescence spectra (**B**) of DMOTT in isopentane. The excitation wavenumber used for the fluorescence spectra was 27030 cm^{-1} and the molar concentration was 3.6 $x10^{-5}$ (for absorption) and 1.8 $x10^{-5}$ (for fluorescence) mol dm^{-3} at room temperature.

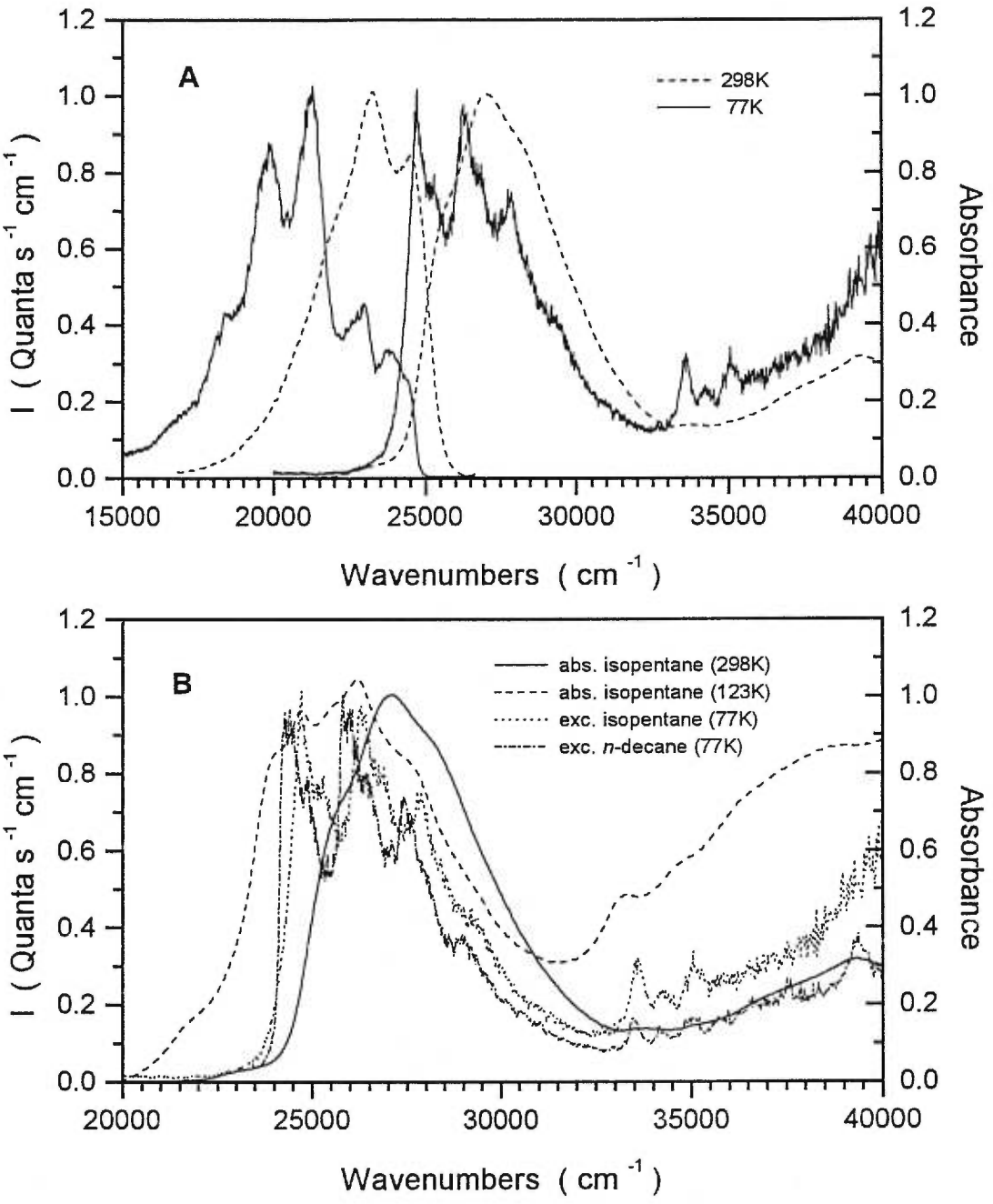

Figure 6 : A: Absorption (298 K), excitation (77 K) and fluorescence spectra of DMOTT in isopentane. The excitation and emission wavenumbers were near the maximum of the absorption (or excitation) and emission spectra respectively. The molar concentration was 2.1 $x10^{-5}$ mol dm^{-3} at room temperature. **B**: Comparison of absorption and excitation spectra of DMOTT in different environments.

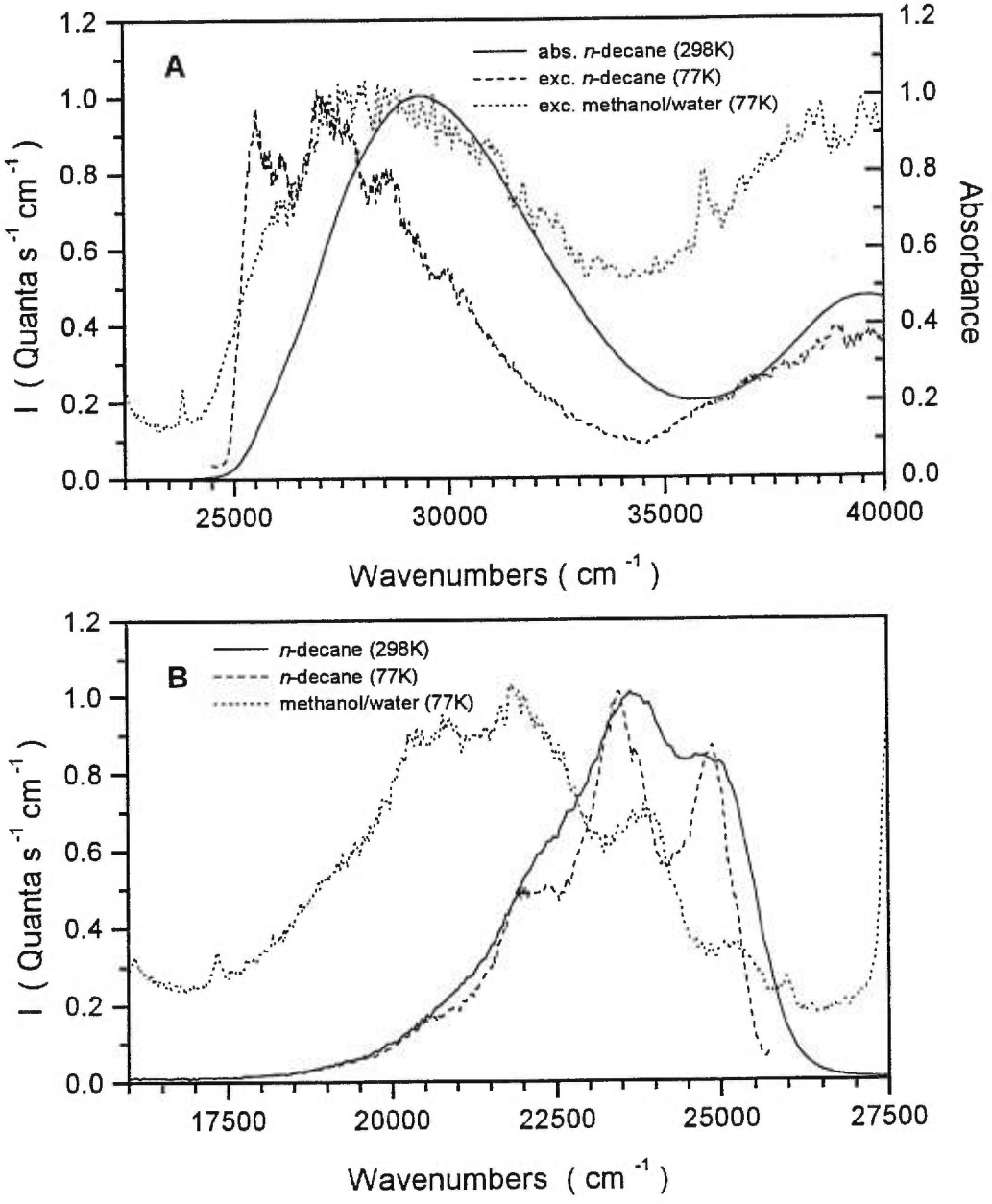

Figure 7 : A: Comparison of absorption and excitation spectra of DMTT in various environments. **B**: Comparison of fluorescence spectra of DMTT in various environments. The excitation and emission wavenumbers were near the maximum of the absorption (or excitation) and emission spectra respectively. The molar concentrations was ~1.6 x10^{-5} mol dm^{-3} at room temperature in the methanol/water mixture.

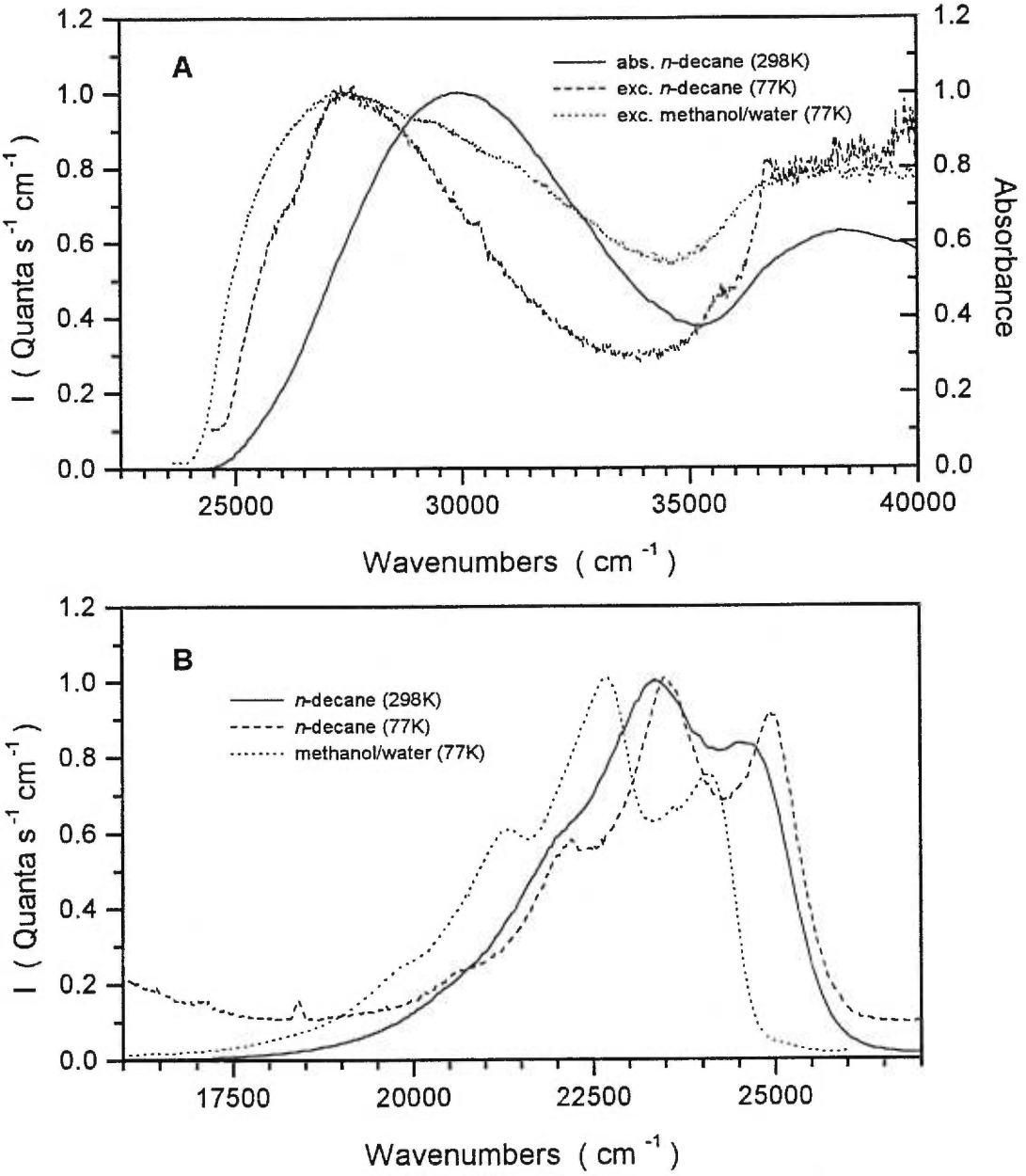

Figure 8 : A: Comparison of absorption and excitation spectra of DHTT in various environments. **B**: Comparison of fluorescence spectra of DHTT in various environments. The excitation and emission wavenumbers were near the maximum of the absorption (or excitation) and emission spectra respectively. The molar concentration was ~3.5 mol dm^3 at room temperature in the methanol/water mixture

Chapitre 8

Étude théorique des interactions intermoléculaires sur les propriétés optiques de dérivés du 2,2':5',2''-terthiophène

Ce chapitre présente la suite de l'article 7 (chapitre 7) et porte sur l'étude théorique des interactions intermoléculaires des dérivés du TT. Afin d'évaluer les effets des changements conformationnels, suivant l'agrégation, et des interactions électroniques entre molécules voisines sur les différents états excités singulets et triplets, nous avons utilisé la méthode théorique ZINDO/S. Développée par le groupe du professeur Zerner, la méthode ZINDO/S est une version améliorée de la méthode INDO conçue spécialement pour l'obtention des propriétés spectroscopiques des molécules.

Afin de simuler les agrégats et d'évaluer les effets des interactions intermoléculaires sur les premières transitions électroniques, nous avions plusieurs recours. Il est possible de construire un dimère (deux molécules) en plaçant de façon aléatoire les deux molécules et d'évaluer les propriétés spectroscopiques en fonction de l'orientation mutuelle des deux molécules et de leurs conformations. Ensuite, il faudrait inclure d'autres molécules et refaire les mêmes démarches afin d'avoir une idée complète des interactions intermoléculaires en fonction de l'orientation, de la conformation et du nombre de molécules. Cette dernière démarche inclut cependant un trop grand nombre de possibilités pour être réalisable. La seule issue possible dans cet esprit est de considérer quelques systèmes types tels les arrangements tête-queues ou "sandwichs", par exemple. Comme la structure des agrégats formés expérimentalement (chapitre 7) n'est pas connue, la comparaison avec des systèmes

types amène une grande incertitude puisque plusieurs types de structures d'agrégat sont susceptibles de donner des résultats similaires. Pour remédier à ce problème, nous avons choisi d'utiliser les structures cristallines des molécules dans les calculs. Toutes les structures cristallines proviennent de cristaux obtenus par précipitation en solution suivant l'agrégation. Il est alors plausible que ces structures cristallines ressemblent à la structure des agrégats formés en solution (chapitre 7). Naturellement, les agrégats étudiés ici sont formés suite à la diminution brusque de la température jusqu'à la formation d'un verre (ou d'une neige selon le cas) alors que les monocristaux utilisés en cristallographie sont formés par précipitation lente. Il est donc prévisible que les agrégats n'aient pas une structure aussi ordonnée que celle du monocristal. Par contre, les structures cristallines nous donnent l'avantage d'être uniques pour chaque dérivé et cette structure est obtenue expérimentalement.

Les mesures des structures cristallines présentées dans ce travail n'ont pas été effectuées dans nos laboratoires mais ont été tirées de la littérature. Malheureusement, la structure cristallographique du DMOTT est jusqu'ici indéterminée et il nous a été impossible d'effectuer ces mesures dans nos laboratoires. Donc, dans ce chapitre, seules les structures cristallines du TT et des deux dérivés alkyls (DMTT, DHTT) seront présentées.

La démarche suivie dans cette partie, pour atteindre nos objectifs, consiste d'abord à évaluer les paramètres spectroscopiques (énergie de la première transition singulet-singulet et de sa force oscillatrice) des molécules isolées ou libres. Pour ce faire, nous avons utilisé les structures moléculaires obtenues à partir des calculs *ab initio* décrits au chapitre 6. Ces résultats sont alors associés aux mesures prises en solution à température ambiante. Afin d'évaluer l'effet des changements conformationnels sur les propriétés spectroscopiques suite à l'augmentation de la planéité à l'état solide (il est à noter que chaque dérivé adopte une conformation plus plane à l'état solide, sans considérer les interactions intermoléculaires) nous avons évalué les paramètres spectroscopiques d'une molécule isolée mais dans sa géométrie cristalline. Ces résultats sont alors comparés aux résultats obtenus dans la

matrice de *n*-décane à 77K. Le paramètre conformationnel étant ainsi évalué, nous avons effectué des calculs sur différents arrangements microcristallins tirés des données cristallographiques. Ces résultats nous renseignent alors sur l'importance relative des interactions intermoléculaires et des changements conformationnels suite à l'agrégation en solution.

Les résultats obtenus des calculs montrent une bonne corrélation avec les résultats expérimentaux présentés au chapitre 7 et appuient les conclusions alors tirées. L'insertion de substituants défavorise grandement un arrangement ordonné et compact et ainsi défavorise les interactions électroniques intermoléculaires. À l'inverse, le TT montre une structure cristallographique bien ordonnée et compacte qui résulte en une importante interaction intermoléculaire et à la formation d'états électroniques de type excitonique.

8.1 Article 8 : Intermolecular interactions in conjugated oligomers: II - Quantum chemical calculations performed on crystalline structures of terthiophene and substituted terthiophenes.

Article publié dans The Journal of Physical Chemistry A, volume 103, numéro 7, pages 803-811 (1999).

Intermolecular Interactions in Conjugated Oligothiophenes: II - Quantum Chemical Calculations Performed on Crystalline Structures of Terthiophene and Substituted Terthiophenes.

Nicolas DiCésare [a], Michel Belletête [a], Mario Leclerc [b] and Gilles Durocher [a]

[a] Laboratoire de photophysique moléculaire
[b] Laboratoire des polymères électroactifs et photoactifs

Département de Chimie, Université de Montréal,
C.P. 6128, Succ. A, Montréal, Québec, H3C 3J7, Canada

Abstract

Quantum-chemical calculations are used to investigate the influence of intermolecular interactions on the absorption spectra of unsubstituted terthiophene (TT) as well as 3,3''-dimethyl-2,2':5',2''-terthiophene (DMTT) and 3',4'-dibutyl-2,2':5',2''-terthiophene (DBTT). The semiemperical ZINDO/S method is employed to calculate the energy of the electronic transitions of a single molecule in this crystalline structure and of interacting molecules in subcrystalline forms of various sizes (2 and 4 molecules). For all molecules investigated, intermolecular interactions lead to a splitting (Davydov's splitting) of the lowest optical singlet transition compared to that calculated for an isolated molecule. These results interpreted through the use of the excitonic model. The splitting of the first electronic transition is very sensitive to the different intermolecular distances and orientations found in the crystalline structures of each molecule. TT shows an important excitonic effect on the first allowed transition whereas the splitting is less important for substituted terthiophenes. The spectral shifts caused by intermolecular interactions are compared with those induced by conformational changes towards planarity for the isolated

molecules in the crystals (packing effects). The results clearly show that the excitonic effect is mainly responsible for the optical properties of TT in its aggregated form whereas, for substituted terthiophenes, the conformational change suggested in part I of this series of papers is the major cause of the red shifts observed in their absorption bands following aggregation.

1. Introduction

In the last twenty years, new organic conjugated polymers have been developed as electrical conductors and active materials in various electronic and opto-electronic devices [1]. For instance, poly(paraphenylenevinylene) (PPV) [2-4] and polythiophenes [5-9] have shown good electro-optical properties. For this reason, a wide variety of experimental investigations has been performed on these systems. The electronic properties of oligothiophenes in the solid state [10-20] have particularly retained the attention since the intermolecular interactions induce important excitonic effect (Frenkel exciton) combined with possible charge transfers and polaron pairs.

Since it is rather difficult to ascribe with certainty the various peaks found in the optical spectra recorded in condensed phases, theoretical methods could be useful to determine the effect of intermolecular interactions on the absorption bands observed experimentally. In the literature, one can find several theoretical analyses dealing with the effect of the chromophore length [21] as well as the presence of lateral substituents [22-27] on the electronic properties and conformations of oligothiophene derivatives. These calculations have provided valuable information about the structure-property relationships of these compounds. For instance, an interesting relationship between the rotational energy barriers of model bithiophene derivatives and the occurrence (or not) of thermochromism in the parent polymers has been established [28]. However, these calculations have been performed on

isolated molecules (representing dilute solutions or the incorporation of the oligomers in inert matrices).

The intermolecular interactions occurring for oligothiophenes in condensed media have not been studied much by theoretical methods [29] but a few calculations involving PPV-oligomer models have been reported in the literature [30-32]. It is shown that, in high-symmetry cofacial configuration, intermolecular interactions induce a splitting (Davydov splitting) of the first excited singlet state (S_1) in two states (S_1 and S_2, called Frenkel exciton states). According to these calculations, the first singlet-singlet electronic transition ($S_1 \leftarrow S_0$) is lower in energy and forbidden by symmetry compared to that of the isolated molecules. On the other hand, the second singlet-singlet electronic transition ($S_2 \leftarrow S_0$) is blue-shifted and allowed. The consequence of this behavior for a highly-symmetric sandwich-type dimer is a blue shift of its simulated absorption spectrum. The largest difference in energy between S_1 and S_2 excited states occurs for an intermolecular distance of 3.5 Å and where the molecules are perfectly parallel. This energy gap rapidly becomes narrower if the intermolecular distance increases or if the symmetry of the system is reduced by an increase of the molecular disorder. The exciton model has been well described by Kasha et al. [33-35].

In order to gain a better understanding of the structure-property relationships of polythiophenes, molecular mechanics coupled to Monte Carlo calculations have been performed on these macromolecules [36,37] and on the crystalline structure of a polythiophene model [38]. These studies have provided valuable informations about the structure of a free polymer chain and about the influence of the motion of the lateral chains on the stacking effect of substituted polythiophenes in their crystalline forms.

Up to now, the electronic interactions occurring for oligothiophene derivatives in condensed media have been investigated by modeling the aggregated forms of unsubtituted systems. As discussed in part I of this series of papers [39], the presence of lateral groups induces important changes in the optical properties of

substituted oligothiophenes following aggregation. We report in this second part a theoretical analysis of the electronic properties of terthiophene (TT) as well as two alkyl-substituted terthiophenes, namely: 3,3''-dimethyl-2,2':5',2''-terthiophene (DMTT) and 3',4'-dibutyl-2,2':5',2''-terthiophene (DBTT) , in their respective aggregated forms. Because intermolecular interactions involve a very large array of associated molecules and because each derivative in its aggregated form has its own molecular conformation, the X-ray data of these compounds have been used. Since the formation of aggregates is obtained in a similar way than the preparation of single crystals used for the crystallographic analysis and since the optical properties involving the oligothiophenes in their aggregated forms are very similar to those in the solid state [39], the molecular structure of the aggregates is expected to be rather similar to the crystalline structures. The electronic excited state energy of different clusters (1-4 molecules) based on the crystalline structures has been calculated using the ZINDO/S (Zerner Intermediate Neglect of Differential Overlap for Spectroscopy) semiempirical method.

These results show that, for all the terthiophene derivatives studied, intermolecular interactions induce an excitonic splitting of the first excited singlet state. The energy differences between these new states are very sensitive to the relative position of the interacting molecules in the crystal and to the size of the aggregate (number of interacting molecules). For TT, the sandwich type aggregate exhibits an important Davydov splitting, which becomes larger as the number of molecules in the configuration is increased, causing a blue shift of the first allowed singlet-singlet transition ($S_2 \leftarrow S_0$). On the other hand, a head-to-tail arrangement of the molecules does not significantly change the energy of the $S_1 \leftarrow S_0$ electronic transition of the isolated molecules. Since the conformational change caused by the packing effect is relatively small for TT [40], the red-shift of the $S_1 \leftarrow S_0$ electronic transition of the isolated molecules caused by the increase of planarity is small compared to the large blue shift of the $S_2 \leftarrow S_0$ transition of the aggregated form. This behavior results in an overall blue shift of the absorption spectrum of TT in its

aggregated form. For the substituted derivatives, the excitonic splitting becomes much less important due to a larger disorder in the crystal structures induced by the presence of the lateral chains and by the twisted conformation of each molecular unit. On the other hand, conformational changes caused by the packing effect in the solid state are much more important for these molecules compared to that of TT [40]. This leads us to conclude that the red shift observed in the absorption spectra of these molecules, following aggregation, is mainly due to conformational changes towards planarity. The structures of the molecules investigated are displayed in Figure 1.

2. Methodology

The crystalline structures of terthiophene (TT) [41], 3,3''-dimethyl-2,2':5',2''-terthiophene (DMTT) [42] and of 3',4'-dibutyl-2,2':5',2''-terthiophene (DBTT) [43] have been reproduced according to these X-ray data. A few neighbouring cells have been built to insure that all intermolecular interactions are considered. A homemade program has been used to convert the cartesian coordinates to hyperchem input files.

Theoretical calculations were performed, on the basis of crystalline data, using the Hyperchem package, release 5.0, for Windows 95 from Hypercube, Inc. The electronic transition energies and their related intensities have been calculated within the framework of the ZINDO/S (Zerner Intermediate Neglect of Differential Overlap for Spectroscopy) Hartree-Fock semiempirical method including configuration interactions (CI). ZINDO/S is a modified INDO method parameterized to reproduce UV/Visible spectroscopic transitions [44,45]. The electron-repulsion integrals were evaluated using the Mataga-Nishimoto formula. CI is chosen in a way to ensure the absence of changes in the spectroscopic parameters when increasing the size of the CI for the size of clusters studied in this paper (1 to 4 molecules).

Simulations of the absorption spectra were done using a gaussian band centered at the transiton energy with a bandwidth of 1000 cm^{-1}. For the aggregated

forms, the sum of each gaussian normalized with the oscillator strength calculated for each transition has been done.

3. Results and Discussion

3.1. Terthiophene (TT)

The unit cell of the crystalline structure of TT is reproduced in Figure 2 [41]. In this arrangement, the molecules form two distinct parallel orientations, one formed by molecules A, C, F and H and a second orientation involving molecules B, D, E and G. These two orientations are not perpendicular to each other but form an angle of ~ 45°. Each terthiophene unit in the crystal is nearly planar in an *anti* conformation with a dihedral angle between thiophene rings (θ) of ~ 172-174°. The increase in planarity, compared to the conformation calculated for the isolated molecules in the gas phase or in dilute solution (θ ~ 147° [40]) is due to the packing effect occurring in the solid phase. The energy of some excited singlet and triplet states for a single molecule and for several molecular aggregates as calculated from ZINDO/S are displayed in Figure 3. The energy values of the first singlet excited states, the oscillator strength (f) of the corresponding singlet-singlet electronic transitions as well as the molecular orbitals (M.O.) numerotation involved in these transitions are reported in Table 1. It is worth mentioning that the absolute values of the transition energies as calculated by ZINDO/S for the "free" or isolated (A) molecules are generally within a 2000 cm^{-1} bracket when compared with the experimental results, see table 2. Indeed, the ZINDO/S energy values correspond only approximately to the 0,0 electronic transitions of the molecules in the gas phase (more acurately it is the vertical transition between the two states) whereas the optical spectra are recorded in solution (where the 0,0 vibronic peak is not well resolved) and rigid media. However, since the goal of this work is to investigate the effect of the intermolecular interactions on the molecular electronic properties, we

will focus our discussion on the spectral shifts resulting from the aggregation process rather than on the exact energy values of the electronic transitions.

The calculated electronic spectrum of a single molecule of TT in this crystalline structure (A from Figure 3) exhibits a first allowed singlet-singlet transition ($S_1 \leftarrow S_0$) located at 24728 cm^{-1} (f = 1.2024) and a second weakly allowed transition ($S_2 \leftarrow S_0$) appearing at 33358 cm^{-1}. The $S_1 \leftarrow S_0$ electronic transition calculated for the same molecular structure but with a dihedral angle of 147° (simulating the expected conformation of free TT in solution [40]) gives an energy value of 26291 cm^{-1} with a slightly smaller oscillator strength (f = 1.113). The increase in the transition energy (1563 cm^{-1}) and the small decrease of f are caused by the partial break of resonance between π orbitals along the oligomer long axis due to the decrease in the dihedral angle. This shift is very close in energy to that observed experimentally between the excitation spectrum of the molecules isolated in a *n*-decane matrix at 77 K (nearly planar conformation) and the absorption spectrum recorded at room temperature in the same solvent (1550 cm^{-1}, see Table 1 and Figure 4 in part I of this series of paper [39] and table 2 of this paper). The $S_2 \leftarrow S_0$ electronic transition is less affected (blue shift of 709 cm^{-1} for the twisted conformer), showing the smaller dependence of this singlet-singlet transition on conformational changes. A similar behavior has been observed experimentally as shown in Figure 4 of part I [39]. One could also perform a ZINDO/S calculation on the basis of an HF/3-21G* molecular optimization [40] for obtaining the transition energy of the "free" molecule, but we have shown that the results obtained are within the 2000 cm^{-1} braket discussed above for all molecules investigated in this paper. We then decided to compare in table 2, experimental transition energies with calculated ones all based on the crystalline structures with the dihedral angle as the only varying parameter for the "free" molecule.

The first triplet state (T_1) appears at a very low energy (A in Figure 3), which is consistent, according to the energy gap law, with the absence of phosphorescence found for TT and other oligothiophene derivatives. Indeed, the high values of the

triplet quantum yield of these molecules would favor the occurrence of phosphorescence [46,47]. One can also see that the T_4 excited state is lying just above the S_1 state in agreement with theoretical results reported elsewhere [21] and with the experimental observation of an activated energy for the deactivation pathway of the S_1 state through the triplet state T_4 [47]. One can note that triplet states discussed throughout this paper are for the planar conformation (A) and that the energy level of the T_1 state is lower than that calculated [47,48] for the more twisted conformations expected in solution.

To investigate the effect of the intermolecular interactions on the different excited states of the isolated molecules, first we have considered the interactions between two adjacent molecules (dimer). As illustrated in Figure 2, two types of association should exist in the TT crystal: a sandwich-type and a head-to-tail interactions. The electronic properties of the A,B dimer (sandwich-type configuration) and the A,E dimer (head-to-tail configuration) have been calculated (see Figure 3 and Table 1). Results show that the interaction between molecules A and B induces a splitting of the S_1 excited state of the isolated molecule (A) in two states. The $S_1 \leftarrow S_0$ electronic transition of the sandwich-type dimer is weak and lower in energy whereas the $S_2 \leftarrow S_0$ electronic transition is much intense and is blue shifted compared to the allowed electronic transition found in the isolated molecule. This excitonic splitting (Davydov splitting) is similar to those observed for oligomer models of PPV [30,32] and is consistent with theoretical models developed by Kasha et al. [33-35]. For a perfect parallel and symmetric TT sandwich-type dimer, a C_{2h} symmetry is observed. For this symmetry group, the $S_1 \leftarrow S_0$ electronic transition between totally symmetric S_0 and S_1 singlet states (A_g) is forbidden by symmetry while the $S_2 \leftarrow S_0$ electronic transition between S_0 (A_g) and S_2 (B_u) singlet states is allowed. One can see that, even if the TT sandwich-type dimer is not perfectly symmetric, the selection rules discussed above are not much relaxed. Figure 3 shows that, after aggregation, the red shift of the S_1 excited state (1944 cm^{-1}) is larger than the blue shift of its S_2 excited state (953 cm^{-1}). Moreover, Table 1 shows that the

$S_1 \leftarrow S_0$ electronic transition involves a mixing of the HOMO (H) → LUMO (L) and H→L+1 molecular orbitals while the $S_2 \leftarrow S_0$ electronic transition involves a mixing of the H-1→L and H-1→L+1 molecular orbitals. It is worth mentioning that ZINDO/S calculations have shown that the energy difference between H and H-1 molecular orbitals (0.17 eV) is larger than that calculated between L and L+1 molecular orbitals (0.09 eV). The same behavior has been reported for oligomer models of PPV [32].

Figure 3 shows that the head-to-tail interactions (dimer A,E) barely affect the electronic properties of the isolated molecule. Indeed, the $S_1 \leftarrow S_0$ electronic transition is allowed and is slightly red-shifted compared to that of the isolated molecule. On the other hand, the S_2 excited singlet state is slightly higher in energy compared to the S_1 excited state of the isolated molecule whereas the $S_2 \leftarrow S_0$ electronic transition of the dimer A,E is forbidden.

Two distinct tetramers have also been considered in these calculations. Molecules A,B,E,F which form a type of tetramer involving sandwich and head-to-tail types of interaction and molecules A,B,C,D which present only a sandwich type of interaction. As illustrated in Figure 3, the tetramer A,B,E,F exhibits a similar excitonic splitting as that of the dimer A,B confirming the above statement that head-to-tail interactions do not induce an important Davydov splitting. However, one can see that the excitonic splitting induces by the tetramer A,B,E,F is slightly smaller than that observed for the dimer A,B. This behavior might imply that head-to-tail interactions partly annihilate the cofacial interactions. In contrast, the tetramer A,B,C,D shows a more important excitonic splitting than that calculated for the dimer A,B. Indeed one can see that the more intense singlet-singlet electronic transition ($S_4 \leftarrow S_0$) of this tetramer is blue shifted by 2513 cm^{-1} compared to the $S_1 \leftarrow S_0$ electronic transition of molecule A (see Figure 3 and Table 1). This shift is much larger than that calculated for the dimer A,B (953 cm^{-1}). On the other hand, the ($S_1 \leftarrow S_0$) singlet-singlet transition of the A,B,C,D aggregate which is also forbidden appears at about the same energy as that of the sandwich-type dimer. Thus the

excitonic splitting (S_4-S_1) of the tetramer (4258 cm^{-1}) is much higher than that of the dimer (2897 cm^{-1}). This is a well known result that the excitonic splitting is more important for larger sandwich-type aggregates [32-35].

In order to compare the theoretical results with the optical properties of TT, Figure 4 displays the absorption spectrum of single molecules isolated (having the crystalline conformation) (A) and free A(147°) and that of the A,B,C,D aggregate. Table 2 compares those calculated data with experiments. One can see that the absorption band of an isolated molecule in the crystal is red-shifted compared to that of the "free" molecule. This is caused by the increase in planarity found in the solid state due to the packing effect. But the intermolecular interactions present for TT in its aggregated form (as exemplified by the tetramer A,B,C,D) induce an overall blue shift of its absorption band compared to that recorded in solution (A with $\theta = 147°$). One can also observe in Figure 4 the red shifted bands caused by intermolecular interactions, which have very low intensities. These theoretical results show a good correlation with the optical spectra of TT reported in part I of this series of paper [39]. However the blue-shift of the $S_4 \leftarrow S_0$ transition following aggregation (A,B,C,D,), as calculated by the ZINDO/S method, is smaller than that measured from the absorption spectra. Indeed, a maximum wavenumber of 27241 cm^{-1} is predicted theoretically compared to 32000 cm^{-1} observed experimentally (see table 2). This might imply that the actual aggregate of TT involves more than four molecules.

3.2. 3,3''-dimethyl-2,2':5',2''-terthiophene (DMTT)

The crystalline structure of DMTT [42], as shown in Figure 5, is much different than that found for TT (see Figure 2). Indeed molecules A and B are parallel but cofacial interactions are limited to one thiophene ring whereas molecules C and D are also parallel. The structure of the single molecule in the solid state is also different than that of TT. Indeed each molecule of DMTT adopts a twisted

conformation of about 30° from planarity whereas a mixture of *syn-gauche* and *anti-gauche* conformers is observed in the crystal. However, the conformation found for DMTT in the solid state is less twisted than that predicted from HF/3-21G* *ab initio* calculations for a "free" molecule ($\theta = 118°$) [40].

The excited singlet and triplet states of the single molecules and of various aggregates are displayed in Figure 6 and the properties of their first singlet-singlet transitions are reported in Table 3 and compared with experimental one in Table 2. For the isolated molecule, the $S_1 \leftarrow S_0$ electronic transition is intense ($f = 1.113$) and is located at 27490 cm^{-1}. This transition energy is higher than that reported above for TT whereas its oscillator strength is smaller. This is a consequence of the twisted conformation found for DMTT in the solid state compared to the nearly planar one for TT. The $S_1 \leftarrow S_0$ electronic transition of DMTT having the same structural parameters but with $\theta = 118°$ (free) appears at a much higher energy (31786 cm^{-1}) giving rise to a blue shift of 4296 cm^{-1} compared to the A form. This shift is much higher than that measured between the absorption and excitation spectra of DMTT in solution and in the *n*-decane matrix at 77K (2250 cm^{-1}). We believe that this behavior arises from an overestimation of the $S_1 \leftarrow S_0$ transition energy for the very twisted conformers as calculated by the ZINDO/S method. This was observed before for heavily twisted conformers [49]. One can see in table 2 that the calculated first singlet transition energy for the free molecule is again in the ~2000 cm^{-1} bracket compared to the experiment as observed for TT. For the isolated molecule and the aggregated form (A,B,C,D), the difference between the observed and calculated transition energies is smaller (~500 cm^{-1}).

According to Figure 5, two main intermolecular interactions may exist in the subcrystalline form: the dimer formed by molecules A and B, which are parallel and the dimer formed by molecules A and D. The dimer A,C (results not shown) has also been considered but the electronic properties were found quasi similar to those of the dimer A,D. Figure 6 shows that the interaction between molecules A and B does not significantly affect the energy of the S_1 excited singlet state of the isolated molecule.

This is explained by the small overlapping between molecules A and B, which gives weak intermolecular interactions. However, the energy of the triplet states are more affected by the interactions involved in the dimer AB. Indeed, one can notice a convergence of the triplet states as observed for the TT aggregates. On the other hand, the interaction between molecules A and D induces a small excitonic splitting of the S_1 excited singlet state. The $S_1 \leftarrow S_0$ electronic transition of the dimer A,D appears at a slightly smaller energy than that of the single molecule and is less intense whereas the $S_2 \leftarrow S_0$ electronic transition is blue shifted and is very intense. It is important to point out that the blue shift observed for the second electronic transition (611 cm^{-1}) compared to that of the single molecule is smaller than that found for the dimer A,B of TT (953 cm^{-1}).

For the tetramer, the $S_1 \leftarrow S_0$ electronic transition appears at about the same energy than that of the isolated molecule and is quite intense (f = 1.1252). But the most allowed singlet-singlet transition, which corresponds to $S_3 \leftarrow S_0$, is blue shifted by 1290 cm^{-1} compared to $S_1 \rightarrow S_0$ of the isolated molecule. The value of this shift is much smaller than that induced by the intermolecular interactions occurring for TT (2513 cm^{-1}). Moreover the red shift of the first allowed singlet transition between the free and isolated molecules caused by the packing effect present in the solid phase of DMTT (4296 cm^{-1} calculated and 2250 cm^{-1} measured, see above) is much larger than the blue shift of the singlet transition between the isolated and aggregated form induced by intermolecular interactions.

The simulated absorption spectra of DMTT using the crystalline structure and possessing dihedral angle values of 30° (in the solid state) and 118° (in solution) are displayed in Figure 7. One can see that the packing effect present for DMTT, for an isolated molecule, in the solid state induces a very large red shift of its absorption band. But, as mentioned above, the energy difference between the $S_1 \leftarrow S_0$ electronic transition of these two conformations could be overestimated by ZINDO/S calculations. On the other hand, the simulated absorption spectrum of the tetramer shows a component at about the same energy than that observed for the isolated

molecule in the solid state but the more intense peak is blue shifted (see Figure 7 and Table 3). The spectral properties shown here for DMTT are quite different than those reported above for TT. Indeed, the main band of the tetramer located at 28780 cm^{-1} is red shifted compared to the absorption band of DMTT in solution (θ = 118°). These theoretical results are in good agreement with the experimental results shown in part I of this series of paper [39] (see figure 9B). Indeed, following the aggregation process, the excitation spectrum of DMTT is red shifted compared to the absorption spectrum recorded in solution. It is worth mentioning here that the excitonic splitting calculated for clusters retaining the perfect crystalline geometry is certainly maximized compared to real life. One expects that for aggregated forms or solid states (evaporated solution of DMTT) [39], the actual splitting is less. Moreover, compared with the excitation spectrum of DMTT molecules isolated in an alkane matrix at 77K, the excitation spectrum of the aggregated forms shows a first band close to the 0,0 vibronic peak (~25100 cm^{-1}). However, the intensity of this peak is weak compared to the rest of the absorption band. The main excitation peak of the aggregated forms appears near 28200 cm^{-1}, which is blue shifted compared to the maximum of the excitation spectrum of the single molecule in the alkane matrix but is red shifted compared with the absorption band of DMTT in solution. The shift between the maximum of the excitation spectra of DMTT in the matrix and in the aggregated forms is ~1000 cm^{-1} (see table 2), which is close to the value of 1290 cm^{-1} calculated between the maximum of the simulated spectra of the molecule isolated in the crystal and that of the tetramer. Obviously, the lack of resolution in the excitation spectra does not preclude the existence of different types of aggregates, which would cause an increase of the bandwidths, making the correlation with theoretical results more qualitative than quantitative.

3.3. 3',4'-dibutyl-2,2':5',2''-terthiophene (DBTT)

The crystalline structure of a unit cell of DBTT [43] is shown in Figure 8. The four molecules are positioned such that no crystal plane is observed. Moreover molecules A and B (or C and D) are nearly perpendicular to each other. The thiophene backbones do not adopt a totally planar conformation but possess a dihedral angle $\theta \sim 30°$ from planarity whereas adjacent thiophene rings have an *anti-gauche* conformation. However, the molecular conformation in the crystal is more planar than the minimum energy conformation optimized for 3',4'-diethyl-2,2':5',2''-terthiophene (DETT) using the HF/3-21G* *ab initio* method [40] as observed for TT and DMTT. Indeed, this lowest energy conformer has a dihedral angle $\theta = 105°$ due to the high steric effect caused by the presence of the alkyl groups. The decrease of the torsion of DBTT in the solid state is caused by the packing effect present in the crystal.

The electronic spectrum of a single molecule is shown in Figure 9 and the spectral characteristics are reported in Table 4. Experimental and calculated parameters are compared in table 2. As observed for TT and DMTT, the $S_1 \leftarrow S_0$ electronic transition is allowed and appears at 25265 cm^{-1} with an oscillator strength of 1.0039. This singlet-singlet transition is blue shifted compared to that of TT due to the increase of the twisting angles in DBTT, but is red shifted compared to that of DMTT. This difference between DMTT and DBTT might be caused by the respective conformation adopted by the molecules (*anti* for DBTT and *anti-syn* for DMTT) and/or might involve the different positions of the substituents on the thiophene rings. The $S_1 \leftarrow S_0$ electronic transition of the isolated molecule having the crystalline structure but a dihedral angle $\theta = 105°$ (free) is located at 32010 cm^{-1} with an oscillator strength of 0.564. As expected, this transition is blue shifted and the oscillator strength is reduced. The energetic difference between the $S_1 \leftarrow S_0$ transitions involving these two conformations is calculated to be 6745 cm^{-1} (see table 2), which is much larger than that observed experimentally (2690 cm^{-1}, see figure 5B

or 10B of part I and table 2 of this paper). As discussed above for DMTT, we believe that ZINDO/S calculations may overestimate the absolute energy of electronic transitions for much twisted conformers. As observed for TT, the comparison between experimental and calculated first allowed transitions (see table 2) is good and inside the 2000 cm^{-1} bracket.

The first dimer considered in the cell unit involves molecules A and B. The electronic spectrum of the dimer A,B is displayed in Figure 9. One can see that the intermolecular interaction between these two molecules caused a Davydov splitting of the S_1 excited singlet state, giving rise to a weak $S_1 \leftarrow S_0$ transition which is red shifted (761 cm^{-1}) and a $S_2 \leftarrow S_0$ transition which is blue shifted (777 cm^{-1}) and more intense compared to the isolated molecule first electronic S_0-S_1 transition. These spectral shifts are smaller than those reported above for TT but slightly larger than those calculated for DMTT. This suggests that the interaction between two DBTT molecules in the solid state is slightly larger than the intermolecular interaction found for DMTT in the same environment. The second type of dimer investigated involving molecules A and C does not show any significant excitonic effect indicating that the intermolecular interaction between these two molecules is weak.

Contrary to the dimer A,B, the first singlet-singlet transition of the tetramer A,B,C,D is located at the same wavelength than that calculated for the isolated molecule (see Figure 9). This behavior is similar to the one discussed above for TT where the S_1 state of the tetramer was not as red shifted as that of the dimer. On the other hand, the most intense transition ($S_3 \leftarrow S_0$) of the tetramer is blue shifted, compared to the single molecule, by exactly the same amount than that calculated for the dimer ($S_2 \leftarrow S_0$). One can also observed that the $S_4 \leftarrow S_0$ transition is more intense and is blue shifted compared to the $S_1 \leftarrow S_0$ and $S_2 \leftarrow S_0$ electronic transitions. As observed for DMTT, the most intense singlet-singlet transition is not as blue shifted (736 cm^{-1}) as that found for TT (2513 cm^{-1}). Moreover the blue shift observed is small compared to the red shift (6745 cm^{-1}) caused by the packing effect present in the solid state, which increases the planarity of the molecules.

The simulated spectra of the various species are shown on Figure 10. It is observed again that the absorption spectrum of the molecule isolated in the crystal and that of the tetramer are close to each other whereas the absorption band of the molecule in solution ($\theta = 105°$) is blue shifted. Once again, these theoretical results provide a good correlation with the experimental results reported in part I of this series of paper [39] (see figure 10B) and in table 2 of this paper.

Overall, it is observed that intermolecular interactions involving substituted terthiophenes lead to a smaller excitonic effect in the absorption spectra of these molecules than that found for TT. This clearly indicates that the addition of side groups to the main chromophore weakens the interaction between these molecules in the solid state. This is certainly due to the different arrangements found in the solid state for these oligothiophenes. Indeed, the presence of the lateral side chains increases intermolecular distances and modifies the orientations, which should decrease the overlap between p_z orbitals of neighboring molecules. Moreover, the non planarity of the thiophene backbones in the crystals could also play a role in the decrease of the intermolecular interactions. To gain a better knowledge of the importance of the last point, ZINDO/S calculations performed on the crystallographic structure of 3,3''-dimethoxy-2,2':5',2''-terthiophene (DMOTT) would be helpful. Indeed, it was shown in part I [39] that this molecule in solution is nearly planar such that no important conformational changes are expected to be induced by the packing effect in the solid state. On the other hand, in the solid state, the intermolecular interactions would be emphasized alone since being the only factors influencing the absorption spectrum. Moreover, the absorption spectrum of DMOTT in its aggregated form reported in part I [39] does not show any excitonic splitting following aggregation. Unfortunately, X-ray data about DMOTT are still missing in the literature. To further investigate the influence of the molecular conformation on the intermolecular interactions, ZINDO/S calculations have been done for the crystalline structure of 3,3'-dimethoxy-2,2'-bithiophene [50]. These results, compared with those performed for the X-ray structure of BT [51], do not

show any important excitonic splitting despite the fact that this molecule is nearly planar [25]. ZINDO/S calculations [52] have also been performed on the crystalline structure of 3,3'''-dimethoxy-2,2':5',2'':5'',2'''-quaterthiophene (DMOQT) [53]. Results show a weaker excitonic splitting on the first allowed singlet transition compared to that calculated for quaterthiophene (QT) despite the fact that the former molecule is nearly planar in the solid state. These results are in agreement with the experimental results. All these experimental and theoretical results indicate that the sole presence of lateral chains prevents the formation of a compact and ordered crystalline structure. Breaking off the highly ordered crystalline form is the principal cause of the weakness of the excitonic effect observed in substituted terthiophenes.

4. Concluding Remarks

It is shown in this paper that sandwich-type intermolecular interactions involve for unsubstituted terthiophene (TT) in its crystalline form induce an important excitonic splitting of its absorption spectrum. On the other hand, head-to-tail intermolecular interactions do not significantly affect the spectral properties of TT. The appearance of a weak red shifted band and an intense blue shifted band in the absorption spectrum of TT in its aggregated form is in good agreement with experimental results reported in part I of this study. The blue shift of the allowed transition increases with the number of molecules in interaction while the red shift of the weak band is reduced. Since TT is not much twisted in solution ($\theta = 150°$), the change of conformation of TT in the solid state caused by the packing effect is relatively weak such that the red shift resulting from the increase of molecular planarity is overcome by the blue shift induced by the formation of aggregates.

In contrast, the crystalline structure of alkyl-substituted terthiophenes is less ordered leading to weaker electronic interactions between neighboring molecules, giving rise to weaker excitonic effects. For these derivatives, the conformational changes occurring in the solid state are large such that the absorption red shift due to

the increase of planarity emcompasses the blue shift resulting from intermolecular interactions present in the solid state. In other words, the chromic effects observed for alkyl-substituted terthiophenes are mainly due to conformational changes instead of excitonic splittings as observed for unsubstituted oligothiophenes.

Acknowledgment

The authors are grateful to the Natural Sciences and Engineering Research Council of Canada (NSERC) and the fonds FCAR (Quebec) for their financial support. N.D.C. is grateful to the NSERC for a graduate scholarship.

References and Notes

[1] Skotheim, T.A., Handbook of Conducting Polymers; Ed.; Marcel Dekker, New-York, 1986; Vols 1 and 2. Brédas, J.L., Silbey, R., Conjugated Polymers: The novel Science and Technology of Highly Conducting and Nonlinear Optically Active Materials; Eds.; Kluwer: Dordrecht, 1991.

[2] Burroughes, J. H.; Bradley, D.D.C.; Brown, A.R.; Marks, R.N.; Friend, R.H.; Burn, P.L.; Holmes, A.B. *Nature* **1990**, *347*, 539.

[3] Pei, Q.; Yu, C.; Zhang, Y.; Yang, Y.; Heeger, A.J. *Science* **1995**, *269*, 1086.

[4] Hide, F.; Diaz-Garcia, M.A.; Schwartz, B.; Anderson, M.R.; Pei, Q.; Heeger, A.J. *Science* **1996**, *833*, 273.

[5] Schopf, G.; Kossmehl, G. *Adv. Polym. Sci.* **1997**, *127*, 1.

[6] Rughooputh, S.D.D.V.; Hotta, S.; Heeger, A.J.; Wudl, F.J. *J. Polym. Sci., Polym. Phys. Ed.* **1987**, *25*, 1071.

[7] Kawai, T.; Kuwabara, T.; Wang, S.; Yoshino, K. *J. Electrochem. Soc.* **1990**, *137*, 3793.

[8] Ohmori, Y.; Uchida, M.; Muro, K.; Yoshino, K. *Jpn. J. Appl. Phys.* **1991**, *30*, L1938.

[9] Morita, S.; Kawai, T.; Yoshino, K. *J. Appl. Phys.* **1991**, *69*, 4445.

[10] Fichou, D.; Horowitz, G.; Xu, B.; Garnier, F. *Synth. Met.* **1992**, *48*, 167.

[11] Oelkrug, D.; Egelhaaf, H.J.; Worrall, D.R.; Wilkinson, F. *J. Fluores.* **1995**, *5*, 165.

[12] Bongiovanni, G.; Botta, C.; Di Silvestro, G.; Mura, A.; Tubino, R. *Phys. Lett. A* **1995**, *208*, 165.

[13] Kanemitsu, Yoshihiko, Shimizu, N. *Phys. Rev. B* **1996**, *54*, 2198.

[14] Oelkrug, D.; Egelhaaf, H.J.; Gierschner, J.; Tompert, A. *Synth. Met.* **1996**, *76*, 249.

[15] Watanabe, K.; Asahi, T.; Fukumura, H.; Masuhara, H.; Hamano, K.; Kurata, T. *J. Phys. Chem. B* **1997**, *101*, 1510.

[16] Lanzani, G.; Nisoli, M.; De Silvestri, S. Abbate, F. *Chem. Phys. Lett.* **1997**, *264*, 667.

[17] Sakurai, K.; Tachibana, H.; Shiga, N.; Terakura, C.; Matsumoto, M.; Tokura, Y. *Phys. Rev. B* **1997**, *56*, 9552.

[18] Lang, P.; Horowitz, G.; Valat, P.; Garnier, F.; Wittmann, J.C.; Lotz, B. *J. Phys. Chem. B* **1997**, *101*, 8204.

[19] Klein, G.; Jundt. C.; Sipp, B.; Villaeys, A.A.; Boeglin, A.; Yassar, A.; Horowitz, G.; Garnier, F. *Chem. Phys.* **1997**, *215*, 131.

[20] Watanabe, K.; Asahi, T.; Fukumura, H.; Masuhara, H.; Hamano, K.; Kurata, T. *J. Phys. Chem. B* **1998**, *102*, 1182.

[21] Beljonne, D.; Cornil, J.; Friend, R.H.; Janssen, R.A.J.; Brédas, J.L. *J. Am. Chem. Soc.* **1996**, *118*, 6453.

[22] Hernandez, V.; Lopez-Navarrete, J.T. *J. Chem. Phys.* **1994**, *101*, 1369.

[23] Aleman, C.; Julia, L. *J. Phys. Chem.* **1996**, *100*, 1524.

[24] Viruela, P.M.; Viruela, R.; Orti, E.; Brédas, J.L. *J. Am. Chem. Soc.* **1997**, *119*, 1360.

[25] DiCésare, N.; Belletête, M.; Leclerc, M.; Durocher, G. *J. Mol. Struct. (TheoChem)*, in press.

[26] DiCésare, N.; Belletête, M.; Raymond, F.; Leclerc, M.; Durocher, G. *J. Phys. Chem. A* **1998**, *102*, 2700.

[27] DiCésare, N.; Belletête, M.; Leclerc, M.; Durocher, G. *Synth. Met.* **1998**, *94*, 291.

[28] DiCésare, N.; Belletête, M.; Leclerc, M.; Durocher, G. *Chem. Phys. Lett.* **1997**, *275*, 533.

[29] Bongiovanni, G.; Botta, C.; Brédas, J.L.; Cornil, J.; Ferro, D.R.; Mura, A.; Piaggi, A.; Tubino, R. *Chem. Phys. Lett.* **1997**, *278*, 146.

[30] Cornil, J.; Heeger, A.J.; Brédas, J.L. *Chem. Phys. Lett.* **1997**, *272*, 463.

[31] Cornil, J.; Beljonne, D.; Heller, C.M.; Campbell, I.H.; Laurich, B.K.; Smith, D.L.; Bradley, D.D.C.; Müllen, K.; Brédas, J.L. *Chem. Phys. Lett.* **1997**, *278*, 139.

[32] Cornil, J.; dos Santos, D.A.; Crispin, X.; Silbey, Brédas, J.L. *J. Am. Chem. Soc.* **1998**, *120*, 1289.

[33] McRae, E.G.; Kasha, M. *J. Chem. Phys.* **1958**, *28*, 721.

[34] Kasha, M. *Radiation Res.* **1963**, *20*, 55.

[35] Hochstrasser, R.M.; Kasha, M. *Photochem. Photobiol.* **1964**, *3*, 317.

[36] Cui, C.X.; Kertesz, M. *Phys. Rev. B* **1989**, *40*, 9661.

[37] Ferro, D.R.; Porzio, W.; Destri, S.; Ragazzi, M. *Macromol. Theory Simul.* **1997**, *6*, 713.

[38] Corish, J.; Feeley, D.E.; Morton-Blake, D.A.; Bénière, F.; Marchetti, M. *J. Phys. Chem. B* **1997**, *101*, 10075.

[39] DiCésare, N.; Belletête, M.; Maranno, C.; Leclerc, M.; Durocher, G. *J. Phys. Chem. A* (part I) **1999**, *103*, 795.

[40] DiCésare, N.; Belletête, M.; Marrano, C.; Leclerc, M.; Durocher, G. *J. Phys. Chem. A* **1998**, *102*, 5142.

[41] Van Bolhuis, F.; Wynberg, H.; Havinga, E.E.; Meijer, E.W.; Staring, G.J. *Synth. Met.* **1989**, *30*, 381.

[42] Chaloner, P.A.; Gunatunga, S.R.; Hitchcock, P.B. *J. Chem. Soc., Perkin Trans. 2* **1997**, 1597.

[43] DeWitt, L.; Blanchard, G.J.; LeGoff, E.; Benz, M.E.; Liao, J.H.; Kanatzidis, M.G. *J. Am. Chem. Soc.* **1993**, *115*, 12158.

[44] Ridley, J.; Zerner, M.C. *Theor. Chim. Acta*, **1973**, *32*, 111.

[45] Forber, C.; Zerner, M.C. *J. Am. Chem. Soc.* **1985**, *107*, 5884.

[46] Becker, R.S.; deMelo, J.S.; Maçanita, A.L.; Elisei, F. *J. Phys. Chem.* **1996**, *100*, 18683.

[47] Rossi, R.; Ciofalo, M.; Carpita, A.; Ponterini, G. *J. Photochem. Photobiol. A* **1993**, *70*, 59.

[48] Belletête, M.; DiCésare, N.; Leclerc, M., Durocher, G. *J. Mol. Struct. (Theochem)* **1997**, *391*, 85.

[49] Unpublished results.

[50] Paulus, E.F.; Dammel, R.; Kampf, G.; Wegener, P. *Acta Cryst.* **1988**, *B44*, 509.

[51] Pelletier, M.; Brisse, F. *Acta Cryst.* **1994**, *C50*, 1942.

[52] Miller, L.L.; Yu, Y. *J. Org. Chem.* **1995**, *60*, 6813.

[53] DiCésare, N.; Belletête, M.; Leclerc, M.; Durocher, G. *J. Phys. Chem*, send for publication.

Table 1

Energy (relatively to the S_0 state), Oscillator Strength and Molecular Orbitals (M.O.) Involved in the First Excited Singlet States of Subcrystalline Forms of TT.

Subcrystalline Forms [a]	Excited Singlet States	Energy cm^{-1} (eV)	f [b]	M.O. [c]
A	S_1	24 728 (3.07)	1.2024	H→L
A,B	S_1	22 784 (2.83)	0.0814	H→L
				H→L+1
	S_2	25 681 (3.18)	2.5107	H-1→L
				H-1→L+1
A,E	S_1	24355 (3.02)	2.3701	H→L
				H-1→L+1
	S_2	25 227 (3.13)	0.0090	H→L+1
				H-1→L
A,B,E,F	S_1	23 288 (2.89)	0.3627	H→L
	S_2	23 518 (2.92)	0.0017	H→L+1
	S_3	25 530 (3.17)	4.3984	-
	S_4	27 071 (3.36)	0.0260	H-2→L+1
A,B,C,D	S_1	22 983 (2.85)	0.0086	H→L
	S_2	23 646 (2.93)	0.0187	H-1→L
	S_3	25 517 (3.16)	0.0200	H-2→L+1
	S_4	27 241 (3.38)	6.3736	-

[a] see figure 2 for the nomenclature.

[b] oscillator strength.

[c] H for HOMO (Highest Occupied Molecular Orbital) and L for LUMO (Lowest Unoccupied Molecular Orbital).

Table 2

Comparison Between Observed and Calculated Absorption Spectra for Various Oligothiophene Species.

Molecule		Exp. [a] (cm^{-1})	Calc. [b] (cm^{-1})	Δ [c] (cm^{-1})
TT	Free (147°)	28 350	26 291	2059
	A	26 800	24 728	2072
	A,B,C,D	24 500	22 983	1517
		32 000	27 241	4759
DMTT	Free (118°)	29 300	31 786	2486
	A	27 050	27 490	440
	A,B,C,D	28 200	27 451	749
			28 780	580
DBTT	Free (105°)	29 940	32 010	2070
	A	27 250	25 265	1985
	A,B,C,D	27 250	25 250	2000
			26 001	1249

[a] Wavenumber of the absorption maximum in fluid *n*-decane solution at 298K(free), isolated in *n*-decane matrix at 77K (A) and in the aggregate forms at 77K (A,B,C,D).

[b] Wavenumber of the absorption spectrum as calculated from ZINDO/S.

[c] Difference between experimental and calculated results.

Table 3

Energy (relatively to the S_0 state), Oscillator Strength and Molecular Orbitals (M.O.) Involved for First Excited Singlet States of Subcrystalline Forms of DMTT.

Subcrystalline Forms [a]	Excited Singlet States	Energy cm^{-1} (eV)	f [b]	M.O. [c]
A	S_1	27 490 (3.41)	1.1330	H→L
A,B	S_1	27 291 (3.38)	2.2449	H→L
				H-1→L+1
	S_2	27 747 (3.44)	0.0000	H→L+1
				H-1→L
A,D	S_1	27 028 (3.35)		H→L+1
				H-1→L
	S_2	28101 (3.48)		H→L+1
				H-1→L
A - D	S_1	27 451 (3.40)	1.1252	H→L
				H-3→L+3
	S_2	28 075 (3.48)	0.0000	H-1→L+2
				H-2→L+1
	S_3	28 780 (3.57)	3.1626	H-1→L+1
				H-2→L+2
	S_4	28 901 (3.58)	0.0000	H→L+3
				H-1→L+2
				H-3→L

[a] see figure 5 for nomenclature.

[b] oscillator strength.

[c] H for HOMO (Highest Occupied Molecular Orbital) and L for LUMO (Lowest Unoccupied Molecular Orbital).

Table 4

Energy (relatively to the S_0 state), Oscillator Strength and Molecular Orbitals (M.O.) Involved for First Excited Singlet States of Subcrystalline Forms of DBTT.

Subcrystalline Forms [a]	Excited Singlet States	Energy cm^{-1} (eV)	f [b]	M.O. [c]
A	S_1	25 265 (3.13)	1.0039	H→L
A,B	S_1	24 504 (3.04)	0.0050	H→L+1
				H-1→L
	S_2	26 042 (3.23)	2.0206	H→L
				H-1→L+1
A,C	S_1	24 969 (3.10)	1.5934	H→L+1
				H-1→L
	S_2	25 680 (3.18)	0.3931	H→L+1
				H-1→L+1
A-D	S_1	25 259 (3.13)	0.0100	H-1→L+2
	S_2	25 265 (3.13)	0.0213	H→L+3
				H-2→L+1
	S_3	26 001 (3.22)	3.0508	-
	S_4	27 427 (3.40)	0.7306	-

[a] see figure 8 for nomenclature.

[b] oscillator strength.

[c] H for HOMO (Highest Occupied Molecular Orbital) and L for LUMO (Lowest Unoccupied Molecular Orbital).

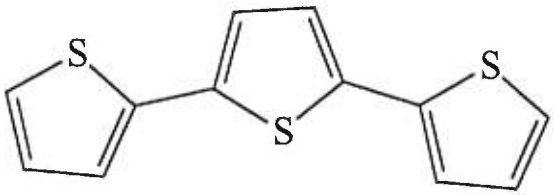

TT

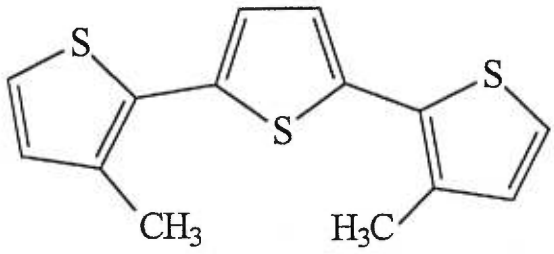

DMTT

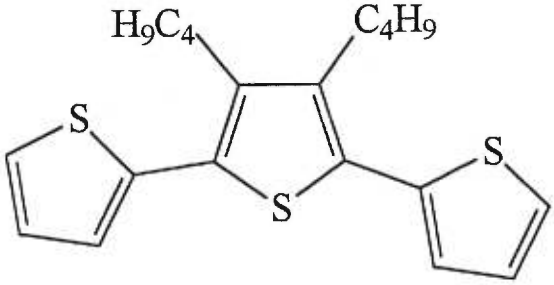

DBTT

Figure 1: Molecular structure and nomenclature used of the molecules investigated.

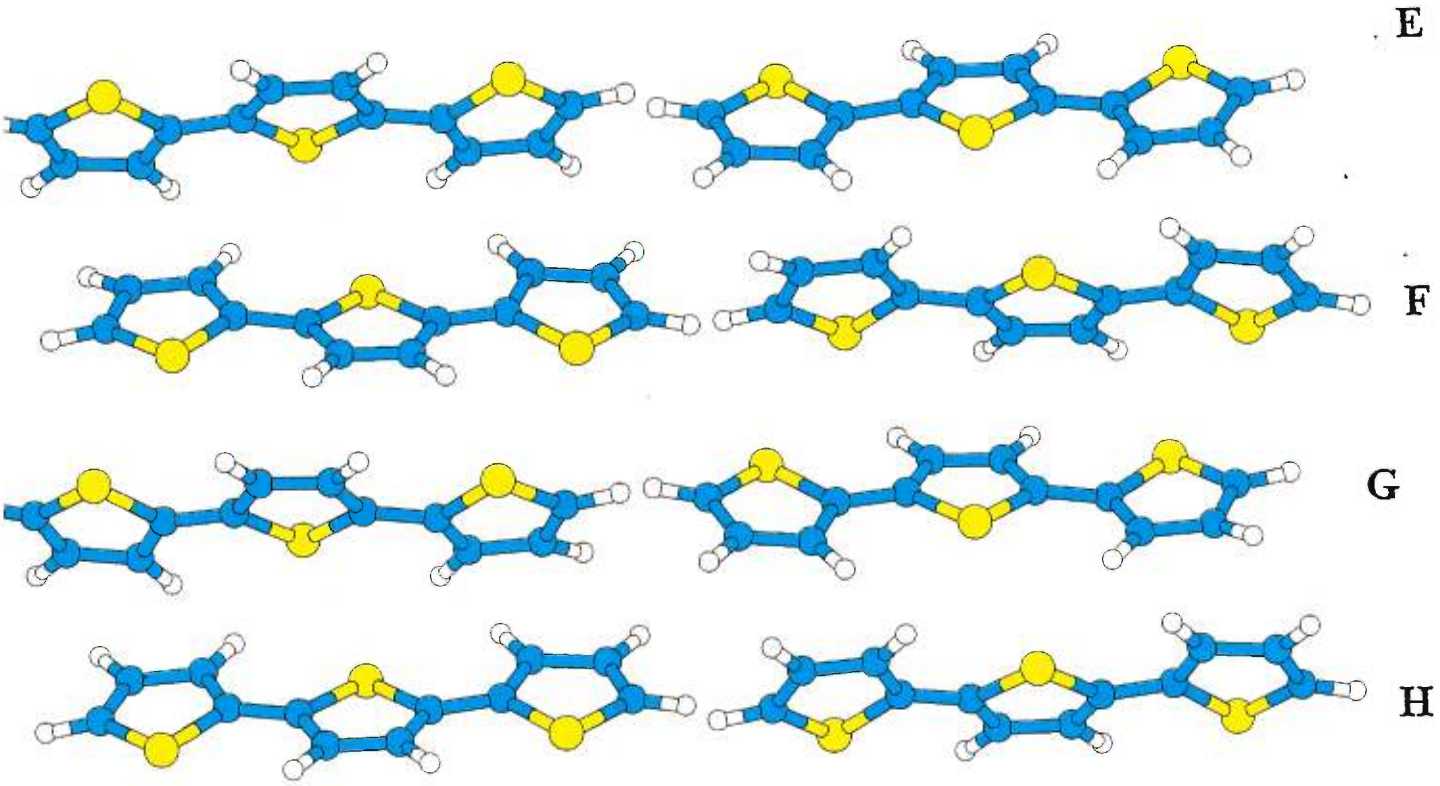

Figure 2: Crystalline structure of TT. Labels (A to H) are used to identify each molecule in subcrystalline structures used for the ZINDO/S calculations.

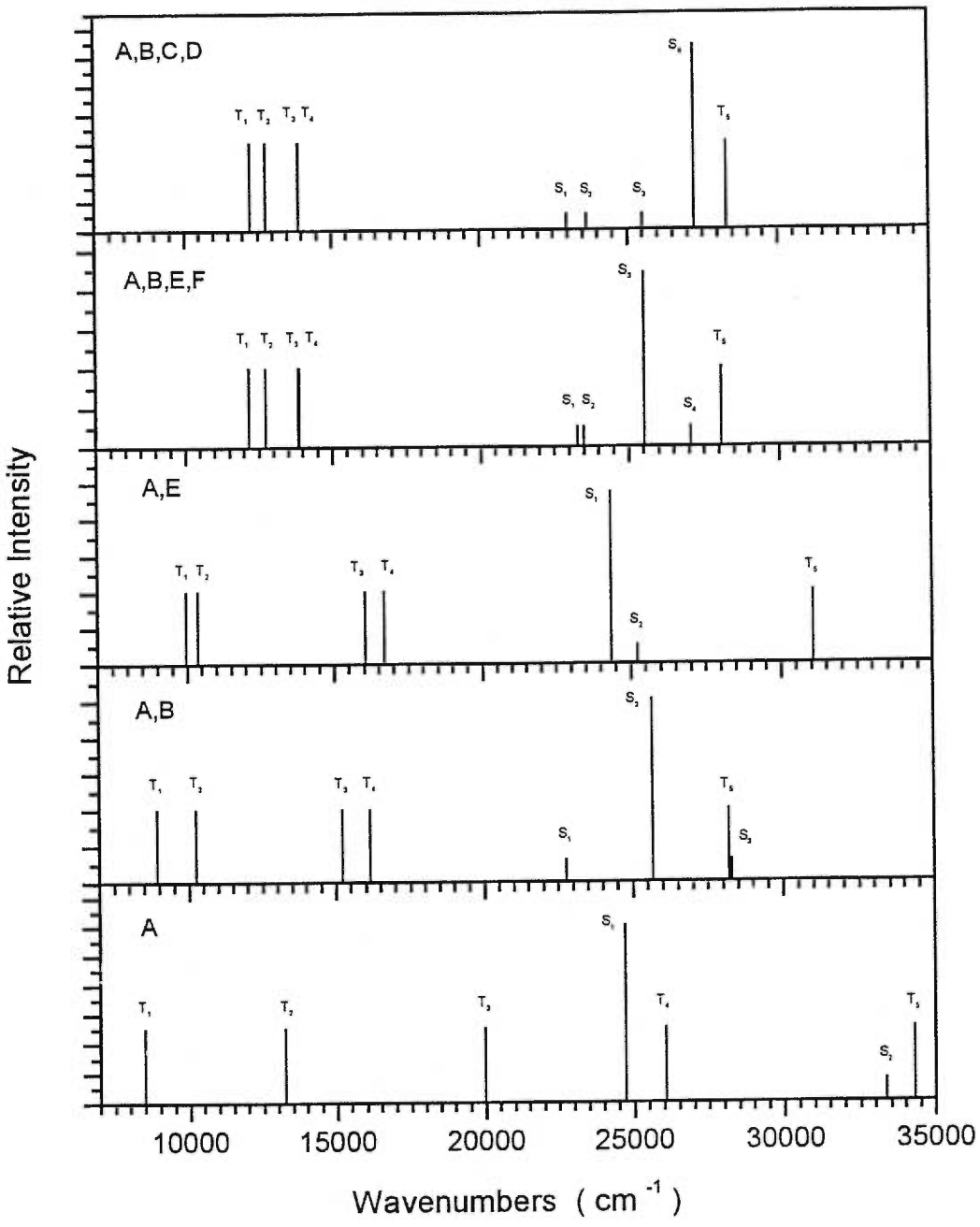

Figure 3: Calculated energy of the singlet-singlet and singlet-triplet electronic transitions of TT. The intensity of the forbidden (or weakly allowed) transitions are increased arbitrarily to be visible. Letters on each window represent the TT molecules (see figure 2) involved in the crystalline forms investigated in the ZINDO/S calculations (from 1 to 4 molecules).

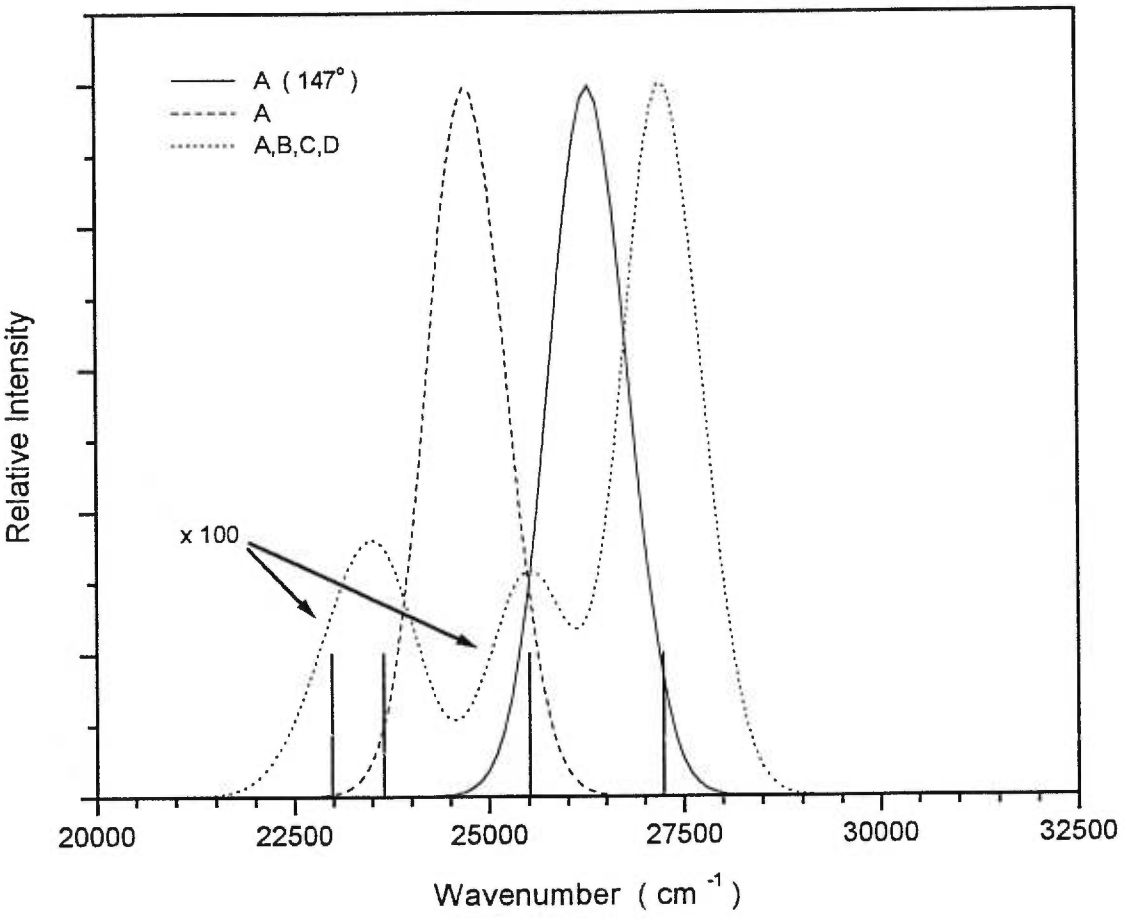

Figure 4: Simulated absorption spectra of TT. Letters in the legend represent the TT molecules (see figure 2) involved in the crystalline form calculated. The spectrum of the free molecule (147°) is obtained as discussed in the text. The normalized transition energies of the tetramer are also indicated.

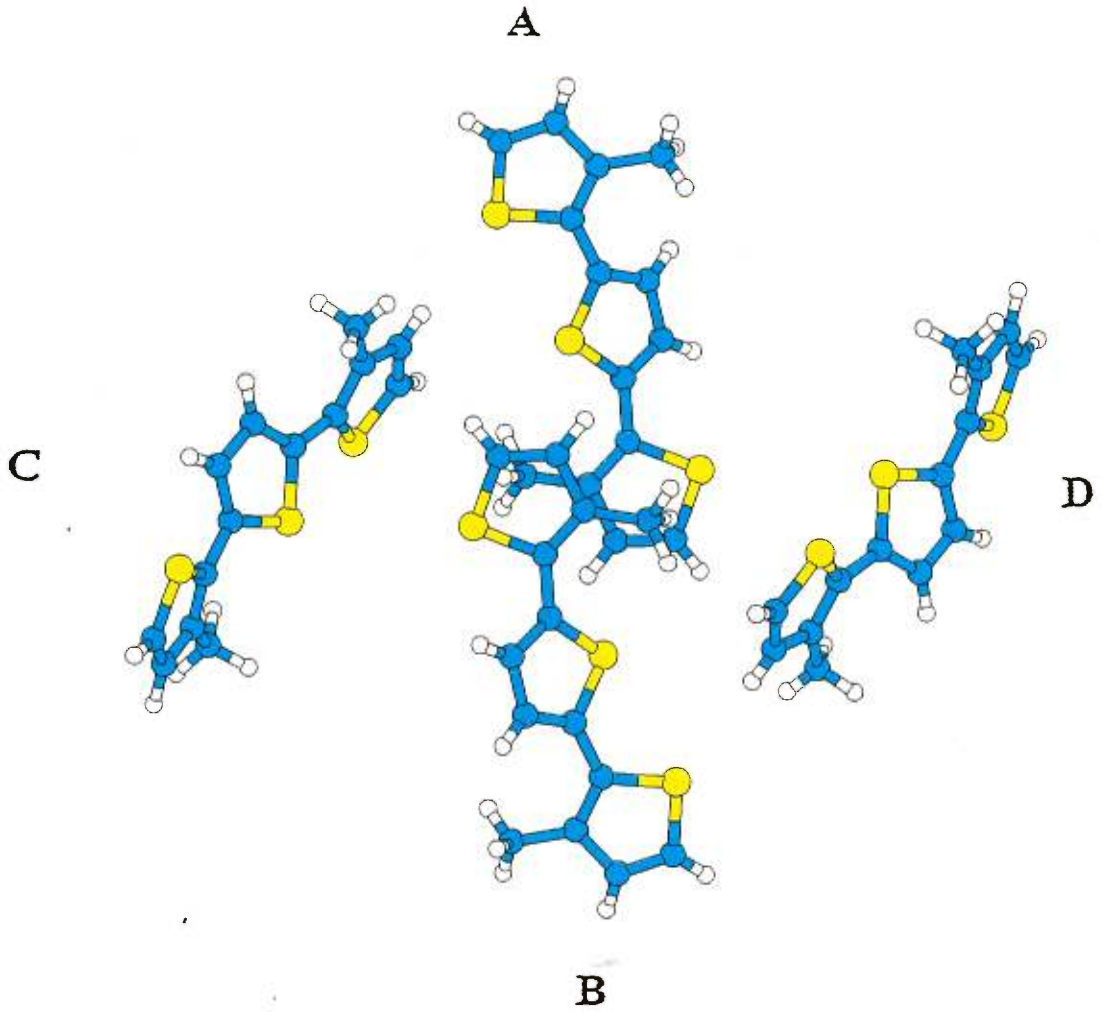

Figure 5: Crystalline structure of DMTT. Labels (A to D) are used to identify each molecule in the subcrystalline structures used for the ZINDO/S calculations.

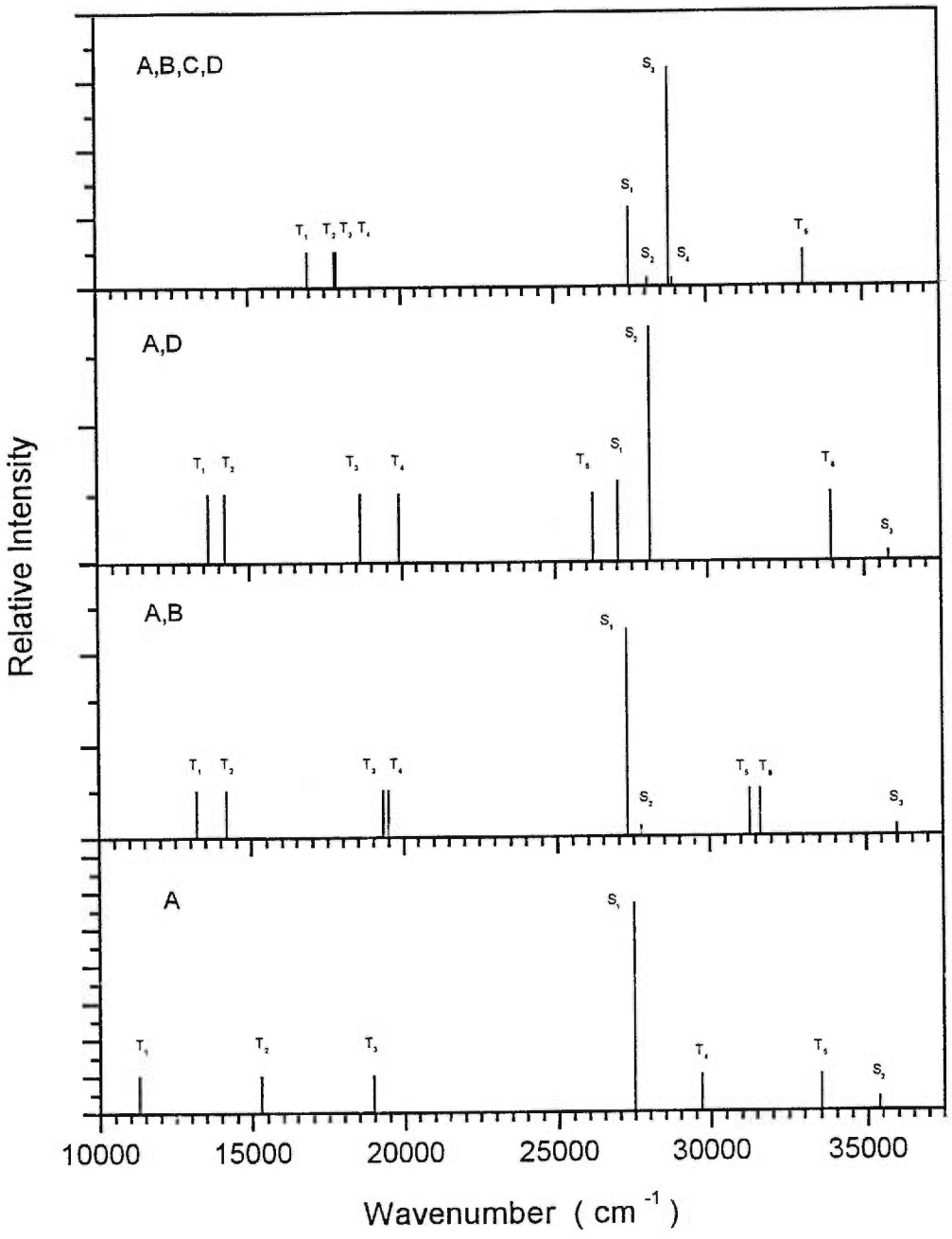

Figure 6: Calculated energy of the singlet-singlet and singlet-triplet electronic transitions of DMTT. The intensity of the forbidden (or weakly allowed) transitions are increased arbitrarily to be visible. Letters on each window represent the DMTT molecules (see figure 5) involved in the crystalline forms investigated (from 1 to 4 molecules).

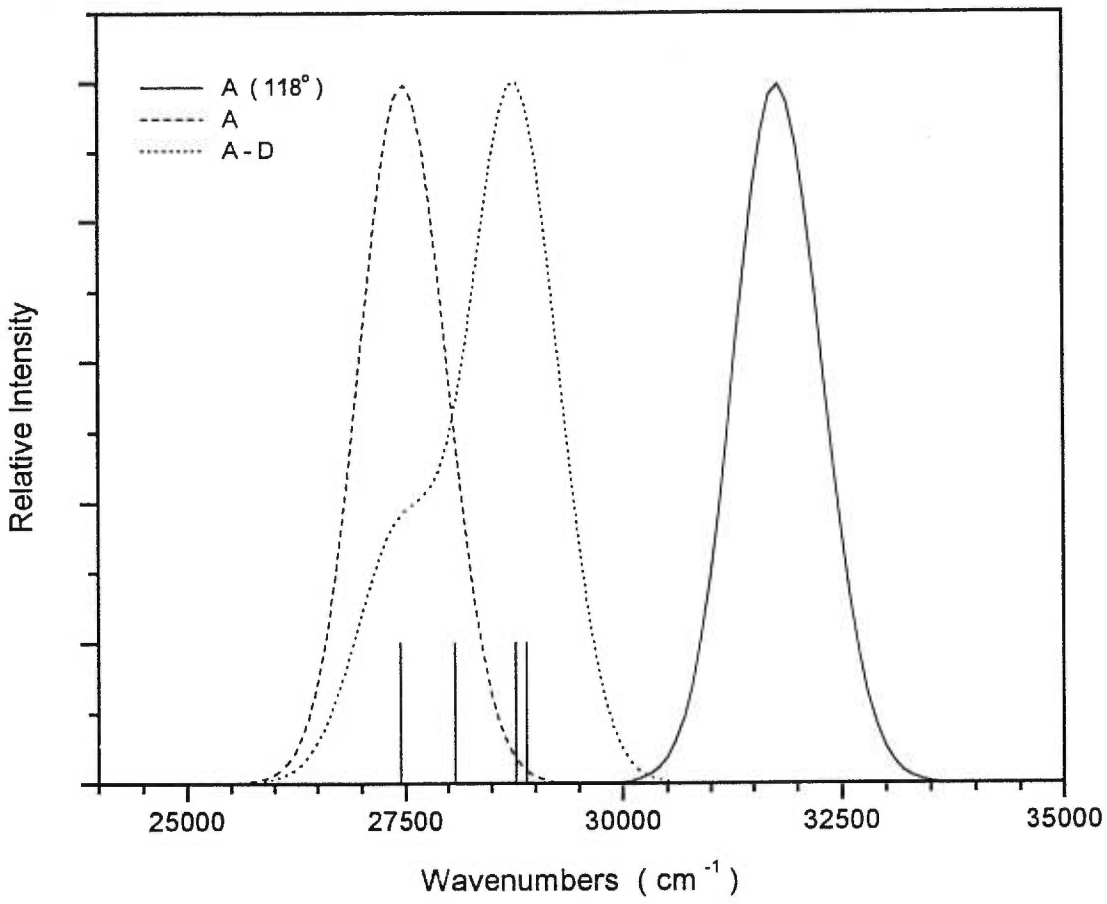

Figure 7: Simulated absorption spectra of DMTT. Letters in the legend represent the DMTT molecules (see figure 5) involved in the crystalline form calculated. The spectrum of the free molecule (118°) is obtained as discussed in the text. The normalized transition energies of the tetramer are also indicated.

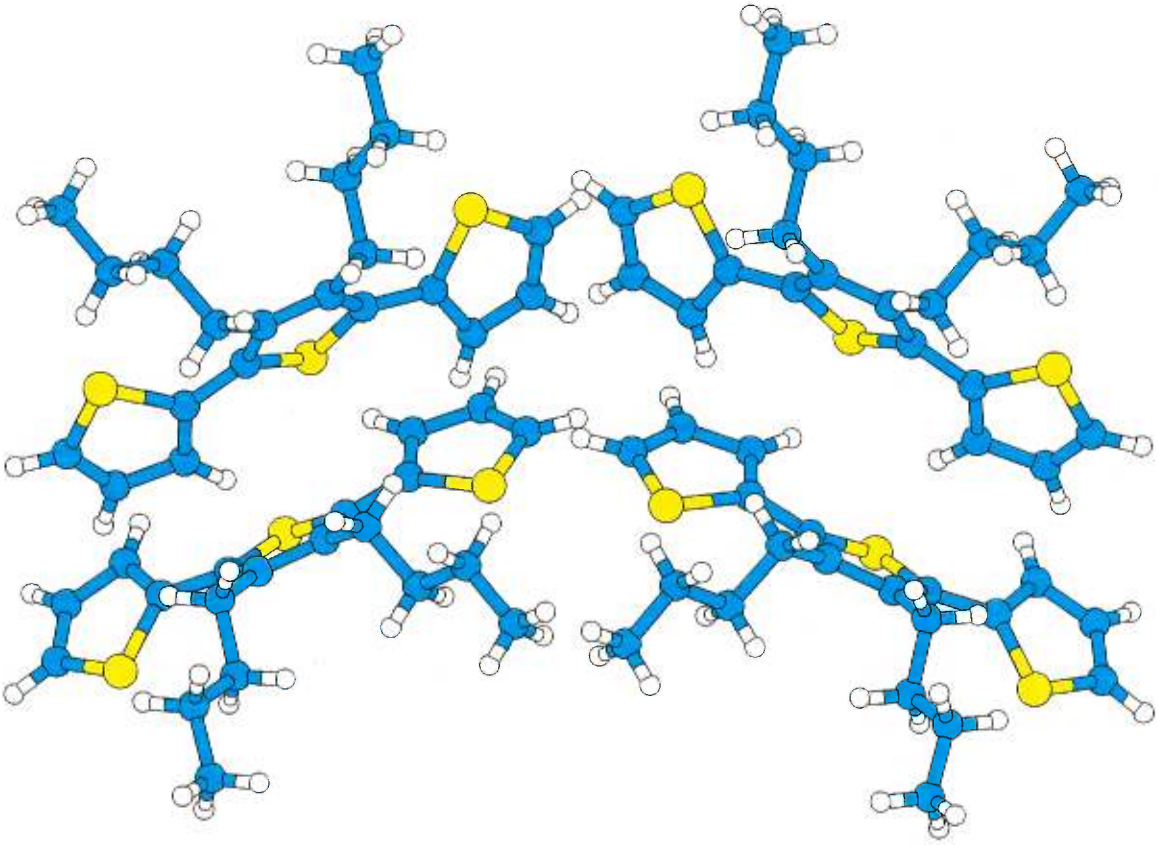

Figure 8: Crystalline structure of DBTT. The labels (A to D) are used to identify each molecule in the subcrystalline structures used for the ZINDO/S calculations.

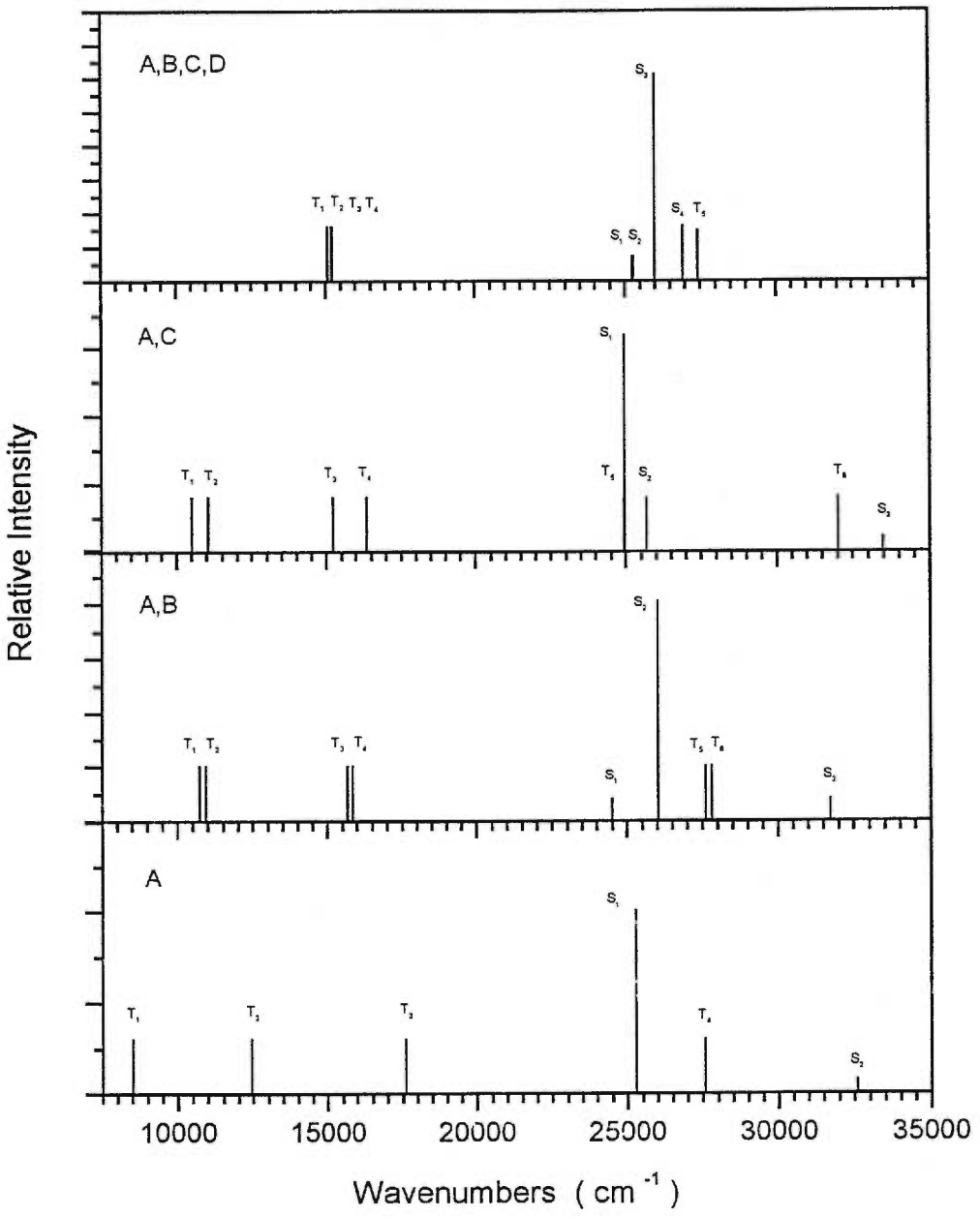

Figure 9: Calculated singlet-singlet and singlet-triplet electronic transitions of DBTT. The intensity of the forbidden (or weakly allowed) transitions are increased arbitrarily to be visible. Letters on each window represent the DBTT molecules (see figure 8) involved in the crystalline form investigated (from 1 to 4 molecules).

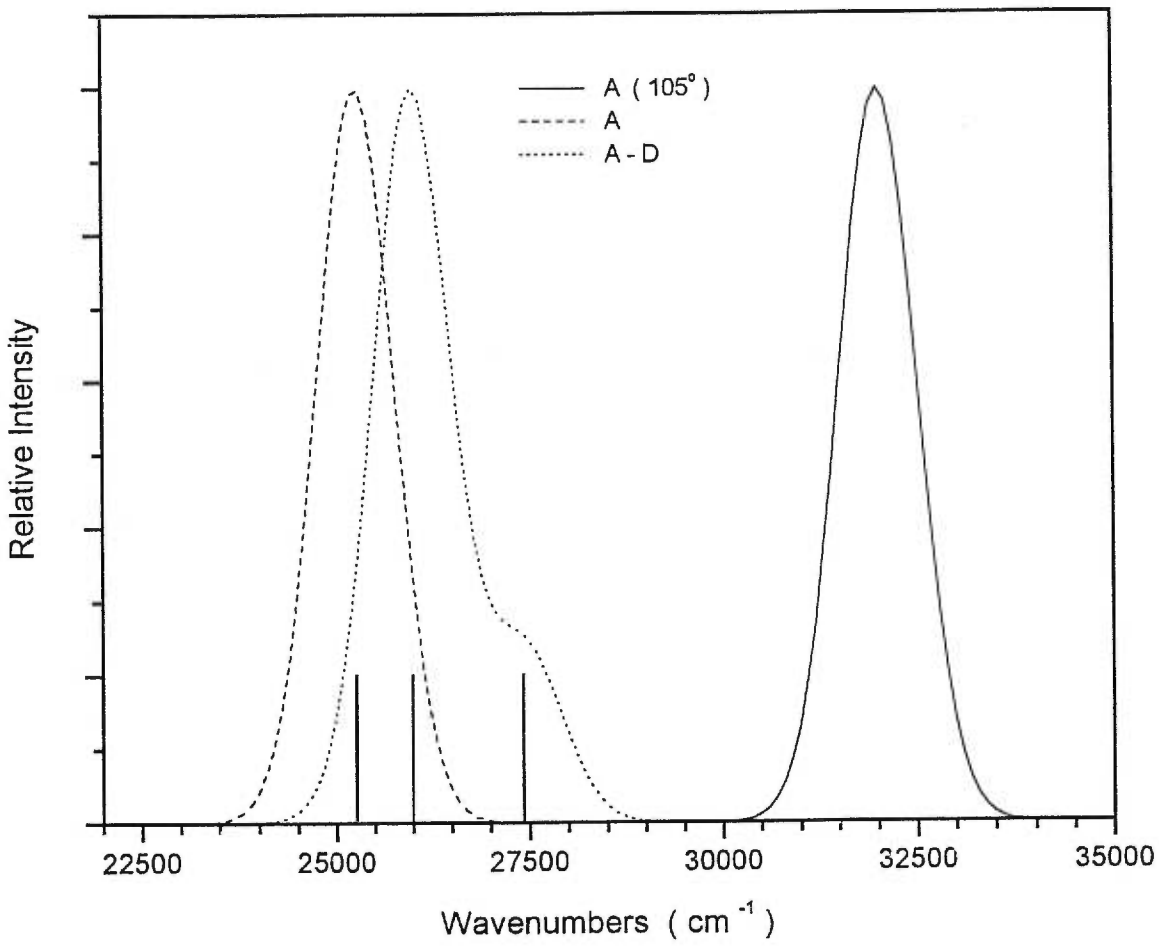

Figure 10: Simulated absorption spectra of DBTT. Letters in the legend represent the DBTT molecules (see figure 8) involved in the crystalline form calculated. The spectrum of the free molecule (105°) is obtained as discussed in the text. The normalized transition energies of the tetramer are also indicated.

Discussion générale

Ici se termine cette incursion dans l'étude des propriétés optiques des oligothiophènes substitués. L'objectif de départ était d'étudier l'effet de l'insertion de chaînes latérales sur la conformation et les propriétés optiques des oligothiophènes. Connaissant cet effet, notre second objectif était d'éclaircir les origines des effets chromiques observés chez ces oligothiophènes et polythiophènes substitués.

1. Propriétés optiques des dimères substitués

Pour atteindre notre premier objectif, nous avons utilisé des dérivés substitués du bithiophène qui ont l'avantage de ne posséder qu'un seul degré de liberté de torsion. La combinaison des mesures spectroscopiques et des calculs théoriques a permis d'identifier de façon claire et précise l'effet de la nature et de la position des substituants sur les paramètres spectroscopiques et sur la conformation du BT. Au premier chapitre (figure 2), nous avons pu voir que le BT possédait une première bande d'absorption non structurée relativement large caractéristique de molécules non planes possédant une barrière rotationnelle faible. L'insertion de substituants en position 4 et/ou 4' n'affecte pas la conformation de la molécule et très peu les paramètres spectroscopiques (chapitre 1, figure 2 et table 1). Ces effets faibles sur les paramètres spectroscopiques des dérivés substitués en 4,4' sont tous identifiés comme dus aux effets donneurs et/ou à l'hyperconjugaison des substituants. À l'encontre, la substitution en position 3 et/ou 3' affecte beaucoup plus les conformations et conséquemment les paramètres spectroscopiques (chapitre 1, figure 3 et table 1).

L'insertion de groupes méthoxys en position 3,3' induit une plus grande planéité entre les cycles thiophènes résultant en un déplacement bathochrome de la première bande d'absorption singulet-singulet (également induit par l'effet donneur et/ou par l'hyperconjugaison des groupes méthoxys) et en une augmentation du coefficient d'extinction molaire en comparaison avec celui du BT. La première bande d'absorption est également plus structurée et plus étroite ce qui est une caractéristique d'une molécule plane et plus rigide (barrière rotationnelle plus élevée) toujours en comparaison avec le BT. À l'inverse des groupements alkoxys, l'insertion de groupements alkyls en position 3 et/ou 3' donne une première bande d'absorption déplacée vers le bleu avec une diminution importante du coefficient d'extinction molaire, en comparaison avec le BT, caractéristique d'une molécule très tordue où la délocalisation entre les deux cycles thiophènes est très réduite. La première bande d'absorption du dérivé alkylthio en position 3,3' (chapitre 4, figure 3 et table 3) est très semblable à celle du dérivé alkyl substitué aux mêmes endroits. C'est-à-dire que nous observons une bande d'absorption déplacée vers les hautes énergies et une réduction importante du coefficient d'extinction molaire comparé au BT. Par contre, comparativement au dérivé alkyl, le coefficient d'absorptivité molaire est plus élevé et la bande d'absorption est étendue sur une plus grande région d'énergie (vers les basses énergies). Ceci démontre que, bien que très tourné, le dérivé alkylthio est tout de même moins tordu et plus flexible que le dérivé alkyl et qu'il possède une barrière rotationnelle moins élevée que ce dernier.

La diminution de la torsion suivant l'insertion de groupes alkoxys est expliquée par un transfert de charge entre le soufre et le carbone en position 3 sur le cycle aromatique. Ce transfert est induit par la présence du groupe alkoxy en position 3 qui diminue grandement la densité de charge sur le carbone en position 3. Ce transfert de charge résulte en une meilleure résonance entre les deux cycles thiophènes et ainsi compense complètement l'encombrement stérique dû aux groupes alkoxys en positions 3,3'. L'augmentation de la torsion entre les cycles thiophènes chez les dérivés alkyl et alkylthio en positions 3,3' est expliquée en terme d'encombrement stérique induit par ces groupes.

Pour tous ces dérivés, les bandes de fluorescence indiquent que la conformation plane est la plus stable au premier état excité singulet relaxé. Il en est de même pour les molécules très tordues à l'état fondamental possèdant une barrière rotationnelle très élevée pour la forme plane. Comme chaque dimère possède une conformation similaire à l'état excité relaxé mais possède des conformations différentes à l'état fondamental, les déplacements Stokes varient beaucoup d'un dérivé à l'autre. Pour les dérivés plus plans à l'état fondamental, le déplacement Stokes est plus petit et il augmente pour les dérivés plus tordus.

2. Analyse conformationnelle des dimères substitués

Les calculs *ab initio* effectués sur les dérivés du BT au chapitre 2 corroborent très bien les mesures expérimentales décrites plus haut. La courbe d'énergie potentielle du BT en fonction de l'angle dièdre entre les deux cycles thiophènes montre un minimum aux environs de 150° (chapitre 2, figure 2 et table 4) avec une très faible barrière rotationnelle (0.4 kcal mol^{-1}) pour la forme plane à 180° et une barrière plus importante (1.49 kcal mol^{-1}) pour la forme perpendiculaire (90°). Ceci est en accord avec les paramètres spectroscopiques d'une molécule tordue où une importante distribution de conformères peut coexister comme décrit au chapitre 1. La surface d'énergie potentielle du DMO33BT (chapitre 3, figure 4) montre un minimum à 180° avec une barrière à 90° plus élevée (6.69 kcal mol^{-1}) que celle du BT ce qui est conforme avec les mesures expérimentales décrites au chapitre 1. La surface d'énergie potentielle du DE33BT (chapitre 2, figure 4) montre un minimum autour de 100° avec une barrière rotationnelle pour la forme plane de 7.6 kcal mol^{-1}. Pour sa part, la surface d'énergie potentielle du DMS33BT présentée au chapitre 4 (figure 2) montre un double minimum à 71.0° et à 120° avec une très faible barrière entre ces deux minimums de 0.11 kcal mol^{-1}, mais une barrière rotationnelle plus importante (2.3 kcal mol^{-1}) pour la forme plane (180°). Ceci montre un très bon accord avec les mesures expérimentales où, pour le DBS33BT, nous obtenions des

paramètres spectroscopiques caractéristiques d'une molécule moins tordue que le DD33BT et comportant une distribution de conformères plus importante (c'est-à-dire une barrière rotationnelle plus faible).

Un seul dimère substitué en position 4,4' a été étudié par les calculs théoriques *ab initio* (chapitre 3). Les calculs effectués sur le DMO44BT montrent bien que la substitution en position 4 et/ou 4' n'affecte pas la conformation du dimère en comparaison avec le BT. Des calculs théoriques ont également été effectués sur d'autres dimères non disponibles pour des mesures expérimentales mais correspondant à des unités répétitives chez certains polythiophènes. Les résultats ont montré que la présence d'un seul substituant en position 3 et/ou 3' donnait le même effet, en moins prononcé, que le dimère possédant deux substituants en position 3,3' décrit précédemment. Ainsi la courbe d'énergie potentielle du DMO34BT (chapitre 3, figure 3) montre une conformation quasi plane (171°) avec une barrière rotationnelle à 90° moins élevée (3.88 kcal mol^{-1}) que celle du DMO33BT. Les surfaces d'énergie potentielle des dérivés DE34BT (chapitre 2, figure 3) et DMS34BT (chapitre 4, figure 4) montrent des conformations moins tordues et des barrières rotationnelles moins élevées que leurs analogues substitués en 3,3'. Nous avons également obtenu les surfaces d'énergie potentielle de deux dérivés comportant des mélanges de substituants, soit le DMODM34BT (chapitre 3, figure 5) comportant deux méthyles (en position 3,4') et deux méthoxys (en position 3',4) et le DMSDM34BT (chapitre 4, figure 5) comportant deux méthyles (en positon 3,4') et deux méthylthios (en positon 3',4). Dans les deux cas, l'encombrement stérique du méthyle favorise une conformation tordue avec une barrière rotationnelle relativement faible dans le cas du DMODM34BT, due à la présence du groupement alkoxy en position 3', mais plus élevée dans le cas du DMSDM34BT, due à l'encombrement stérique combiné des deux groupes en positions 3 et 3'.

3. Relation entre conformation et thermochromisme

Dans une première étape, pour étudier les origines des effets chromiques chez les polythiophènes et oligothiophènes substitués, nous avons comparé les possibilités de changements conformationnels (conformation minimum et barrière rotationnelle) des dimères, qui correspondent à des unités répétitives chez des polythiophènes, avec le thermochromisme observé (ou non) chez ces polythiophènes substitués (chapitre 5). Nous avons pu observer que chez les dimères ayant une conformation plane à l'état libre (et donc ne pouvant pas changer de conformation suivant un changement de phase induisant l'agrégation), le polymère correspondant ne montrait aucun effet chromique. C'est le cas pour le DMO33BT et le DMO34BT ainsi que leur polymères correspondants, le poly(3-alkoxythiophène) et le poly(3,3'-dialkoxy-2,2'-bithiophène). De même, pour les dimères très tordus et possédant une barrière rotationnelle très élevée pour la forme plane (où les changements conformationnels sont défavorisés), les polymères correspondants ne montraient aucun effet chromique notable. C'est le cas pour le DE33BT et son polymère correspondant, le poly(3,3'-dialkyl-2,2'-bithiophène). Dans tous les autres cas (sauf pour le BT et son polymère, le PT, qui n'est pas soluble), les dimères sont tordus et possèdent des barrières rotationnelles pour les formes planes moins élevées et plus facilement franchissables. Leurs polymères correspondants montrent tous des effets chromiques plus ou moins importants selon le cas. Ces résultats favorisent et appuient fortement la thèse du changement conformationnel pour expliquer les effets chromiques des polythiophènes substitués.

Quoique cette corrélation entre la mobilité des unités répétitives et les effets chromiques observés appuie l'hypothèse du changement conformationnel comme origine du thermochromisme, elle ne nous informe aucunement sur la présence réelle de ce changement conformationnel et sur la nature des interactions intermoléculaires ou interchaînes présentes suivant l'agrégation ou à l'état solide.

4. Origine du thermochromisme chez les trimères substitués

Les résultats des calculs théoriques ainsi que les mesures spectroscopiques effectuées chez les trimères substitués, et présentés au chapitre 6, ont permis d'identifier les conformations de ces molécules dans leur état libre, c'est-à-dire en solution à la température ambiante. La comparaison de ces mesures avec celles obtenues dans une matrice d'alcane à 77K (chapitre 7, figures 2,3) ont permis d'identifier clairement que ces molécules pouvaient changer de conformation dépendamment de l'environnement. Ces conclusions sont également en accord avec les données cristallographiques qui présentent tous ces dérivés dans une conformation moins tordue à l'état solide que celle prédite par les calculs théoriques et les données spectroscopiques à l'état gazeux ou en solution. La comparaison des changements des propriétés optiques dus aux changements conformationnels avec ceux induits par l'agrégation (donnant les effets thermochromes) (chapitre 7, figures 6-8) a clairement démontré que, pour les dérivés substitués, les changements conformationnels sont l'origine la plus importante (et peut être la seule) des effets chromiques observés chez ces molécules. À l'inverse, les interactions intermoléculaires de type excitonique sont à l'origine des changements dans les propriétés optiques suivant l'agrégation pour le TT. Les calculs ZINDO/S des propriétés électroniques de microcristaux, présentés au chapitre 8, ont également appuyé cette conclusion. Cette différence entre les dérivés substitués et le TT est due à l'augmentation du désordre, induit par la présence des substituants, entre molécules voisines dans l'agrégat ou le cristal (chapitre 8, figures 5,8). Ce désordre défavorise les interactions électroniques et la formation d'exciton. D'autre part, le TT qui présente une structure cristalline beaucoup plus ordonnée et compacte présente une scission excitonique importante (chapitre 8, figure 2).

5. Répercussion des résultats et applications

Pour terminer, ce travail a montré les différentes étapes et résultats qui ont permis d'atteindre les objectifs visés. Les expériences et la méthodologie utilisées dans le cadre de ce travail étaient précises et concluantes. Elles ont permis de tirer rapidement des conclusions importantes et nettes. Ce travail contribue à n'en pas douter, à accroître nos connaisances dans ce domaine et permettra sans doute l'émergence de nouvelles idées par les chercheurs travaillant dans le domaine du développement de nouveaux matériaux polymères. La connaissance précise des effets des substituants sur la conformation et ses répercussions sur les propriétés optiques de ces matériaux donnera aux chercheurs un outil supplémentaire de travail. Ceci permettra de mieux cibler le type de matériaux pouvant posséder les caractéristiques recherchées. Comme les effets thermochromes sont une caractéristique importante pour la mise au point de certains détecteurs, la connaissance de son origine est d'une grande importance pour pouvoir exploiter cette caractéristique au maximum. Du fait que les origines du thermochromisme ne résultent pas d'interactions intermoléculaires spécifiques entre molécules (ou polymères) identiques, les changements optiques peuvent donc être applicables pour des systèmes où la molécule (ou le polymère) est isolée. Ainsi, les changements optiques d'une molécule (ou un polymère) se trouvant isolée dans un milieu restreint (tel un gel, une membrane biologique, milieu biologique etc.), peuvent être utilisés pour caractériser ce milieu.

Ce travail a également permis de mettre en évidence les relations entre conformations moléculaires et propriétés optiques, ce qui est d'un grand intérêt dans la compréhension de la chimie moderne. Spécialement dans le développement de nouveaux matériaux organiques entrant comme composante électronique tel les diodes luminescentes ou les interrupteurs électroniques. L'utilisation de ces matériaux pour de telles composantes implique une compréhension des phénomènes moléculaires (conformation, interactions intermoléculaires, structure électronique

etc.) qui sont à l'origine des phénomènes macroscopiques souhaités. C'est ainsi que ce travail apporte une contribution dans ces applications actuelles et futures.

Conclusion Générale

Dans le cadre de ce travail, nous avons pu identifier les effets de l'insertion de substituants sur la conformation et les propriétés optiques d'oligothiophènes. Le BT possède une conformation non plane (minimum à 150°) et relativement souple. L'insertion de substituants en position 4 et/ou 4' n'affecte pas la conformation et très peu les paramètres optiques comparativement à ceux du BT. À l'encontre, l'insertion de substituants en position 3 et/ou 3' affecte de façon plus marquée la conformation et les propriétés optiques du BT. L'insertion de groupements alkyls et alkylthios induit une plus grande torsion entre les cycles thiophènes due à l'augmentation de l'encombrement stérique créé par ces groupes. À l'inverse, l'insertion de groupements alkoxys en position 3 et/ou 3' induit une plus grande planéité. Cette augmentation de la planéité est expliquée par un transfert de charge entre l'atome de soufre et le carbone à la position 3 du cycle thiophène.

La comparaison des surfaces d'énergie potentielle des dimères substitués avec le thermochromisme des polythiophènes correspondants montre que les changements conformationnels peuvent être à l'origine des effets thermochromes observés chez ces polymères. Les polythiophènes, possédant des unités répétitives très encombrées avec une barrière rotationnelle élevée pour la forme plane, ne sont pas thermochrome. Il en est de même pour les polythiophènes dont l'unité répétitive est plane. Dans les deux derniers cas, il ne peut y avoir de changements conformationnels du polymère entre la forme libre et agrégée (ou à l'état solide). Par contre, tous les polythiophènes substitués possédant des unités répétitives non planes avec des barrières rotationnelles relativement faibles pour les formes planes sont thermochromes.

Les mesures de thermochromisme effectuées sur les oligothiophènes (trimères dans ce travail) nous conduisent à la même conclusion que les résultats théoriques. Les déplacements des bandes d'absorption, suite à un changement conformationnel, sont très similaires à ceux causés par l'agrégation (condition pour observer le thermochromisme chez les polymères). Pour tous les trimères substitués, les effets excitoniques ne semblent pas présents ou beaucoup moins importants que les effets conformationnels. À l'encontre, les effets excitoniques sont la cause majeure des effets thermochromes observés chez le TT. Les calculs ZINDO/S effectués sur les structures cristallines des trimères corroborent les résultats expérimentaux. L'insertion de substituants empêche un empilement bien ordonné et compact et ainsi défavorise les interactions intermoléculaires menant à des scissions de nature excitonique mais favorise néanmoins une augmentation de la planéité moléculaire.

Annexe 1

Toutes les méthodes de calculs théoriques présentées dans la thèse ont comme point commun la résolution de l'équation de Schrödinger : $H\Psi = E\Psi$ où Ψ représente la fonction d'onde de l'état d'énergie E décrit par l'opérateur H (Hamiltonien). Dans le cas d'un système atomique ou moléculaire, les mouvements électroniques sont considérés comme indépendants des mouvements nucléaires. Selon cette approximation, nommée approximation de Born-Oppenheimer, nous pouvons séparer les termes d'énergie nucléaire et électronique de l'Hamiltonien :

$$H_{elec}\Psi_{elect} = E_{elec}\Psi_{elec}$$

où l'Hamiltonien électronique comporte les termes d'énergie cinétique des électrons, les termes d'énergie potentielle d'attraction électron-noyau et les termes d'énergie potentielle de répulsion électron-électron. Les fonctions d'onde obtenues (appelées orbitales moléculaires, ϕ_i) sont constituées d'une combinaison linéaire d'orbitales atomiques Ψ_k (approximation MO-LCAO):

$$\phi_i = \sum c_{ik}\Psi_k$$

Un problème se pose pour l'obtention des termes d'énergie potentielle de répulsion électron-électron. Nous ne pouvons pas tenir compte dans les calculs des répulsions entre un électron et les n-1 autres électrons. Pour solutionner ce problème, nous considérons qu'un électron interagit avec un champs unique moyen constitué par tous les autres électrons. Alors un autre problème se pose, ce champs moyen dépend de la distribution des électrons dans les orbitales et inversement la distribution des électrons dans les orbitales dépend du champs moyen des électrons voisins. En d'autres mots, ils ne sont pas auto-cohérents. Pour solutionner ce

problème, nous distribuons les électrons dans des orbitales "acceptables", nous calculons un champs moyen pour cette distribution, par la suite nous recalculons les orbitales avec ce champs. Avec ces nouvelles orbitales, nous recalculons un nouveau champs et le tout se poursuit jusqu'à convergence des orbitales moléculaire. Ainsi toutes les méthodes de calculs HF (Hartree-Fock) et semi-empiriques se basent sur ces principes. La différence majeure entre ces techniques est dans les subtilités mathématiques utilisées pour résoudre les équations.

La méthode Hartree-Fock (HF) se base sur la résolution exacte de l'équation de Schödinger ce qui rend ce genre de calcul long et exigeant. Le seul paramètre à fixer est la base utilisée pour la construction des orbitales atomiques qui servent à la construction des orbitales moléculaires. Plus la base proposée est grande (beaucoup de fonctions) plus le temps de calcul sera long mais plus les orbitales obtenues seront acceptables. Dans le cadre de cette thèse, deux types de bases ont été utilisées, soit la base STO-3G et 3-21G*. La base STO-3G est une base minimale constituée d'exponentielles de Slater ($e^{-\alpha x}$). Comme les intégrales constituées de fonctions de Slater sont difficiles à résoudre, on utilise souvent (dans la majorité des cas) des fonctions à base de gaussiennes ($\exp(-\alpha x^2)$). La base 3-21G* est constituée de fonctions gaussiennes pour représenter les fonctions de type s et p. L'étoile indique que nous rajoutons des fonctions de type d (pour les atomes où $Z > 2$) permettant ainsi la polarisation des orbitales p.

Cette méthode ab initio (HF) comporte certaines insuffisances. Elle ne tient pas compte de l'effet de la corrélation électronique et ne permet pas la dissociation inter-atomique. Pour des optimisations de géométrie de molécules simples (telles que les molécules étudiées dans le cadre de la thèse), ces effets sont souvent considérés négligeable et la méthode HF donne de très bons résultats si la base utilisée est suffisamment élaborée.

Pour les méthodes semi-empiriques, les équations de base sont les mêmes que pour la méthode HF. Par contre, la différence est dans la résolution de ces équations. Toutes les méthodes semi-empiriques partent du déterminant séculaire d'Hartree-Fock mais on ajoute une variété d'approximations de façon à réduire le temps de calculs. Ces approximations ne veulent pas dire que les résultats des méthodes semi-empiriques donnent nécessairement des résultats moins valables que la méthode HF. Les méthodes ab initio sont elles-mêmes imparfaites pour

reproduire certaines propriétés. Ceci est principalement vrai pour de gros systèmes où plusieurs compromis doivent être considérés pour obtenir un calcul physiquement réalisable et dans un temps raisonable. Ainsi, les approximations des méthodes semi-empiriques réduisent le temps de calcul et permettent souvent d'obtenir de meilleurs résultats. Les approximations utilisées sont la négligence des électrons de cœurs qui sont considérés comme formant un tout avec le noyau, la négligence de certaines intégrales comme les intégrales à trois et quatre centres qui sont très longues à résoudre et l'incorporation de paramètres ajustables à partir des résultats expérimentaux. Il faut faire très attention au choix de la méthode utilisée. Il existe plusieurs méthodes semi-empiriques du fait que selon des approximations effectuées et la nature des résultats expérimentaux utilisés, les résultats seront souvent valables pour certaines propriétés et non valables pour d'autre. Également, les approximations seront valables, ou ont été considérées, pour un certain type de molécules et la méthode s'appliquera seulement pour ce type de molécules.

Les méthodes AM1 et PM3 (développées par Dewar et coll.) sont des méthodes INDO (Intermediate Neglect of Diatomic Différentiel) modifiées. Dans ces calculs, les intégrales d'échange sont considérées. Ces deux méthodes incorporent des paramètres empiriques de façon à améliorer la corrélation avec l'expérience. Elles s'appliquent particulièrement pour les optimisations de géométrie de molécules organiques.

La méthode ZINDO/S (développée par Zerner et coll.) est également une méthode INDO modifiée. Cette méthode se base sur des paramètres obtenus par calculs ab initio pour ensuite reproduire les résultats expérimentaux. Il a été observé que les paramètres requis pour reproduire l'ordre énergétique des orbitales et les spectres UV sont différents de ceux requis pour reproduire les structures moléculaires. Ainsi la méthode ZINDO/S est principalement utilisée pour prédire les propriétés des spectres électroniques.

Annexe 2

Définition des descriptions des conformations.

Dans la thèse, deux systèmes sont utilisés pour la description des angles dièdres (θ) entre les cycles thiophènes.

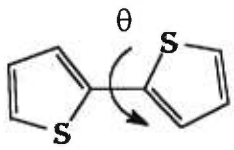

Lorsque nous avons des conformations planes (θ = 0° ou 180°), nous utilisons les termes *cis* ou *syn* pour un angle θ = 0°, et *trans* ou *anti* pour un angle θ = 180°. Les termes *cis* et *trans* sont empruntés à la nomenclature des alcènes pour représenter des molécules planes. Les termes *syn* et *anti* sont employés de façon plus générale en chimie pour la description 3D de molécules.

Le terme *gauche* est utilisé pour décrire les conformations non-planes. Ce terme représente plusieurs conformations. En générale, le terme *gauche* est utilisé pour désigner une conformation comportant un angle voisin de 60°. Pour nos systèmes, ceci peut correspondre à un angle θ = 60° ou θ = 120°. Pour faire la différence entre ces deux régions de conformations, nous utilisons le terme *syn*-gauche pour θ ~ 60° et le terme *anti*-gauche pour θ ~ 120°. Il est important de mentionner que les termes *syn*-gauche et *anti*-gauche ne correspondent pas à un angle unique mais à une région comportant plusieurs conformères. La distinction entre ces deux régions de conformations est importante puisque la distance entre les atomes de soufres (des cycles thiophènes) est primordiale pour l'énergie de la conformation. Ainsi, la région *syn*-gauche

regroupe les conformations non-planes où les deux atomes de soufre sont voisins. La région *anti*-gauche regroupe les conformations non-planes où les atomes de soufre pointent dans des directions opposées.

Bibliographie

[1] C.K. Chiang, C.R. Fincher jr., Y.W. Park, A.J. Heeger, H. Shirakawa, E.J. Louis, S.C. Gau et A.G. MacDiarmid, Phys. Rev. Lett., 39 (1977) 1098.

[2] Handbook of Conducting Polymers, Marcel Dekker, New York (1986).

[3] G. Kossmehl, Makromol. Chem., Macromol. Symp., 4 (1986) 45.

[4] J. Roncali, Chem. Rev., 92 (1992) 711.

[5] G. Schopf et G. Kossmehl, Adv. Polym. Sci., 129 (1997) 1.

[6] Handbook of Organic Conductive Molecules and Polymers vol. 1-4, Ed. Hari Singh Nalwa, Englend (1997).

[7] K. Tashiro, T. Ono, Y. Minagawa, M. Kobayashi, S. Kawai, K. Yoshini, J. Polym. Sci., 29 (1991) 1223.

[8] A. Bolognesi, M. Catellani, S. Destri, W. Porzio, Makromol. Chem. Rapid. Commun., 12 (1991) 9.

[9] A. Bolognesi, W. Porzio, F. Provalosi, Makromol. Chem., 194 (1993) 817.

[10] T-A. Chen, X. Wu, R.D. Rieke, J. Am. Chem. Soc., 117 (1995) 233.

[11] F. Bertinelli, C. Della Casa, Polymer, 37 (1996) 5469.

[12] O.R. Konestubo, K.E. Aasmundtreit, E.J. Samuelsen, E. Bakken, P.H.J. Carlsen, Synth. Met., 84 (1997) 589.

[13] C. Yang, S. Holdcruft, Synth. Met., 84 (1997) 563.

[14] P. Buvat, P. Hourquebie, Macromolecules, 30 (1997) 2685.

[15] F. Goldoni, D. Iarossi, A. Mucci, L. Schenetti, M. Zambianchi, J. Mater. Chem., 7 (1997) 593.

[16] C. Roux, J-Y. Bergeron, M. Leclerc, Makromol. Chem., 194 (1993) 869.

[17] K. Faïd, M. Leclerc, J. Chem. Soc.; Chem. Commun., 11 (1993) 962.

[18] C. Roux, M. Leclerc, Chem. Mater., 6 (1994) 620.

[19] K. Faïd, M. Fréchette, M. Ranger, L. Mazerolle, I. Lévesque, M. Leclerc, Chem. Mater., 7 (1995) 1390.

[20] G. Rumbles, I.D.W. Samuel, L. Magnani, K.A. Murray, A.J. DeMello, B. Crystall, S.C. Moratti, B.M. Stone, A.B. Holmes, R.H. Friend, Synth. Met., 76 (1996) 47.

[21] I. Lévesque, M. Leclerc, Chem. Mater., 8 (1996) 2843.

[22] M. Leclerc, M. Fréchette, J-Y. Bergeron, M. Ranger, I. Lévesque, K. Faïd, Macromol. Chem. Phys., 197 (1996) 2077.

[23] R. Hanna, M. Leclerc, Chem. Mater., 8 (1996) 1512.

[24] B.M.W. Langeveld-Voss, E. Peeters, R.A. Janssen, E.W. Meijer, Synth. Met., 84 (1997) 611.

[25] F. Raymond, N. DiCésare, M. Belletête, G. Durocher et M. Leclerc, Adv. Mater, 10 (1998) 599.

[26] S-C. Ng, P. Miao, H.S.O. Chan, Chem. Commun. (1998) 153.

[27] T. Yamamoto, D. Komarudin, M. Arai, B-L. Lee, H. Suganuma, N. Asakawa, Y. Inoue, K. Kubota, S. Sasaki, T. Fukuda, H. Matsuda, J. Am. Chem. Soc., 120 (1998) 2047.

[28] G. Horowitz, D. Fichou, X.Z. Peng, G. Xu, F. Garnier, Solid State Commun., 72 (1989) 381.

[29] J. Roncali, Chem. Rev., 92 (1992) 711.

[30] F. Garnier, A. Yassar, R. Hajlaoui, G. Horowitz, F. Deloffre, B. Servet, S. Ries, P. Alnot, J. Am. Chem. Soc., 115 (1993) 8716.

[31] G. Horowitz, P. Delannoy, H. Bouchriha, F. Deloffre, J-L. Fave, F. Garnier, R. Hajlaoui, M. Heyman, F. Kouki, P. Valat, V. Wintgens, A. Yassar, Adv. Mater., 6 (1994) 752.

[32] A. Dodabalapur, L. Torsi, H.E. Katz, Sciences, 268 (1995) 270.

[33] Y. Kunugi, L.L. Miller, T. Maki, A. Canavesi, Chem. Mater., 9 (1997) 1061.

[34] H.E. Katz, J. Mater. Chem., 7 (1997) 369.

[35] J.A. Pople, D.L. Beveridge, Approximate Molecular Orbital Theory, McGraw Hill, New-York, 1970.

[36] J.N. Murrell, A.J. Harget, Semi-Empirical Self-Consistent-Field Molecular Orbital Theory of Molecules, Wiley Interscience, New-York, 1971.

[37] W. Thiel, Tetrahedron, 44 (1988) 7393.

[38] J.J.P. Stewart, J. Comput. Chem., 10 (1989) 10.

[39] J.J.P. Stewart, J. Comput. Chem., 10 (1989) 221.

[40] J.J.P. Stewart, Reviews of Conputational Chemistry, K. Lipkovitz, D.B. Boyd, Eds. VCM Publishers, New-York, 1990.

[41] T.H. Dunning, P.J. Hay, Modern Theoretical Chemistry, Plenum, New-York, 1976.

[42] A. Szabo, N. Ostlund, Modern Quantum Chemistry, Macmillan, New-York, 1982.

[43] N. DiCésare, M. Belletête, A. Donat-Bouillud, M. Leclerc, G. Durocher, J. Luminesc., 81 (1999) 111.

[44] N. DiCésare, M. Belletête, A. Donat-Bouillud, M. Leclerc, G. Durocher, Macromolecules, 31 (1998) 6289.

[45] N. DiCéare, M. Belletête, M. Leclerc, G. Durocher, Synth. Met., 98 (1998) 31.

[46] N. DiCésare, M. Belletête, M. Leclerc, G. Durocher, Chem. Phys. Lett., 291 (1998) 487.

[47] N. DiCésare, M. Belletête, E. Riviera, M. Leclerc, G. Durocher, J. Phys. Chem., soumis pour publication.